

NASA Contractor Report 3692

Dynamic Effects of Internal Spur Gear Drives

**Adam Pintz, R. Kasuba,
J. L. Frater, and R. August**

**GRANT NAG3-186
JUNE 1983**

NASA

NASA Contractor Report 3692

Dynamic Effects of Internal Spur Gear Drives

Adam Pintz, R. Kasuba,
J. L. Frater, and R. August
Cleveland State University
Cleveland, Ohio

Prepared for
Lewis Research Center
under Grant NAG3-186



National Aeronautics
and Space Administration

Scientific and Technical
Information Branch

TABLE OF CONTENTS

CHAPTER	PAGE
I. INTRODUCTION	1
1.1 General Remarks	1
II. LITERATURE REVIEW	9
2.1 External Spur Gears	9
2.2 Internal Spur Gears	25
III. ANALYTICAL INVESTIGATION	30
3.1 Problem Formulation	30
3.2 Assumptions	35
3.3 Method of Solution	37
3.4 Static Analysis	38
3.4.1 Nomenclature	38
3.4.2 Local and Global Coordinate Systems	39
3.4.3 External and Internal Gear Tooth Profile	41
3.4.4 Contact Points Between Gear Tooth Pairs	48
3.4.5 Line of Action, Contact Ratio and Interference Conditions	54
3.4.6 Deflections and Stiffness of the Teeth and Their Supporting Structure	56
3.5 Dynamic Analysis	62
3.6 Computer Program	74
3.6.1 Program Structure	74
3.6.2 Description of the Executive Programs and Subroutines	77
3.6.2.1 Module 1	77

CHAPTER	PAGE
3.6.2.2 Module 2	78
3.6.2.3 Module 3	79
IV. RESULTS, DISCUSSION AND SUMMARY	80
4.1 Results and Discussion	80
4.1.1 Introduction	80
4.1.2 Static Analysis	81
4.1.2.1 Comparison of ISG and ESG Set Performance	81
4.1.2.2 ISG Drives of Practical Interest . .	88
4.1.2.3 Effects of Radial Deflection on Static Performance	89
4.1.3 Dynamic Analysis	91
4.1.3.1 Comparison of ISG and ESG Drive Dynamic Performance	91
4.1.3.2 ISG Drives of Practical Interest . .	102
4.1.3.3 Effect of Radial Deflection on Dynamic Performance	102
4.2 Summary and Conclusions	105
BIBLIOGRAPHY	108
APPENDICES	110
A Spur Gear Formulae and Involute Profile Development	110
A-1 Standard Spur Gear Relations for the ISG Drive	111
A-2 Development of the Involute Profile . .	114
B Deflections	118
B-1 Bearing Deflections	119
B-2 Radial Ring Gear Deflection	120
B-3 Circumferential Deformation of Gear Teeth	121

APPENDICES (Cont'd)

B-3.1	Deflection of Point of Contact Due to Deformation of Teeth	121
B-3.2	Deformation of the Teeth Due to Rotation of Their Foundation	125
B-3.3	Deflection of the Teeth Due to Circumferential Deformation of the Rim and Gear Ring	128
B-3.4	Hertzian Deformation at Contact Point	132
C	Computer Program Package	135
C-1	Listing and Sample Run of the Static Analysis Program "Internal Static"	136
C-2	Listing and Sample Run of the Dynamic Analysis Program "Internal Dynamic"	198
C-3	Listing and Sample Run of the Stress Analysis "Internal Stress"	248
C-4	Entering of Input Data	271
D	Glossary of Terms	276

CHAPTER I
INTRODUCTION

1.1 GENERAL REMARKS

Spur gears have been utilized for many years and are of great importance in transmitting power from one rotating shaft to another. To affect power transmission, two or more gears are combined in a variety of arrangements. The most common and best understood configuration is the use of two external spur gears side-by-side as shown in Figure 1. This arrangement of the gears is used in single and multiple pairs or stages, and is referred to as a parallel shaft gear transmission or "gear box". Parallel shaft gear boxes are economic in the power range 0 to 1500 KW, but become large, heavy and less economic above these power levels.

More compact arrangements are achieved with the use of an external gear inside an internal gear as shown in Figure 2. This configuration is referred to as internal gear drive and is applied for the movement of turntables, tank turrets, radar systems, and the transmission of power in wind turbines, wheel drives of off-the-road vehicles, etc. The internal gear drives can be used either as speed reducers or speed increasers.

Because of their inherently higher cost, selection of internal gear drives is predicated on the need for compactness or the opportunity of sharing components with another function in the system. Examples

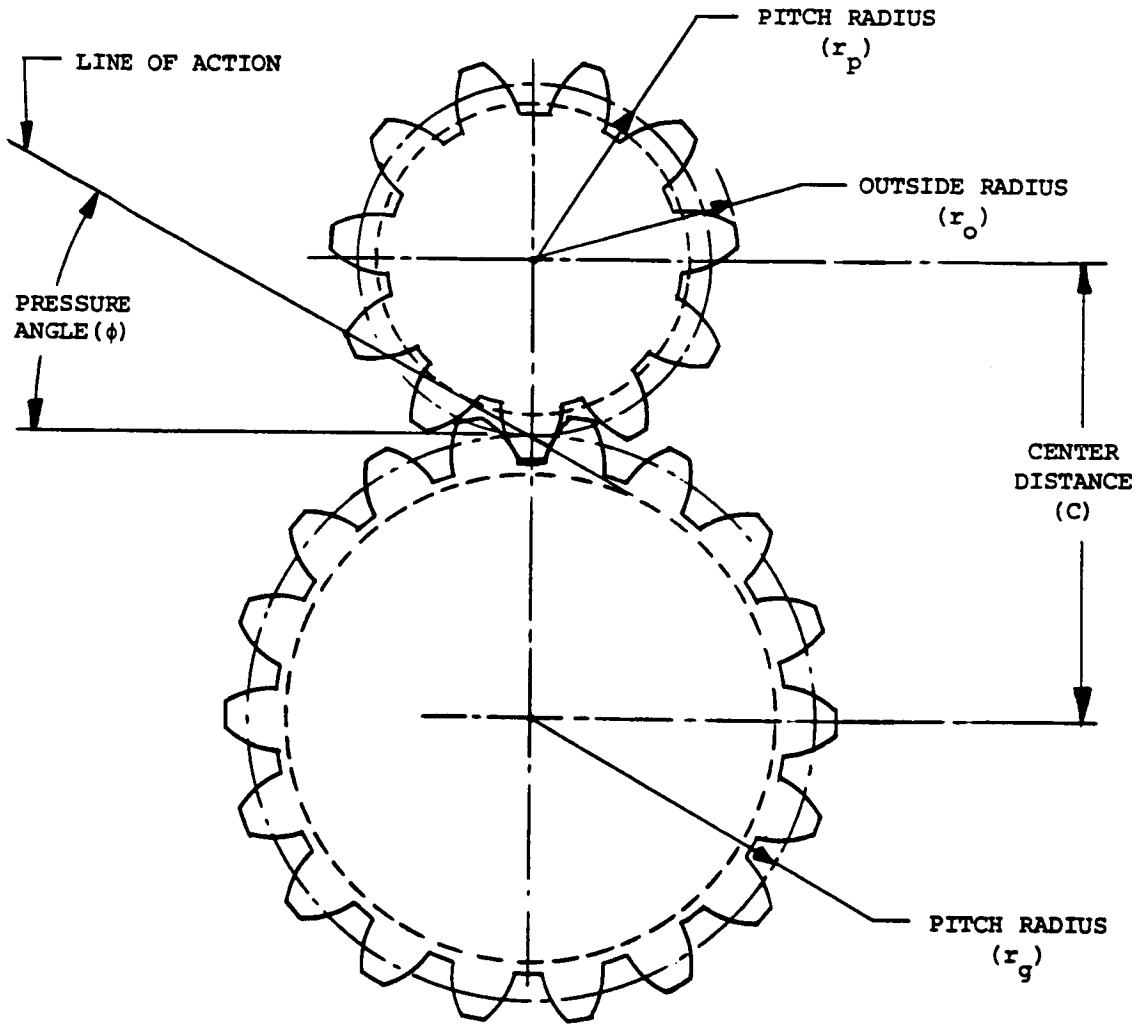


Figure 1 - External Spur Gear Arrangement

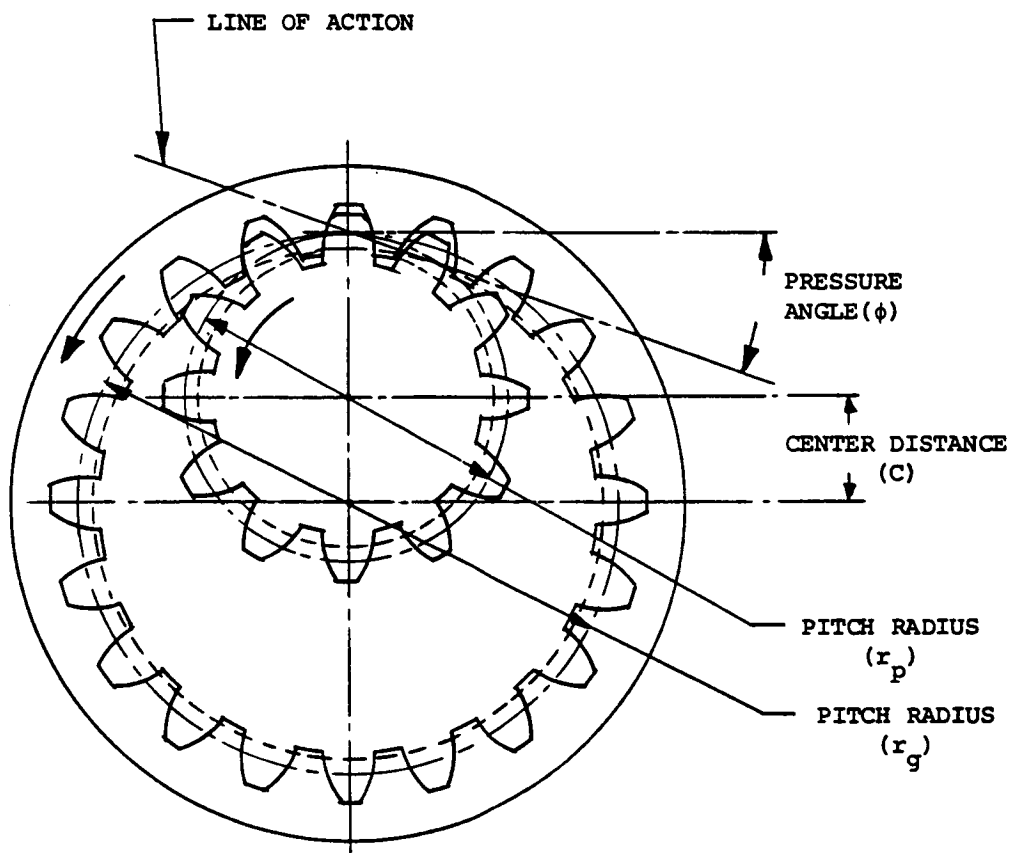


Figure 2 - Internal Gear Drive (ISG)

of either possibility are shown in Figures 3 and 4. The radar gear reduction unit of Figure 3 is actually a combination or hybrid of external and internal gear reduction stages. The compactness of the design is obvious.

Figure 4 is an example where two functions are combined in one component. In this application the rotor of a wind turbine is supported at the inner race of a large ball bearing. Also, the inner race is used as the first stage speed increaser for the wind turbine. As shown in Figure 4, internal gear teeth at the bore of the inner race engage with the external mating gear. The mating gear is mounted at the far side of the bearing. A long drive shaft connects the first stage speed increaser to the two-stage final speed increaser. Finally, the electric generator is connected to the final speed increaser and is shown at the far side of the drive shaft. The cost of a separate bearing support for the rotor and a three-stage speed increaser is higher than the arrangement shown in Figure 4.

Other examples of internal gear arrangements can be found in epicyclic gearing (Figure 5). As can be seen, an epicyclic gear train has a central "sun" gear, several "planets" meshing with the sun and spaced uniformly around the sun, and an internal gear or ring gear meshing with the planets. The name epicyclic is derived from the fact that points on planets trace out epicycloidal curves in space. Because of the multiple use of planet gears, epicyclic gearing is the most compact arrangement of all the spur gear systems.

At present, concerted efforts are being made to increase the power-to-transmission weight ratio. These efforts are not limited to the aerospace industry alone because of the high cost of material,

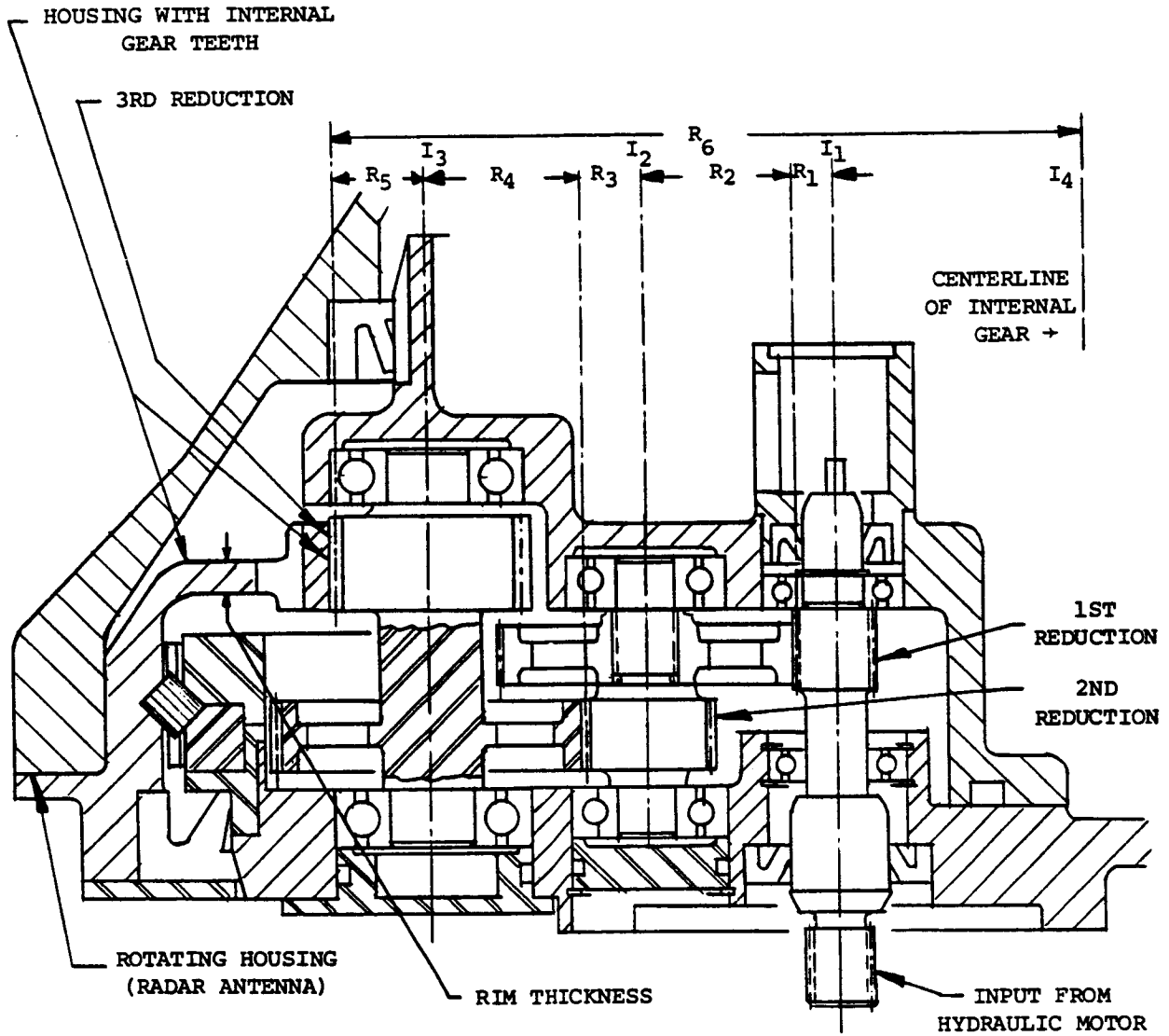


Figure 3 - Assembly Drawing of Radar Gear - Reduction Unit

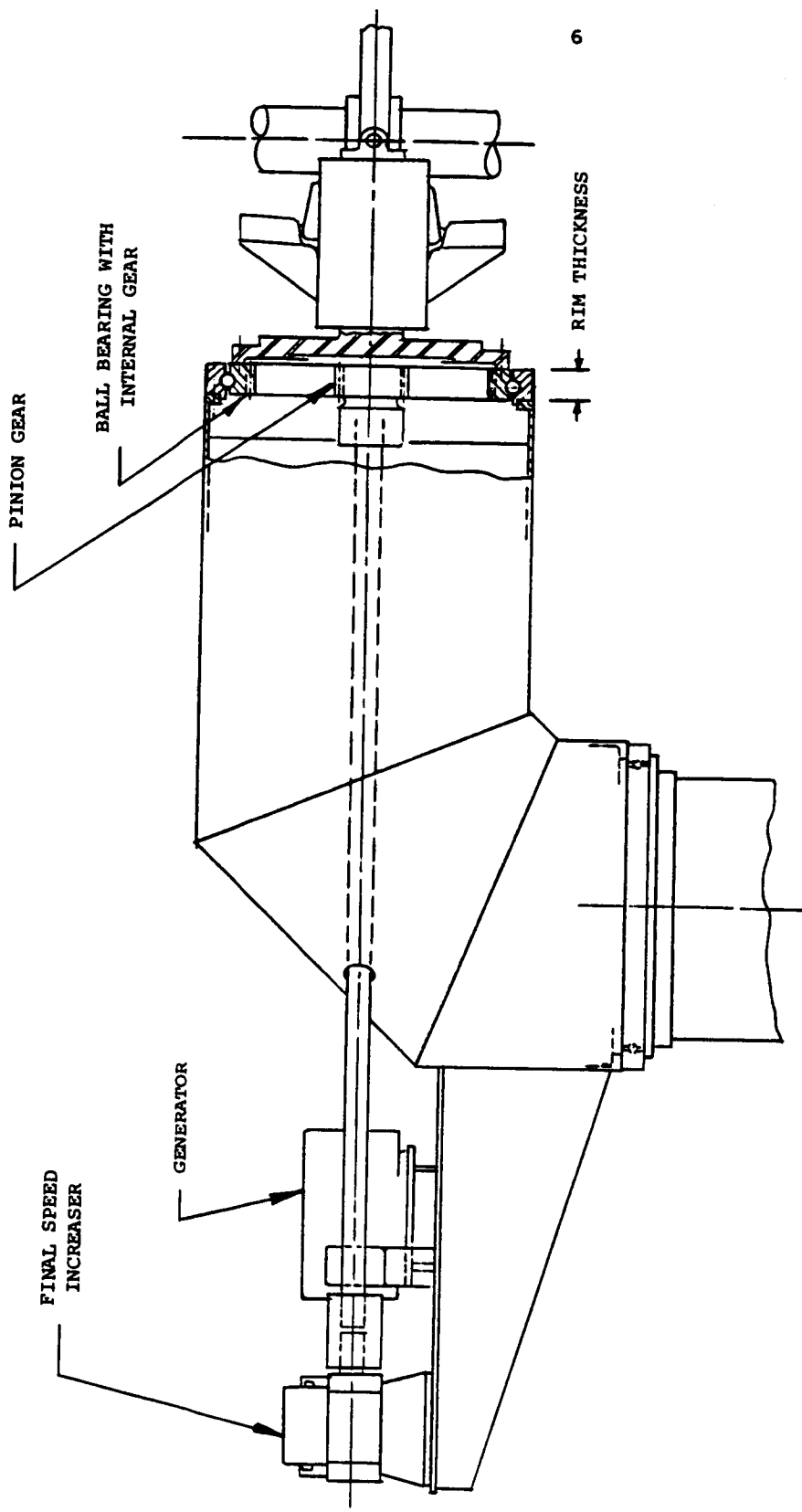


Figure 4 - Wind Turbine Concept Utilizing Internal Gear Drive

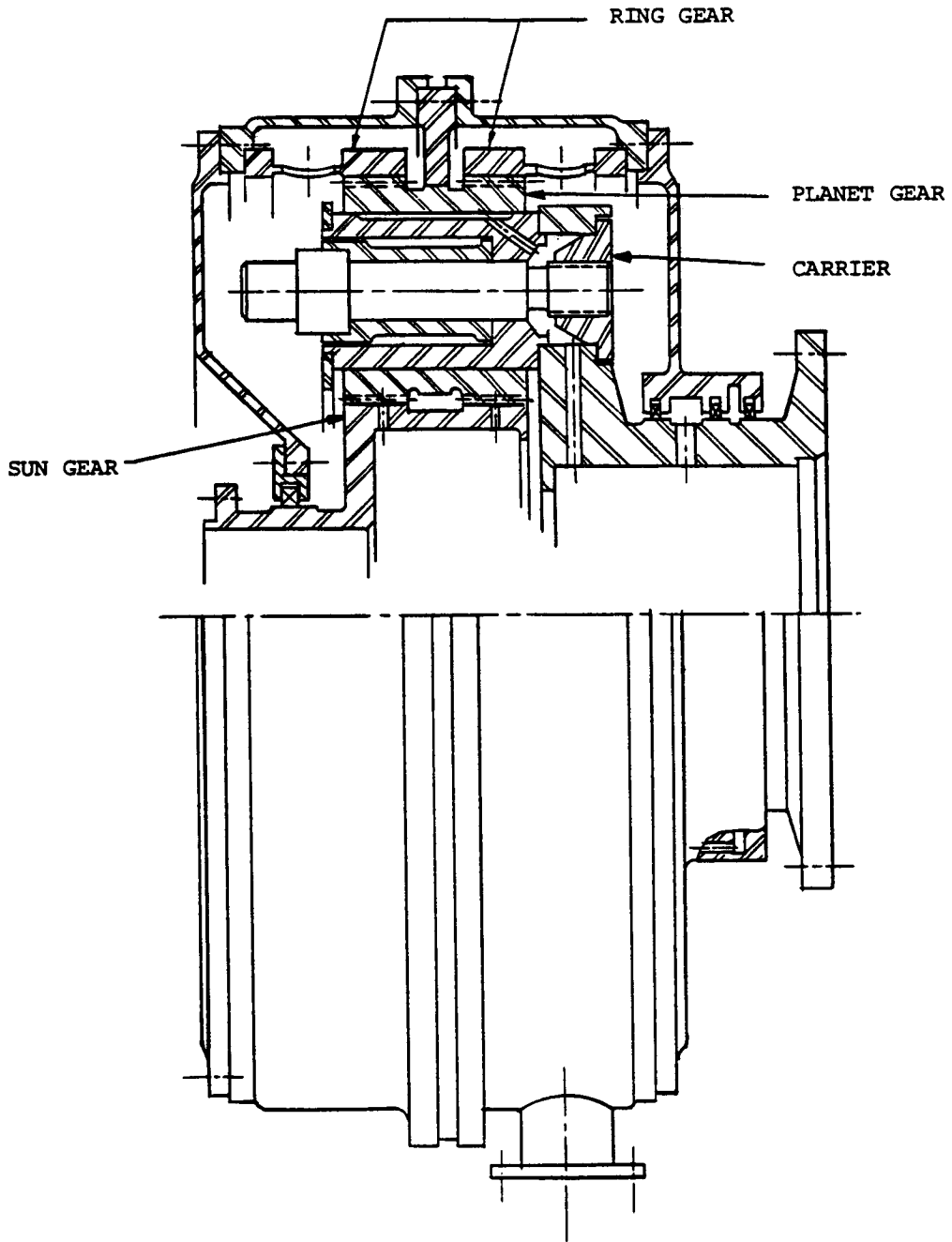


Figure 5 - Epicyclic Gear Box

labor and energy. Savings in weight normally imply less material with some savings in cost of the transmission.

Consequently, extension of the state-of-the-art in spur gearing is a continuing requirement. Unfortunately, spur gearing investigations are concentrated almost exclusively to external gears as is evident from the literature review in the next section. For example, the latest investigations utilize large scale digital computer programs to analyze external spur gearing for both static and dynamic conditions. These sophisticated computer programs for external gears help to move the analytical simulation closer to the actual behavior. Prior to this research work, no such analytical tools were known to exist for internal spur gear (ISG) drives.

The design of ISG drives was based principally on extrapolations of external gearing procedures by the American Gear Manufacturer's Association (AGMA) and the International Standard Organization (ISO). In either case, these procedures represent the technology known in the 1950's. The basic drawback of these procedures is that they are based on highly idealized relationships, which in real applications hardly exist. Thus, a multitude of safety and application factors are imposed on the procedures which can result in considerable overdesign.

CHAPTER II

LITERATURE REVIEW

As mentioned earlier the study of spur gearing is concentrated to a great extent on investigations of external spur gears. Therefore, this literature review relies heavily on the information for external spur gears in showing the progress and current status of spur gear technology. The information is presented chronologically, and in separate sections for the external and internal spur gearing respectively.

2.1 EXTERNAL SPUR GEARS

In 1892 Lewis ^{[1]*} used the form of the gear tooth as one of the factors in a formula for the Strength of External Gear Teeth. He related the tooth load to the material working stress using simple beam theory and developed equation (1), known as the Lewis Equation

$$W = SPFY \quad \dots(1)$$

where

W = transmitted load, lb.

S = safe working stress in material, psi

P = circular pitch, in.

F = face width of gears, in.

Y = tooth-form factor

*Superscripts refer to entries in references.

Lewis also recognized that the instantaneous load of the teeth was affected by the velocity of the system. Barth^[10] took note of this fact and developed a formula which resulted in an adjustment of the allowable stress as follows:

$$S_d = S \frac{600}{600 + V} \quad \dots(2)$$

where

S = safe static stress, psi

V = pitch line velocity, fpm

This modified design stress was then used as the design stress in the Lewis Equation. Today, the American Gear Manufacturer's Association (AGMA) recommended practice for bending strength uses the Lewis Equation in modified form.

In the 1920's and the early 1930's the American Society of Mechanical Engineers (ASME) Research Committee investigated gear tooth loads and available design criteria in order to develop a unified approach to gear design. Tests were conducted by Lewis and Buckingham to determine the effects of production errors and pitch line velocity on the load capacity of gears. The resulting report indicated a procedure to determine the so-called dynamic load increment due to dynamics of gears in mesh and the error of the gear teeth. Buckingham presented the dynamic load increment calculation in his text^[1] as follows:

$$F_t = F + \sqrt{F_A [2 F_2 - F_A]} \quad \dots(3)$$

where

$$F_2 = F [(e/D) + 1]$$

$$F_A = \frac{F_1 F_2}{F_1 + F_2} \quad \dots(4)$$

F_t = instantaneous load, lb.

F = average transmitted load (calculated from the horsepower to be transmitted and considering the force to act tangential to the pitch circle)

F_A = acceleration load on gear teeth, lb.

F_2 = force required to deform the teeth the amount of the effective error, lb.

e = measured error in action (maximum), in.

D = displacement of gear tooth under load F , in.

F_1 = force required to accelerate the masses of the gear and pinion as rigid bodies, lb.

The instantaneous load determined by equation (3) should be less than the safe allowable load determined from the Lewis Equation.

Probably, the most important finding by the ASME Research Committee testing program was that most gear failures were not due to insufficient bending strength in gear teeth. In many cases teeth failed in wear, primarily by progressive pitting. Again, Buckingham developed the wear equation which is used today in modified form.

Tuplin was one of the first to publish a more refined method of determining the dynamic loads in gear teeth.^[2] He considered an equivalent spring-mass system as shown in Figure 6 that represents gears in mesh. He states that passage of a "high" tooth through the meshing zone is equivalent to the rapid insertion of a thin wedge between loaded teeth of stationary gears and that the model in Figure 6 represents this condition. The mass M is determined from equivalent masses of gears concentrated at the gear pitch circles. Spring stiffness K is that of two teeth acting together and is determined from the

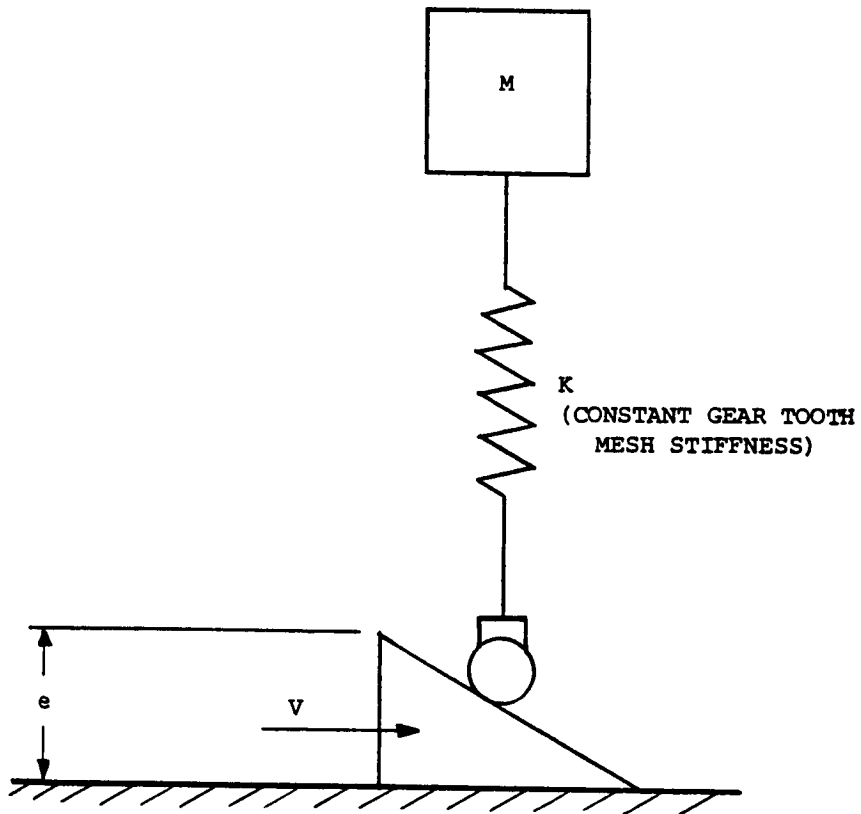


Figure 6 - Tuplin's Model

static load-deflection relationship. In this model, e and V represent the maximum pitch error and rate of insertion of the wedge (average pitch line velocity of gears), respectively.

Tuplin's results indicate the dynamic load increment to be

$$I = \frac{Ke}{1 + 6.6(t/T)^2} \quad \text{for } t \leq 0.3 \quad \dots(5)$$

$$I = \frac{0.815 \times Ke}{[1 + 6.6(t/T)^2]^{\frac{1}{2}}} \quad \text{for } t > 0.3 \quad \dots(6)$$

where

I = dynamic increment of load (the load above the average load), lb.

K = spring constant of teeth in mesh, lb./in.

e = maximum pitch error, in.

T = natural period of vibration of equivalent spring-mass system, sec.

t = time of insertion of wedge, sec.

It is especially interesting to note that the dynamic increment determined by Tuplin's equation has no relation to the average load being transmitted between gears. Also, the equations do not account for multiple tooth contact or damping in the system.

Attia^[3] performed experiments to determine the actual instantaneous load. He found that Buckingham's equation gave high values of dynamic increment while Tuplin's equation gave values nearer to those measured. Also, Attia's measurements illustrated sudden rises and drops in the load curves, indicating that gearing errors caused several impacts throughout engagement rather than smooth load transmission, and that the maximum load did not occur at a particular phase of engagement. From the results he inferred that the simple analyses presented by

Buckingham and Tuplin were not adequate to describe the transmitted load behavior.

Reswick^[4] conducted a more rigorous analyses by including the effects of multiple tooth engagement. He also considered the effects of heavily and lightly loaded gears.

Niemann and Rettig^[5] found in their test program that larger masses caused higher dynamic loads, but that as the average load became larger the effect of larger masses became unimportant. They also found that "very heavily loaded" gears showed no appreciable dynamic load increment, whereas in "lightly" and "moderately loaded" gears dynamic load increments of considerable magnitude were observed.

Harris^[6] carried out a photoelastic investigation concerning dynamic loads of gears. He concluded that when spur gears are isolated from external forcing functions, the dynamic load is caused by

1. Error in the velocity ratio measured under the working load (gears can only approach a constant velocity ratio under one deflection which depends on the applied load and profile modification).
2. Parametric excitation due to the stiffness variation of the teeth.
3. Nonlinearity caused by tooth separation (backlash).

Munro's^[7] work in gear dynamics indicated that transients do not decay as quickly as previously thought. Hence, he strongly suggests that single tooth studies are inadequate, since essential nonrepetitious errors are considered. He found that after a tooth with error had passed through an engagement cycle, subsequent engaging teeth were affected by the preceding tooth's error.

Richardson^[8] completed an analyses of static load, stress and deflection cycles of gear teeth and substantiated his results with experimental measurements. He then developed a dynamic model to predict the instantaneous load by first considering two gears in mesh as shown in Figure 7. Newton's laws of motion were applied to this physical system and then the system of equations were transformed. The model shown in Figure 8 is the result of the transformed equations. Assumptions made in order to make the problem of determining the instantaneous transmitted loads tractable were:

1. Input and output torques remain constant and the output torque is inversely proportional to the velocity ratio.
2. The total mass M of the model is determined considering the equivalent mass of the gears concentrated at the base circles of the gears.
3. Coulomb friction is considered negligible.
4. The viscous friction force W_f and all other friction are considered as a single damping term.
5. The stiffness of the gear teeth is assumed to be the same for all teeth and constant.
6. Error functions act as forcing functions on the system.
7. The cam moves at the pitch line velocity of the gears.
8. Curved ends of the cam result from a "no load separation analysis" as described by Richardson. (The attempt is to make the gears engage gradually, rather than abruptly).

Two modes of dynamic operation were considered:

1. Heavily loaded gears where the relative displacement or static displacement of gears is greater than the errors

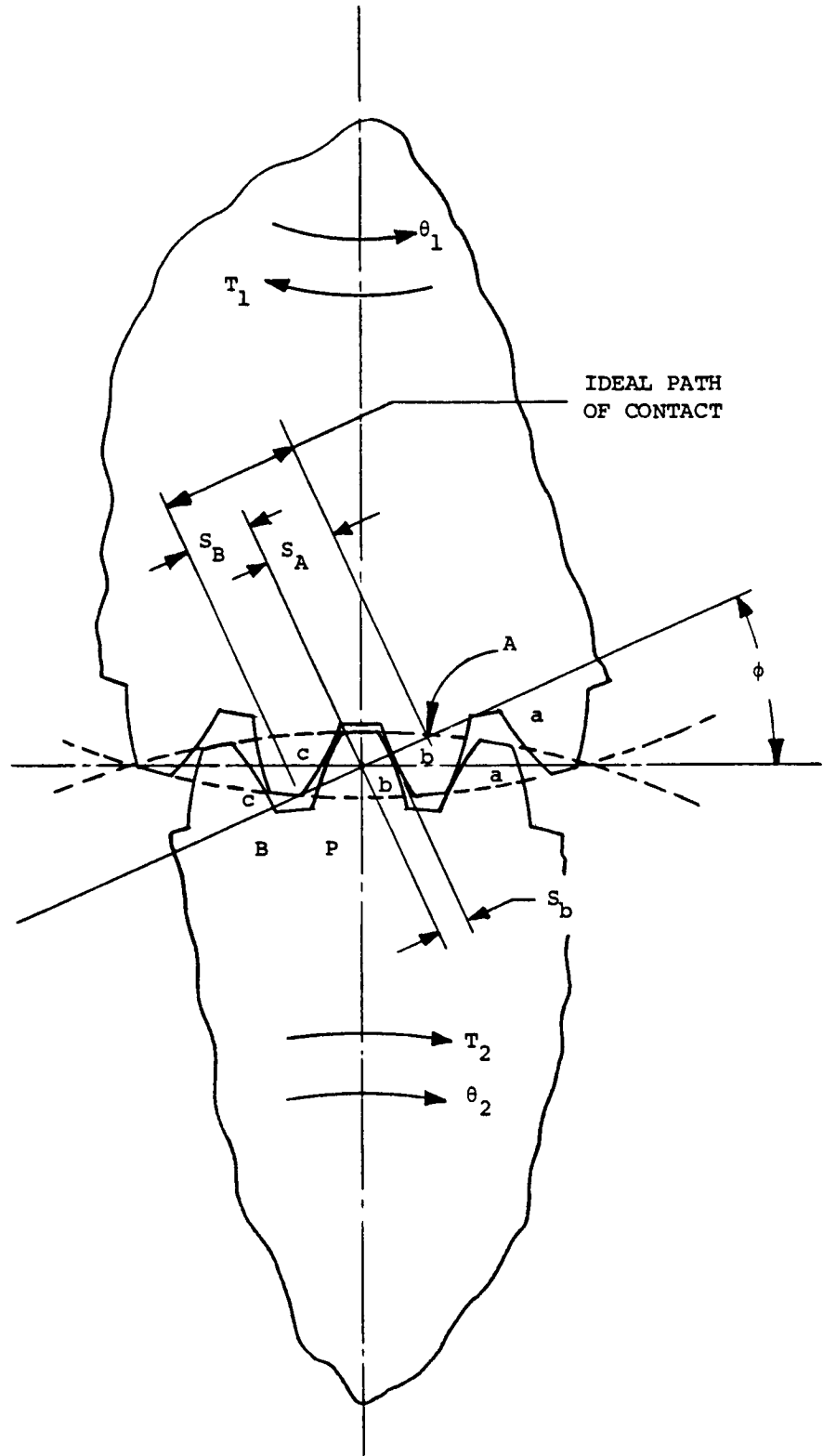


Figure 7 - Two Gears in Mesh

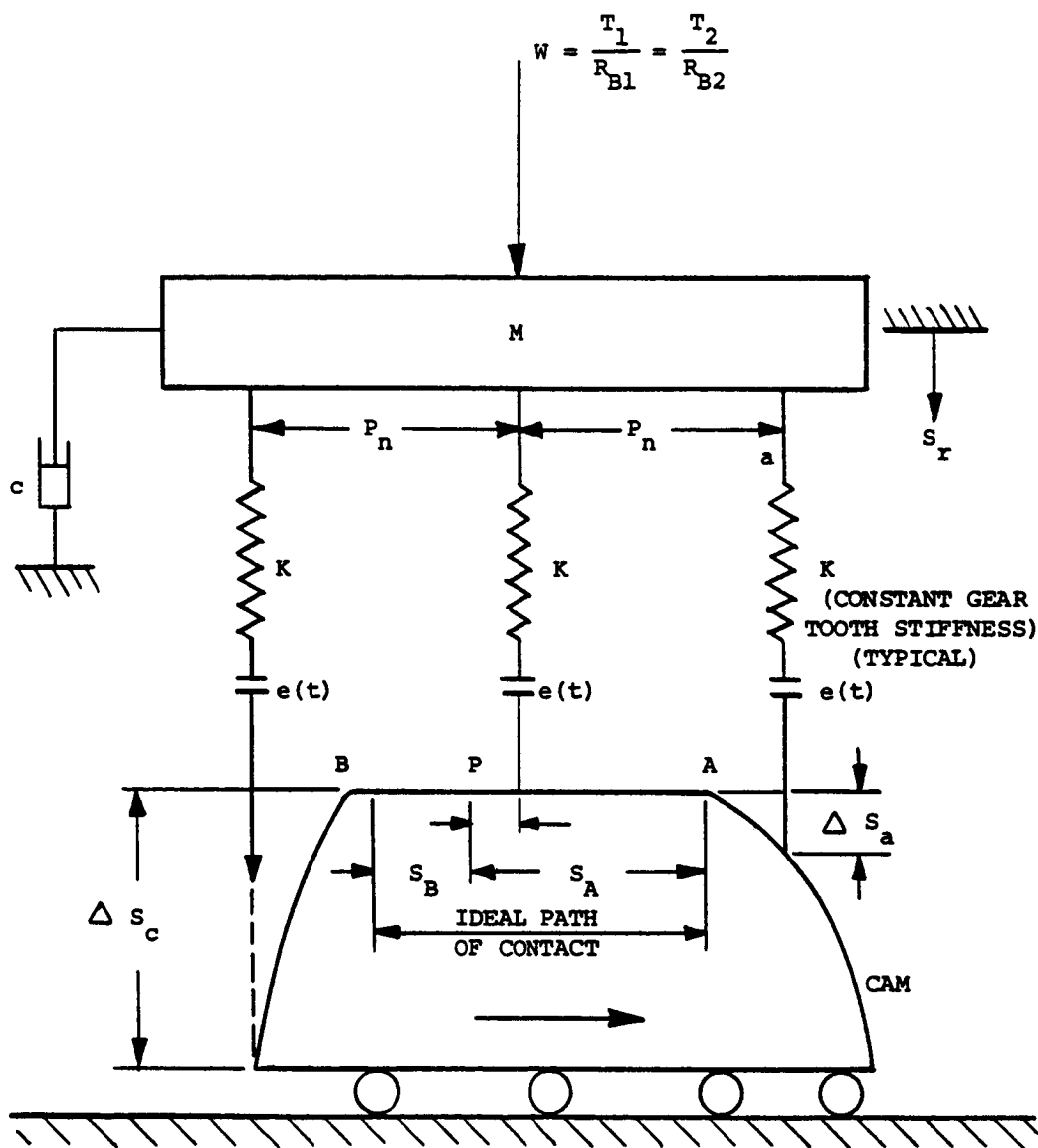


Figure 8 - Richardson's Model

involved.

2. Lightly loaded gears where the errors are much greater than the relative displacement, single tooth action predominating.

Richardson's work, for the most part, substantiated each mode of operation. His equations are presented in such a manner that the only forcing functions acting on the model are error functions; however, his error function did not allow for the condition of tooth separation. It is felt that tooth separation is important in lightly loaded systems.

Kasuba^[9] analyzed heavily loaded gears, and developed a model similar to Richardson, but rather than using a cam and an error to impress displacement upon the spring, he used a simulated engagement error, $s(t)$. His model, after conversion to a spring-mass system, is shown in Figure 9. He also considered a planetary system and used it both for analytical and experimental investigation. For the planetary system he employed the model shown in Figure 10. The model representing the planetary system accounts for the reaction of the system to errors. This is the first attempt to consider system effects. Dynamic load factors found by Kasuba are generally smaller than those obtained previously. He recommended that the actual contact ratio under load should be used. The entire system of gears should be considered when attempting to determine the instantaneous load to which teeth are subjected. Also, the tooth stiffness should be considered a variable accounting for multiple tooth contact.

Bollinger^[10] considered tooth stiffness as a trapezoidal function. Results of the study correlated very well the experimental and analytical work. He found that under different running conditions,

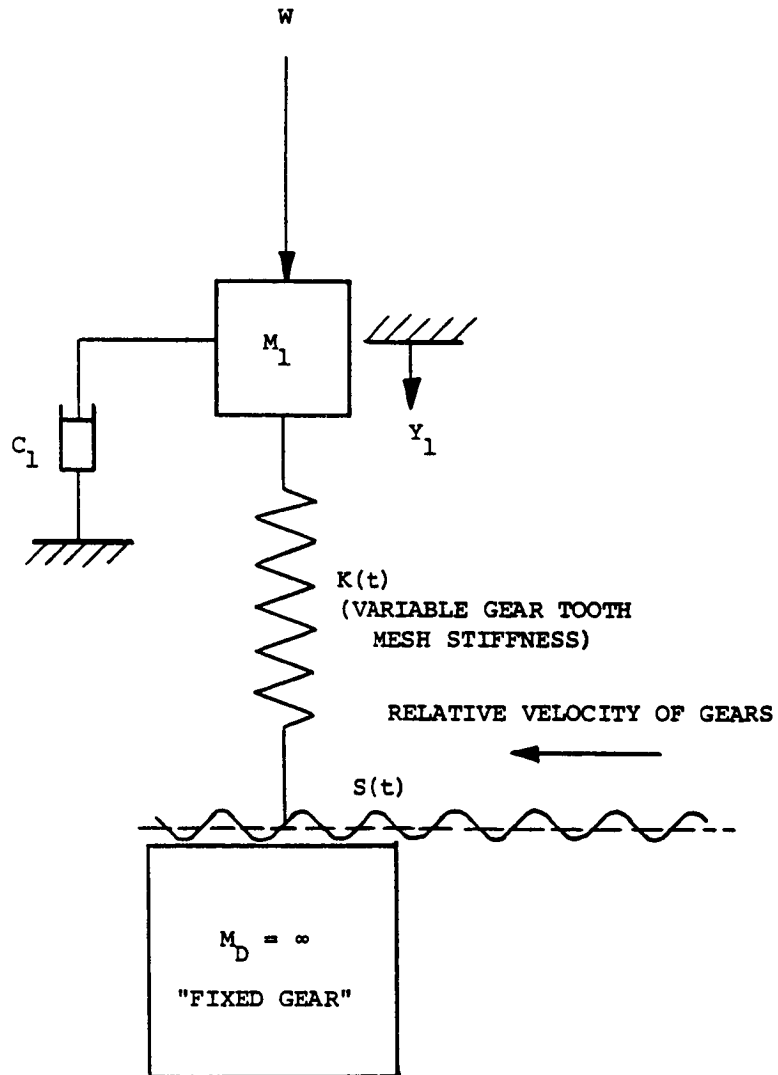


Figure 9 - Kasuba's Single Degree of Freedom Model
Corresponding to a Compound Differential Gear Train Model

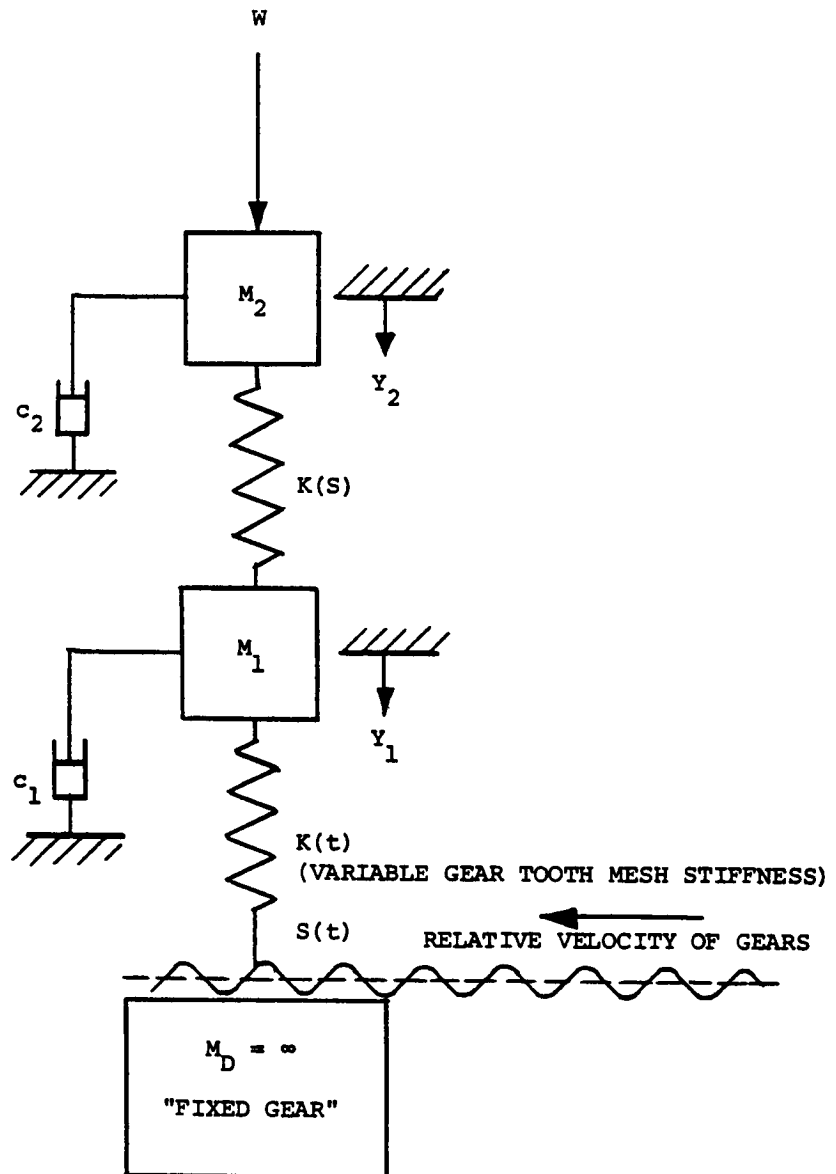


Figure 10 - Kasuba's Two Degree of Freedom Model
Corresponding to a Compound Differential Gear Train Model

the trapezoidal stiffness function for the same pair of gears changed. He determined the stiffness function experimentally and used it in his analytical investigations.

Many investigations have been made to determine the gear tooth deflections. Baud and Peterson^[11] proposed equations for the deflection of gear teeth, considering the tooth as a cantilever beam of variable cross section. Walker^[12] deduced a formula for the deflection of the gear tooth following an experimental investigation carried out on one tooth fixed to a frame. Both investigations assumed the tooth to behave as a cantilever beam fixed to a rigid wheel. Weber^[13] considered the actual shape of the tooth profile in his analysis using strain energy techniques. He accounts for normal, shear, and bending energy in the tooth and a small surrounding area of the gear to which the tooth is considered attached. He also considers Hertzian deformation assuming tooth profile radii of curvature as equivalent cylinders. Attia^[14] expanded Weber's model by including the circumferential deformation of the gear rim, and the deflection of a tooth under the effect of loaded neighboring teeth. Further improvements were made by Cornell^[15] in the treatment of the fillet/foundation deflection. He defined the deflection of three different fillet configurations, whereas previous studies assumed a given fillet angle of 75°. He evaluated the resulting compliance analysis against available test, finite element and exact transformation analyses, and found that the calculated compliance results agreed well with measurements. Premilhat, Tordion and Baronet^[16] determined the elastic compliance through the use of appropriate stress functions resulting from the complex transformation of the tooth profile. Their analysis resulted in a slightly larger

compliance than Weber's analysis. Chabert, Tran and Matis^[17] made yet a different evaluation of stresses and deflection of spur gear teeth by finite element methods. Formulas were developed for a simple calculation of the maximum stresses and compared the results with ISO and AGMA standard formulas for the strength of gear teeth.

Cornell and Westervelt^[18] developed a time history, closed form solution of a dynamic model of spur gear systems. Their analysis determines the dynamic response of the gear system and the associated tooth loads and stresses. The dynamic model is based on Richardson's cam model but treats the teeth as a variable spring. Included in the analysis are the effects of the nonlinearity of the tooth pair stiffness during mesh, the tooth errors, and the profile modifications. The analysis showed that tooth profile modification, system inertia and damping, and system critical speeds can affect the dynamic gear tooth loads and stresses significantly.

Kasuba and Evans^[19] concluded that the gear mesh stiffness in engagement is probably the key element in the analysis of gear train dynamics. Also, the gear mesh stiffness and contact ratio are affected by many factors such as the transmitted loads, load sharing, gear tooth errors, profile modifications, gear tooth deflections, and position of contacting points.

By introducing these aspects, the calculated gear mesh stiffness can be defined as being a variable - variable mesh stiffness (VVMS). The VVMS model is an improvement over the previous periodic varying mesh stiffness which the authors^[19] called fixed - variable mesh stiffness (FVMS).

They developed a large scale digitized gear model including the

VVMS method which investigates in one uninterrupted sequence the static and dynamic conditions.

An iterative procedure was used to calculate the VVMS by solving the statically indeterminate problem of multi-pair contacts, changes in contact ratio, and mesh deflections. The developed method can be used to analyze both normal and high contact ratio gearing.

The associated computer program package calculates the VVMS, the static and dynamic loads, and variations in transmission ratios, sliding velocities, and the maximum contact pressures acting on the gear teeth as they move through the contact zone.

Their findings for typical single stage external spur gear systems are:

1. The gears and the adjacent drive and load systems can be matched for optimum performance in terms of minimum allowable dynamic loads for a wide range of operating speeds.
2. Torsionally flexible design of gear bodies/hubs/rims offers an excellent means of absorbing or minimizing the geometrical errors in mesh.
3. The gear mesh stiffness and its distribution are significantly affected by the transmitted loads and tooth profile imperfections.
4. The dynamic factors can be decreased by increasing the damping and/or contact ratio. Local damping appears to be the most efficient means for decreasing the dynamic load factors.
5. The high contact ratio (HCR) gearing has lower dynamic

loads and peak Hertz stresses than the normal contact ratio (NCR) gearing.

The studies by Kasuba and Evans provide one of the most detailed and advanced models available at this time.

2.2 INTERNAL SPUR GEARS

Buckingham^[1] indicated that there are almost an infinite number of forms which can be used as gear tooth profiles. However, the most common profile for transmission of power is the involute form. He developed the kinematic formulations under which involute gears transmit uniform rotary motion. The constant velocity action between such teeth is called conjugate gear tooth action. Buckingham's formulations of the conjugate gear-tooth action and interference prediction for the internal spur gear are readily applicable for present day use.

Dudley^[20] further pointed out that a comparison between the internal and external spur gear sets assuming the same number of teeth produced the following advantages of the internal spur gear set:

1. Greater length of action.
2. Relative sliding of the teeth at the start and end are less.
3. Center distance is smaller and thus leads to a more compact arrangement.
4. Contact area is larger because of the mating of a concave and convex surface. This increased contact area results in larger resistance to pitting and wear. Also, the distribution of the load among more teeth decreases the intensity of the stress.

An additional advantage is derived because the tooth strength of an internal gear is greater than that of an equivalent external gear.

Dudley acknowledges that there is no AGMA standard covering internal gears. He recommends that the methods of design for the external spur gear may be applied to the internal spur gear. In light

of the obvious advantages of the internal set, it is understandable that the external spur gear design methods would lead to a satisfactory internal gear design. Incidentally, the available methods for external gears that Dudley refers to are primarily based on static analysis of the system. In this study the internal spur gear set will be analyzed from the dynamical point of view.

Dudley also lists several disadvantages to the internal gear set. These disadvantages can be removed by introducing more accurate and, consequently, more costly manufacturing operations.

The first of these disadvantages is tip interference. In this type of interference, the external gear cannot be assembled radially with the internal gear. Only axial assembly is possible. If a shaper cutter having a number of teeth equal to or greater than the external gear is used to cut the internal gear, then it will cut its way into mesh but in so doing will remove some material from the flanks of a few of the teeth that should have been left in place for good tooth operation. This cutting action is also known as "trimming". Such teeth will have poor contact and will tend to be noisy.

The second problem is sometimes known as "fouling". In this case the internal gear teeth interfere with the flanks of the external toothed gear if there is too small a difference in numbers of teeth between the external and internal gears.

The third problem is in the manufacture of internal gears.^[21] The necessity for the generating tool to work within the gear body restricts cutter and machine dimensions, which in turn limits tool accuracy, rigidity and the resultant precision. Finish grinding of the teeth is especially difficult because of the large size of the grinding

wheel. Generally, internal gear sets are not used for precision gear trains unless the applications must utilize their unique internal features as an advantage. Examples of such applications are indicated in Section 1.1, "General Remarks".

Clearly, any detailed investigation of the ISG drives, such as this thesis work, must consider the previously mentioned findings and recommendations by Buckingham and Dudley. However, the above findings must be used in conjunction with the modern thinking of gear behavior as was indicated in the literature search for external gears. This modern thinking must include consideration of the elastic deformation of the internal gear teeth and their supporting ring structure, and dynamic analysis of the system.

To date, the number of investigations related to the elastic analysis of the internal spur gear teeth and the supporting ring are limited.

Karas^[22] was the first to evaluate the deflection of the internal spur gear tooth due to bending, shearing and Hertzian contact deformation. He assumed a trapezoidal shape for the tooth profile and a rigid support at the root. He did not consider any deformation of the supporting ring. Ishikawa^[23] regarded the root of the gear tooth as a semi-infinite body, and then calculated the deflection due to the tooth rotation at the root of the gear tooth. He also did not consider the deformation of the ring. Hidaka^[24] superimposed the above four deflections into one final tooth deflection. He then compared this deflection against a finite element representation of the tooth and portions of the ring. The boundaries of the ring portions were then fixed against translation or rotation. He concluded that the results of his four deflection relations and the finite element analyses were

similar. Thus, he decided to use the four relations for deflection due to bending, shear, Hertzian contact stress and rotation at the root in the analysis of planetary spur gear systems.

The first treatment of the ring gear deflection was by Sinkevich.^[25] He replaced the ring gear with a perfect ring having an equivalent stiffness. The equivalent thickness was expressed as a function of module/diametral pitch, whole depth of the tooth, backlash and the number of teeth.

Hidaka^[24] later compared Sinkevich's relations against a finite element representation of the ring. He treated the deflection as a plane stress problem using different finite element mesh sizes and different thickness. Having arrived at an optimum mesh size and thickness he then modified Sinkevich's deflection relations based on the equivalent thickness concept. However, Hidaka's final relations for ring deflection are not applicable to the present ISG ring gear deflection investigations due to the following reasons:

1. His investigation is for a planetary gear system in which the loading is symmetric around the circumference. The ISG drive has a single point loading.
2. He assumed thin ring relations (i.e., thickness over radius ratio $< 1/10$). In many cases the ring gear of the ISG drive is a thick ring.

Hidaka also points out that the finite element method of solution for the deflection of gear teeth requires a finely meshed model. This approach can quickly exhaust the capacity of the computer.

Because of the limited available information for deflections of the ISG drives, the author of this thesis decided to utilize the

applicable and proven methods for determining the stiffness of external gearing systems to the ISG drive. The work by Weber^[13] and Attia^[14] on external gear teeth and hubs will be adapted to the internal tooth profile and then will be used as a basis for comparison of results.

CHAPTER III

ANALYTICAL INVESTIGATION3.1 PROBLEM FORMULATION

A comprehensive analysis of the dynamic loading in internal spur gear (ISG) drives presents a difficult task even under ideal geometry conditions because of the continuously changing interactions as the gears move through the meshing cycle. Further complications arise when the gear tooth deflections, backlash, profile errors and multiple gear tooth pair loading are introduced. The complexity of the meshing process can be illustrated by following the action of the teeth through one complete mesh cycle. Figure 11 shows the two gears at the start of the cycle where the driver engages the driven tooth at its tip. Under load the teeth deform to a noninvolute shape which changes the line of action and, thus, the loading between the teeth. Other in-plane deformations, both tangential and radial, take place in the tooth support structure, the adjacent teeth and the remaining drive train. Figure 12 depicts this deformed condition. If the deflection continues, then contact will be made between another tooth pair and an indeterminate load sharing condition is entered. Backlash or a tooth that is too thin increases the deflection slightly but in general decreases the chance of multi-tooth contact. A tooth that is too thick leads to premature engagement and jamming between teeth. A pit in the profile can cause sudden disengagement and subsequent clashing between teeth.

As the driver pushes through the mesh cycle, the loading changes from root to tip contact and finally disengagement. The unloaded teeth will regain almost all of their original shape immediately, and then completely as additional teeth become unloaded. A typical combined stiffness pattern for error free teeth is shown in Figure 13. This periodically repeating pattern will be distorted by identical profile errors in the teeth. The nonlinear dynamic process leads to instantaneous load fluctuations in the teeth even in the presence of constant external load conditions. Also, the magnitude of the load and the fluctuations are influenced by the damping effect of the lubricant, and the proximity of component natural frequencies with any of the forcing frequencies. Figure 22 shows a practical internal gear drive system model used in this study.

Having thus identified the physical problems it can be stated here that adequate mathematical tools are available for their solution. However, the capacity of the present large scale digital computers and the scope of this investigation are such that certain limitations must be imposed on the treatment of the problem. These limitations or assumptions are treated next.

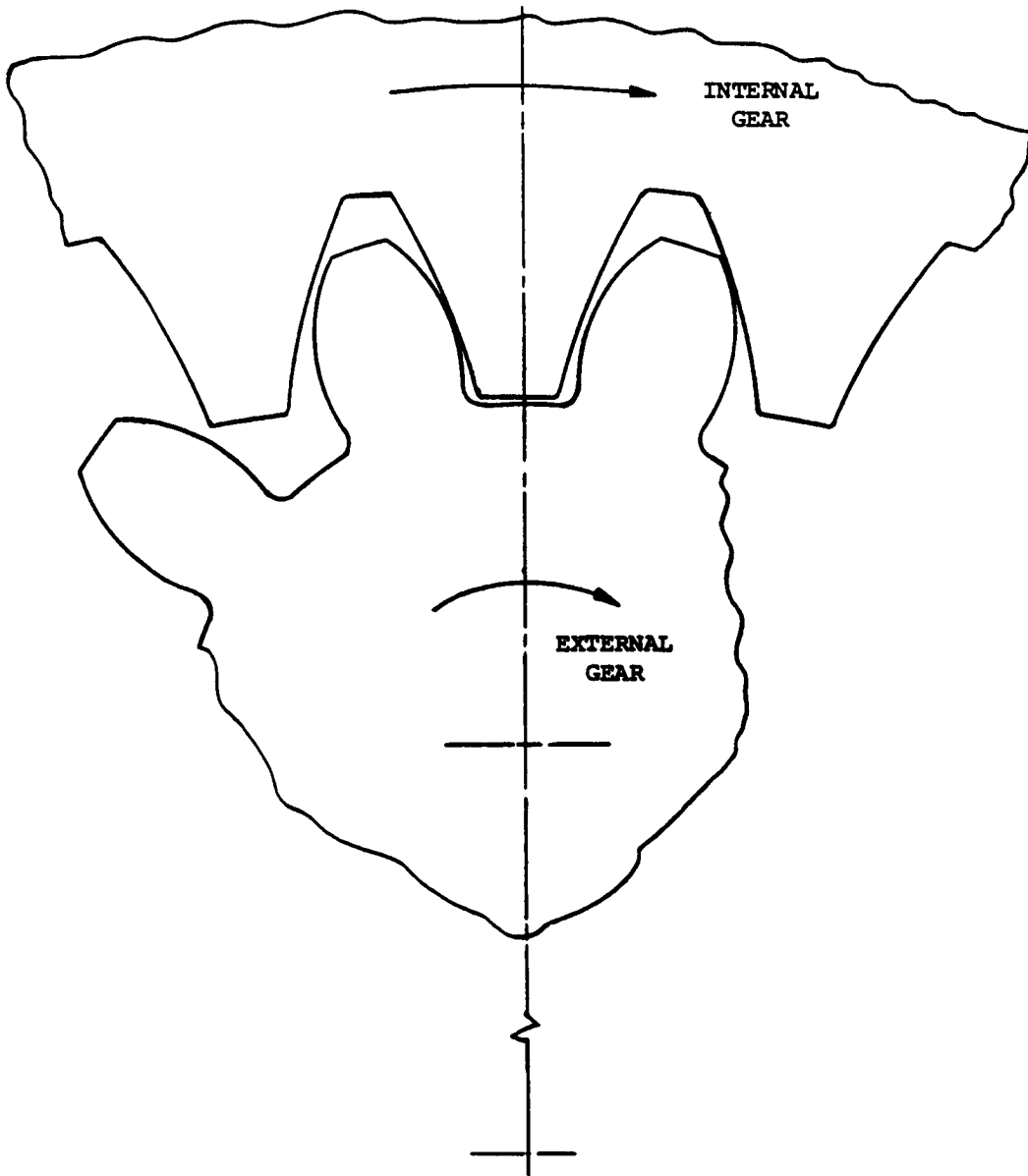


Figure 11 - Internal-External Gears at Start of Mesh Cycle Under No-Load

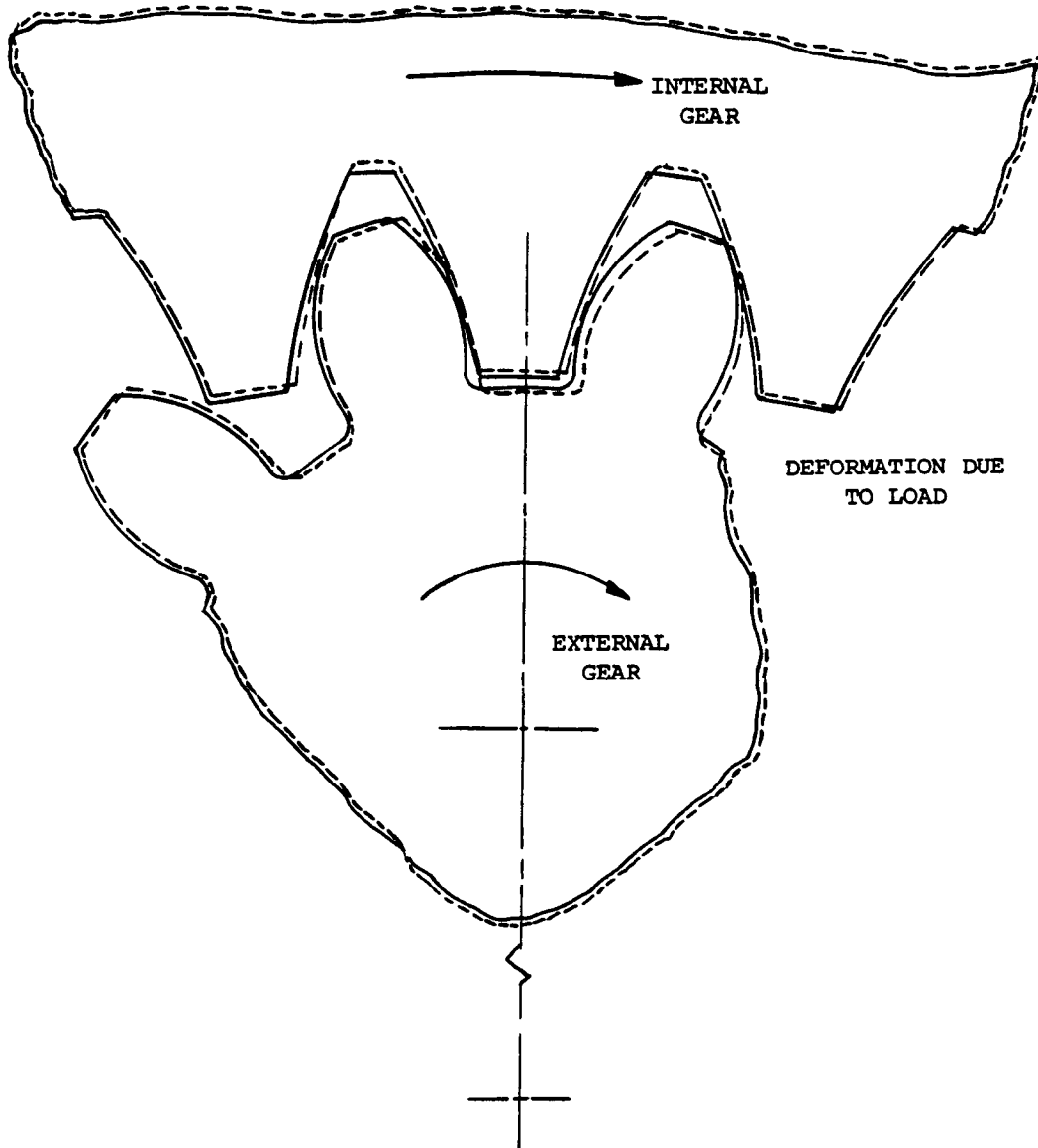


Figure 12 - Internal-External Gears Under Load

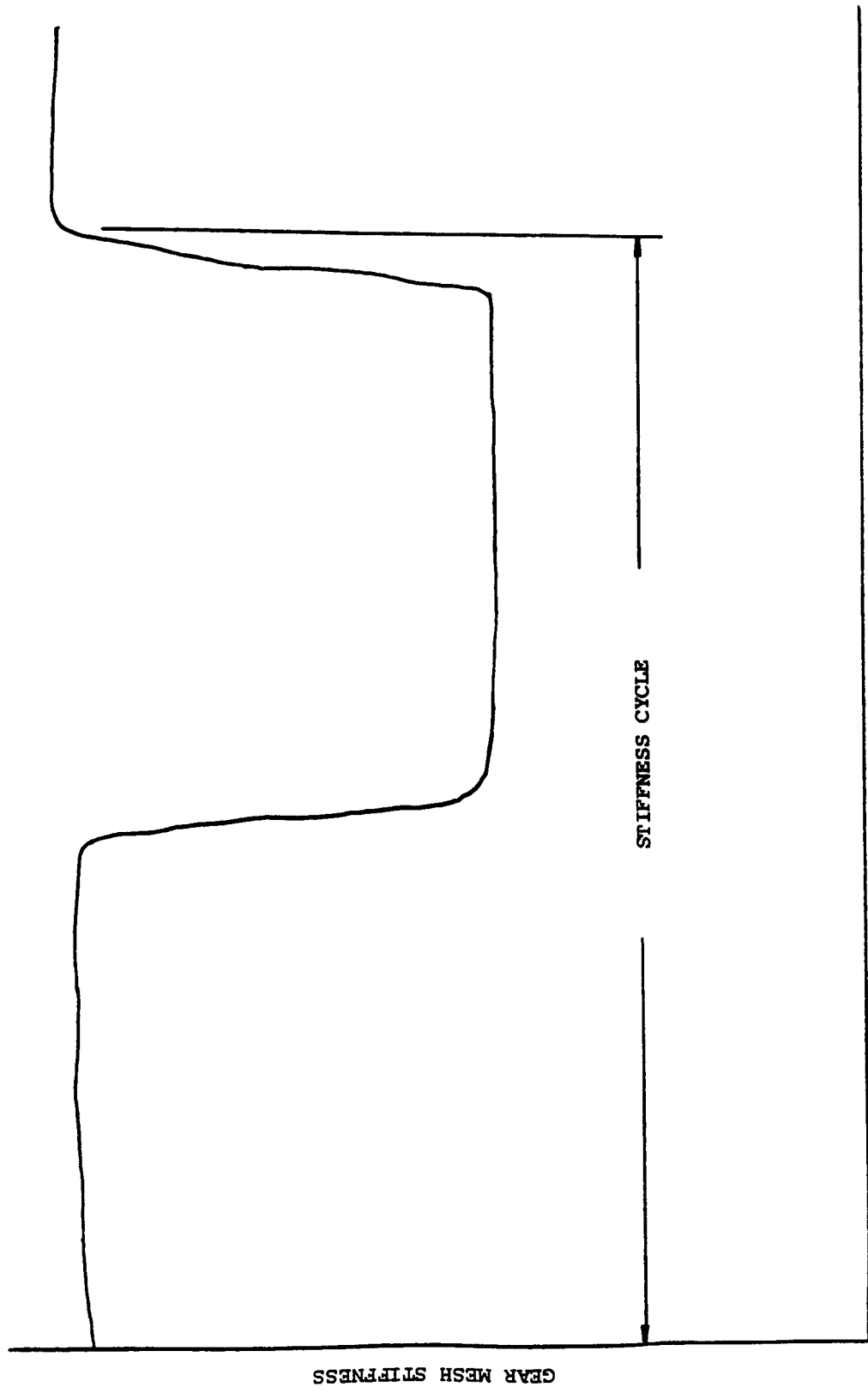


Figure 13 - Combined Stiffness Pattern of External-Internal Spur Gears

3.2 ASSUMPTIONS

The following simplifying assumptions and conventions are used to make the analysis manageable and still realistic:

1. The dynamic process is defined in the rotating plane of the gears. The torsional stiffness of the shafts and gears in engagement, and their masses are acting in the plane. This assumption is considered realistic because of the symmetry of the rotating axes. Also, the out-of-plane twisting and misalignment are prevented by proper design and careful assembly procedures.
2. Damping due to lubrication of gears and bearings are expressed as constant damping coefficients. Their effect on the load dynamics is investigated by parametric studies.
3. The dynamic process is investigated through several complete engagement or mesh cycles.
4. The differential equations of motion are expressed along the instantaneous rather than the theoretical line of action of the teeth which permits evaluation of noninvolute action.
5. The deformations of the tooth support structure and shafting are determined from equations which were developed in solid mechanics for simple shapes. For more complicated shapes the deformations have to be determined experimentally or by finite element techniques. The computer program is structured so that the deflection values from experiment or finite

element analysis can be entered into the analysis process by means of data sets.

6. Multi-tooth contact is determined by analyzing five gear tooth pairs. The central or middle tooth is used to establish the instantaneous position of the teeth and monitor their progress through a complete mesh cycle.
7. The presence of backlash may lead to tooth separation under dynamic conditions which must be accounted for in the analysis methodology.

3.3 METHOD OF SOLUTION

The purpose of this investigation is to develop an analytical method for determining the static and dynamic behavior of the ISG drive. In order to obtain dynamic information, it is first necessary to get the static supporting data. For this reason, it has been convenient to divide the investigation into static and dynamic sections. In each section, the appropriate analytical model is comprised of relations available from references in gearing, strength of material, mathematics, vibration analysis, and the publications on deflections by Weber, [13] Attia, [14] etc. In the interest of timely solutions, an attempt was made to solve for the required information directly. Where this was not possible, iterative search techniques and numerical solutions, along with suitable acceptance criteria, were substituted.

The developed analytical methods were combined in a sequence of digital computer programs which can be used on a large scale computer like the IBM 370/158 at Cleveland State University (CSU). For parametric studies, the program can be used more efficiently in three parts (modules). The first module determines the static information and stores it on a tape. The second module uses the static data to initiate the dynamic solution and then solves for the dynamic information. The third module calculates the static or dynamic tooth bending stress at the critical fillet location. In a similar fashion, the program can be further subdivided for incorporation on a mini-computer like the Hewlett-Packard 1000.

The next three sections of this report present a detailed development of the static and dynamic analysis procedures as well as a summary description of the computer program. For reference purposes, Appendix A and B contain all of the standard equations which were utilized in this investigation. Appendix C contains the computer program listings.

3.4 STATIC ANALYSIS

The task of the Static Analysis Procedure is twofold. First, it must provide all of the supporting and final information needed from a static analysis of a gear system. The analysis procedure must be structured so that the desired information is obtained efficiently. Some of the structural requirements and the needed information can be identified as follows:

1. A suitable nomenclature for documentation and computer use.
2. Suitable local and global coordinate systems.
3. External and internal gear tooth profiles.
4. Contact points between gear tooth pairs.
5. Line of action.
6. Contact ratio.
7. Interference conditions.
8. Deflection and stiffness of the teeth and their supporting structure.
9. Load sharing among neighboring teeth.
10. Sliding action between mating teeth.
11. Static load per tooth pair.

Second, the static analysis must file this information for use in the dynamic and stress analyses, and for printing of selected portions of this information.

3.4.1 Nomenclature

The nomenclature for the static and dynamic analysis has been selected from symbols used in gearing, strength of materials, mathematics and publications by Weber, Attia, etc. When the required

symbols were not available from these sources, special symbols were introduced to describe the particular parameters in short form.

3.4.2 Local and Global Coordinate Systems

Three Cartesian coordinate systems are employed in the static analysis. The first is a local system using the symbols X and Y. It has its origin at the root of each tooth. The Y-axis coincides with the tooth centerline. In all, there are ten such X-Y local coordinate systems to account for five gear tooth pairs under investigation in each gear. Transformation from one tooth coordinate in a given gear to another tooth is readily possible because of the fixed geometric relation between the teeth. These local tooth coordinate systems are used to define the discrete tooth profile locations and appropriate deflections of the teeth.

The coordinates of the second system are labeled W and Z. These systems are local to each gear and rotate with the gear. Each W-Z coordinate system is parallel to its respective X-Y system. There are ten W-Z coordinate systems also. The Z-axis coincides with the tooth centerlines.

The third system is global and fixed at the center of the internal gear. This system is identified as the U-V system. The arrangement of the three coordinate systems is shown in Figure 14. The transformations between the coordinate systems for each gear pair are:

$$W1(I) = X1(I)$$

$$W2(I) = -X2(I)$$

$$Z1(I) = RRO1 + Y1(I)$$

$$Z2(I) = RRO2 - Y2(I)$$

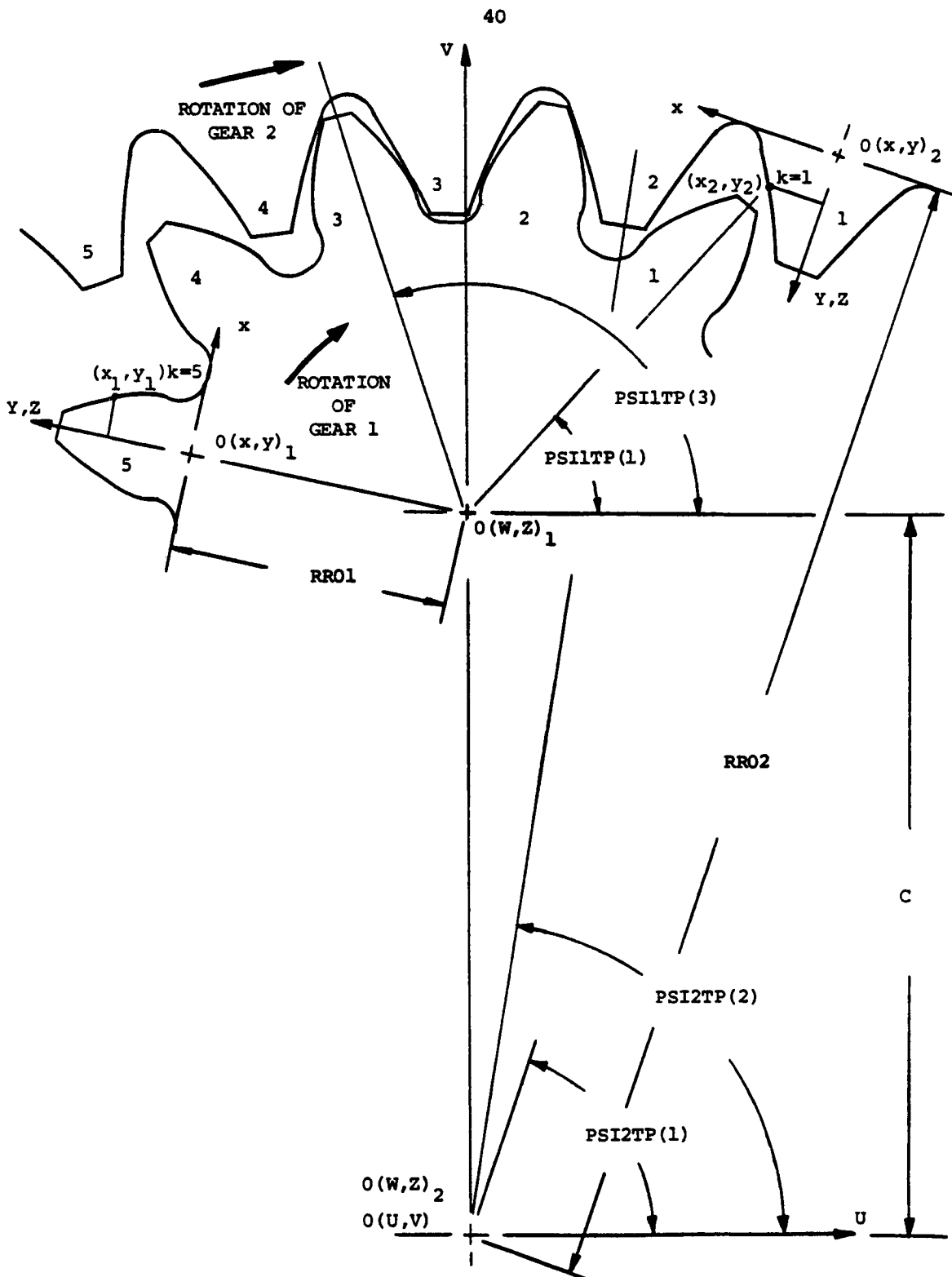


Figure 14.- Internal-External Gear Tooth Coordinate System

$$\begin{aligned}
 U1(I) &= W1(I) \times \text{SIN}[\text{PSI1TP}(I)] + Z1(I) \times \text{COS}[\text{PSI1TP}(I)] \\
 V1(I) &= -W1(I) \times \text{COS}[\text{PSI1TP}(I)] + Z1(I) \times \text{SIN}[\text{PSI1TP}(I)] \\
 &\quad + C \\
 U2(I) &= -\{Z2(I) \times \text{SIN}[\text{PSI2TP}(I) - 0.5\pi] - W2(I) \times \\
 &\quad \text{COS}[\text{PSI2TP}(I) - 0.5\pi]\} \\
 V2(I) &= Z2(I) \times \text{COS}[\text{PSI2TP}(I) - 0.5\pi] + W2(I) \times \\
 &\quad \text{SIN}[\text{PSI2TP}(I) - 0.5\pi] \qquad \dots(7)
 \end{aligned}$$

where

I = gear pair 1 through 5

1 = external gear

2 = internal gear

3.4.3 External and Internal Gear Tooth Profiles

Development of the involute profile of a tooth follows well known geometric relations which are shown in Appendix A for convenient reference. Also shown in Appendix A are construction of the involute profile, and the respective external and internal local and global coordinates of the computer program.

In actual practice, deviations from the theoretical involute profile are introduced because of manufacturing tolerances, errors and by intent. A fourth potential source of modification is due to damage during operation. The intentional modifications are introduced to overcome the detrimental effects of profile deviations and tolerances in the remaining system. As a rule, gears are fabricated with backlash on their teeth. Additional modifications are made to the tip to improve engagement between mating teeth, and to the root to avoid interference. Damage during operation exhibits itself as local burnishing, pits or spalling. The condition of a tooth profile can be

determined by means of a gear checker. This machine follows the tooth surface as the gear is rolled off its base circle. A moving pen and chart instrument then draws the profile as a function of the roll angle. A true involute produces a straight line and any deviation from this line is indicative of the degree of modifications and/or faults.

Thus, it is customary in gear analysis to define the profile modifications and errors by means of a profile chart. Figure 15 illustrates the relationship of the profile and involute chart for the external spur gear tooth. As indicated before, the profile modification of the tip deviates from the straight line of the true involute. A similar chart holds for the internal spur gear tooth. Figure 16 depicts samples of possible tooth profile modifications which can be used alone or in combination to simulate a large number of practical cases. Various profile modifications for the external and internal tooth are shown in Figures 17 and 18 respectively.

Analytically, the profile modifications can be expressed by means of a product consisting of the maximum amplitude of the modification and an appropriate shape function. This shape function uses the roll angle as the independent variable which can be structured so that the straight-line, parabolic, sinusoidal and pit like modifications of Figure 16 are faithfully represented. In this manner, the surface faults of a particular profile are combined with the true involute profile, as developed in Appendix A, to simulate the actual tooth shape. The X-Y coordinates of such a tooth profile from the tip to the beginning of the fillet are defined by the following general expression:

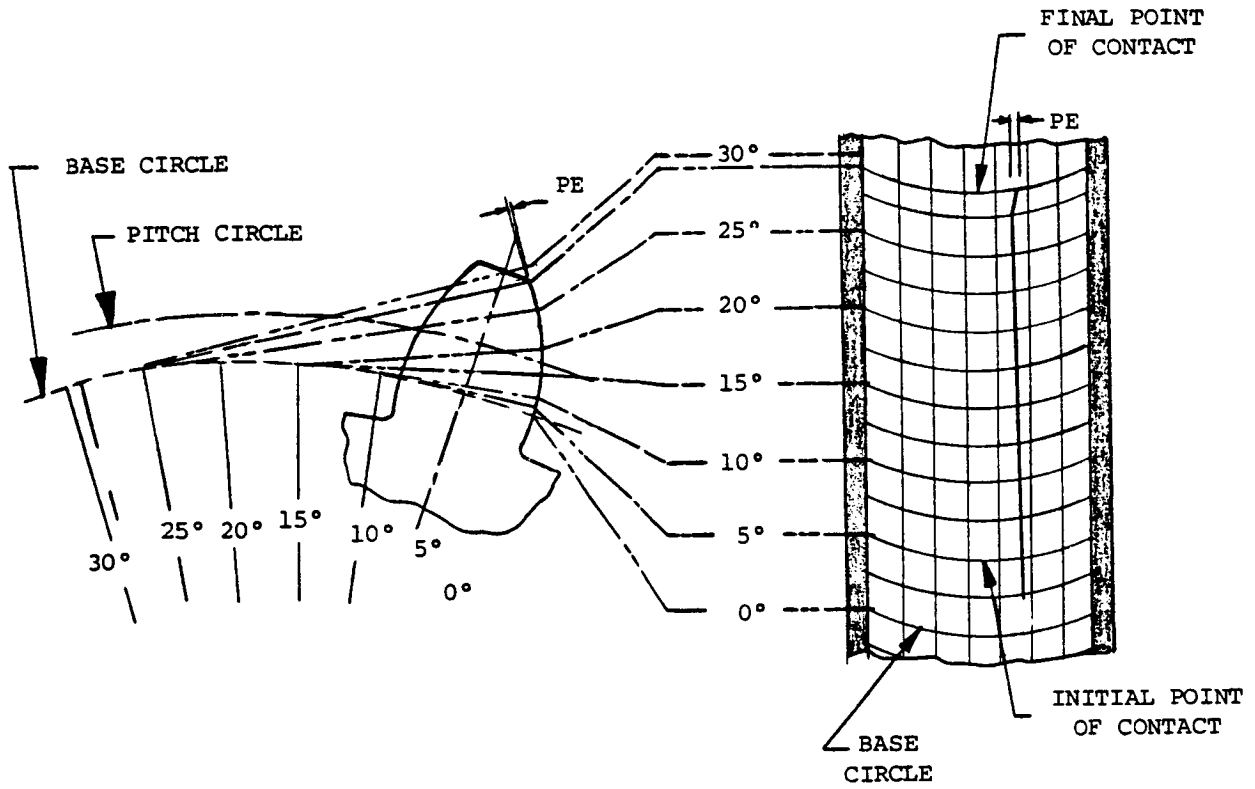


Figure 15 - Involute Chart - Profile Relationship

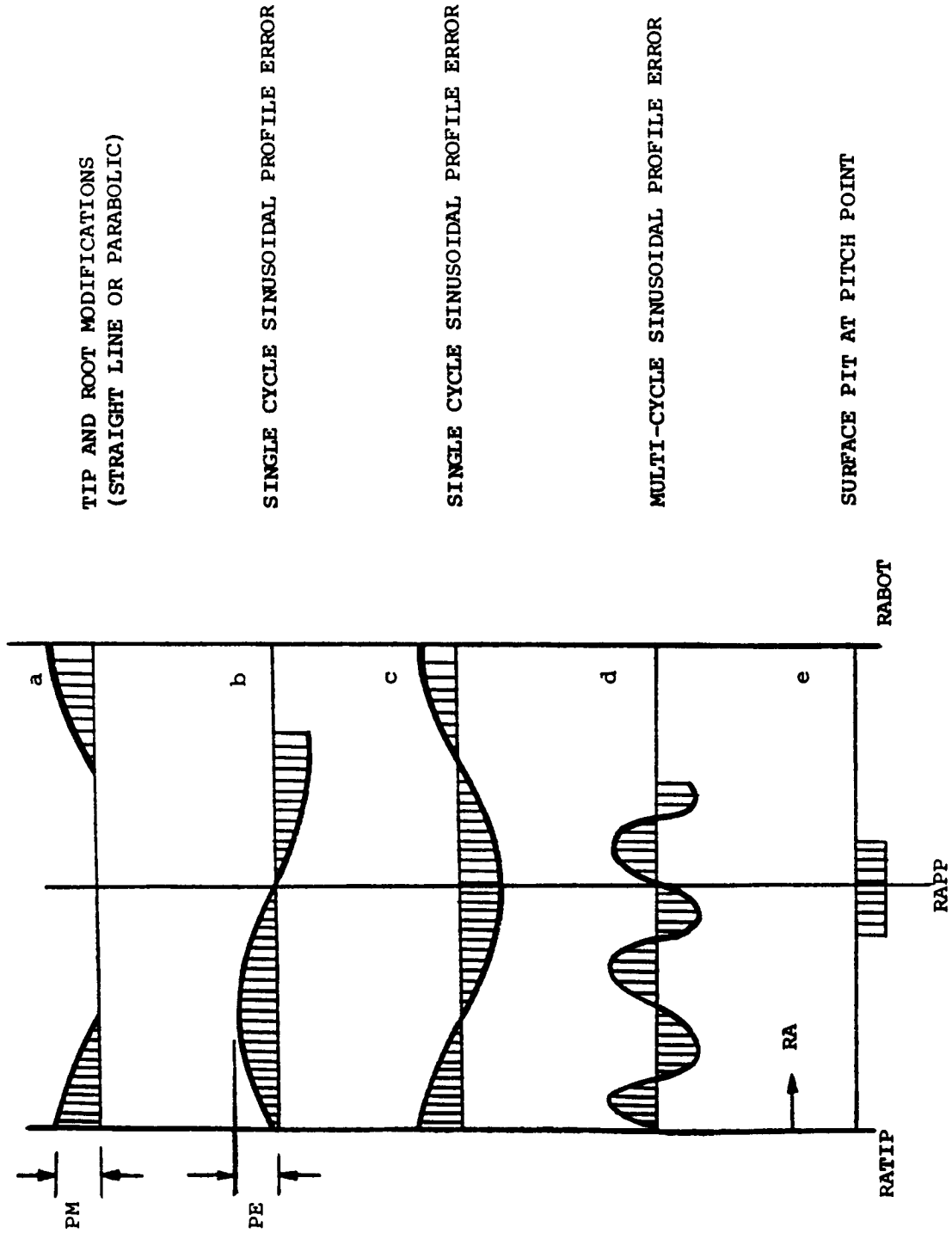


Figure 16 - Sample Simulated Gear Tooth Profile Charts

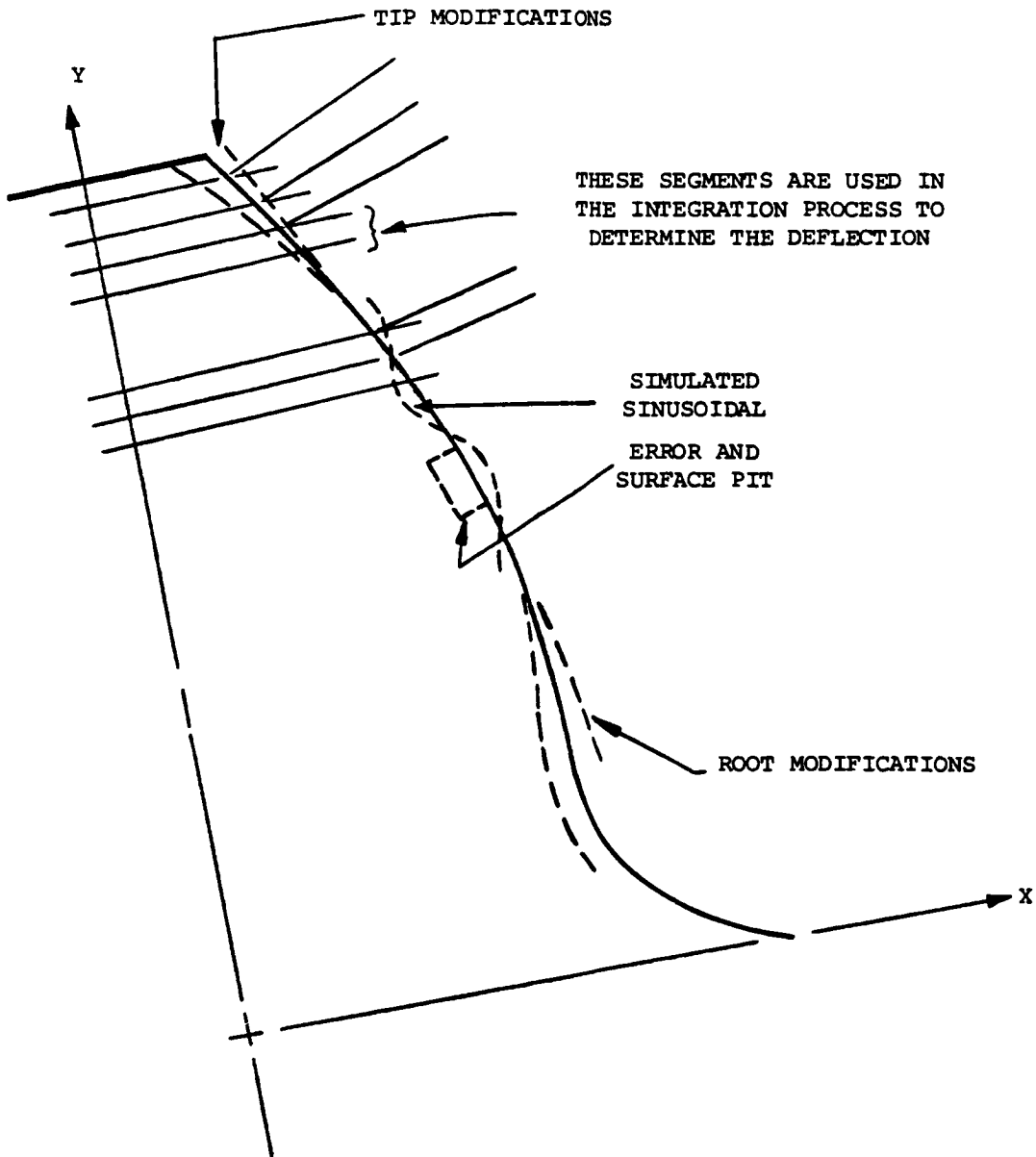


Figure 17 - External Gear Tooth Profile Model

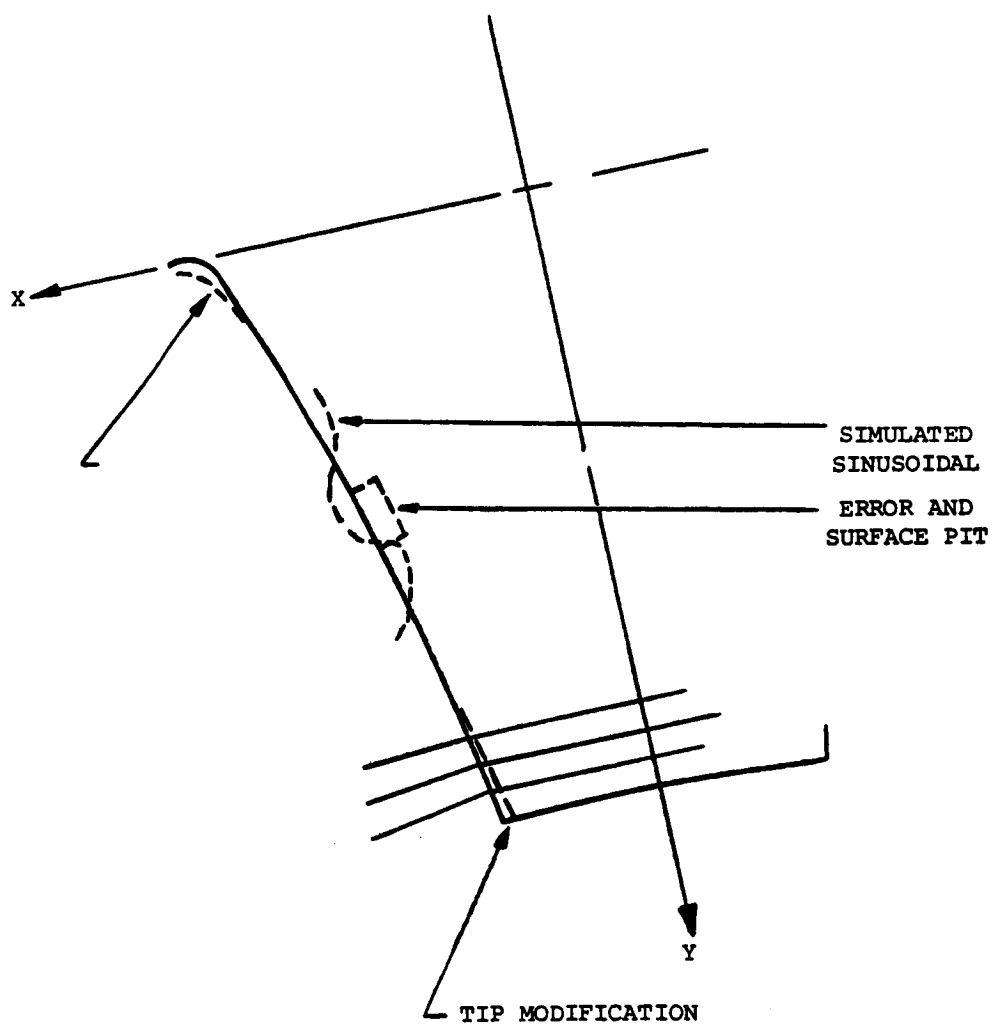


Figure 18 - Internal Gear Tooth Profile

External Tooth (subscript 1 omitted)

$$\begin{aligned}
 X &= R \sin\beta \pm \frac{STTM}{\cos\theta} \left[\frac{RA - RAM}{RATM} \right] \pm \frac{PATM}{\cos\theta} \left[1 - \left(\frac{RAT - RA}{RATM} \right)^{\frac{1}{2}} \right] \\
 &\pm \frac{PER}{\cos\theta} \sin \left[\pi(RAM - RA) \frac{CYC}{RATIP} + PAP \right] - DEEP \\
 &\pm \frac{STBM}{\cos\theta} \left[\frac{RA - RAN}{RABM} \right] \pm \frac{PABM}{\cos\theta} \left[1 - \left(\frac{RA - RABI}{RABM} \right)^{\frac{1}{2}} \right] \\
 Y &= R \cos\beta - RRO \qquad \dots(8)
 \end{aligned}$$

Internal Tooth (subscript 2 omitted)

$$\begin{aligned}
 X &= -\left[R \sin\beta \pm \frac{STTM}{\cos\theta} \left[\frac{RA - RAM}{RATM} \right] \pm \frac{PATM}{\cos\theta} \left[1 - \left(\frac{RAT - RA}{RATM} \right)^{\frac{1}{2}} \right] \right. \\
 &\pm \frac{PER}{\cos\theta} \sin \left[\pi(RAM - RA) \frac{CYC}{RATIP} + PAP \right] - DEEP \\
 &\left. \pm \frac{STBM}{\cos\theta} \left[\frac{RAN - RA}{RABM} \right] \pm \frac{PABM}{\cos\theta} \left[1 - \left(\frac{RABI - RA}{RABM} \right)^{\frac{1}{2}} \right] \right] \dots(9)
 \end{aligned}$$

where

STTM = magnitude of straight line modification at tip

RA = roll angle

RAM = roll angle at end of modification at tip

RATM = length of tip modification in degrees of roll

PATM = magnitude of parabolic modification at tip

PER = maximum profile error

CYC = number of sinusoidal error cycles

RATIP = roll angle from end of modification to roll
angle at the pitch point

PAP = angle from start of sinusoidal error to start
of involute

DEEP = depth of pit

STBM = magnitude of straight line modification at bottom

PABM = magnitude of parabolic modification at bottom

RABM = length of root modification in degrees of roll

RABI = roll angle at the bottom of involute

RAN = roll angle at end of modification at bottom

and the remaining parameters are defined in Appendix A. In the computer program, the tooth profile is represented by a finite number of points. The spacing between points is selected so that the segment between two points can be represented by a straight line. Depending on the size of the tooth, either one or two hundred points are used.

Thus by specifying the appropriate parameters any profile configuration of Figures 17 and 18 can be represented by equations (8) and (9) in digital form. The development of the fillet coordinates is shown in Appendix A.

3.4.4 Contact Points Between Gear Tooth Pairs

The location of the contacting gear teeth and the number of contacting gear tooth pairs cannot be determined directly by analytical means because of the possible presence of tooth modifications and the deformation of the loaded teeth. However, it is possible to determine the line of action, and initial and final points of contact of teeth with true involute profiles. Figure 19 shows the arrangement for an external-internal gear pair. The theoretical initial and final points of contact as shown in Figure 19 are used in this investigation as the starting points for a two step iterative search of the actual contact points as the gears rotate through a complete meshing cycle. The search for this actual contact considers first the unloaded (rigid body) motion of the gears and then repeats this search again while the gears rotate under load:

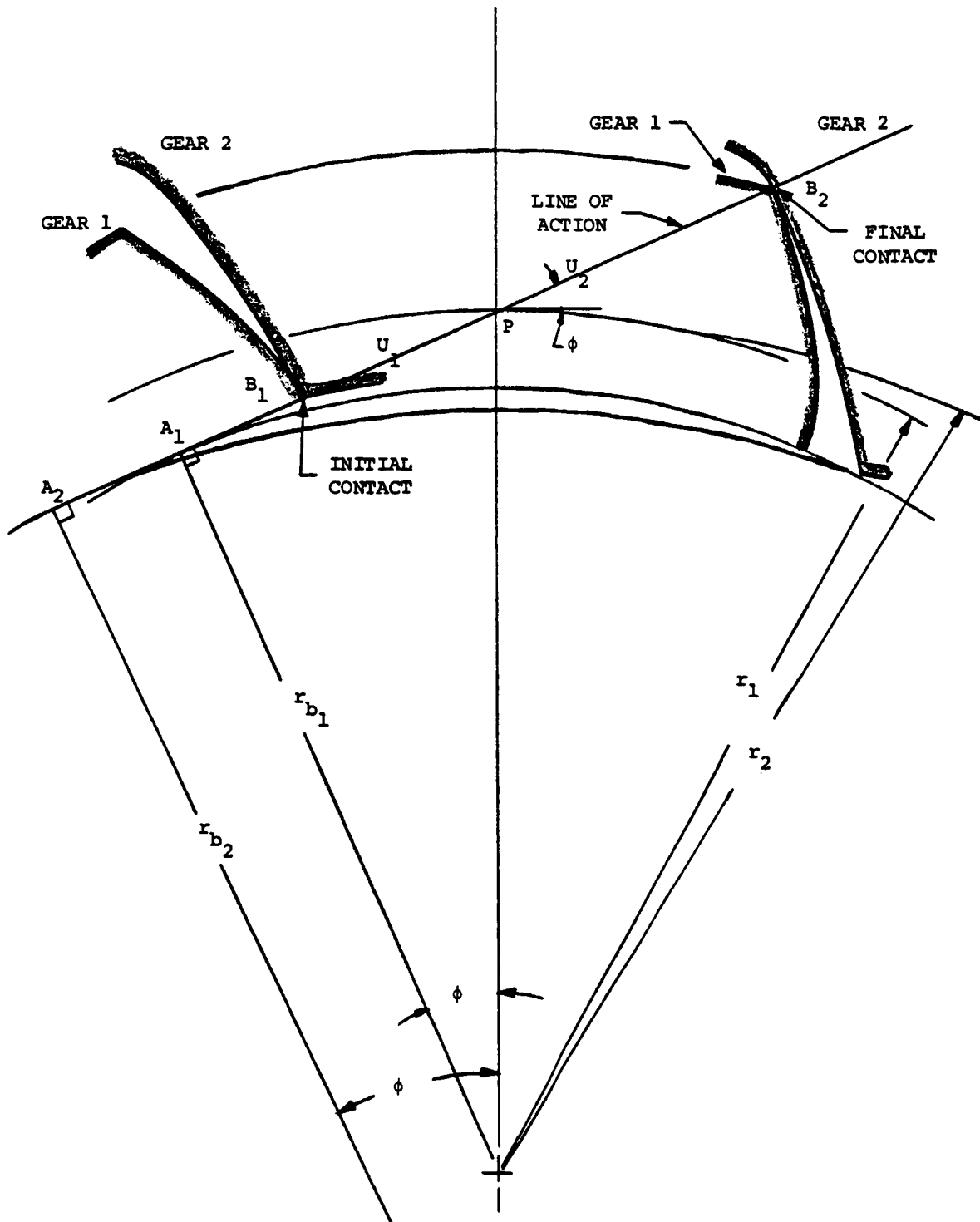


Figure 19 - Initial and Final Points of Contact, and Line of Action of an Involute External-Internal Gear Pair

Step One - Rigid Body Motion

1. Transfer the local X-Y coordinates of the digitized tooth profiles to the rotating W-Z and global U-V coordinates. This transfer fixes the tooth (assumed to be the third of five) unto the respective gear and establishes the geometric arrangement between the two gears.
2. Determine the theoretical initial and final points of contact from the standard gear relations of Appendix A and the geometric arrangement of the two gears as shown in Figure 19.
3. The theoretical initial and final position of the center of the tooth are determined. The angular arc between the two angles is divided into forty-nine equal intervals. Since the true and actual positions of contact for modified involute profiles may differ, it is necessary to search for these positions. This search is accomplished by rotating each gear several intervals counter clockwise and then the proximity of each profile point of gear 1 and 2 is compared. When the proximity of any profile points of gear 1 and 2 fall within the specified acceptance criterion of $|.0025|$ mm then actual contact is considered to be made. This search is performed at the initial and final point of contact. The angular arc is again determined and divided into forty-nine intervals. This new interval is used as the angle with which the gears will be rotated in forty-nine increments resulting in one complete mesh cycle. When the proximity of any

profile point is not acceptable, then the two gears are rotated clockwise a fraction of an interval and a new comparison is made until contact is found. For unloaded teeth with true involute profiles, the contact occurs near the theoretical point of contact. For modified profiles, this search may continue beyond the original theoretical point of contact. In Figure 20, the distance $U_{11} - U_2(L)$ represents the closest distance between the tip of the internal gear tooth and end of the involute profile of the external gear tooth. The point U_{11} is determined from the surrounding profile points and by using the relation between similar right triangles:

$$U_{11} = \frac{V_2(L) - V_1(J)}{V_1(J+1) - V_1(J)} [U_1(J+1) - U_1(J)] + U_1(J) \quad \dots(10)$$

The final contact position is determined in a similar fashion except here the tip of the external gear tooth and the end of the involute profile of the internal gear tooth are in contact.

4. The initial and final tooth center position of tooth number one is determined by subtracting two circular pitches from the angular position of the third gear tooth center. Incrementing in integral values of a circular pitch results in initial and final positions of teeth two through five. At this point the unloaded initial and final positions of all five teeth of the internal and external gear are established, and tooth

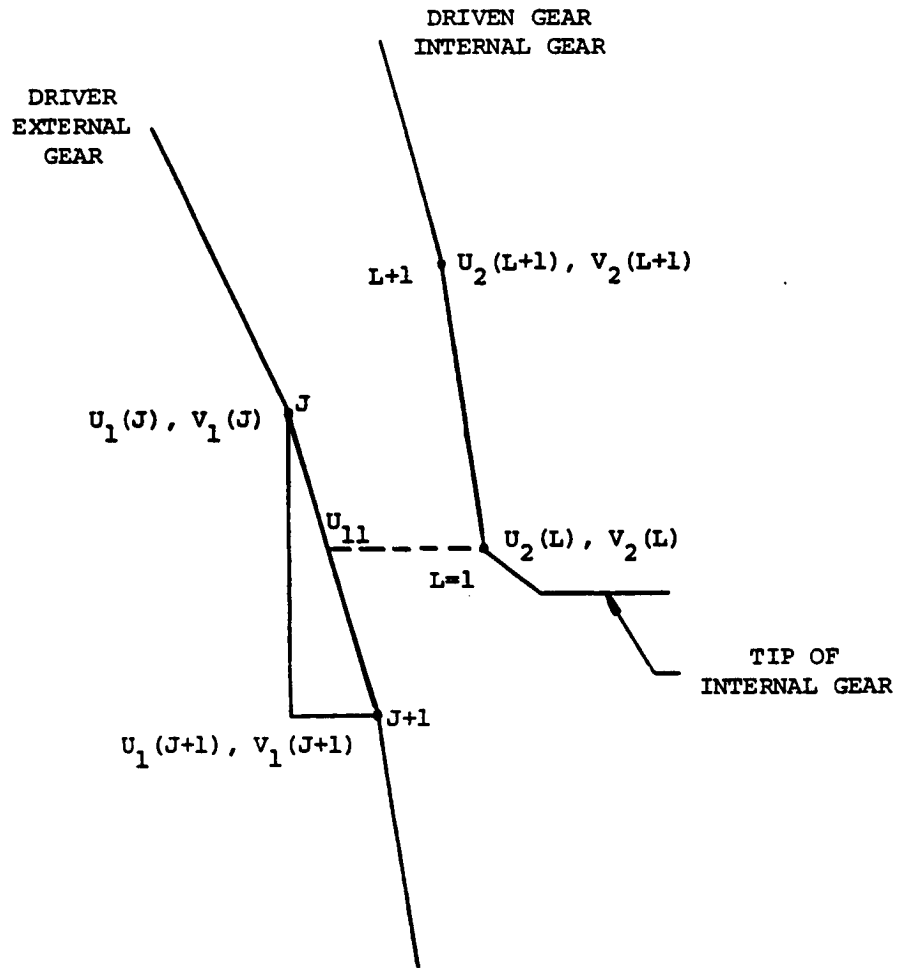


Figure 20 - Search for Initial Mesh Arc Contact

pair number three is contacting at the beginning of its mesh cycle.

5. A complete contact search for all five tooth pairs is made at fifty positions from initial through final contact of tooth no. 3. Actual contact at every mesh point for all five teeth and the contact position for tooth number three and any other teeth is recorded. At this point single or multiple tooth contact for all fifty mesh positions is determined. In case of multiple tooth contact the load will be shared between the contacting teeth. Each tooth carries a fraction of the total load proportional to its own tooth stiffness and the combined stiffness of all the contacting teeth. For the i^{th} contacting tooth the shared load $Q(k)_i$ is

$$Q(k)_i = \frac{KP(k)_i}{KG_i}(Q_t) \quad \dots(11)$$

where $KP(k)_i$, KG_i and Q_t are the stiffness of the i^{th} tooth, total mesh stiffness and total load at that mesh position respectively. Details of the methods for tooth deflection and stiffness calculations are discussed in Section 3.4.6. From these methods and knowledge of the shared load on each tooth it is now possible to determine the deflection of each tooth profile point. This completes the first search for contact assuming rigid body motion of the two gears.

Search for Contact of the Loaded Gears

1. The gear tooth deflections can be considered as another

form of tooth modification causing premature engagement and delayed disengagement. Points A' and B' of Figure 21 demonstrate this action. Thus, by adding the tooth deflection, the whole procedure of the first search routine must be repeated. At the end of the procedure the actual contact positions, mesh stiffness and static loading for fifty positions of the total meshing arc are determined. Also calculated are the deflections of each profile point for all five tooth pairs at each of fifty mesh angles.

3.4.5 Line of Action, Contact Ratio and Interference Conditions

The line of action of an unloaded involute tooth pair is tangent to the base circle of gears 1 and 2, and its inclination is represented by the theoretical pressure angle, ϕ (see Figure 19). Under load the mating teeth deflect and the instantaneous line of action is no longer tangent to both circles. The line of action will change with changes in load, speed and position. Thus, we are concerned with the theoretical and instantaneous lines of action (see Figure 21). Other parameters that can be thought of as changing at any instant are pressure angles, base radii, pitch radii, transmission ratios, etc. The net effect of the change in line of action is to reduce the transmission ratio, TR, or the ability to transmit the torque.

As mentioned before, the circumferential deflection of the teeth causes premature engagement and delayed disengagement. This condition is beneficial to the action of the gears since it increases the arc of contact between the mating teeth. In Figure 21 the angular arcs A-B and A'-B' represent the theoretical and instantaneous contact arcs.

- PPD' = Instantaneous Pitch Radius
- A = Theoretical Contact Point
- A' = Actual Instantaneous Contact Point
- B = Theoretical Final Contact Point
- B' = Actual Final Contact Point
- TLA = Theoretical Line of Action
- ILA = Instantaneous Line of Action
- δ_1 = Deflection of Tooth at A, Gear 1
- δ_2 = Deflection of Tooth at A, Gear 2
- RCP1 = $O_1 - A'$
- RCP2 = $O_2 - A'$
- RCCP1 = $C_1 - A'$
- RCCP2 = $C_2 - A'$

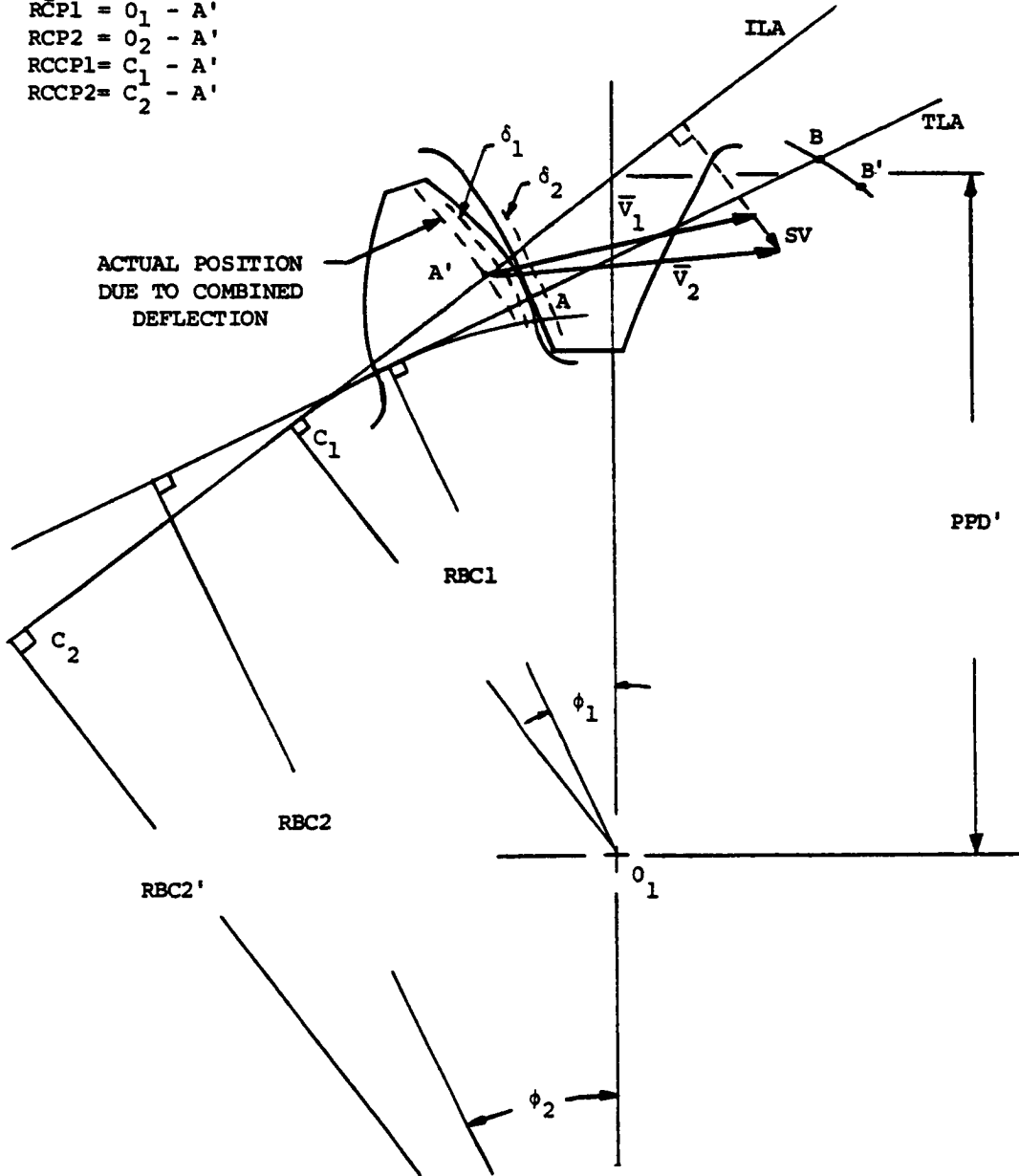


Figure 21 - Instantaneous Contact Point for Tooth Pair

Thus the loaded contact ratio, CR, for an error-less gear pair can be approximated as

$$CR = \frac{A' - B'}{p'} \quad \dots (12)$$

where

p' = circular pitch under load

The deflection of the gear tooth under load enters into another consideration, namely, the possibility of interference. Formulae for avoiding the various interference conditions of external-internal involute gears have been derived from unloaded gears in terms of limit radii or angles. For the loaded condition the deflection of the teeth may increase the potential for interference. Thus, it is necessary to conduct two interference calculations using the ideal and instantaneous gear geometries.

Of course, any deviation from the involute action will increase the amount of sliding action between the teeth.

3.4.6 Deflections and Stiffness of the Teeth and Their Supporting Structure

When the teeth of a pinion and gear come into contact, transmission of load causes deflections in the gearing system as indicated in Figure 12. For the external-internal gear combination the overall deformation may be sufficiently large to influence the mesh characteristics and, thus, affect the static and dynamic behavior of the gear system. The actual deflection may be considered to consist of the summation of several deflection components starting with the Hertzian deformation at the contact point and extending into the foundation of the system. For the dynamic analysis it is necessary to consider inertial and damping effects as well which can best be treated by

subdividing the gearing system into smaller parts of masses, dampers and springs. In the context of this system subdivision, the deflections pertaining to the contacting gear teeth are radial and circumferential. The radial component is due to the radial deflection of the support bearings and shafts and the internal gear ring. The radial deflection of the pinion is negligible due to its rigid construction. Expressions for the radial deflection of bearings and shafts are readily available from standard textbooks. [26][27] A listing of deflection equations of bearings suitable for the ISG drives is given in Appendix B. The radial deflection of the ring gear is not as readily available because of its single point loading and complex geometry (see Figure 3). In general, experimental means or three-dimensional finite element analysis must be resorted to for an accurate assessment of the deflection. However, these measures may not be needed for the ISG drive because it is usually designed to minimize radial deflection. In Figure 4, the support bearing for the ring has been placed directly over the load preventing radial deformation of the ring. In Figure 3, the ring thickness over the internal gear teeth is heavy causing nearly rigid body loading of the outer cylindrical section. For this configuration a worst case condition can be assumed to occur as outlined in Appendix B-2. The worst case solution of Appendix B-2 is then used to evaluate the performance of the gears. Because of the rigid design, the radial deflections are held to the same order of magnitude as the circumferential deflection. Nevertheless, the radial deflection causes radial movement of the gears with a resulting reduction in contact length of the gears.

For a given design, selection of the appropriate bearing deflection equation from Appendix B-1 and bracketing of the ring deflection

leads to a combined radial deflection as follows

$$\delta_R = \delta_{REB} + \delta_{RIB} + \delta_{RES} + \delta_{RR} \quad \dots(13)$$

where

δ_{REB} = deflection of external gear bearing

δ_{RIB} = deflection of internal gear bearing

δ_{RES} = deflection of external gear shaft

δ_{RR} = deflection of ring

The deflection along the gear circumference is due to Hertzian deformation, bending, shear, compression and rotation of the teeth at their root, and due to torsion of the pinion and gear ring.

The combined external-internal gear tooth pair deflections can be expressed in the following form:

$$\delta(k)_i = \delta_E(k)_i + \delta_I(k)_i + \delta_H(k)_i \quad \dots(14)$$

where

$\delta_E(k)_i$ = deflection of the k^{th} tooth of the external gear at mesh arc position i

$\delta_I(k)_i$ = deflection of the k^{th} tooth of the internal gear at mesh arc position i

$\delta_H(k)_i$ = localized Hertzian deformation at the point of contact

For the contacting pairs, the gear tooth deflections $\delta_E(k)_i$ and $\delta_I(k)_i$ incorporate a number of constituent deflections. For the external gear:

$$\delta_E(k)_i = \delta_{ME}(k)_i + \delta_{SE}(k)_i + \delta_{NE}(k)_i + \delta_{BE}(k)_i + \delta_{RE}(k)_i \quad \dots(15)$$

In equation (15),

δ_{ME} = gear tooth deflection due to bending moment

δ_{SE} = gear tooth deflection due to shear force

δ_{NE} = gear tooth deflection due to normal force

δ_{BE} = gear tooth deflection due to deformation of
the surrounding hub area (rocking action)

δ_{RE} = gear tooth deflection due to torsion of the
rim or hub (circumferential deformation of hub)

For the internal gear, the deflection for the k^{th} tooth pair at mesh arc position i is

$$\delta_{I(k)}_i = \delta_{MI(k)}_i + \delta_{SI(k)}_i + \delta_{NI(k)}_i + \delta_{BI(k)}_i + \delta_{RI(k)}_i \quad \dots(16)$$

where

δ_{MI} = gear tooth deflection due to bending moment

δ_{SI} = gear tooth deflection due to shear force

δ_{NI} = gear tooth deflection due to normal force

δ_{BI} = gear tooth deflection due to deformation of
the surrounding ring area (rocking action)

δ_{RI} = gear tooth deflection due to torsion of the
supporting ring (circumferential deformation
of the ring)

Expressions for the constituent deflections of the external gear have been derived by strength of material techniques [13]

In this investigation, the same methods have been applied to the internal gear. A detailed account of all the circumferential deflections in the ISG drive is shown in Appendix B-3

The circumferential deformations of the hub and ring affect the deflections on all teeth whether they are loaded or not. Thus, if the rigid body contact search of Section 3.4.4 does not find contact between

two teeth, it is possible that the two unloaded teeth would be declared in contact in the second contact search as a result of the attendant circumferential deformation. In this case, the final load sharing and deflections will be recalculated on the basis of this additional contacting tooth pair.

Both the radial and circumferential deflections affect the mesh stiffness and contact ratio characteristics. The radial deflection primarily affects the contact ratio and to a smaller degree the stiffness value. The circumferential deflection has a much more significant influence on the mesh stiffness. These effects are shown in Figures 26 & 29.

Thus, for any mesh arc position i , the calculated k^{th} gear tooth pair stiffness $KP(k)_i$, mesh stiffness KG_i , and load sharing incorporate the effects due to manufactured profile errors, profile modifications, and radial and circumferential deflections by means of the iterated numerical solutions of equations (13) through (18).

The individual gear tooth pair stiffness can be expressed as

$$KP(k)_i = \frac{Q(k)_i}{\delta(k)_i} \quad \dots (17)$$

If the effective errors prevent contact, $KP(k)_i = 0$.

The sum of gear tooth pair stiffnesses for all pairs in contact at position i represents the variable mesh stiffness KGP

$$KGP_i = \sum_1^K KP(k)_i \quad \dots (18)$$

The load carried by each of the pairs moving through the mesh arc in the static mode can be determined as

$$Q(k)_i = \frac{KP(k)_i}{KGP_i} (P) \quad \dots (19)$$

where P is the total normal static load carried by the gears at any mesh position in the static mode

$$P = \sum_{i=1}^K Q(k)_i \quad \dots (20)$$

The static analysis thus described determines the variable mesh stiffness (KGP), transmission ratios (TR), and the contact position vectors (RCP1, RCP2, RCCP1, as shown in Figure 21) for subsequent dynamic calculations.

3.5 DYNAMIC ANALYSIS

The gear train shown in Figure 22 was modelled for the dynamic solution. This gear train is found in practical applications like turbine driven pumps, motor driven tank turrets or wind turbines as in Figure 4. The model consists of input and output devices, the external-internal gear transmission and interconnecting shafts and bearings. The analysis considers constant input and fluctuating output torque, damping in shafts, gears and bearings, backlash, noninvolute action caused by deflections and tooth modifications, and loss of contact between gear teeth. The coordinate system used in the static analysis is used also in the dynamic analysis. The instantaneous parameters which were determined for the fifty mesh arc positions in the static analysis will be combined with the equations of motion for the dynamical solution of the system.

For the model of Figure 22, the differential equations of motion can be given in the following form:

$$\begin{aligned}
 J_D \ddot{\theta}_D + C_{BD} \dot{\theta}_D + C_{B1} \dot{\theta}_D + C_{DS} (\dot{\theta}_D - \dot{\theta}_2) \\
 + K_{DS} (\theta_D - \theta_1) = T_D \quad \dots (21)
 \end{aligned}$$

$$\begin{aligned}
 J_{G1} \ddot{\theta}_1 + C_{B2} \dot{\theta}_1 + C_{DS} (\dot{\theta}_1 - \dot{\theta}_D) + K_{DS} (\theta_1 - \theta_D) \\
 + [CGP_i (RBC1 \dot{\theta}_1 - RBC2' \dot{\theta}_2) + KGP_i (RBC1 \theta_1 \\
 - RBC2' \theta_2)] RBC1 = 0 \quad \dots (22)
 \end{aligned}$$

$$\begin{aligned}
 J_{G2} \ddot{\theta}_2 + C_{B3} \dot{\theta}_2 + C_{B4} \dot{\theta}_2 + C_{LS} (\dot{\theta}_2 - \dot{\theta}_L) \\
 + K_{LS} (\theta_2 - \theta_1) + [CGP_i (RBC2' \dot{\theta}_2 - RBC1 \dot{\theta}_1) \\
 + KGP_i (RBC2' \theta_2 - RBC1 \theta_1)] RBC2' = 0 \quad \dots (23)
 \end{aligned}$$

$$\begin{aligned}
 J_L \ddot{\theta}_L + C_{BS} \dot{\theta}_L + C_{BL} \dot{\theta}_L + C_{LS} (\dot{\theta}_L - \dot{\theta}_2) + K_{LS} (\theta_L - \theta_2) \\
 = - T_D \times TR' = - T_L (TR') \quad \dots(24)
 \end{aligned}$$

Importantly, the equations of motion are based on the instantaneous rather than the theoretical line of action. In equation (24), the load torque is written as a function of the instantaneous transmission ratio TR' . The bracketed terms in equations (22) and (23) represent the dynamic gear mesh force which is dependent on the dynamic displacements of the engaged gears, gear mesh stiffness and damping in the mesh.

The mesh stiffness, KGP_i in equations (22) and (23), represents the combined effects of gear tooth profile errors and modifications, radial and circumferential deflections of the gear teeth, sharing of the load between teeth, height of engagement, and the angular position in the gear mesh cycle. Representative mesh stiffness cycles are shown in Figures 26 and 27. For a constant input torque, the variable mesh stiffness and the changes in transmission ratio due to noninvolute action represent major sources of dynamic excitation. The output torque, T_L , is a function of the input torque, the instantaneous transmission ratio and losses in the system.

During operation of the system in Figure 22, the dynamic excitation sources can create situations during which momentary disengagement of the mating gear teeth can occur. The information whether separation takes place can be obtained by reviewing the equations of motion.

The term $(RBC1 \theta_1 - RBC2' \theta_2)$ represents the relative dynamic displacement of gear 1 and 2. Considering that gear 1 is the driving gear, the following situations can occur:

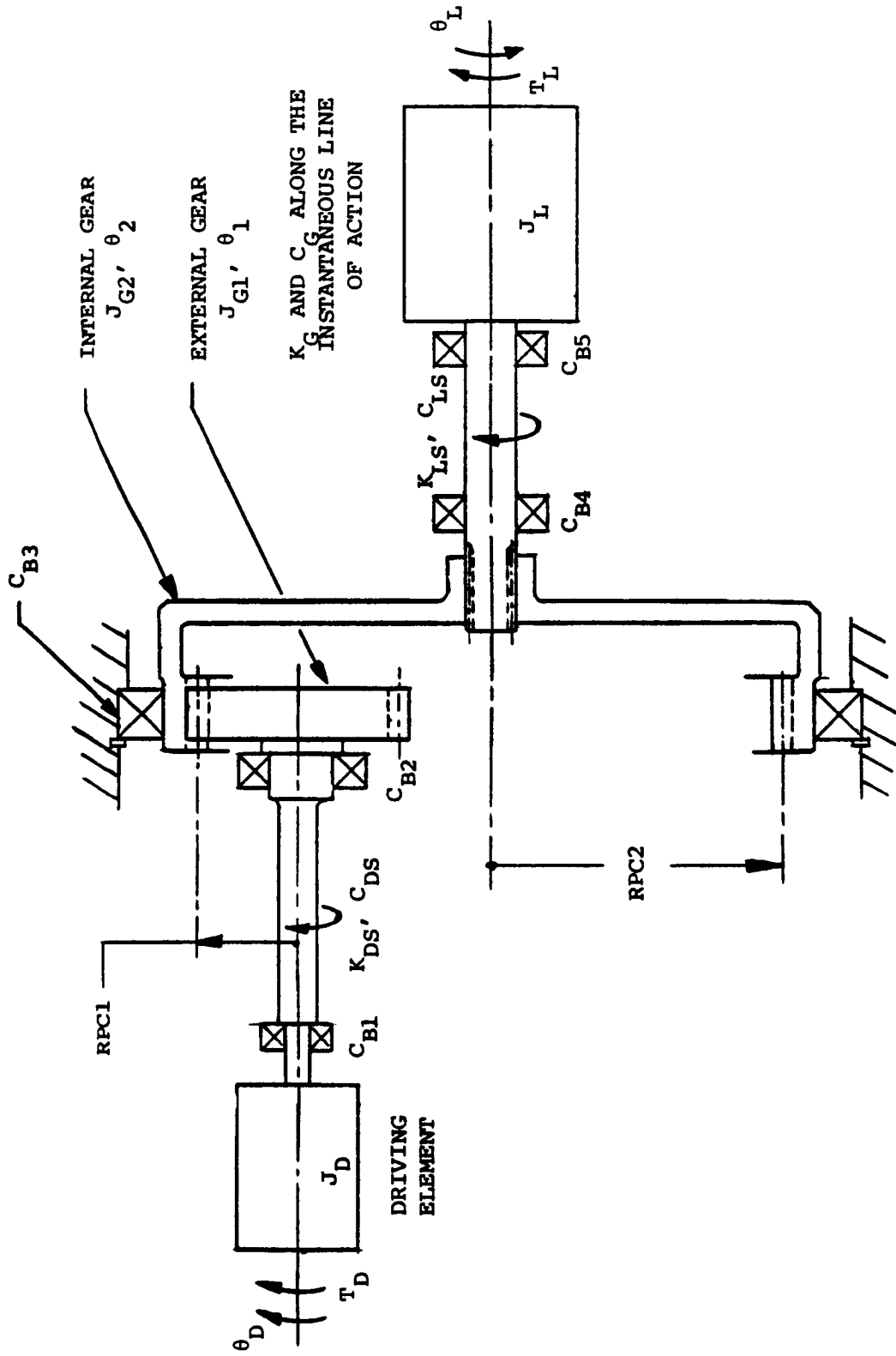


Figure 22 - Internal-External Gear Train Used in the Dynamic Analysis

When $RBC1 \theta_1 > RBC2' \theta_2$

we have normal operation of the gear system and the dynamic mesh force is defined by

$$\begin{aligned} (QDT)_i &= CGP_i (RBC1 \theta_1 - RBC2' \theta_2) \\ &+ KGP_i (RBC1 \theta_1 - RBC2' \theta_2) \end{aligned} \quad \dots(25)$$

If $RBC2' \theta_2 \geq RBC1 \theta_1$ and $RBC2' \theta_2 - RBC1 \theta_1 < BGM$

then the gears will separate and contact between the gears will be lost. For this case,

$$(QDT)_i = 0 \quad \dots(26)$$

If $RBC2' \theta_2 > RBC1 \theta_1$ and $(RBC2' \theta_2 - RBC1 \theta_1) > BGM$

$$\begin{aligned} (QDT)_i &= CG_i (RBC1 \theta_1 - RBC2' \theta_2) \\ &+ KGP_i [(RBC1 \theta_1 - RBC2' \theta_2) - BGM] \end{aligned} \quad \dots(27)$$

in this case, gear 2 will hit gear 1 on the backside.

Also when $KGP_i = 0$; $(QDT)_i = 0$

An example of zero stiffness can be obtained from a pit extending across the tooth profile.

The equations of motion (21) through (24) contain damping terms for all components in the system. For this investigation, the damping in the bearing nearest the driving or driven element has been combined with the respective damping of those elements. Damping in the shafts is due to material damping which, by experiment, [29] has been found to be between 0.005 and .007. Expressed as a critical damping ratio, a representative value of .005 has been assigned for the shafts. For the

shafts, the effective damping is then

$$C_{DS} = 2\xi_S \sqrt{\frac{K_{DS}}{\frac{J_D + J_{G1}}{J_D \times J_{G1}}}} \quad \dots (28)$$

$$C_{DS} = 2\xi_S \sqrt{\frac{K_{LS}}{\frac{J_L + J_{G2}}{J_L \times J_{G2}}}} \quad \dots (29)$$

where

$$\begin{aligned} \xi_S &= \text{critical damping ratio} \\ &= .005 \end{aligned}$$

and the shaft masses are lumped into the masses J_D , J_{G1} , J_{G2} and J_L .

Also, the effective damping of the gear mesh is:

$$CGP_i = 2\xi_G \sqrt{\frac{KGP_i}{\frac{(RBC1)^2}{J_{G1}} + \frac{(RBC2)^2}{J_{G2}}}} \quad \dots (30)$$

where

$$\xi_G = \text{critical damping ratio of gear mesh}$$

System response measurements of geared systems [6][9][8] indicated that ξ_G ranges between 0.03 and 0.10. In equation (30) the average gear mesh stiffness is used and the equivalent masses of gears 1 and 2 are concentrated at the base circles to reflect their effect along the line of action.

The equations of motion (21) through (24) are numerically integrated using a fourth order Runge-Kutta scheme. [28] This method is described in a number of references and will not be repeated here.

Before the integration can be performed, initial values, integration

time increment and integration duration must be determined. For a given design condition the initial displacements $\theta_D(0)$, $\theta_L(0)$, $\theta_2(0)$ and $\theta_1(0)$ are determined by applying the input and output torques to the system. For convenience, the first gear is used as the null point. The subsequent driver movement is considered plus and the driven movement as negative. The initial velocities $\dot{\theta}_D(0)$, $\dot{\theta}_1(0)$, $\dot{\theta}_2(0)$ and $\dot{\theta}_L(0)$ have been assigned the anticipated steady state velocities.

The integration time step must be selected short enough to avoid inaccuracies and instability in the integration process and yet long enough to minimize computer time. A measure of the optimum time step can be obtained by determining the undamped torsional natural frequencies of the system. The undamped equations of motion rewritten in matrix form appear below

$$[J]\{\ddot{\theta}\} + [K]\{\theta\} = 0 \quad \dots(31)$$

where the inertia matrix is

$$\begin{bmatrix} J_D & 0 & 0 & 0 \\ 0 & J_{G1} & 0 & 0 \\ 0 & 0 & J_{G2} & 0 \\ 0 & 0 & 0 & J_L \end{bmatrix} \quad \dots(32)$$

and the stiffness matrix is

$$\begin{bmatrix} K_{DS} & -K_{DS} & 0 & 0 \\ -K_{DS} & K_{DS} - KGP_{AVE} \times RBC1^2 & -KGP_{AVG} \times RBC1 \times RBC2 & 0 \\ 0 & -KGP_{AVG} \times RBC1 \times RBC2 & K_{DS} + KGP_{AVG} \times RBC2^2 & -K_{LS} \\ 0 & 0 & -K_{LS} & K_{LS} \end{bmatrix} \quad \dots(33)$$

In equation (33) the weighted average of gear mesh stiffness, KGP_{AVE} , is introduced to simplify the solution for eigenvalues. KGP_{AVE} is determined by summing up the discrete stiffness values, KGP_i , over one cycle and dividing by the number of discrete mesh positions in the cycle.

The undamped equations of motion are solved for the eigenvalues and eigenvectors by a Jacobi iteration technique. For the integration time step stable solutions have been obtained consistently by using one tenth of the shortest system natural period or less than two percent of the mesh stiffness period. The duration of the integration time step is predicated on the time needed for the start-up transients to decay. Review of the output data revealed essentially steady state behavior for integration time lengths equal to five times the longest system natural period.

As a first step, the dynamic force in the mesh as defined by equations (25) through (27) is calculated in the dynamic analysis subroutine FAST. Next, FAST interacts with the static subroutine SLOWM to determine the sharing of the dynamic load, the variation of the load through the mesh cycle, the sliding velocity, the maximum Hertz pressure and the velocity-Hertz pressure product along the tooth profiles.

The sliding velocity vector relationship at a given mesh position can be seen from Figure 21. In vector notation

$$SV(k)_i = \bar{V}_1 - \bar{V}_2 = RCP1'(k) \dot{\theta}_1 - RCP2'(k) \dot{\theta}_2 \quad \dots (34)$$

where

$RCP1'(k)_i$ and $RCP2'(k)_i$ are the instantaneous radii to the contact point of tooth k at mesh position i . In scalar form equation

(34) can be expressed as

$$SV(k)_i = \sqrt{(V_1)^2 + (V_2)^2 - 2V_1V_2 \cos(\alpha_{A1} - \alpha_{A2})} \quad \dots (35)$$

For the same position the dynamic load $QD(k)$ was established as

$$QD(k)_i = \frac{KP(k)_i}{KG_i} QDT_i \quad \dots (36)$$

and two dynamic load factors as

$$(DF1)_i = \frac{QDT_i}{Q_t} \quad \dots (37)$$

$$(DF2)_i = \frac{QD(k)_i}{Q(k)_i} \quad \dots (38)$$

where DF1 is defined as the ratio of total dynamic mesh force to the total static mesh load. DF2 is the dynamic load ratio for any given pair in engagement.

Two stress conditions are evaluated for the contacting teeth:

1. Hertzian Contact Stress using the equivalent cylinder approach for Hertzian deflection outlined in Section 3.4.6:

$$P_H(k)_i = \sqrt{\frac{QD(k)_i}{\pi FA} \left(\frac{1}{RCCP1'(k)} - \frac{1}{RCCP2'(k)} \right)} \quad \dots (39)$$

where

$RCCP1'(k), RCCP2'(k)$ = equivalent instantaneous radii
of curvature

F = minimum gear tooth face width

$$A = \frac{(1 - \mu_1^2)}{E_1} + \frac{(1 - \mu_2^2)}{E_2}$$

Using equations (35) and (39), the product $P_H(k)_i \times SV(k)_i$

is determined as an indication of the severity of the wear condition at the tooth profile surfaces.

2. Bending stress of the teeth using a modified Heywood formula suggested by Cornell: [15]

$$\sigma_B = \frac{QD(3)_j}{F} \cos \theta_j \left[1 + .26 \left(\frac{X_{js}}{RF_j} \right)^{.7} \right] \frac{3Y'_{js}}{2X_{js}^2} + \sqrt{\frac{.36}{X_{js} Y_{js}}} \left(1 - \frac{X_j}{X_{js}} \mu \text{TAN } \theta'_j \right) - \frac{\text{TAN } \theta_j}{2 X_{js}} \quad \dots (40)$$

where

$$j = 1 \text{ or } 2$$

For the modified Heywood formula, the position of the maximum stress in the fillet, γ_{js} is found by iteration

$$\text{TAN } \gamma_{js(l+1)} = (1 + .16 A_{jl}^{.7}) A_{jl} / [B_{jl} (4 + .416 A_{jl}^{.7}) - (\frac{1}{3} + .016 A_{jl}^{.7}) A_{jl} \text{TAN } \theta_{jl}] \quad \dots (41)$$

where

l = iteration number starting with 1

$$A_{jl} = \frac{2 X_{jo}}{RF_j} + 2(1 - \cos \gamma_{jsl})$$

$$B_{jl} = \frac{Y_{jo}}{RF_j} + \text{SIN } \gamma_{jsl}$$

and the remaining nomenclature is as in Figures 23 and 24.

Equation (40) predicts the maximum tensile fillet stress within about 5% to 10% of finite element methods. [15] It also predicts fairly well the location of the peak stress in the fillet. Because of its relative ease of use and the expected low stresses in the rigid

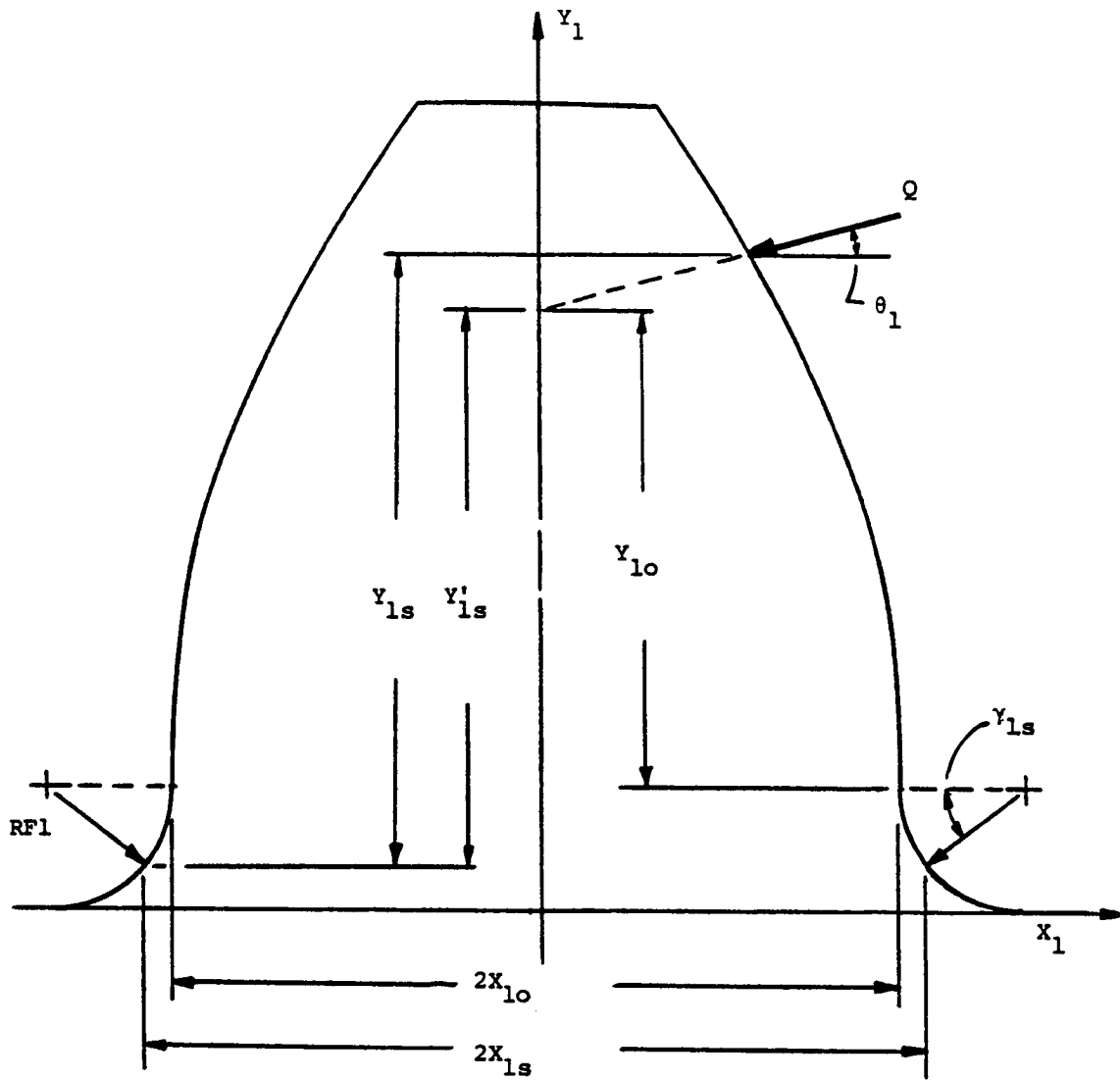


Figure 23 - Nomenclature for Modified Heywood Formula -
External Gear Tooth

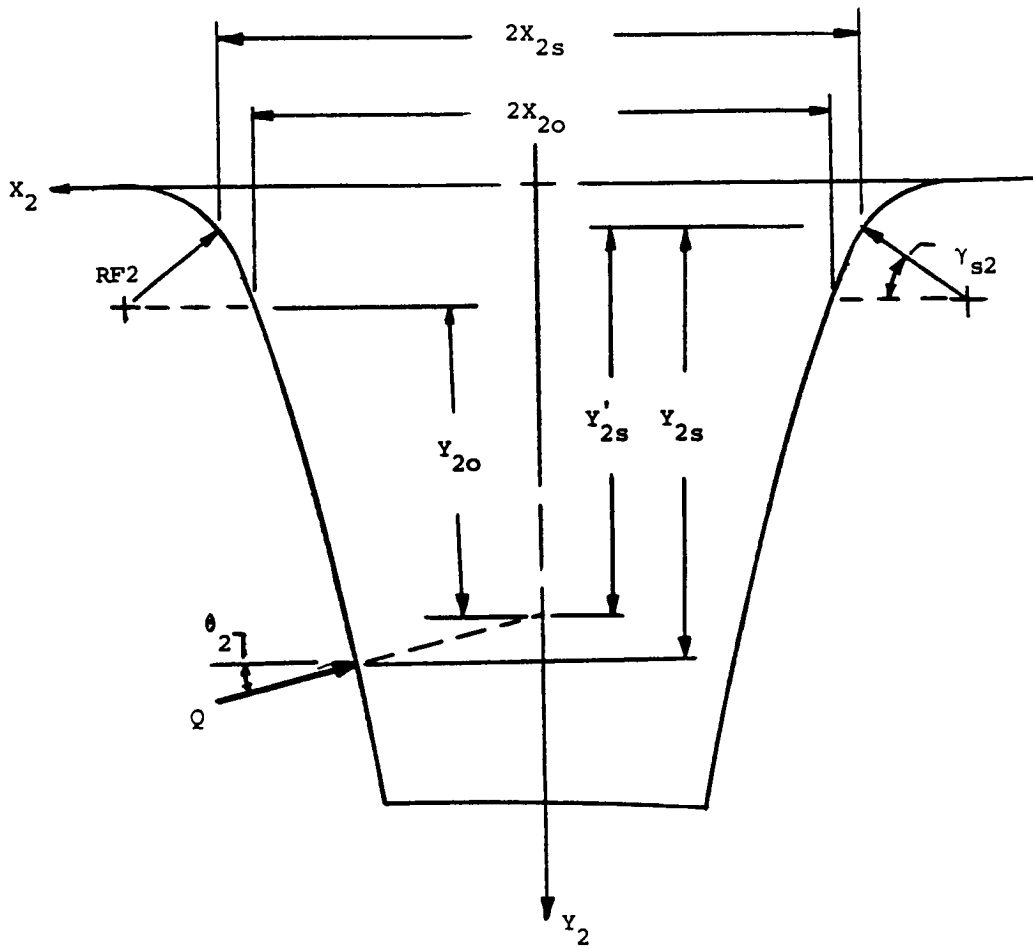


Figure 24 - Nomenclature for Modified Heywood Formula -
Internal Gear Tooth

hub and ring, equation (40) is considered to be representative of the peak stresses of gear 1 and 2.

3.6 COMPUTER PROGRAM

The development of a digital computer program for the comprehensive analysis of the static and dynamic behavior of internal spur gear (ISG) drives was one of the tasks of this dissertation effort. The existing external spur gear program developed at CSU was used as the nominal starting point for the structure and nomenclature of the new ISG drive program. The ISG computer program package in its entirety, along with sample output print-out, is included in Appendix C. Highlights of the computer program, its structure, nomenclature and the input data required for the analysis of an external-internal spur gear drive are discussed in this section.

3.6.1 Program Structure

The ISG drive computer program package is written in Fortran IV G1 for use on the Cleveland State University IBM 370/158 digital computer. It has been prepared in three modules for operator convenience (see Figure 25). Module 1 represents the static analysis discussed in Section 3.4. In this module, the operator has the following options:

1. INTERNAL STATIC permits the operator to make changes to the program and conduct a static analysis. This ability to change the program is desirable for future improvements. The program is compiled after every submittal and thus takes over 2 minutes of computer time on the CSU IBM 370/158 digital computer.
2. The current INTERNAL STATIC can be compiled and it becomes now EXECUTE INTRSTAT. However, before the compiling is done, it is first necessary to delete the

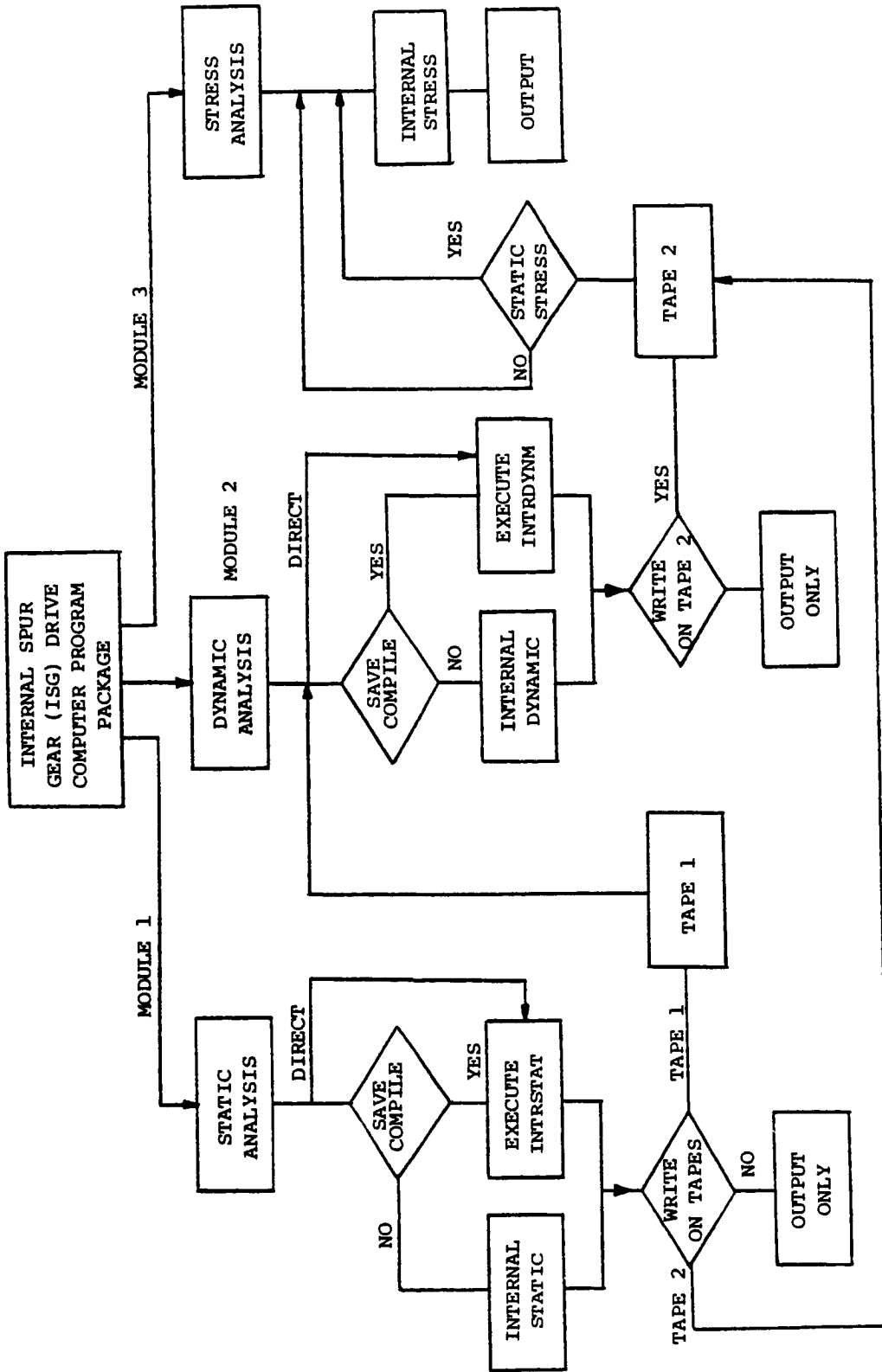


Figure 25 - Block Diagram of Computer Package for External-Internal Spur Gears

old EXECUTE INTRSTAT. Then the empty space on the file is compacted, the old INTERNAL STATIC is deleted, the new INTERNAL STATIC version is transferred to the deleted section and then compiled. Now the new EXECUTE INTRSTAT is ready.

3. EXECUTE INTRSTAT permits no changes to the program, but the computer time is reduced to less than 2 minutes. Thus, parametric studies are made most efficiently directly from the current EXECUTE INTRSTAT version.

Option 1 and 3 provide the additional feature to the operator of being able to write output data on two tapes. Tape 8 and 9 are needed for the dynamic and stress analysis respectively.

Module 2 represents the dynamic analysis as discussed in Section 3.5. In this module the operator has the same options as before but the uncompiled and compiled versions are now called INTERNAL DYNAMIC and EXECUTE INTRDYNM. Once again, EXECUTE INTRDYNM can be used directly for parametric studies. Both versions of the dynamic analysis, in addition to input data, require the data from Tape 8, and can write dynamic data on Tape 9 for use in the stress analysis.

Module 3 calculates the maximum tooth bending stress at the fillet using the stress formulae discussed in Section 3.5. Tape 9 information is needed for this analysis in terms of the 50 contact points, and whether static or dynamic loading is used.

The three modules consist of an executive program and a number of subroutines. Portions of the executive program are common to all modules and some subroutine sections are shared by Module 1 and 3. The input data is entered into the executive program by use of namelist

parameters, and Tapes 8 and 9. Again, some of the namelist parameters are common between the three modules. Thus, the resultant overall program package is larger than would be obtained with a combined program. However, the advantage of operator flexibility and quick computer turn-around made the "three module" approach far more convenient. Also, an initial step has been made towards preparing the analysis package for use in the CSU mini-computer HP 1000.

3.6.2 Description of the Executive Programs and Subroutines

The executive program of all modules is called MAIN. It contains the read statements for the namelist parameters and tapes, the call statements for the subroutines and the write statements for input data, diagnostics and output data. Each MAIN program has its own set of namelist parameters, subroutine call statements, and read and write statements suitable for the type of analysis of the given module.

3.6.2.1 Module 1

In addition to MAIN, Module 1 uses MAIN1 for additional executive control and write instructions. The MOD subroutine defines the digitized tooth profiles, checks for interference between mating teeth and determines the theoretical contact ratio. SLOWM first locates the geometric arrangement of the gears with respect to each other. Next it establishes the points of contact, number of contacting gear tooth pairs, sliding velocity vectors, length of dynamic cycle, and loaded contact ratio. Subroutine DEFLECT calculates the deflections except the Hertzian deformation due to a unit load. This unit load deflection is combined with the Hertzian deformation in SLOWM to determine the stiffness of the individual pairs, the variable mesh

stiffness, the static load and the deflection due to this loading.

3.6.2.2 Module 2

The FAST subroutine of this module analyzes the three degree of freedom, four mass, mathematical model of the geared torsional system depicted in Figure 22. Calculations in FAST are based on a dynamic cycle which starts with the initiation of contact on a tooth entering the contact zone and ends with the initiation of contact with the tooth following it. The length of this cycle is established in subroutine SLOWM by examining the stiffness function. The position of tooth no. 3 when tooth no. 4 comes into contact is defined as IEP. Consequently, (IEP-1) is the endpoint of the dynamic cycle started when tooth no. 3 came into contact (Figure 27). FAST calculates the dynamic force in the mesh as defined by equations (25) through (27). The integration is performed in two small subroutines using the very efficient Runge-Kutta integration scheme by Franks.^[28] The RKUTTA subroutine contains the integration step size and keeps track of the iterations across the integration interval. The actual integration is done in subroutine MORERK. Subroutine VIBS uses a Jacobi iteration technique to determine eigenvalues of the gear train. This information is returned to FAST for determination of the natural frequencies, eigenvectors, integration time step and duration. FAST also calculates the instantaneous angular position and velocities, sliding velocities, Hertzian pressure, dynamic loads, dynamic load factors, and transmission ratio. Subroutines STORE and XPLOT are used to store the data and then plot as many as four dependent variables against a single independent variable (see Appendix C for sample output plots).

3.6.2.3 Module 3

Module 3 is set aside for calculating the maximum bending stress of the tooth fillet. Portions of MAIN and MAIN1 have been modified for executive control and printing of pertinent information. Subroutine MOD has been modified to provide not only the tooth profile points but also a more refined breakdown of the fillet contour. This additional refinement is needed for the iterative search routine of the maximum fillet stress location as indicated by equation (41). The actual stress calculation is done in subroutine CORNEL.

CHAPTER IV

RESULTS, DISCUSSION AND SUMMARY4.1 RESULTS AND DISCUSSION4.1.1 Introduction

The internal spur gear (ISG) analysis methodology, which was developed for this report, was used to perform a series of comparative parametric studies in order to assess the ISG drive performance. Since there are no ISG drive performance data available, comparisons were made with known solutions of external spur gear drives. In particular, the results of the ESG study by Kasuba and Evans^[19] can be used to compare the static and dynamic performance of internal versus external spur gear drives under identical load, speed and geometry conditions. From the study by Kasuba and Evans, this author selected one external gear set which was of practical interest to the internal gear design. The selected external spur gear (ESG) set consists of the following design parameters:

Number of Teeth on 1st and 2nd Gear	32 & 96
Pressure Angle	14.5°
Diametral Pitch	8
Face Width	25.4 mm

The analyses of the ESG set consider variations in tooth profiles, tooth support stiffness, critical damping ratios and shaft stiffness. For the ISG drive, static and dynamic computer analyses were conducted

under identical conditions. Next, ISG drives of practical interest were investigated for the same output information to allow comparisons between external and internal drives. Additional analyses were conducted to investigate the effects of radial deflection of the bearings, shafts, hub and gear rings on the ISG drive performance. Also, the tooth bending stress program was used to determine the static and dynamic stress for all fifty gear mesh positions.

4.1.2 Static Analysis

The dynamical model shown in Figure 22 was also used in the static analysis (with all masses taken to be zero). The behavior of the internal and external gear teeth were investigated for various structure support conditions and load magnitudes. In the static analysis the information of interest for the gear teeth consists of the deflection, stiffness, load sharing, bending stress, unit sliding velocities and Hertz pressure.

4.1.2.1 Comparison of ISG and ESG Set Performance

The results presented in Table 1 and Figure 26 show a comparison of the mesh stiffness characteristics between error-less external and internal spur gear sets. The results indicate the influence of the tooth support stiffness on the overall gear mesh stiffness for both ESG and ISG sets. By increasing the support torsional stiffness (higher HSF, Appendix B-3.3), the loaded contact ratio decreases, mesh stiffness increases, changes in instantaneous transmission ratio decrease, and sensitivity to gear tooth errors increases. The opposite occurs by decreasing the support stiffness. In the case of the ISG set, the gear ring stiffness can be reduced effectively only

by decreasing the thickness of the rim (see Figures 3 and 4).

Table 2 demonstrates the significantly higher theoretical contact ratio of the ISG versus the ESG set. Also, the tabulated results in Table 1 indicate substantial changes in contact ratio with increasing loads and/or support flexibility. For different load magnitudes ranging from 88 to 700 N/m (500 to 4000 lbs./in.) the contact ratios change by 13% and 7% for the respective ISG and ESG sets. At the maximum load condition, the contact ratio of the ISG set is 3.09, i.e., three pairs are in continuous contact. This high contact ratio is obtained by the internal gear set, even with high gear tooth support stiffness ($HSF = 1.0$).

Profile errors and pitting affect the mesh stiffness characteristics of the ISG and ESG sets to varying degrees. For the case of only the pinion or gear having a narrow pit 0.5 mm wide (0.02 in.) at the pitch line, the torsionally stiff ISG gears absorbed the fault without a change in the mesh stiffness pattern whereas the ESG gears could not absorb this fault. Thus, causing significant interruptions of the mesh stiffness pattern. Only when the pit width was increased to 2.0 mm did the error affect the ISG mesh stiffness characteristics (Figure 27). The unabsorbed error caused non-contacting zones with resulting substantial changes in the mesh stiffness characteristics, i.e., the flexibilities in the mesh were able to bridge the non-contact zones. For the pit shown in Figure 27, the flexibility of the mesh was able to absorb a portion of the error by eliminating about 60% of the mesh stiffness interruption. The reason for this effective bridging of the non-contact zones can be found in the torsional ring flexibility and the inherent high contact ratio of the ISG set. In normal contact ratio gears as can be encountered with ESG sets, the mesh stiffness,

TABLE 1

EFFECTS OF GEAR HUB/RING FLEXIBILITY ON MESH STIFFNESS,
TRANSMISSION RATIO AND CONTACT RATIO FOR
INTERNAL AND EXTERNAL SPUR GEAR SETS

Gears: 32 & 96 T, 8 DP, 14.5° PA, $CR_T = 2.625$ (INTERNAL),
 $CR_T = 2.14$ (EXTERNAL)

Normal Load: 4450 N (1000 lb.) or 175 N/mm (1000 lb./in.)

GEAR TYPE	RH1 _f mm	RH2 _f mm	KG _{max} N/m	KG _F N/m ²	HSF	ΔTR* %	CR
ISG	12.7	218.5*	6.12×10^8	2.41×10^4	.88	1.8	2.853
	12.7	218.5	6.15×10^8	2.42×10^4	.89	1.8	2.853
	12.7	171.7	6.15×10^8	2.42×10^4	.89	1.8	2.853
	47.2	156	6.94×10^8	2.73×10^4	1.0	1.5	2.81
ESG	10	14.5	3.07×10^8	1.21×10^4	.476	2.4	2.47
	12.7	18.3	3.80×10^8	1.50×10^4	.591	1.9	2.42
	12.7	38.1	5.08×10^8	2.0×10^4	.794	1.6	2.36
	38.1	114.3	6.36×10^8	2.5×10^4	.992	1.0	2.32
	47.2	148.8	6.45×10^8	2.54×10^4	1.0	1.0	2.32

KG_{max} = maximum attainable stiffness in meshing arc

$F_1 = F_2 = FH1 = FH2 = 25.4$ mm (1.0 in.)

RRC1 = 47.25 mm RRC2 = 156 mm for internal gears

RRC1 = 47.25 mm RRC2 = 148.84 mm for external gears

$$KG_F = \frac{KG_{max}}{F}$$

All gears without errors or modifications

*Rim thickness of ring gear = 10 mm

TABLE 2

LOAD EFFECTS ON MESH STIFFNESS, TRANSMISSION RATIO
AND CONTACT RATIO FOR INTERNAL AND EXTERNAL
SPUR GEAR SETS

Gears: 32 & 96 T, 8 DP, 14.5° PA, $CR_T = 2.625$ (INTERNAL),
 $CR_T = 2.14$ (EXTERNAL), HSF = 1.0

GEAR TYPE	LOAD N/m	KG_{max} N/mm	KG_F N/mm ²	ΔTR %	CR
ISG	88	6.94×10^8	2.73×10^4	1.15	2.731
	175	6.94×10^8	2.73×10^4	1.51	2.81
	350	6.94×10^8	2.73×10^4	1.83	2.895
	525	6.94×10^8	2.73×10^4	2.05	3.02
	700	6.94×10^8	2.73×10^4	2.16	3.09
ESG	88	6.36×10^8	2.5×10^4	0.8	2.29
	175	6.36×10^8	2.5×10^4	1.0	2.32
	350	6.36×10^8	2.5×10^4	1.0	2.38
	525	6.36×10^8	2.5×10^4	1.8	2.43
	700	6.36×10^8	2.5×10^4	2.2	2.45

KG_{max} = maximum attainable stiffness in meshing arc

$F_1 = F_2 = FH1 = FH2 = 25.4$ mm (1.0 in.)

RRC1 = 47.25 mm RRC2 = 156 mm for internal gears

RRC1 = 47.25 mm RRC2 = 148.8 mm for external gears

$$KG_F = \frac{KG_{max}}{F}$$

All gears without errors or modification

Gears as listed in Table 1; HSF = 1.0 and Load = 175 N/m
 Angle of approach is negative; Angle of recess is positive

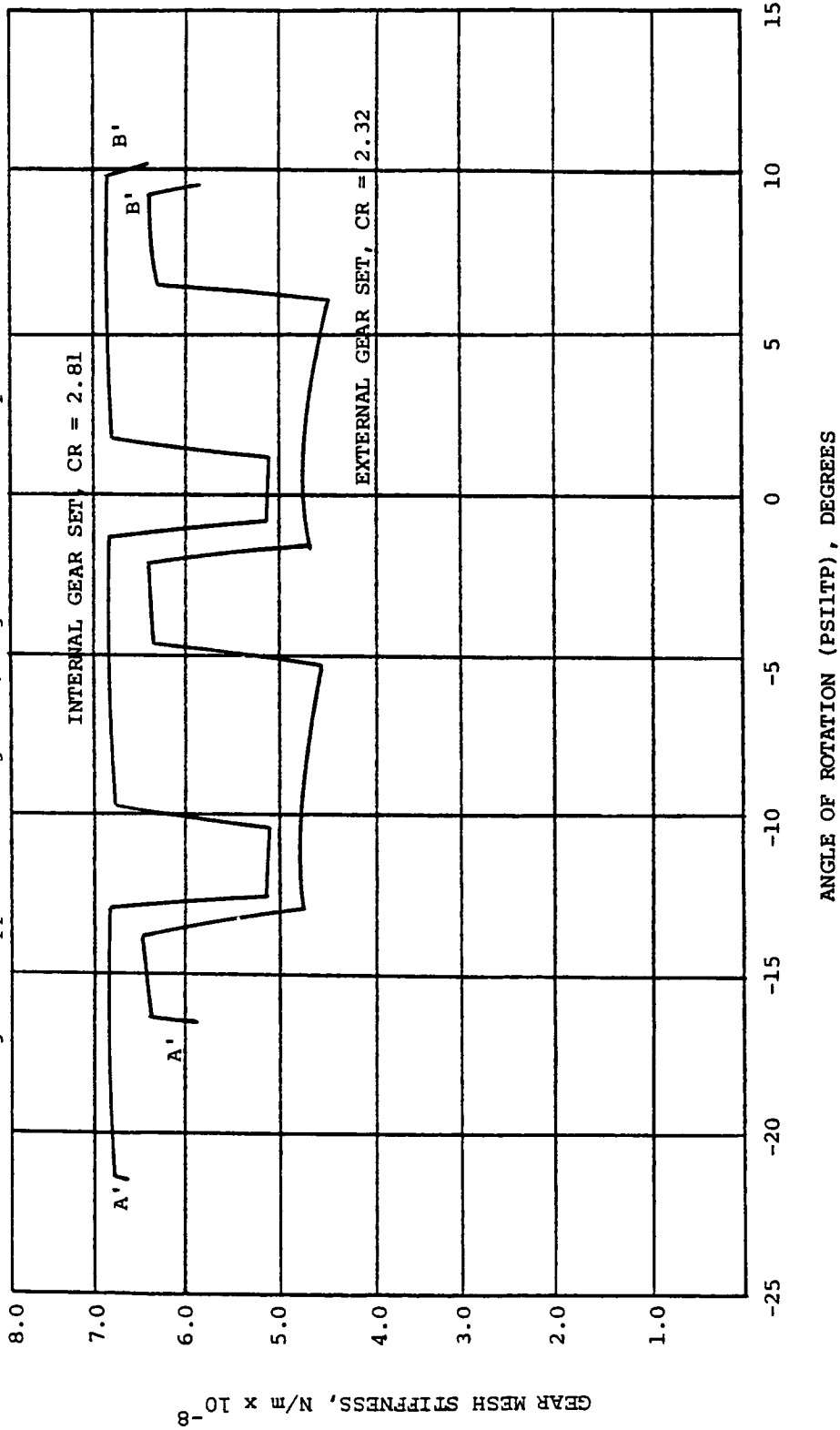


Figure 26 - Typical Gear Mesh Stiffness for ISG and ESG Drives

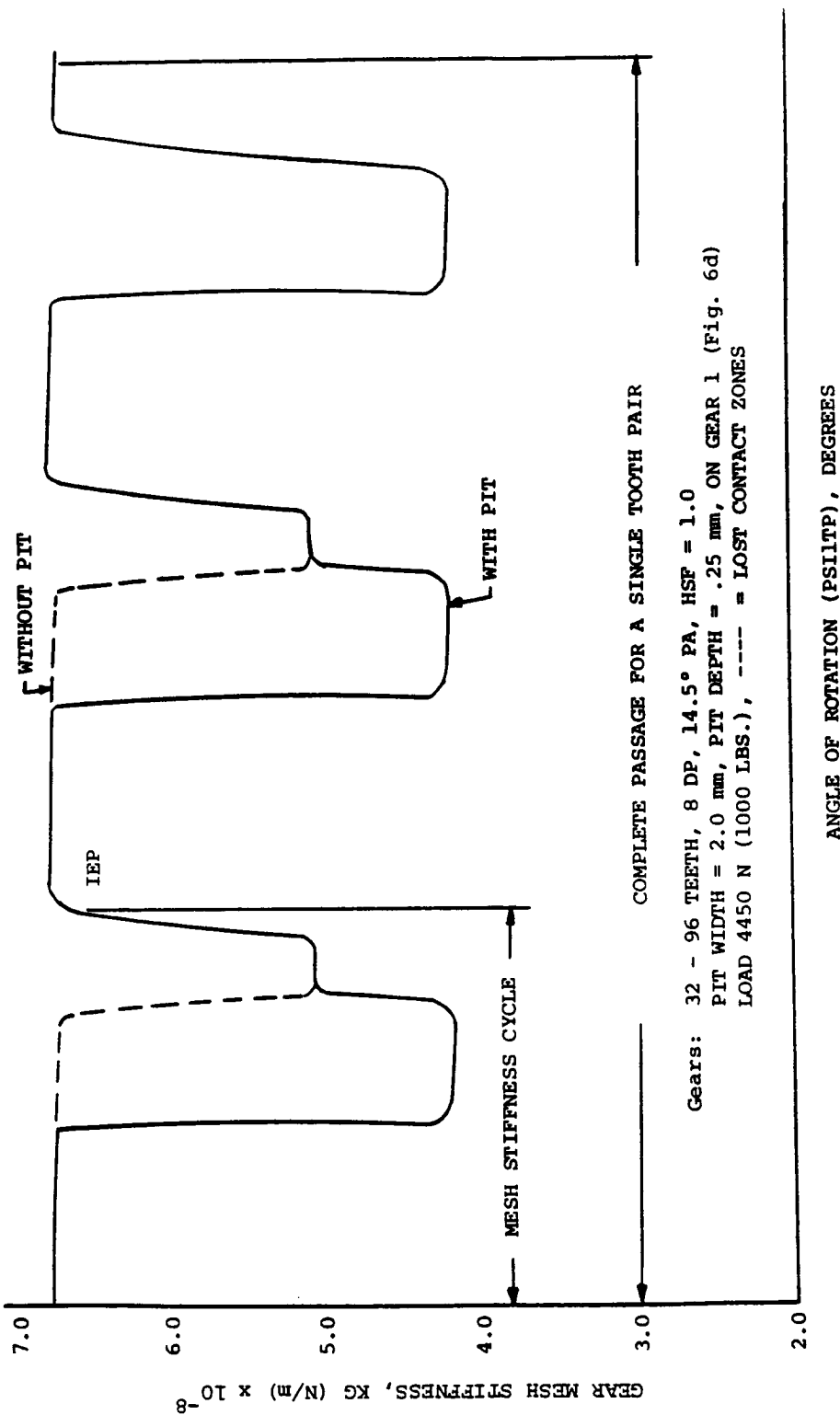
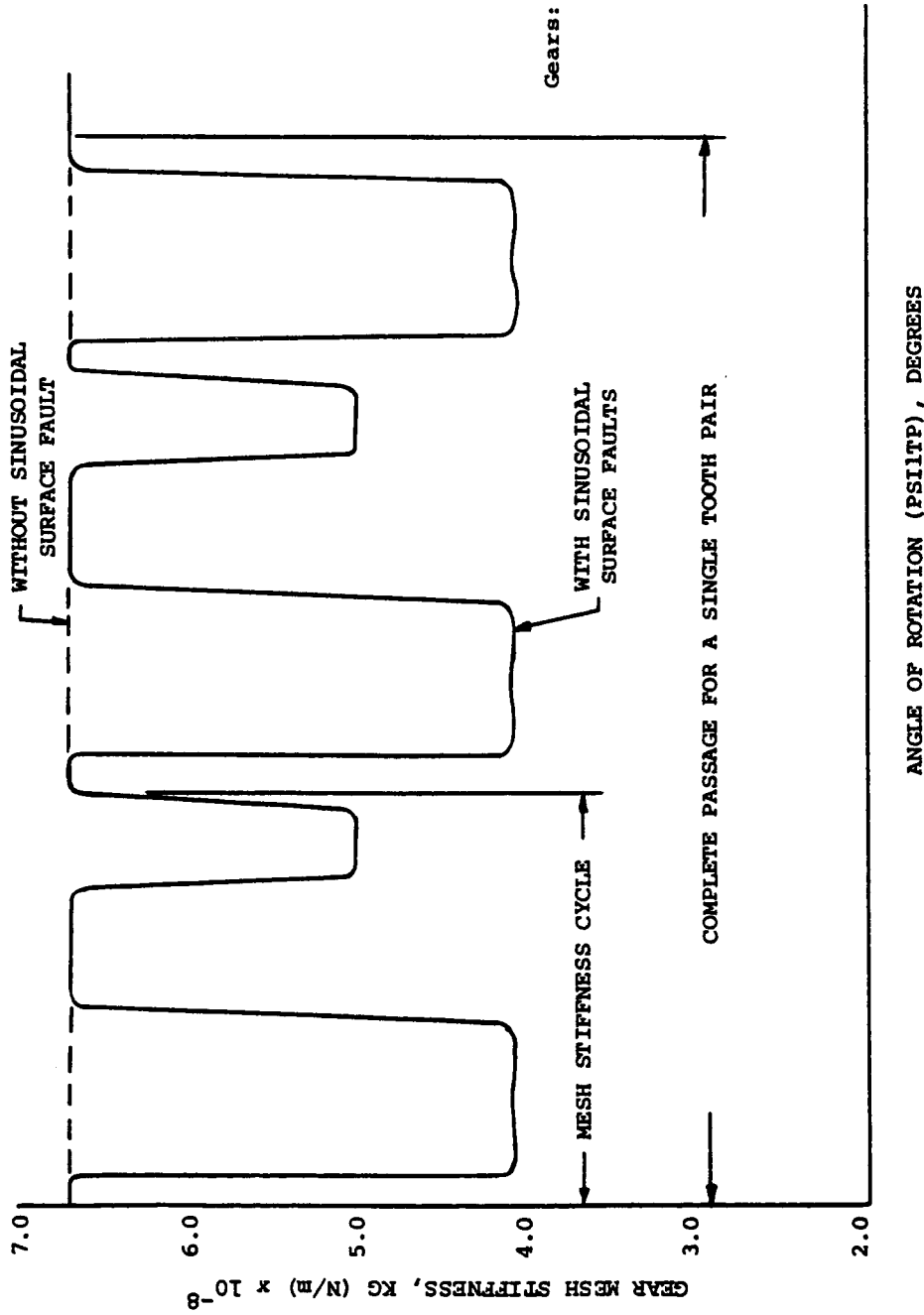


Figure 27 - Effect of Surface Pit on ISG Mesh Stiffness



Gears: 32 - 96 TEETH
 8 DP, 14.5° PA
 F = 25.4 mm
 HSF = 25.4;
 CR = 2.81
 LOAD = 175 N/m
 PEL = 0.028 mm
 (Fig. 6c)
 ---- LOST CONTACT ZONE

Figure 28 - Effect of Sinusoidal Error on ISG Mesh Stiffness

KG, would equal zero when these non-contacting zones due to errors occur. Sinusoidal errors of 0.013 mm (.0005 in.) on either the pinion or gear of the ISG drive caused non-contact zones and the resulting changes in mesh stiffness characteristics of Figure 28 due to its high torsional rigidity. In contrast, a torsionally flexible ESG drive was able to absorb the fault without affecting the mesh stiffness characteristics. [19]

The analysis procedure can also be used to investigate other surface fault-error combinations acting on both gears. For example, errors of Figure 16c caused mesh stiffness reductions over a longer span of the meshing cycle than were obtained when the identical error was on one gear only as in Figure 28. Thus, it must be concluded that each profile condition and mesh system flexibility will cause unique mesh stiffness patterns. The gear tooth contacts due to deflections do not coincide with the theoretical line of action. This results in noninvolute action producing variations in the transmission ratio, ΔTR . For the investigated cases in Tables 1 and 2, the trend in ΔTR for the ISG and ESG sets was the same. The magnitude of the ISG ΔTR was about 50% higher but not exceeding 2.7%. However, the transmission ratio of the ISG set is higher.

4.1.2.2 ISG Drives of Practical Interest

Review of the maximum stiffness, KG_{max} , in Table 1 reveals a 13% higher stiffness value for the torsionally stiff ISG drive which does not reduce significantly with changes in hub or ring radii changes. The reason for this small variation in stiffness can be attributed to the rather rigid internal gear ring. In order to reduce this circumferential stiffness of the ring, the rim thickness has to be reduced to 20% or less of the face width of the gear teeth. However, ISG drives of practical interest do not exhibit such small rim thicknesses in order

to minimize deflections in the radial direction (Figures 3 and 4). The inference is that ISG drives will be inherently stiffer than ESG drives and, because of their closely matched contours, will be less tolerant to sinusoidal imperfections or similar irregularities of the surface. This intolerance to surface irregularities can become limiting since grinding of the internal teeth is not practical.

4.1.2.3 Effects of Radial Deflection on Static Performance

Radial deflections due to bearings, shafts, pinion hub and gear ring cause radial movement of the gears in the rotating plane with a resultant reduction of contact length of the gears. This fact can readily be deduced from a plot of contact ratio versus radial deflections (Figure 29). The plot indicates a sharp reduction of contact ratio with small radial deflections. At .025 mm (.001 in.) radial deflection, the reduction of contact ratio levels off and reaches the theoretical contact ratio, CR_T of 2.625 at a radial deflection of 0.05 mm (.002 in.). Additional radial deflection causes the contact ratio to drop below the CR_T . For the gear and loading combination of Figure 29 practical combined bearing, shaft, pinion hub and gear ring deflections can be held to 0.05 mm (.002 in.). Thus, it appears that the actual loaded contact ratio probably will not exceed the CR_T because of the ever present radial deflection unless design and assembly practice offsets the radial deflection with an equal amount of reduction in center distance. It is interesting to note that the combined circumferential deflection of the two ISG drive gears of Figure 29 has a significantly greater and opposite effect on contact ratio than does the radial deflection.

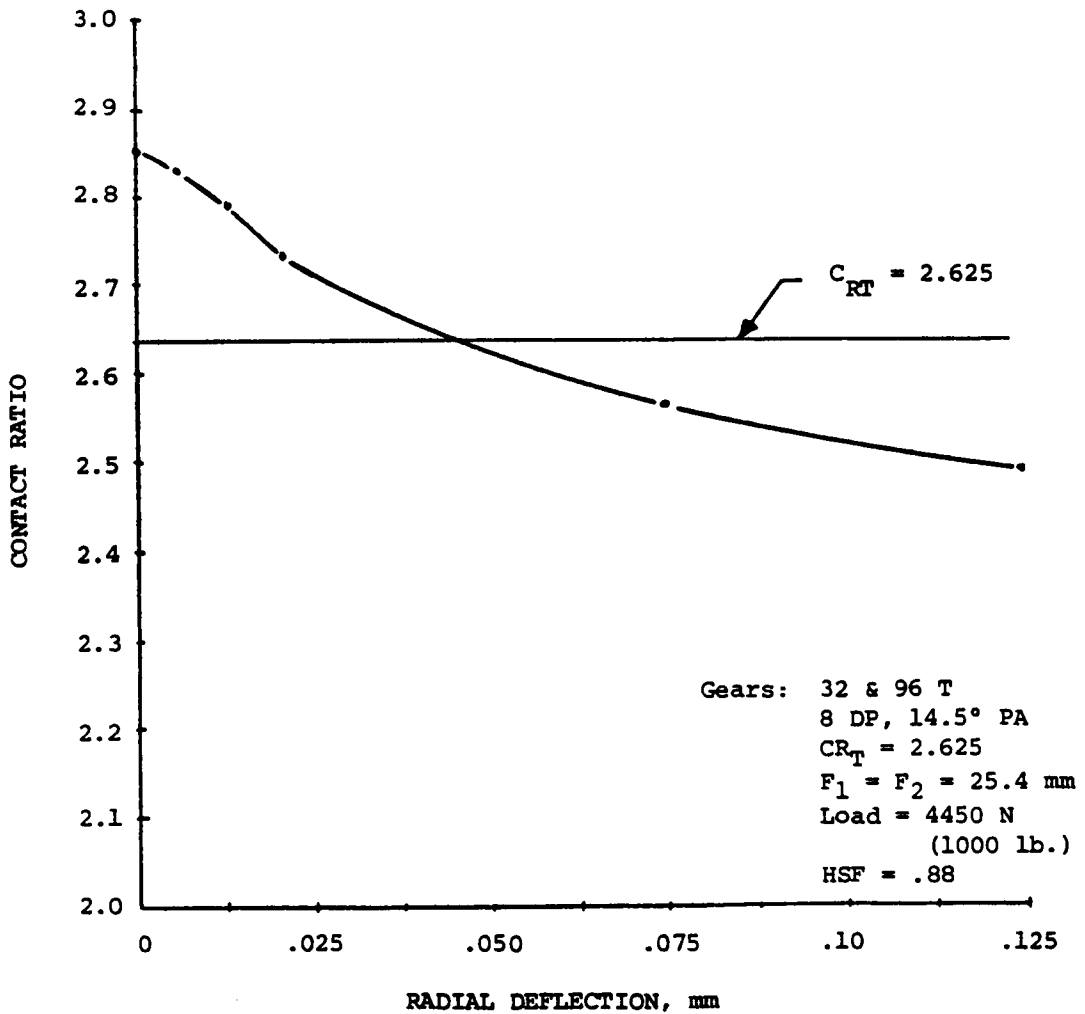


Figure 29 - Effect of Radial Deflection of ISG Drive on Contact Ratio

For the load condition of Figure 29, the two deflections offset each other at a radial deflection of .05 mm (.002 in.) and a corresponding maximum circumferential deflection of .015 mm (.0006 in.).

The contact search for radial deflections of 0.025 mm or less can be accomplished with the contact search method as discussed in Section 3.4.4. For larger radial deflections the contact search method was changed to include non-uniform rotation ("wiggling") for establishing of the limiting mesh points.

4.1.3 Dynamic Analysis

The gear train of Figure 22 was modeled for the dynamic analysis. The solution of the dynamic equations of motion (equations 21 through 24) leads to dynamic loads which depend on the magnitudes of the mass moments of inertia of all elements, shaft stiffness, transmitted loads, gear mesh stiffness characteristics, damping in the system, amount of backlash and speed.

4.1.3.1 Comparison of ISG and ESG Drive Dynamic Performance

For comparison purposes, identical geometry and operating conditions were applied to the ISG drive model of Figure 22 and the ESG drive model.^[19] Figures 30 and 31 show the results of a series of analyses on error-less ISG and ESG gear trains using low and high stiffnesses for the shafts and teeth supports and varying amounts of damping. Review of the resulting curves indicates a smoother performance in terms of lower peak dynamic factors for the ISG drive.

Figure 32 demonstrates the dramatic effect of severe mesh stiffness interruptions due to sinusoidal errors on dynamic performance. For this type of error the two drives exhibit similarly violent

dynamic fluctuations. The performance of the ISG versus ESG drive due to the effect of a surface pit is considerably smoother (Figure 33). In this error condition, locating the pit on either the pinion or gear of the ISG drive had little effect on performance.

There is a requirement for a minimum amount of damping to prevent the Mathieu-Hill type instabilities.^[9] For the considered ISG drive of 32 and 96 gear teeth, there was no such instability encountered within the operating range of 0 to 12,000 rpm with $\xi_G = .05$ and $\xi_S = .005$. Because of the large support bearing of the ring gear (Figures 3 and 4) the combined bearing and gear mesh damping, ξ_G , is probably near .15, and thus Mathieu-Hill instabilities are unlikely to be encountered with ISG drives.

The ISG analysis procedure has the capability for analyzing the distribution of the dynamic loads, dynamic factors (Figures 30 through 33), load sharing, contact Hertz stress (P_H), contact stress-sliding velocity product (PV) and maximum tooth bending stress for the entire meshing zone. Figures 34 and 35 show the range of the maximum P_H and maximum PV values corresponding to the dynamic conditions illustrated in Figures 30 and 33. In general, the higher contact ratio ISG drive appeared to show lower values.

Figure 36 shows the maximum tensile tooth bending stress versus all fifty gear mesh positions for the static and the 8000 rpm operating condition of the ISG drive depicted in Figure 30, case d. As expected, the pinion shows higher stress values both for the static and dynamic condition. The peak stress values occur in the gear mesh position range from 14 to 18 and 33 to 38. These gear mesh positions represent the change over from three to two tooth contact. Figures 37 and 38 show the stress pattern for the ESG drive.

Gears: 32 & 96 T, 8 DP, 14.5° PA, NO ERRORS
 LOAD 175 N/mm

System: $J_D = 0.011, J_{G1} = 0.00021$ m²-kg
 $J_L = 0.011, J_{G2} = 0.017$ m²-kg
 $\xi_S = .005; \xi_G = 0.05$

Curves: a. EXTERNAL-EXTERNAL } HSF = .65; $K_{DS} = 8400$,
 b. EXTERNAL-INTERNAL } $K_{LS} = 36400$ N.m/rad
 c. EXTERNAL-EXTERNAL } HSF = 1.0; $K_{DS} = 102,000$,
 d. EXTERNAL-INTERNAL } $K_{LS} = 102,000$ N.m/rad

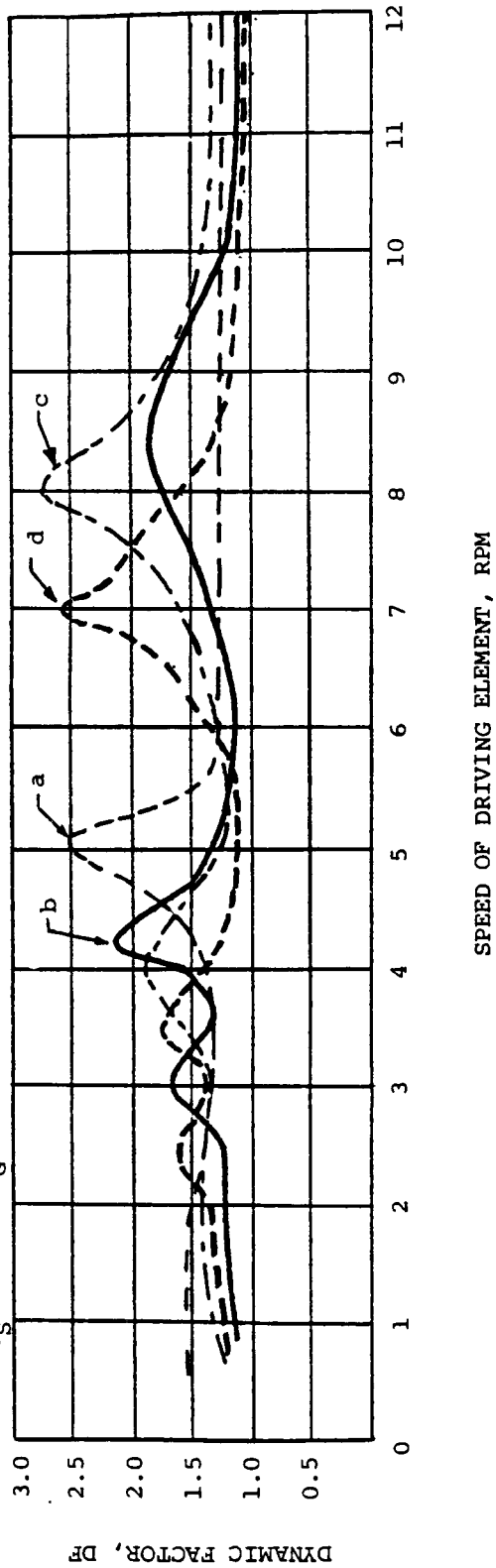


Figure 30 - System Flexibility Effects on Dynamic Factors of Error-Less ISG and ESG Drives

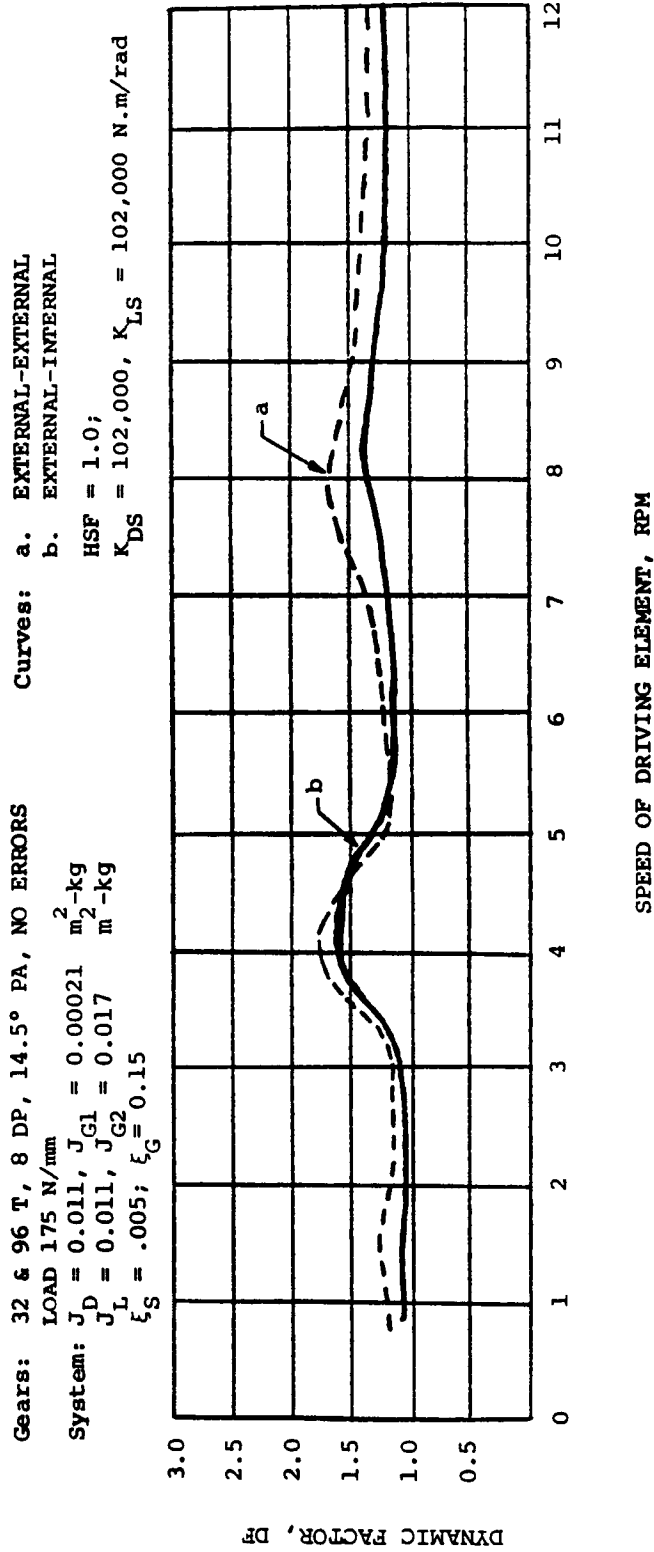
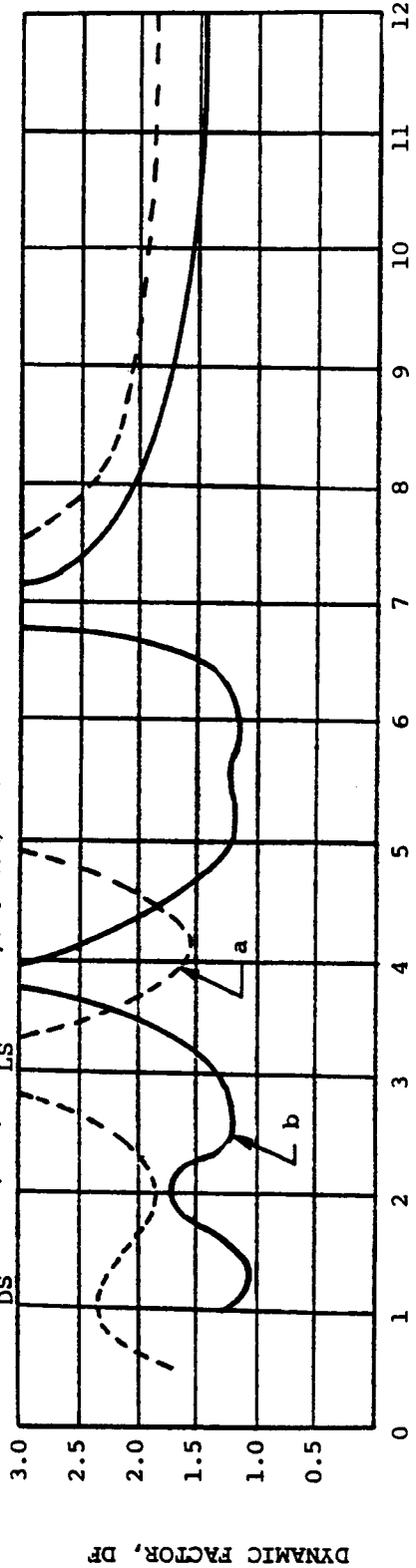


Figure 31 - Effect of High Damping on Dynamic Factors of Error-Less ISG and ESG Drives

Gears: 32 & 96 T, 8 DP, 14.5° PA, HSF = 1.0
 LOAD = 175 N/mm, $\delta_s = 0.005$, $\delta_2 = .05$
 System: $J_D = 0.011$, $J_{G1} = 0.00021$ m²-kg
 $J_L = 0.011$, $J_{G2} = 0.017$ m²-kg
 $K_{DS} = 102,000$; $K_{LS} = 102,000$ N.m/rad

Curves: PE1 = 0.27 mm (1 CYCLE)
 a. EXTERNAL-EXTERNAL (ESG)
 b. EXTERNAL-INTERNAL (ISG)



SPEED OF DRIVING ELEMENT, RPM

DYNAMIC FACTOR, DF

Figure 32 - Influence of Sinusoidal Error on Dynamic Factors for ISG and ESG Drives

Gears: 32 & 96 T, 8 DP, 14.5° PA, HSF = 1.0
 LOAD = 175 N/mm, $\xi_g = 0.005$, $\xi_G = 0.05$
System: $J_D = 0.011$, $J_{G1} = 0.00021$ m²-kg
 $J_L = 0.011$, $J_{G2} = 0.017$ m²-kg
 $K_{DS} = 102,000$; $K_{LS} = 102,000$ N.m/rad

Curves: PIT 0.5 mm WIDE, 0.25 MM DEEP
 a. PIT ON GEAR OF EXTERNAL-EXTERNAL GEARS
 b. PIT ON PINION OF EXTERNAL-INTERNAL GEARS
 c. PIT ON GEAR OF EXTERNAL-INTERNAL GEARS

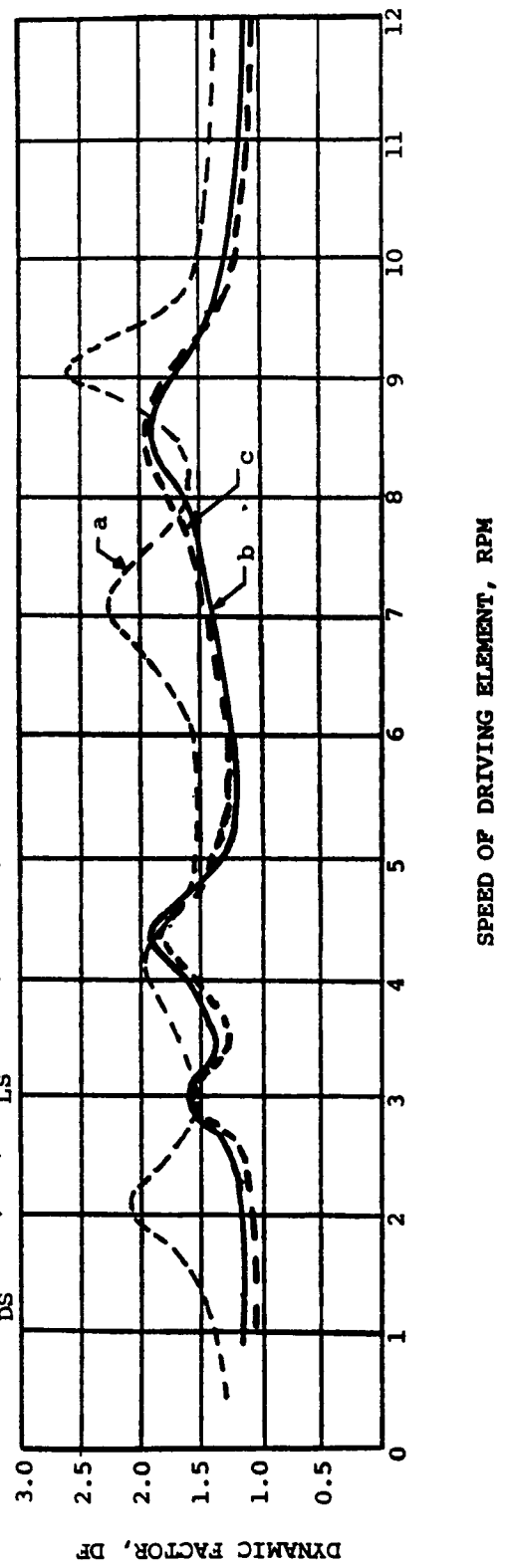


Figure 33 - Influence of Pit on Dynamic Factors for ISG and ESG Drives

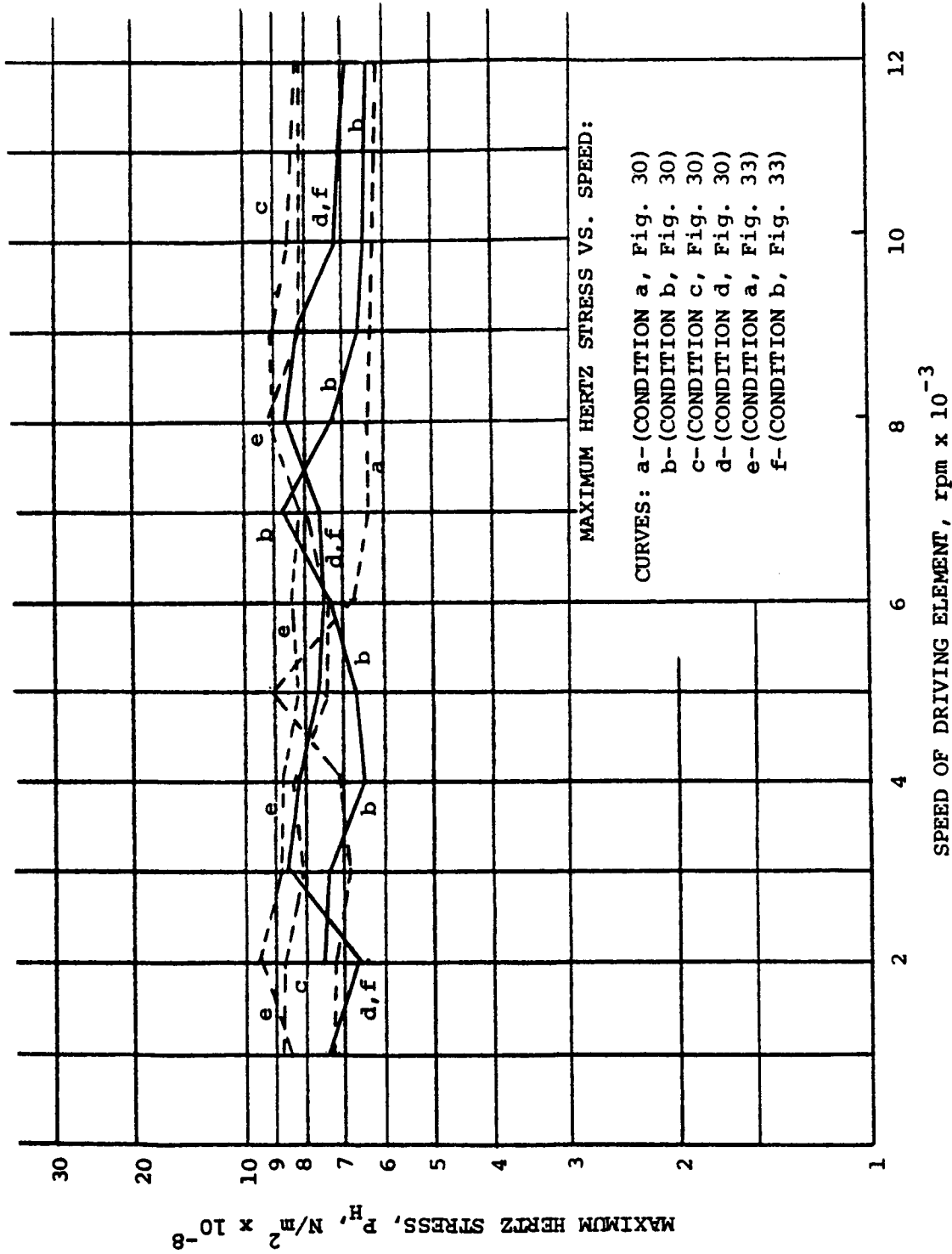


Figure 34 - Maximum Hertz Stress in Contact Zone for Various ISG and ESG Operating Conditions

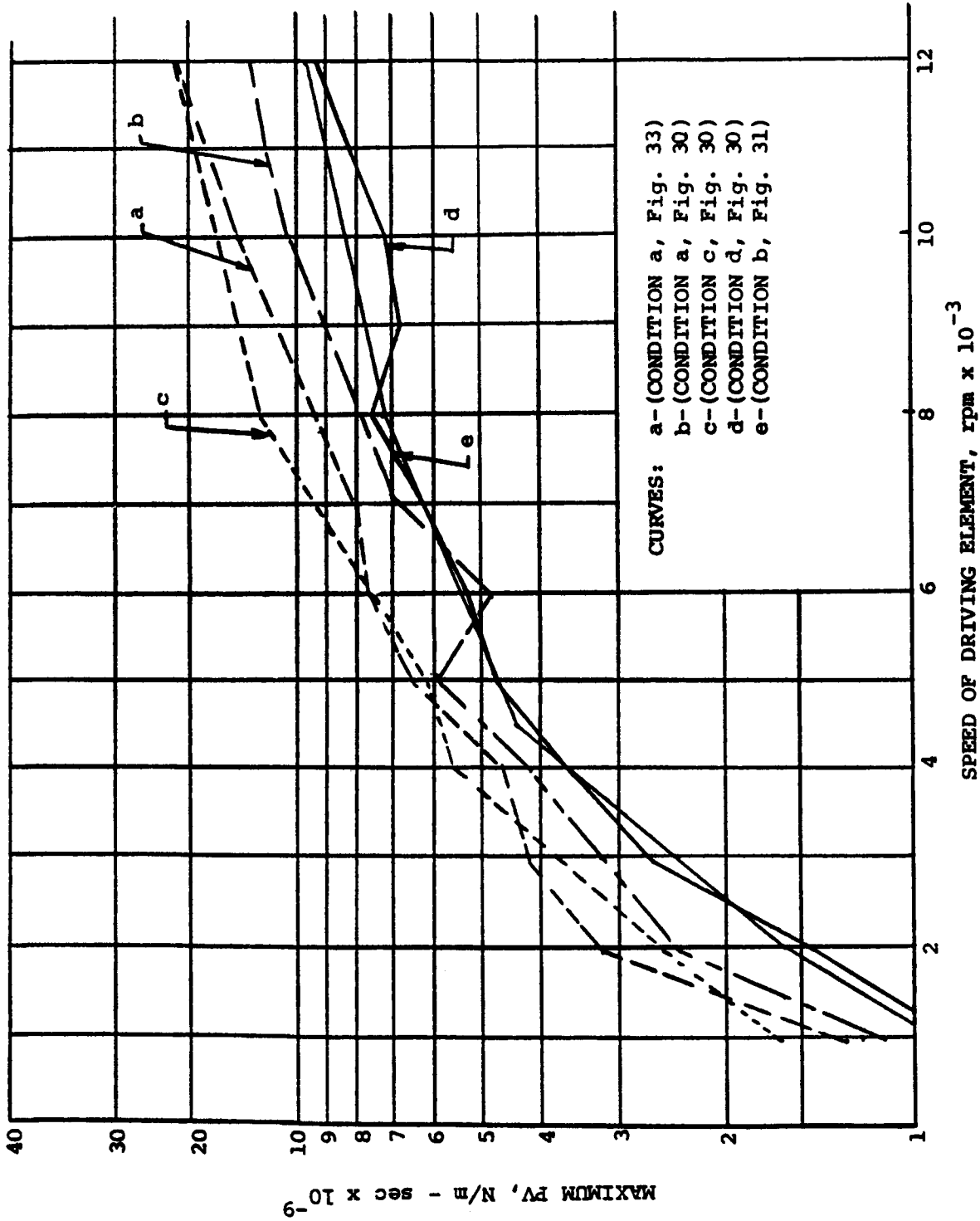


Figure 35 - Maximum Product of Hertz Stress and Sliding Velocity in Contact Zone for Various ISG and ESG Drives

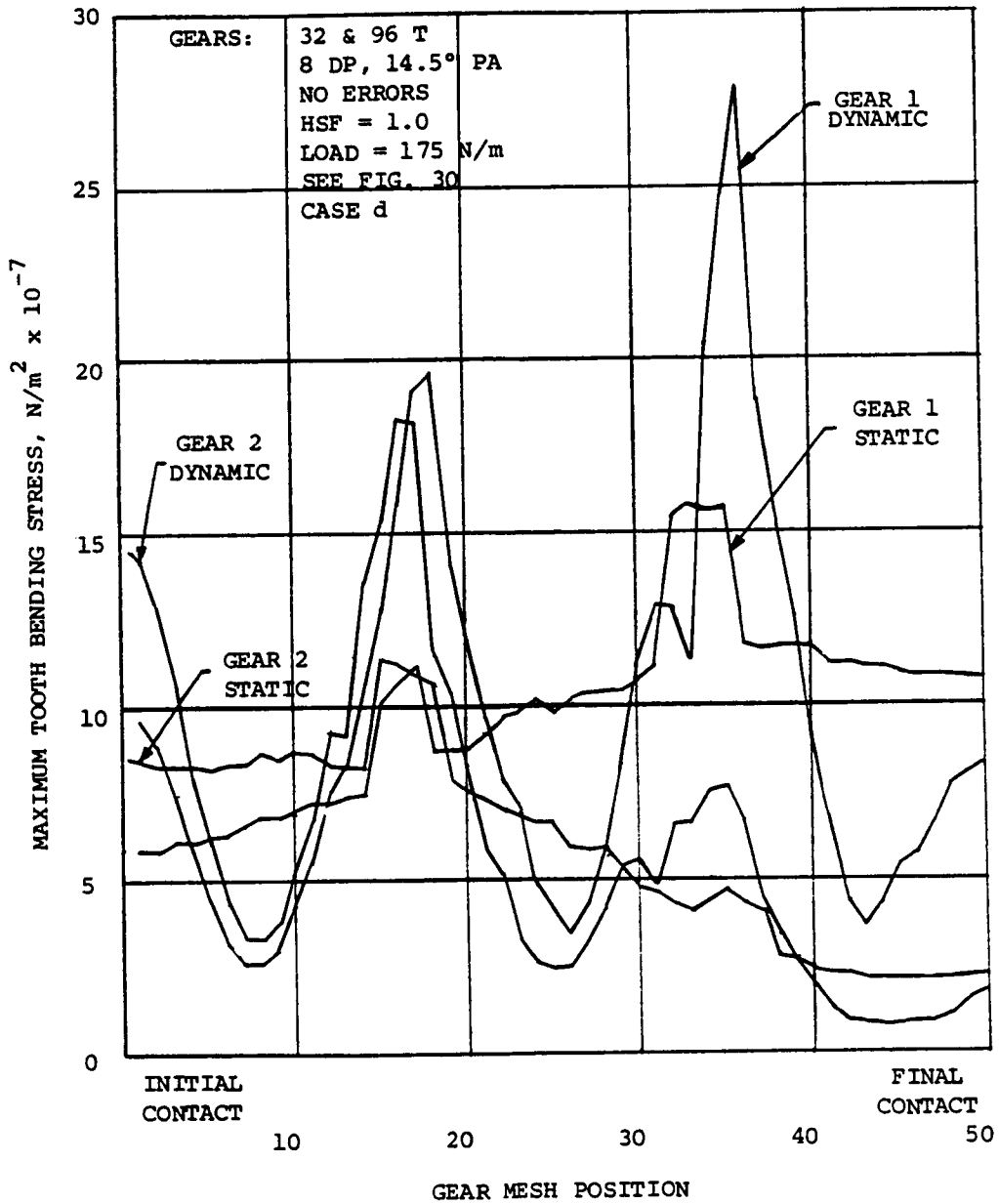


Figure 36 - Maximum Tooth Bending Stress Versus Gear Mesh Position for the Static and 8000 rpm Operating Condition of the ISG Drive

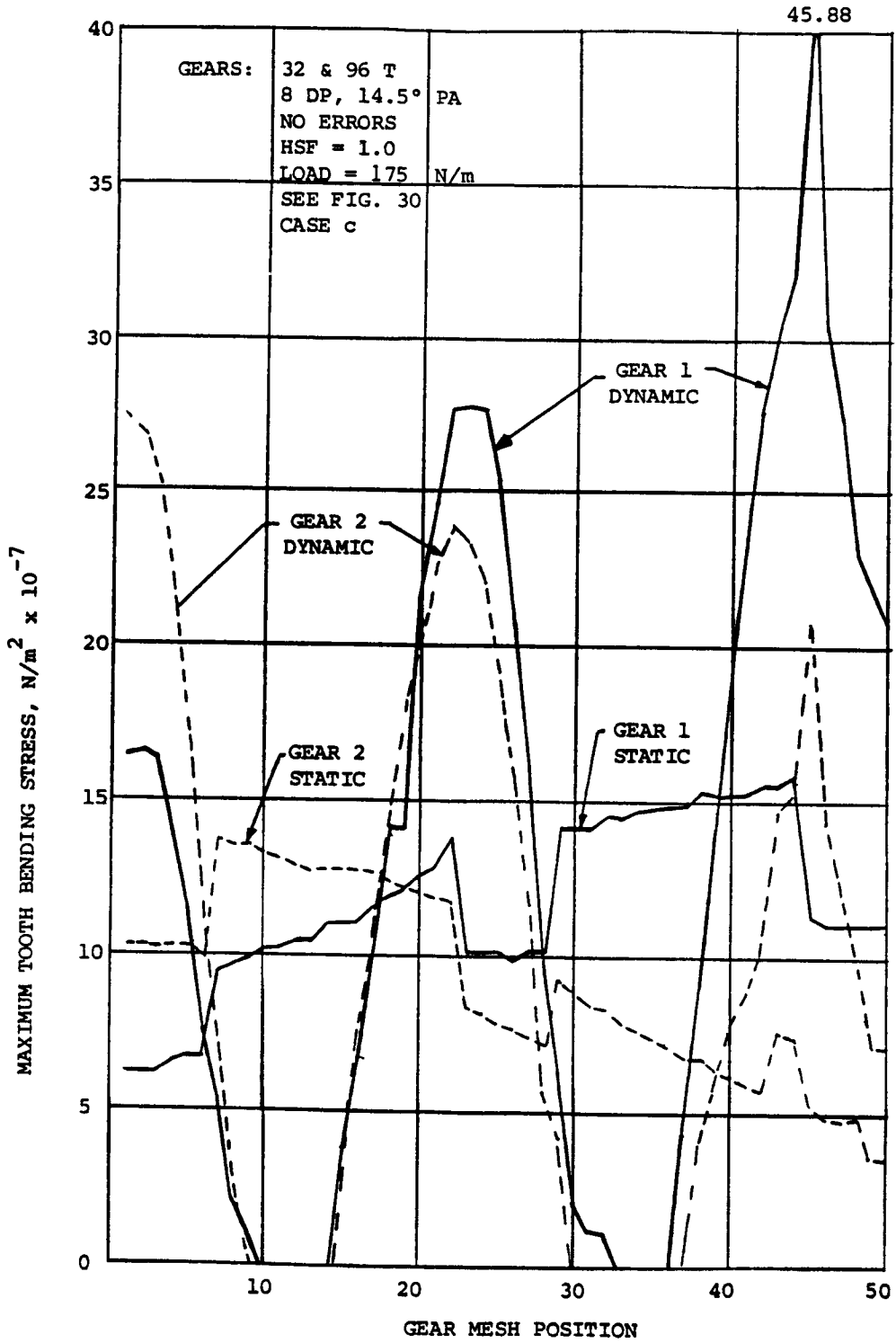


Figure 37 - Maximum Tooth Bending Stress Versus Gear Mesh Position for the Static and 8000 rpm Operating Condition of the ESG Drive

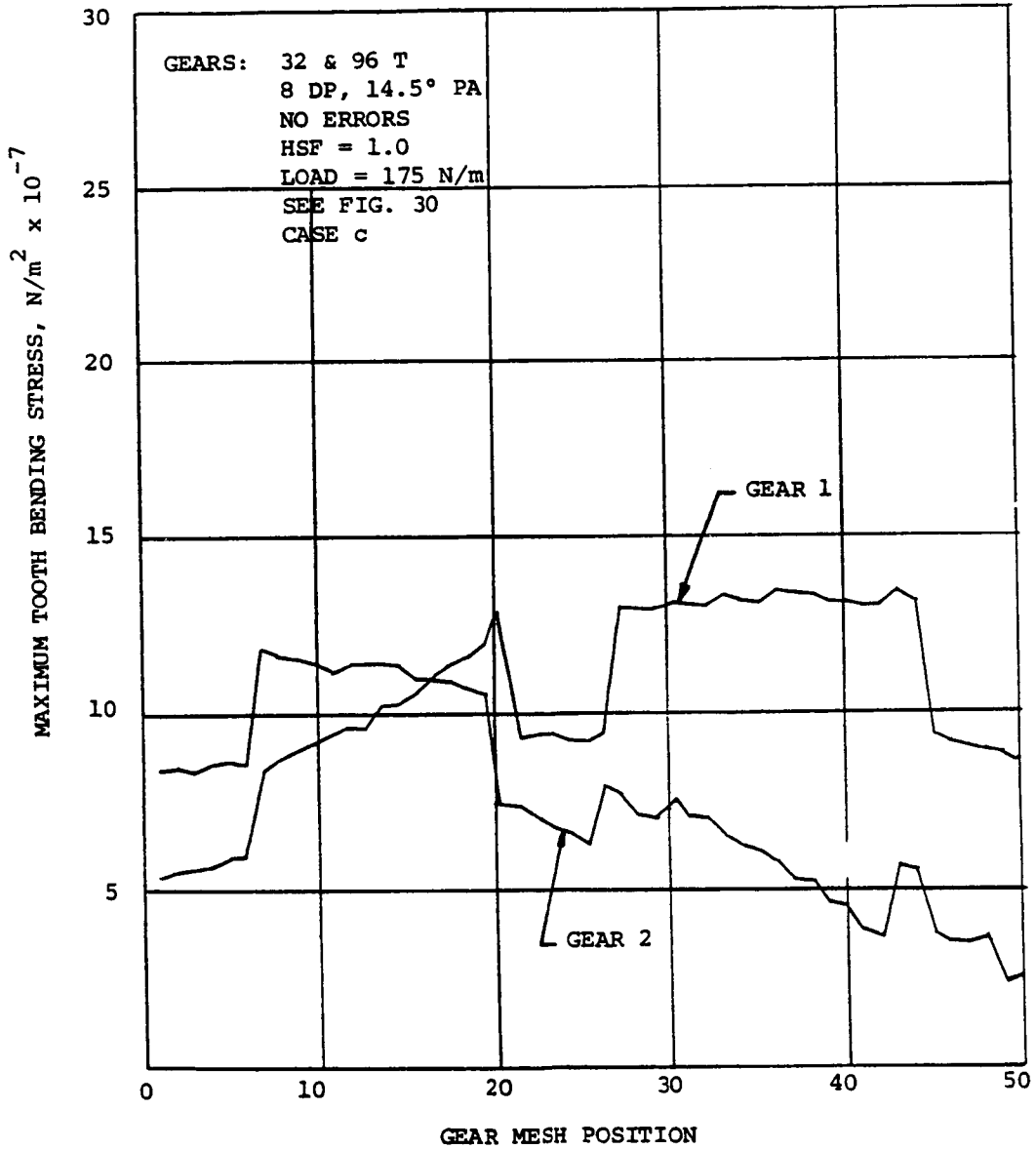


Figure 38 - Maximum Tooth Bending Stress Using AGMA Formula Versus Gear Mesh Position for the Static Operating Condition of the ESG Drive

4.1.3.2 ISG Drives of Practical Interest

For similar construction, ISG drives are torsionally stiffer than ESG drives because of the large outside diameter of the internal gear. Thus, the torsionally soft case of $HSF = .65$ and mass moment of inertia, $J_{G2} = 0.017 \text{ m}^2\text{-kg}$ (Figures 30 through 33), can only be achieved with a severe reduction of the internal gear rim thickness (Figures 3 and 4). The dynamic load factors of ISG drives of practical interest with various mass moments of inertia, J_{G2} , and different gear mesh and shaft stiffnesses are shown in Figure 39. For the four cases investigated, the best performance, in terms of lowest gear dynamic load factors, was obtained for the ISG drive of high mass moment of inertia, high shaft stiffness and low torsional stiffness, $HSF = .88$. The ESG drive of equal shaft stiffness, $HSF = 1.0$ (Figure 30, Curve c) exhibited the highest dynamic load factors. The results of the analysis of practical ISG drives demonstrates the need for tuning of the various constituent elements in the model of Figure 22. The general trend indicates smoother performance from ISG drives of practical interest versus similar ESG drives.

4.1.3.3 Effect of Radial Deflection on Dynamic Performance

Figure 40 shows three cases of ISG drives subject to different radial deflections. Review of the results shows larger dynamic load factors with increase in radial deflection. The performance of the ISG drives exhibits considerable missing and "backhitting" of the gear teeth similar to the performance of gears with sinusoidal profile errors. Significant reduction of the dynamic load factors was evident with increase in gear mesh damping.

Gears: 32 & 96 T

8 DP, 14.5° PA

LOAD = 175 N/m

NO ERRORS

System: $J_D = 0.011$, $J_{G1} = 0.00021 \text{ m}^2\text{-kg}$

$J_L = 0.011 \text{ m}^2\text{-kg}$

$\zeta_S = 0.005$, $\zeta_G = 0.05$

Curves: ISG DRIVES,

$K_{DS} = K_{LS} = 102,000 \text{ N-m/RAD COMMON}$

TO CURVES a, b & c

a. $J_{G2} = 0.026 \text{ m}^2\text{-kg}$, HSF = .65

b. $J_{G2} = 0.026 \text{ m}^2\text{-kg}$, HSF = 1.0

c. $J_{G2} = 0.017 \text{ m}^2\text{-kg}$, HSF = 1.0

d. $J_{G2} = 0.026 \text{ m}^2\text{-kg}$, HSF = 1.0

$K_{DS} = 8400$; $K_{LS} = 36,400 \text{ N-m/RAD}$

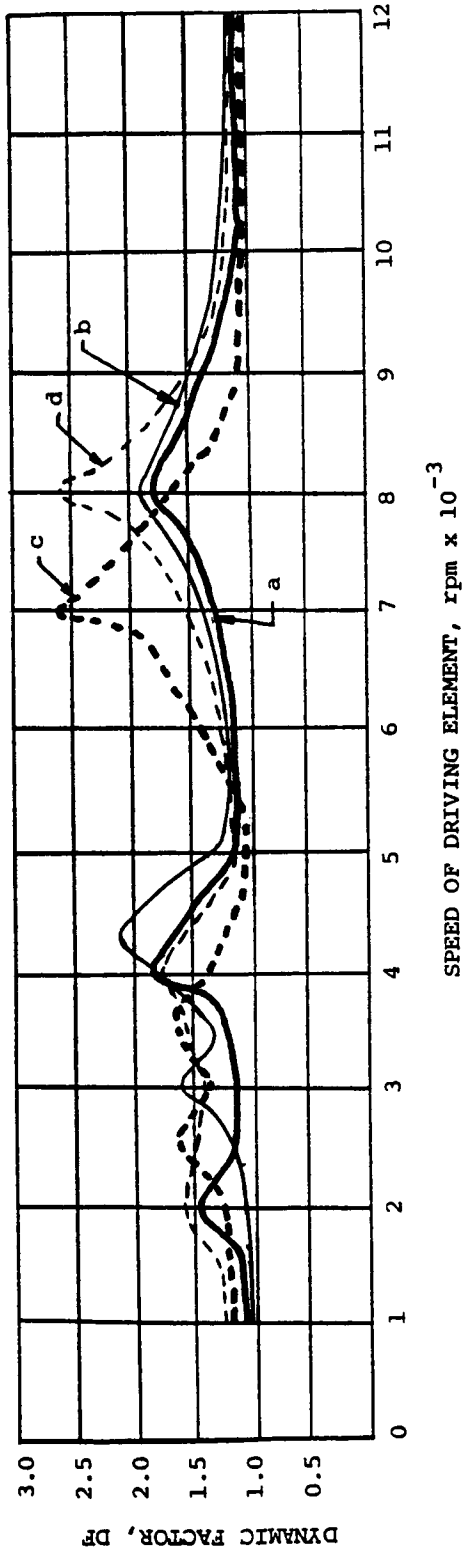


Figure 39 - Dynamic Load Factors for Various ISG Configurations

Gears: 32 & 96 T, 8 DP, 14.5° PA
 LOAD = 175 N/m, NO ERRORS

System: $J_D = 0.011$, $J_{G1} = 0.00021$ m²-kg
 $J_L = 0.011$ m²-kg
 $\xi_S = 0.005$

Curves: ISG DRIVES
 $J_{G2} = 0.026$ m²-kg
 $K_{DS} = K_{LS} = 102,000$ N-m/RAD
 $HSP = 0.88$

a. RADIAL DEFLECTION, $\delta_R = .076$ mm, $\xi_G = .05$
 b. $\delta_R = .076$ mm, $\xi_G = .15$
 c. $\delta_R = .023$ mm, $\xi_G = .05$

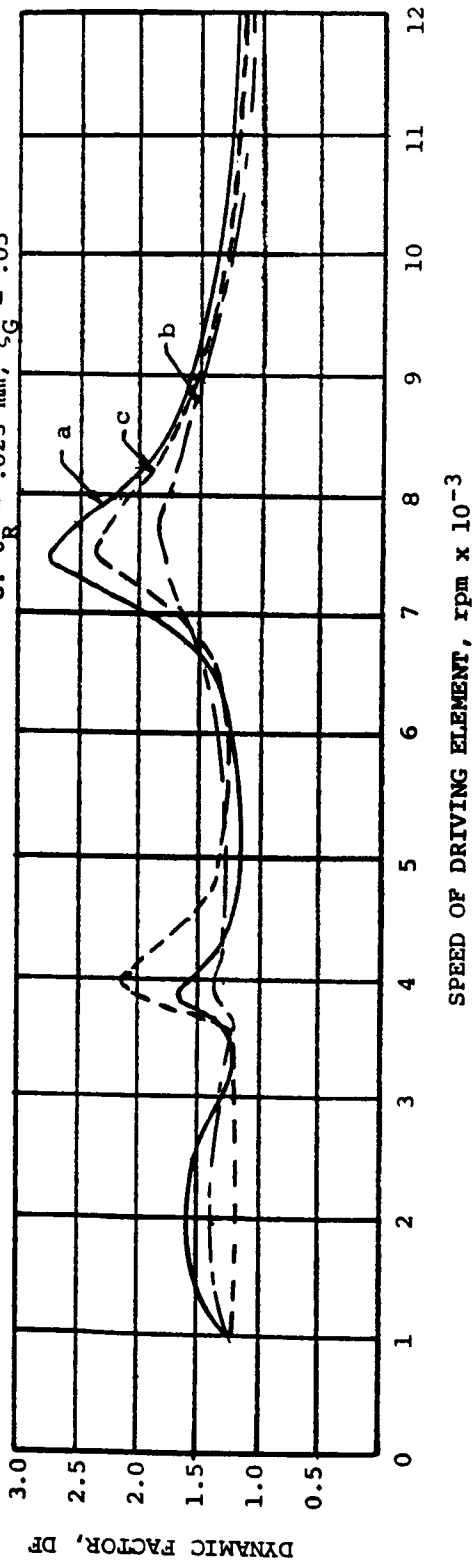


Figure 40 - Effect of Various Radial Deflections and Gear Mesh Damping Ratio on Dynamic Load Factors of ISG Drives

4.2 SUMMARY AND CONCLUSIONS

A new methodology has been developed for the static and dynamic load and stress analysis of the internal spur gear (ISG) drive. Prior to this report, there were no established methods for the above analyses. The currently published design techniques for ISG drives reflect the technology of the 1950's.

The analysis procedure is applicable to involute profiles and minor deviations from this profile as a result of modifications, imperfections and circumferential deflections. Because of the potential noninvolute profile and the effect of radial deflection on tooth position, an iterative procedure is used to calculate the statically indeterminate problem of multi-tooth contacts, circumferential deflection and contact ratio. The developed method can be used in gear combinations leading up to and exceeding the "very high contact ratio" (VHCR) of three. The static analysis can also be adapted for determining the gear mesh stiffness of a planet and ring gear assembly. For this adaptation it is necessary to supply the ring gear stiffness relying on strength of materials, finite element or experimental means. The maximum tooth bending stress of the external and internal gear is determined by "Cornell's method". This method is a modification of the empirical formula for stress of loaded projections based on photoelastic experiments by Heywood.

The new methodology was computerized with the computer package consisting of three modules which perform the static, dynamic and stress analyses respectively. The output from the three modules includes the static and dynamic loads, variations in transmission ratio, sliding velocities, maximum contact pressures and tooth bending stress

acting on the gear teeth at the fifty mesh positions. The results of the parametric computer studies yielded the following conclusions:

1. For equal geometries, the ISG drive achieves higher contact and transmission ratios than the ESG drive. For the investigated 32 and 96 tooth combination, the heavily loaded ISG drive reached the "very high contact ratio" of three. The unloaded or theoretical contact ratio is 2.625.
2. Because of the high contact ratio and the concave-convex tooth contours, the ISG drive is able to absorb pits across the surface better than ESG drives. However, the opposite effect is encountered when sinusoidal or similar surface irregularities are present.
3. ISG drives tend to be torsionally stiffer and heavier than ESG drives because of the large internal gear. Nevertheless, when both systems are sized optimally, then the ISG drive performance in terms of peak dynamic loading is better.
4. Radial deflections of shafts, bearings and gears reduce the contact ratio of ISG and presumably ESG drives. The effect on mesh stiffness is minor but the pattern is changed. The dynamic loading increases with radial deflection.
5. The dynamic factors of ISG drives can be reduced with increases in damping ratio. This effect is also evident in drives experiencing radial deflections.
6. The maximum product of Hertz stress and sliding velocity

is consistently lower than the ESG drive. The maximum Hertz stress performance is distorted because of the different peak dynamic loading of the various cases that were investigated. In general, the maximum Hertz stress appears lower also for the ISG drive. Peak bending stress of the pinions were the same whereas the gear of the ISG drive experienced an 18% lower stress value.

The derived new analysis procedure has established a method exclusively for the analysis and prediction of dynamic performance of the internal-external spur gear set. The list of advantages, as derived from this study, of the ISG drive over the ESG drive is quite impressive, and should lead to renewed interest in applying the ISG drives in advanced transmissions.

Recommendations for future work might include a finite element method for the ring gear deflections and an efficient contact search technique which would satisfy the intentionally built-in large radial deflections such as found in the planetary gear rings.

BIBLIOGRAPHY

1. Buckingham, E., "Analytical Mechanics of Gears", Dover Publications, Inc., N. Y. (1949).
2. Tuplin, W. A., "Dynamic Loads on Gear Teeth", Machine Design, p. 203 (Oct. 1953).
3. Attia, A. Y., "Dynamic Loading of Spur Gear Teeth", Journal of Engineering for Industry, ASME Transactions, Vol. 81, Ser. B, p. 1 (Feb. 1959).
4. Reswick, J. B., "Dynamic Loads on Spur and Helical - Gear Teeth", Transactions of American Society of Mechanical Engineers, Vol. 77, p. 635 (July 1954).
5. Nieman, G., and Rettig, H., "Error Induced Dynamic Gear Tooth Loads", Proceedings of the International Conference on Gearing, p. 31 (1958).
6. Harris, S. L., "Dynamic Loads on the Teeth of Spur Gears", Proceedings of the Institution of Mechanical Engineers, London, Vol. 172, p. 187 (1958).
7. Munro, R. G., "The Dynamic Behavior of Spur Gears", Unpublished Ph.D. Dissertation, University of Cambridge, England (1962).
8. Richardson, H. H., "Static and Dynamic Load, Stress and Deflection Cycles in Spur-Gear System", Unpublished Ph.D. Dissertation, Massachusetts Institute of Technology (1958).
9. Kasuba, R., "An Analytical and Experimental Study of Dynamic Loads on Spur Gear Teeth", Unpublished Ph.D. Dissertation, University of Illinois (1962).
10. Bollinger, J. G., "Darstellung Des Dynamischen Verhaltens Eines Nichtlinearen Zahnrad - Getriebesystems Auf Dem Analogrechner", Industrie Anzeiger, Nr. 46, S. 961 (June 7, 1963).
11. Baud, R. V., and Pederson, R. E., "Load and Stress Cycle in Gear Teeth", Mechanical Engineering, Vol. 51, pp. 653-662 (1929).
12. Walker, H., "Gear Tooth Deflection and Profile Modification", The Engineer, Vol. 166, pp. 409-412 and 434-436 (1938).
13. Weber, C., "The Deformation of Loaded Gears and the Effect on Their Load Carrying Capacity", Sponsored Research (Germany), British Department of Scientific and Industrial Research, Report No. 3 (1949).
14. Attia, A. Y., "Deflection of Spur Gear Teeth Cut in Thin Rims", ASME Paper No. 63-WA-14 (1964).

15. Cornell, R. W., "Compliance and Stress Sensitivity of Spur Gear Teeth", ASME Paper No. 80-C2/Det-24 (1980).
16. Premilhat, A., Tordion, G. V., and Baronet, C. N., "An Improved Determination of the Elastic Compliance of a Spur Gear Tooth Acted on by a Concentrated Load", Journal of Engineering for Industry, ASME Transactions, pp. 382-384 (May 1974).
17. Chabert, G., Dang Tran, T., and Mathis, R., "An Evaluation of Stresses and Deflection of Spur Gear Teeth Under Strain", Journal of Engineering for Industry, ASME Transactions, pp. 85-93 (Feb. 1974).
18. Cornell, R. W. and Westervelt, W. W., "Dynamic Tooth Loads and Stressing for High Contact Ratio Spur Gears", ASME Paper No. 77-Det-101 (1977).
19. Kasuba, R., and Evans, J. W., "An Extended Model for Determining Dynamic Loads in Spur Gearing", ASME Paper No. 80-C2/Det-90 (1980).
20. Dudley, D. W., "Gear Handbook", McGraw-Hill Book Company (1962).
21. George, W. Michael, "Precision Gearing - Theory and Practice", John Wiley & Sons, Inc. (1966).
22. Karas, F., "Elastische Formänderung und Lastverteilung Beim Doppeleingriff Gerader Stirnradzähne, V.D.I. Forschungsheft 406, V. 12, p. 17 (Jan./Feb. 1941).
23. Ishikawa, N., Bulletin T.I.T., Series A, No. 3 (1957).
24. Hidaka, T., Terauchi, Y., "Dynamic Behavior of Planetary Gear, Third Report", Bulletin of JSME, Vol. 20, No. 150 (Dec. 1977).
25. Sinkevich, Yu., B. and Sholomov, N., "Russian Engineering Journal", 51-6, p. 25 (1971-6).
26. Tedric, A. Harris, "Rolling Bearing Analysis", John Wiley & Sons, Inc. (1966).
27. Deutschman, Aaron D., Michels, Walter J., and Wilson, Charles E., "Machine Design Theory and Practice", MacMillan Publishing Co. (1975).
28. Franks, R. G. E., "Modeling and Simulation in Chemical Engineering", John Wiley & Sons, Inc. (1972).
29. Hahn, W. F., "Study of Instantaneous Load to Which Gear Teeth are Subjected", Unpublished Ph.D. Dissertation, University of Illinois (1969).

APPENDIX A

SPUR GEAR FORMULAE AND INVOLUTE PROFILE DEVELOPMENT

This Appendix lists standard spur gear geometry relations and develops the involute profile for the internal and external tooth. It forms the basis for the definition of the actual tooth profiles in Section 3.4.3.

A-1 Standard Spur Gear Relations for the ISG Drive

A-2 Development of the Involute Profile

A-1 STANDARD SPUR GEAR RELATIONS^[20] FOR THE ISG DRIVEDefinitions

P = diametral pitch	F = face width
M = module	B = backlash
r = pitch radius	ϕ_n = normal pressure angle
r_o = outside radius	ϕ = pressure angle
r_r = root radius	θ = involute polar angle
r_a = addendum radius	γ = angle between pitch point and center of tooth
r_d = dedendum radius	a = addendum
r_b = base circle radius	d = dedendum
r_l = limit radius	h_t = whole depth
r_f = fillet radius	ϵ = roll angle
r_T = edge radius of generating tool	u = interval of contact
N = number of teeth	m_G = gear ratio
C = center distance	m_p = contact ratio
p = circular pitch	T_{in} = input torque
p_b = base pitch	F_t = tangential load

Subscripts

1 = external gear	o = outside
2 = internal gear	r = root
b = base	t = tangent, total
F = fillet	T = tool
G = gear	p = pitch
l = limit	in = input
n = normal	

Standard Formulae

$$r = \frac{N}{2P} \quad \text{A-1}$$

$$C = r_2 - r_1 \quad \text{A-2}$$

$$p = \frac{\pi}{P} \quad \text{A-3}$$

$$P_b = p \cos \phi_n \quad \text{A-4}$$

$$R_f = 0.7 \left[r_T + \frac{(h_t + a - r_T)^2}{r + h_t - (a + r_T)} \right] \quad \text{A-5}$$

$$r_b = r \cos \phi_n \quad \text{A-6}$$

$$\phi = \cos^{-1} \frac{r_b}{r_a} \quad \text{A-7}$$

$$u_1 = -(r_2 - a_2) \sin \phi_2 + r_2 \sin \phi_n \quad \text{A-8}$$

$$u_2 = (r_1 + a_1) \sin \phi_1 - r_1 \sin \phi_n \quad \text{A-9}$$

$$\epsilon_1 = \frac{r_1 \sin \phi_n + u_2}{r_{b1}} \quad \text{A-10}$$

$$\epsilon_2 = \frac{r_2 \sin \phi_n + u_2}{r_{b2}} \quad \text{A-11}$$

$$r_{\ell_1} = \frac{r_{b1}}{\cos \phi_{\ell_1}} \quad \text{A-12}$$

$$r_{\ell_2} = \frac{r_{b2}}{\cos \phi_{\ell_2}} \quad \text{A-13}$$

$$m_p = \frac{u_1 + u_2}{P_b} \quad \text{A-14}$$

$$\epsilon = \tan \phi_n \quad \text{A-15}$$

$$\theta = \text{TAN } \phi_n - \phi_n \quad \text{A-16}$$

$$F_t = \frac{T_{in}}{r_b} \quad \text{A-17}$$

$$\gamma = \frac{\pi}{2N} \quad \text{A-18}$$

$$h_t = a + d \quad \text{A-19}$$

$$r_o = r + a \quad \text{EXTERNAL GEAR} \quad \text{A-20}$$

$$r_r = r - d \quad \text{EXTERNAL GEAR} \quad \text{A-21}$$

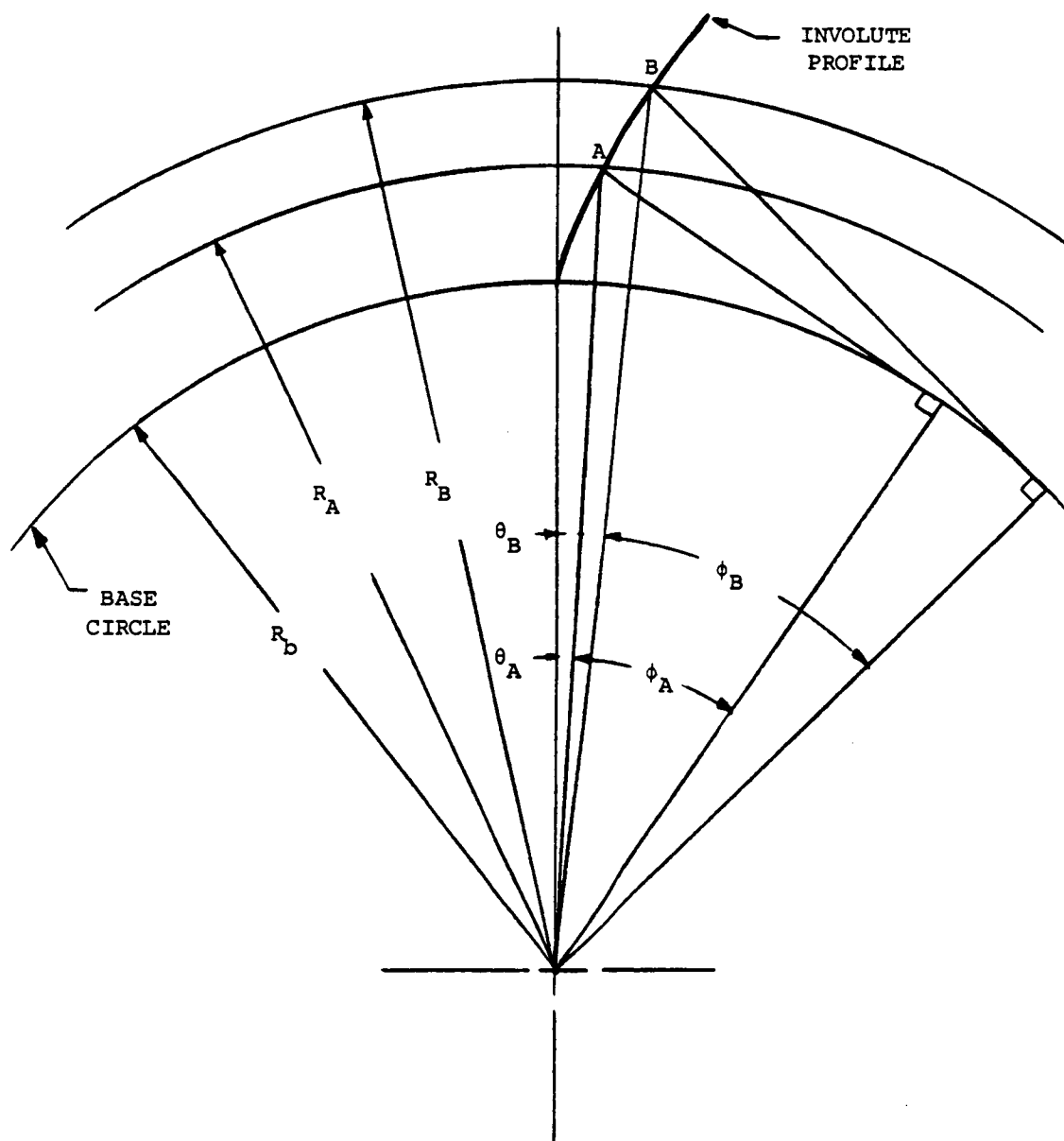
$$r_o = r - a \quad \text{INTERNAL GEAR} \quad \text{A-22}$$

$$r_r = r + d \quad \text{INTERNAL GEAR} \quad \text{A-23}$$

$$M = \frac{25.4}{P} \quad \text{A-24}$$

A-2 DEVELOPMENT OF THE INVOLUTE PROFILE

The construction of the involute spur gear tooth follows exact geometric relations as indicated by the standard formulae in Section A-1. Thus, from knowledge of a few parameters all the other parameters can be determined. General design practice starts with an assumption of the number of teeth, diametral pitch, addendum, working depth, fillet radius and pressure angle at the pitch point. The radial distance, R , to any point along the involute line is now determined from the base radius and the pressure angle at that point (see Figure A-1). The involute can then be drawn by connecting finely spaced radial points with straight lines. In the computer program either one or two hundred points are used depending on the size of the tooth. Any position between two points is determined by linear interpolation. The external and internal tooth have the same involute profile. The distinction between the two arises from the fact that their tooth center is either on the concave or convex side of the involute profile. Figures A-2 and A-3 respectively show the construction of the internal and external involute tooth along with the fillet configuration and the position of the local and global tooth coordinate system.



ROLL ANGLE, $\epsilon = \phi + \theta$

Figure A-1 - Involute Development

APPENDIX B

DEFLECTIONS

The radial and circumferential deflections of the external-internal gear support bearings, gear ring and teeth as discussed in Section 3.4.6 are summarized in this Appendix.

B-1 Bearing Deflections

B-2 Radial Ring Gear Deflections

B-3 Circumferential Deformation of Gear Teeth

B-3.1 Deflection of Point of Contact Due to Deformation
of Teeth

B-3.2 Deformation of the Teeth Due to Rotation of Their
Foundation

B-3.3 Deflection of the Teeth Due to Circumferential
Deformation of the Rim and Gear Ring

B-3.4 Hertzian Deformation at Contact Point

B-1 BEARING DEFLECTIONS

Rolling element bearings are preferred for their use in ISG drives because of their load carrying capacity, durability and low maintenance. The deflection in rolling element bearings is mainly due to Hertzian contact deformation. Because the maximum elastic contact deformation is dependent on the rolling element loads, it is necessary to analyze the load distribution occurring within the bearing prior to determination of the bearing deflection.

Harris [26] suggests an approximate solution for the maximum ball or roller load, Q_{\max} as:

$$Q_{\max} = \frac{5 F_r}{Z \cos \alpha} \quad \dots (B1-1)$$

where

F_r = radial load

Z = number of balls or rollers

α = contact angle

The deflection of a ball or roller bearing are respectively:

$$\delta_r = 1.58 \times 10^{-5} \frac{Q_{\max}^{2/3}}{D^{1/3} \cos \alpha} \quad \dots (B1-2)$$

$$\delta_r = 4.33 \times 10^{-6} \frac{Q_{\max}^{3/4}}{\ell^{1/2} \cos \alpha} \quad \dots (B1-3)$$

where

D = ball diameter

ℓ = length of roller

B-2 RING DEFLECTION

The ring gear of Figure 3 is subject to a single load which is reacted by an inclined roller bearing. The ring gear consists of the internal teeth, intermediate tooth support ring, outer ring and cylindrical support. Under load the intermediate and outer ring act rigidly and thus transfer the load uniformly into the support cylinder. This represents nearly cantilever loading and its deflection represents a "best possible" solution. In the extreme, the cylinder can be looked at as reacting to the equal and opposite loading of a ring. This deflection represents the "worst possible" condition.

The applicable equations for either ring deflection are:

Cantilever

$$\delta_r = \frac{F_r L^3}{3 EI} \quad \dots (B2-1)$$

where

$$I = \frac{\pi}{64} (D^4 - d^4) \quad \dots (B2-2)$$

D = outside diameter of cylinder

d = inside diameter of cylinder

Ring

$$\delta_r = .0745 \frac{F_r R^3}{EI} \quad \dots (B2-3)$$

where

R = mean diameter of cylinder

I = moment of inertia of ring cross-section

$$= \frac{b h^3}{12}$$

h = ring thickness

b = ring gear width

B-3 CIRCUMFERENTIAL DEFORMATION OF GEAR TEETH

B-3.1 Deflection of Point of Contact Due to Deformation of Teeth

Weber^[13] solved for the deflection at the point of application of an external gear tooth by equating the stress energy to the deforming work, $\frac{1}{2} P\delta$. In his formulation, the stress energy is composed of the partial energies due to the bending moment, the shearing force and the normal forces as seen in Figure B3-1.

$$\frac{1}{2} Q\delta = \frac{1}{2} \int_0^{Y_c} \frac{M^2}{EI} dy + \frac{1}{2} \int_0^{Y_c} \frac{V^2}{GFA} dy + \frac{1}{2} \int_0^{Y_c} \frac{N^2}{EA} dy \quad \dots (B3-1)$$

In Figure B3-1 the applied force Q is transferred to the center of the tooth resulting in an equivalent loading set

$$M = Q(Y_c - Y'_n) \cos \theta \quad \dots (B3-2)$$

$$V = Q \cos \theta \quad \dots (B3-3)$$

$$N = Q \sin \theta \quad \dots (B3-4)$$

and for this cantilever loading

$$I = \frac{1}{12} \ell (2x)^3 \quad \dots (B3-5)$$

$$A = \ell 2x \quad \dots (B3-6)$$

$$F = \frac{5}{6} \text{ for spur gear teeth} \quad \dots (B3-7)$$

if we replace, E by

$$G = \frac{E}{2(1 + \mu)} \quad \dots (B3-8)$$

and $\mu = 0.3$

then substitution and simplification leads to the expression for deflection at the point of contact

$$\delta = \frac{Q}{E} \cos^2 \theta \left[12 \int_0^{Y_c} \frac{(Y_c - Y)^2}{(2x)^3} dy + 3.12 \left(1 + \frac{\tan^2 \theta}{3.12} \right) \int_0^{Y_c} \frac{dy}{2x} \right] \quad \dots (B3-9)$$

In this equation x and y are the local coordinates of the involute or modified involute profile. By considering the digitized profile points of Figure B3-1, it is possible to solve for the deflection at the contact point by numeric integration. In this investigation the integration is carried out to the intersection of the fillet with the root radius, $RRCl$. Thus, a slight improvement over Weber's disregard of the fillet has been achieved.

Comparison of the more pronounced profile curvature of the external versus the internal gear tooth leads to the conclusion that Weber's solution equally applies to the internal tooth (see Figures B3-1 and B3-2). Equation B3-9 can be used for the deflection of the external or internal gear tooth by substituting the appropriate local coordinates for the respective tooth.

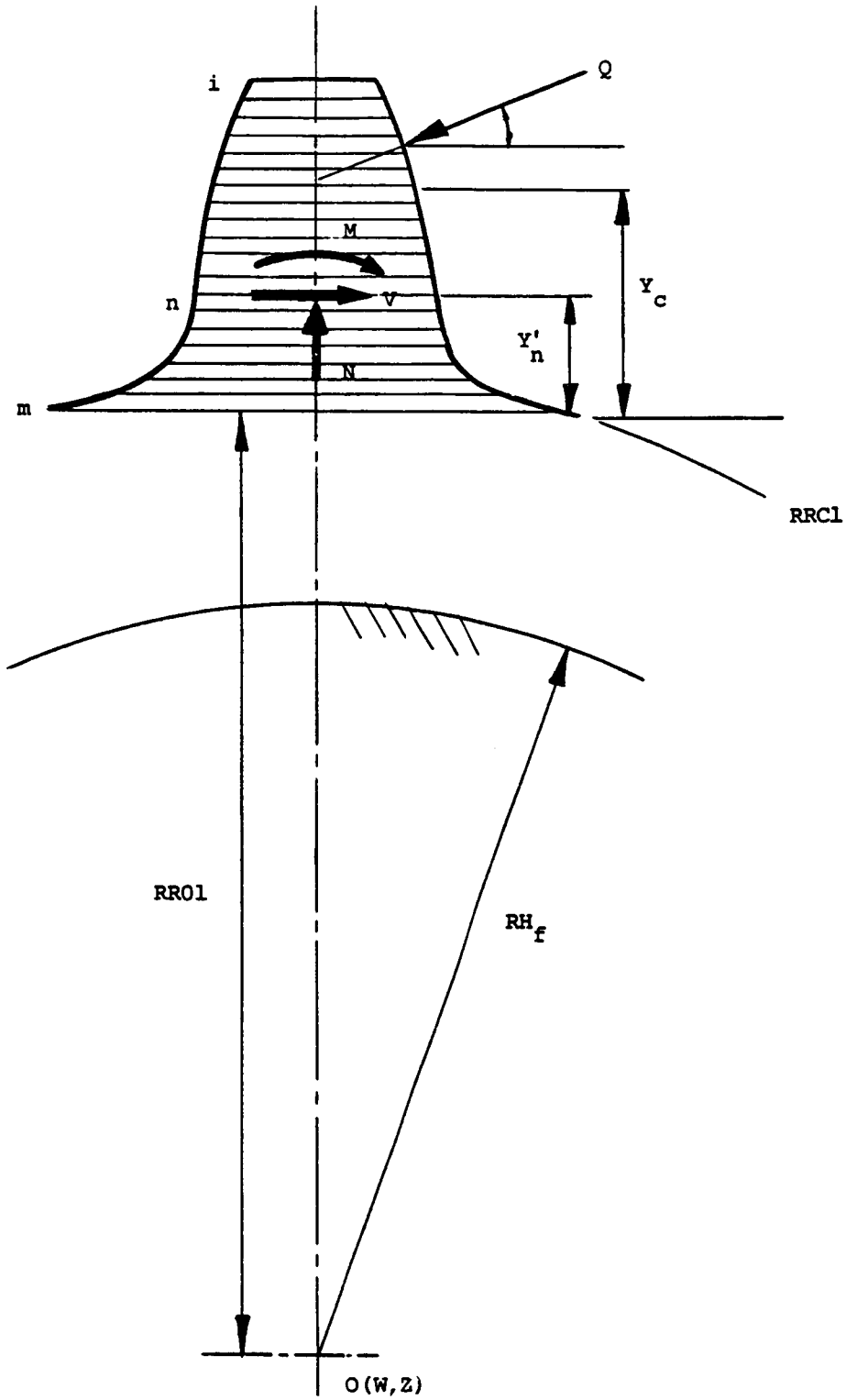


Figure B3-1 - External Gear Tooth Bending, Shear and Normal Deflection Model

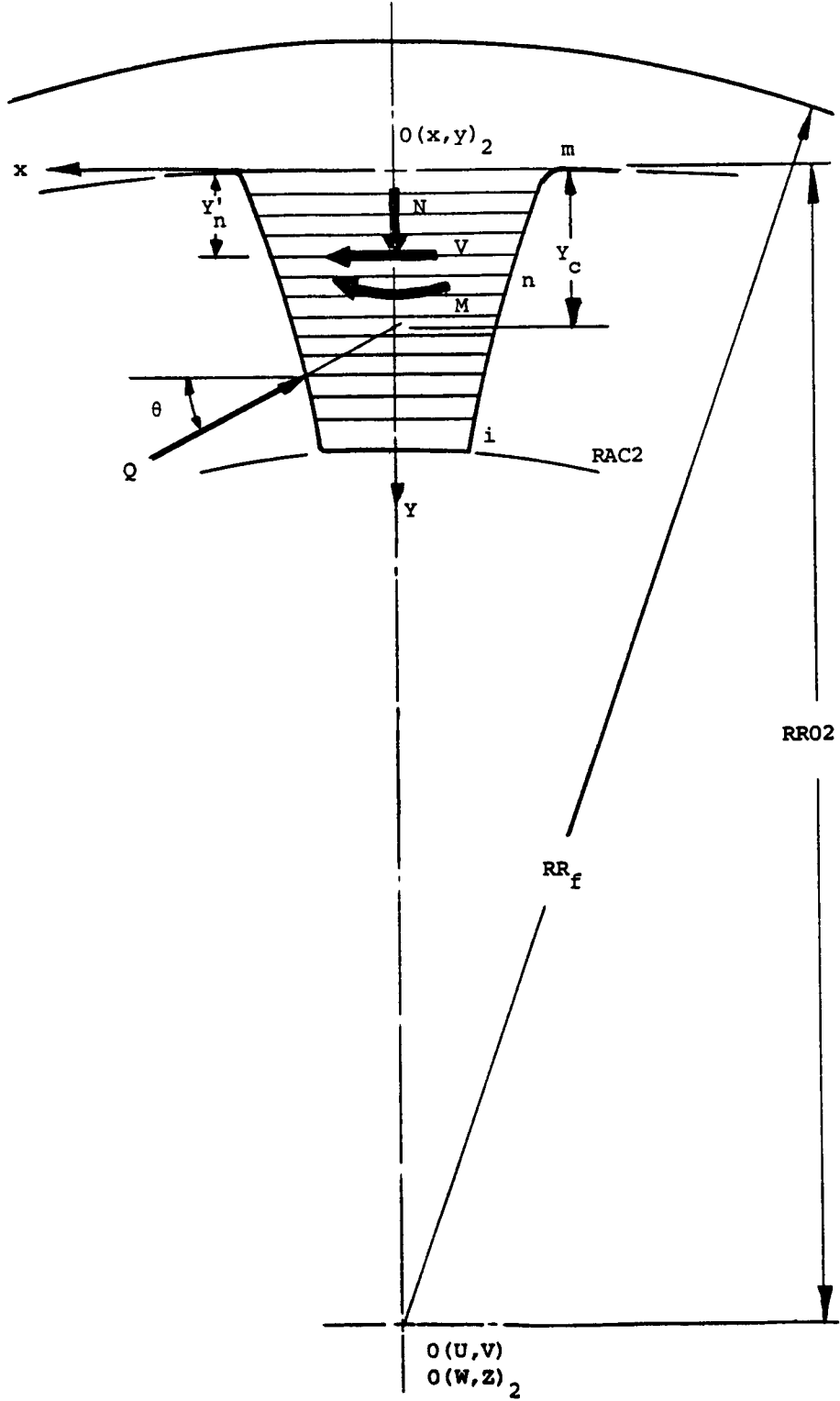


Figure B3-2 - Internal Gear Tooth Bending, Shear and Normal Deflection Model

B-3.2 Deformation of the Teeth Due to Rotation of Their Foundation

Weber^[13] investigated the effect of the elastic support of the teeth on the deflection at the contact point. For this investigation he assumed that a rigid tooth is acting on a semi-infinite support structure represented by the gear hub or ring, and that the loading is transferred to the support as indicated in Figures B3-3a through B3-3d. He then proceeded to find a stress function which satisfied all of the boundary conditions for the semi-infinite support. Again, equating the deforming work and stress energy:

$$\frac{1}{2} Q\delta = C_{11} M^2 + 2C_{12} MV + C_{22} V^2 + C_{33} N^2 \quad \dots (B3-10)$$

where C_{11} , C_{12} , C_{22} and C_{33} are factors whose determination is outlined as follows.

By potential functions we obtain the deflection in the Y-direction, where

$$v_{\text{boundary}} = \frac{2(1-\mu^2)}{E} \frac{6M}{\ell b^2} x \frac{2}{\pi b} \left\{ \frac{1}{2} \left[x^2 - \left(\frac{b}{2}\right)^2 \right] \ell n \left| \frac{b+x}{b-x} \right| - \frac{xb}{2} \right\} \quad \dots (B3-11)$$

and $b = 2 x_{\text{min}} \quad \dots (B3-12)$

$$x_{\text{min}} = \text{x-dimension at fillet-to-root intersection}$$

Now consider the work done by the load at the boundary due to M; the expression for the strain energy $C_{11} M^2$ is

$$C_{11} M^2 = \frac{1}{2} \int_{-b/2}^{+b/2} \sigma_{y_{\text{boundary}}} v_{\text{boundary}} \ell dx \quad \dots (B3-13)$$

where σ_y is the stress. Therefore,

$$\sigma_{y_{\text{boundary}}} = \frac{2x}{b} \frac{6M}{\ell b^2} \quad \dots (B3-14)$$

By substituting $\sigma_{y_{\text{boundary}}}$, v_{boundary} in equation (B3-13) and integrating

$$C_{11} M^2 = - \frac{(1 - \mu^2)}{\pi E} \left(\frac{6M}{Lb^2} \right) \times \frac{4\ell}{b^2} \times \left(- \frac{b^4}{16} \right) \quad \dots (B3-15)$$

$$C_{11} = \frac{9}{\pi} \frac{(1 - \mu^2)}{E} \frac{1}{Lb^2} = \frac{9(1 - \mu^2)}{\pi E L b^2} \quad \dots (B3-16)$$

By similar procedure we get

$$C_{12} = \frac{(1 + \mu)(1 - 2\mu)}{2E\ell b} \quad \dots (B3-17)$$

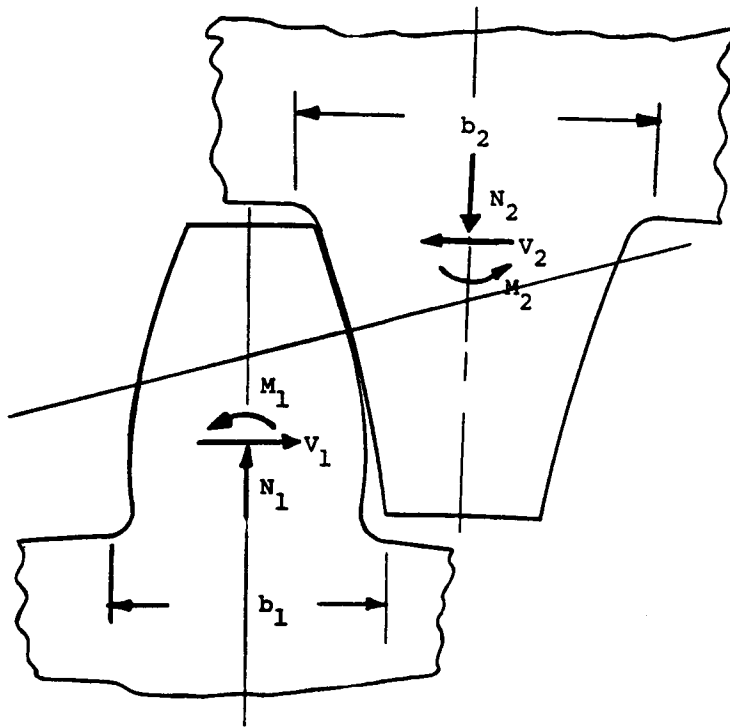
$$C_{22} = \frac{2.4(1 - \mu^2)}{\pi E \ell} \quad \dots (B3-18)$$

and
$$C_{33} = C_{22} \left(1 + \frac{\text{TAN}^2 \theta}{3.1} \right) \quad \dots (B3-19)$$

Substituting the expressions for C_{11} , C_{12} , C_{22} and C_{33} in equation (B3-10) and the load set $M = Y Y_c \cos \theta$, $V = Q \cos \theta$ and $N = Q \sin \theta$ we get:

The deflection of the point of contact due to rotation of the support structure

$$\delta = \frac{Q}{E} \cos^2 \theta \left[\frac{5.2 Y_c^2}{b^2} + \frac{Y_c}{b} + 1.4 \left(1 + \frac{\text{TAN}^2 \theta}{3.1} \right) \right] \quad \dots (B3-20)$$



(a)

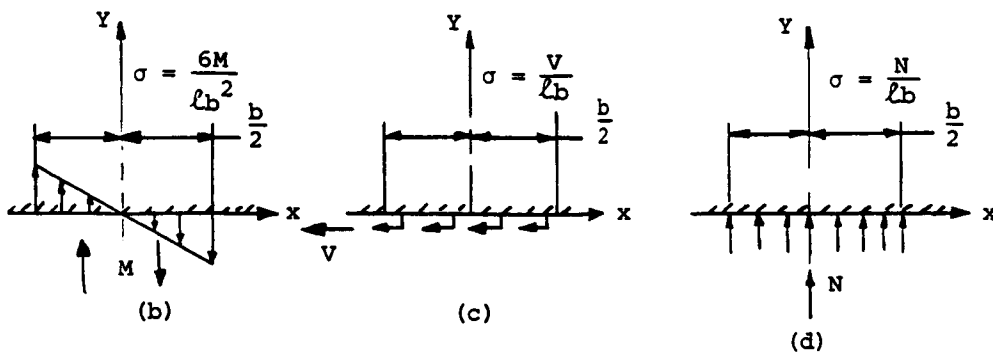


Figure B3-3 - Stress Distribution on Support Structure

B-3.3 Deflection of the Teeth Due to Circumferential Deformation of the Rim and Gear Ring*

Assume the external gear is held rigidly as in Figure B3-4. Under the effect of tangential force Q , the line HW is deformed and takes the position HW'. Any differential element ABCD is deformed to A'B'C'D'. The movement of A'B' relative to C'D' gives an angular rotation $d\theta$ about the center of the gear.

Total angular displacement of the point W = $\theta_t = \int d\theta$. From Figure B3-4, $r d\theta = \gamma dr$; therefore

$$d\theta = \frac{\tau}{G} \frac{dr}{r} \quad \dots (B3-21)$$

and
$$\theta_t = \int_{r_i}^{r_o} \frac{\tau}{G} \frac{dr}{r} \quad \dots (B3-22)$$

For equilibrium, the total shearing force on any concentric surface is equal to the applied torque T ; therefore

$$T = 2\pi r^2 F \tau \quad \dots (B3-23)$$

and
$$\theta_t = \frac{T}{2\pi LG} \int_{r_i}^{r_o} \frac{dr}{r^3} = \frac{Q r_i}{4\pi LG} \left(\frac{1}{r_i^2} - \frac{1}{r_o^2} \right) \quad \dots (B3-24)$$

The deflection, δ_E , of the point of contact due to the circumferential deformation due to force Q

$$\delta_E = \frac{Q \cos \theta}{4\pi FG} r_i^2 \left(\frac{1}{r_{i1}^2} - \frac{1}{r_{o1}^2} \right) \quad \dots (B3-25)$$

where

F = hub face width

r_i = radius to the contacting point

r_{o1} = outside hub/rim radius

r_{i1} = effective radius of circumferential hub fixity

*These derivations are primarily based on [14].

For the internal gear ring deflection a similar rationale as for the external gear leads to the expression for deflection (see Figure B3-5).

$$\delta_I = \frac{Q \cos \theta}{4\pi FG} r_2^2 \left(\frac{1}{r_{i2}^2} - \frac{1}{r_{o2}^2} \right) \quad \dots (B3-26)$$

where

r_2 = radius to contacting point on internal gear

r_{i2} = root circle radius of gear ring

r_{o2} = effective radius of circumferential gear
ring fixity

A torsionally rigid hub is obtained if the effective hub fixity radius coincides with the root circle, i.e., $\delta = 0$. The hub stiffness factor, HSF, is used to indicate a degree of influence of the hub/ring flexibility on the overall gear mesh stiffness.

$$HSF = \frac{KG_{\max}}{KG_{s \max}} \quad \dots (B3-27)$$

where

$KG_{s \max}$ = maximum mesh stiffness with torsionally
rigid hubs/rings; $\delta_E = \delta_I = 0$

KG_{\max} = maximum mesh stiffness with designated
hubs or rings, δ_E and $\delta_I \neq 0$

A combination of a rigid external gear hub and rigid internal gear ring is identified as $HSF = 1$.

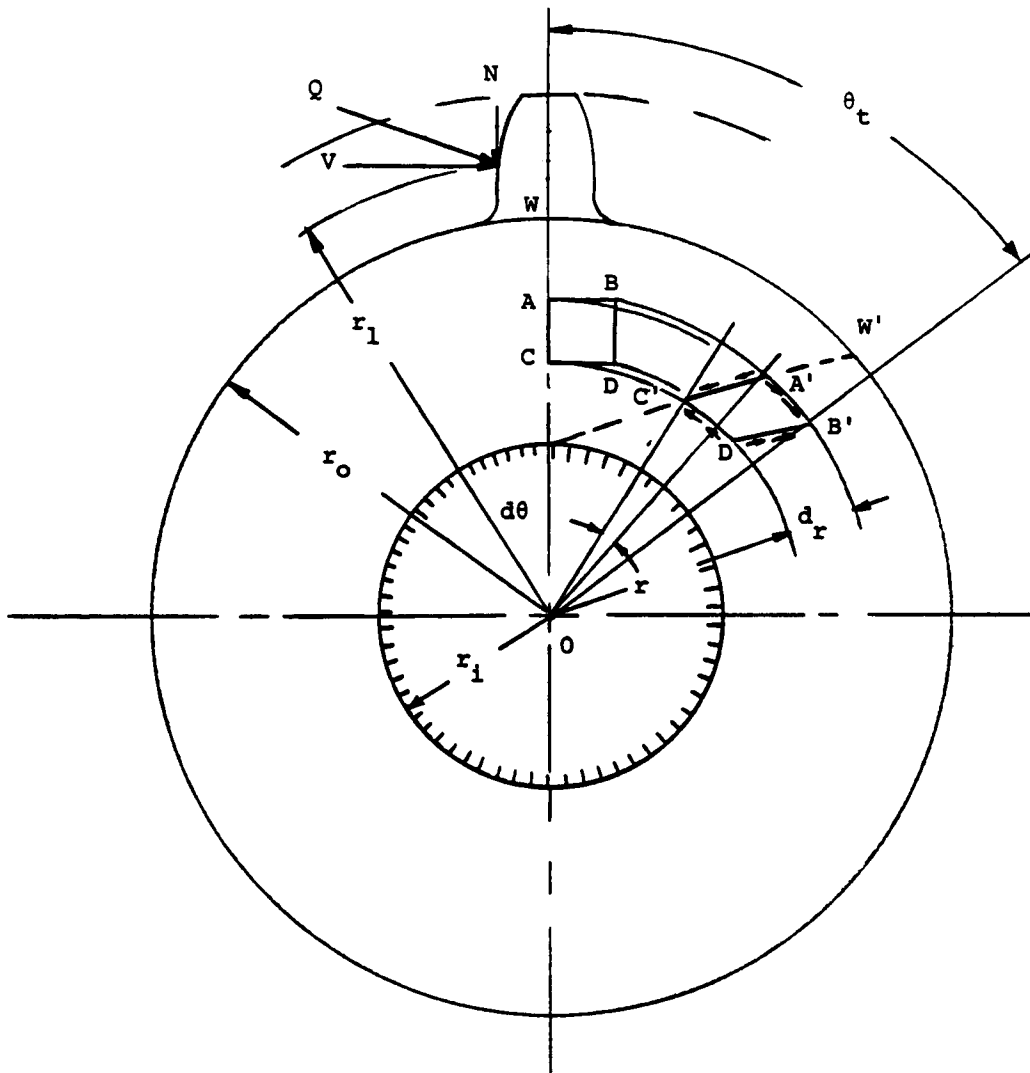


Figure B3-4 - Circumferential Deformation
of External Gear Hub

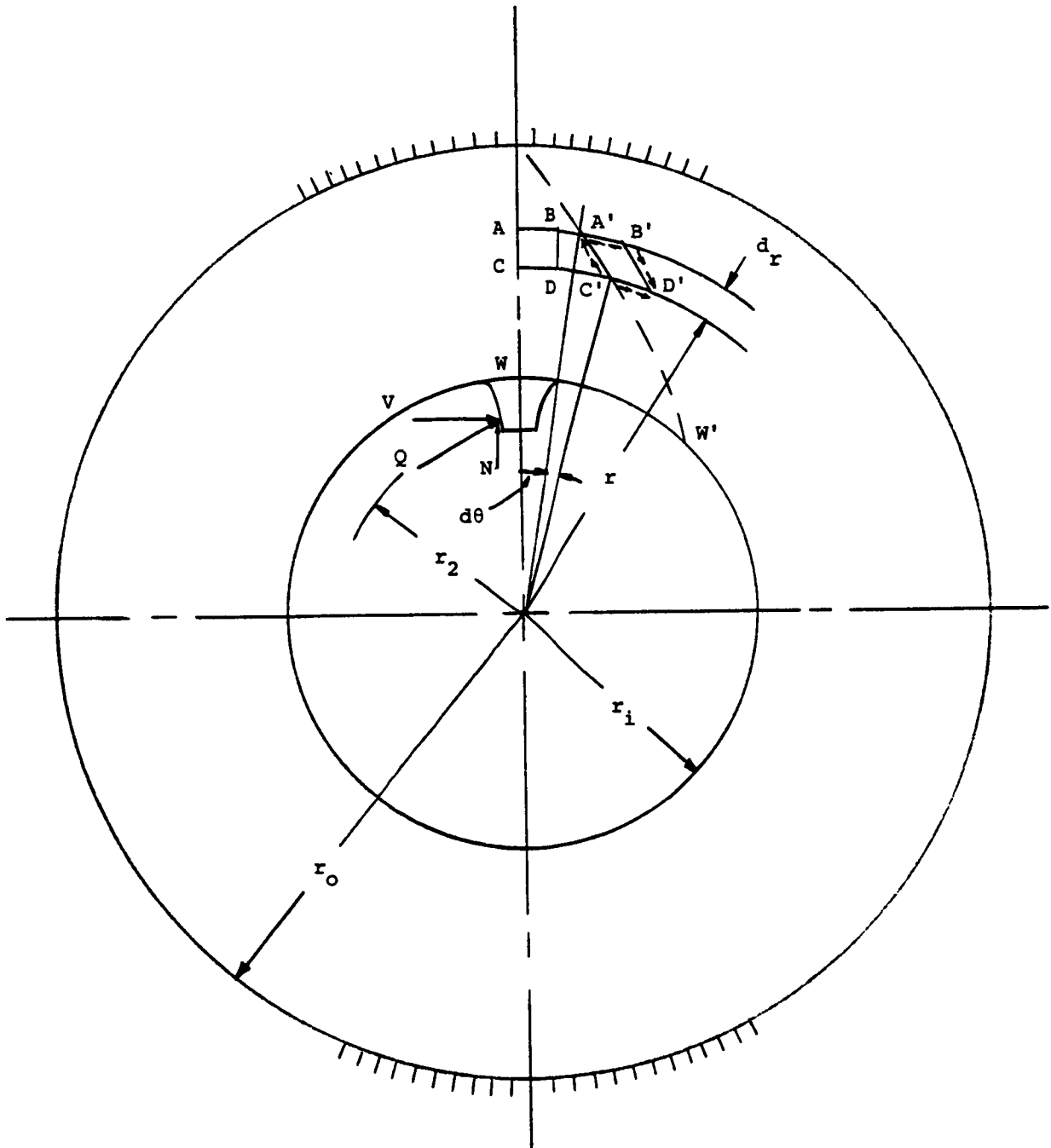


Figure B3-5 - Circumferential Deformation
of Internal Gear Ring

B-3.4 Hertzian Deformation at Contact Point

Weber^[13] applied Hertz's solution between two loaded cylinders in contact to the deformation of spur gears. In his formulation he used the following rationale:

The force at the contact point is distributed to the center of the tooth and then transmitted to the gear body. The tooth is cantilever which has an equivalent loading at the center consisting of bending, compression and shear. The shear load is distributed over the cross-section in the form of a parabola. The Hertzian stress is due to the shear component and reaches to the center of the tooth where it is transmitted as a transverse stress. The Hertzian compression is calculated from the point of contact in the direction of the applied force to the center of the tooth.

The teeth are treated as cylinders of lengths equal to the face width and radii equal to the radii of curvature at the contact point. For involute teeth the radii are the distances from the contact point to the tangent point of the respective base circles. For noninvolute profiles instantaneous base circles must be used. Figure B3-6 depicts the previously discussed geometry considerations as applied to the ISG drive. Distances h_1 and h_2 are along the line of action from the contact point to the center of the teeth.

Using Hertz's formulation for contact between cylinders

$$b^2 = 8 Q r (1 - \mu^2) / \pi E \quad \dots (B3-28)$$

For the external-internal gear combination

$$\frac{1}{r} = \frac{1}{r_2} - \frac{1}{r_1} \quad \dots (B3-29)$$

and

Q = load per tooth face width

r_1 = radius of curvature of external gear

r_2 = radius of curvature of internal gear

also,

$$P_{\max} = \frac{2Q}{\pi b}$$

Considering the contacting gear teeth as slightly curved semi-infinite planes the Hertzian deformation

$$\delta = \delta_E + \delta_I = \frac{Q}{E} \frac{4(1 - \mu^2)}{\pi} \times \left[\ln \frac{\sqrt{h_1 h_2}}{2r(1 - \mu^2)P_{\max}} - \frac{\mu}{1 - \mu} \right]$$

... (B3-30)

where

δ_E and δ_I are the deflection due to the Hertzian deformation of the external and internal tooth

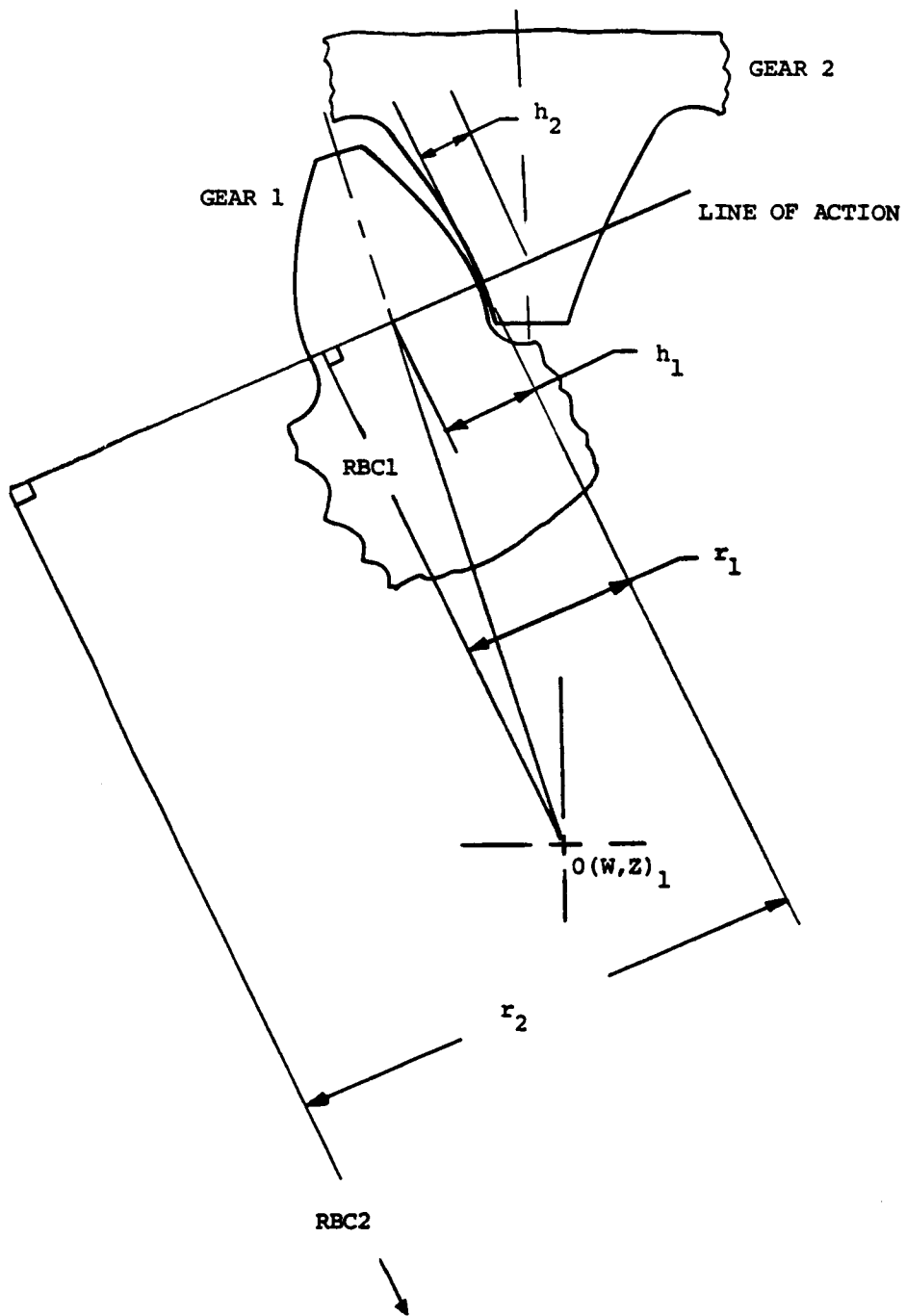


Figure B3-6 - Tooth Model for Hertzian Contact Deformation

APPENDIX C

COMPUTER PROGRAM PACKAGE

This section contains the computer listing of all three modules, typical output data and instructions for entering the data.

C-1 Listing and Sample Run of the Static Analysis Program

"Internal Static"

C-2 Listing and Sample Run of the Dynamic Analysis Program

"Internal Dynamic"

C-3 Listing and Sample Run of the Stress Analysis "Internal

Stress"

C-4 Entering of Input Data

C-1 LISTING AND SAMPLE RUN OF THE STATIC ANALYSIS PROGRAM
"INTERNAL STATIC"


```

COR3, COR4
* NAMELIST/PARAME/MLIM, MLIM, DELT, JJJJ, LLLL, DPSL11, DPSL12, DPEL1, DPEL2
NAMELIST/PRFDEF/PATM, STTM, RATM, PABM, STBM, RABM, PER, PAP, CYC, IPIT1,
IPIT2, DEEP
* PI=3.141592654
IBYPSS=0
C
  READ(5, HEDING)
  READ(5, CONTRL, END=999)
  READ(5, PHYPAR)
  READ(5, GENPAR)
  READ(5, GEOPAR)
  READ(5, PARAME)
  IF(MODF.EQ.YES) MODCOD=1
  IF (MODCOD.EQ.1) READ(5, PRFDEF)
C
  3 OCODE=1
C
  IF (OUTPUT.EQ.SI) OCODE = 2
  IF (INPUT.EQ.SI) DP=1/M
  ICHMG=0
C
  6 PHI=PHID*PI/180.
  TOUT=TIN*TG(2)/TG(1)
  RPMOUT=RPMIN*TG(1)/TG(2)
  G(1)=0.5*E(1)/(1.+PR(1))
  G(2)=0.5*E(2)/(1.+PR(2))
  PD1=TG(1)/DP
  PD2=TG(2)/DP
  RPC1=0.5*PD1
  RPC2=0.5*PD2
  IF (INPUT.EQ.ENGL) GO TO 7
  IF (RI(1).EQ.0.0) RI(1)=(16.*TIN/(PI*TAUMAX))**(1./3.)*26.270218
  IF (RI(1).EQ.0.0) RI(1)=(16.*TIN/(PI*TAUMAX))**(1./3.)*.5
  IF (JG(1).EQ.0.) JG(1)=.5*GAMA(1)*PI*FH(1)*RPC1**4/386.
  IF (JG(2).EQ.0.) JG(2)=.5*GAMA(2)*PI*FH(2)*RPC2**4/386.
  C = -RPC1 + RPC2
  GP = PI/DP
  BP = CP*COS(PHI)
  RF1=.7*(GRRF(1)+(WD(1)-AD(1)-GRRF(1))**2/(.5*PD1+WD(1)-AD(1)-
  &GRRF(1)))
  RF2=.7*(GRRF(2)+(WD(2)-AD(2)-GRRF(2))**2/(.5*PD2+WD(2)-AD(2)-
  &GRRF(2)))
  RAC1=RPC1+AD(1)

```

```

RAC2=RPC2-AD(2)
RRC1=RAC1-WD(1)
RRC2=RAC2+WD(2)
IF (RI(2).EQ.0.0) RI(2)=1.2*RRC2
RBC1 = RPC1*COS(PHI)
RBC2 = RPC2*COS(PHI)
DELR1 = RAC1 - RRC1
DELR2 = RRC2-RAC2
DELTAR = DELR1
IF(DELR2.GT.DELTAR) DELTAR = 0ELR2
L1=DELTAR*100.
IF(DELTAR.LE.1.0) L1 = 100
IF(DELTAR.GE.2.0) L1 = 200
L2 = L1

C
WRITE(6,21) TITLE1,TITLE2,TITLE3
WRITE(6,22) TITLE1,TITLE2,TITLE3
WRITE(6,35) PHID
IF(OCODE.EQ.2) GO TO 8
WRITE(6,37) DP,TIM,TOUT
GO TO 10
8 WRITE(6,38) M,TIN,TOUT
10 WRITE(6,40) RPMIN,RPMOUT
WRITE(6,50)
WRITE(6,60) TG,PD1,LENGTH(OC),PD2,LENGTH(OC),RAC1,LENGTH(OC),RAC2,
&LENGTH(OC),RBC1,LENGTH(OC),RBC2,LENGTH(OC),RRC1,LENGTH(OC),RRC2,
&LENGTH(OC)
WRITE(6,65) RF1,LENGTH(OC),RF2,LENGTH(OC),RI(1),LENGTH(OC),RI(2),
&LENGTH(OC),RT1,LENGTH(OC),RT2,LENGTH(OC)
&FW(1),LENGTH(OC),FW(2),LENGTH(OC),E(1),MODLUS(OC),
&E(2),MODLUS(OC),GAMA(1),SPWGHT(OC),GAMA(2),SPWGHT(OC),PR

C
CALL MAIN1(INF,LINF)
IF ((INF.EQ.2).OR.(LINF.EQ.2)) GO TO 1

C
GO TO 1
999 STOP

C
21 FORMAT(1H1,T38,'STATIC AND DYNAMIC ANALYSIS OF A GEAR PAIR SYSTEM'
&/T38,49('*')//)
22 FORMAT(' ',T38,20A4)
35 FORMAT(//T50,F5.1, DEGREE PRESSURE ANGLE'//)
37 FORMAT(T49,'DIAMETRAL PITCH IS',F10.3//T46,'INPUT TORQUE IS',

```



```

&F11.2,' IN-LBF'//T46,'OUTPUT TORQUE IS',F11.2,' IN-LBF'//)

38 FORMAT(T53,'MODULE IS',F11.3//T46,'INPUT TORQUE IS',F11.2,' NT-M
&'//T46,'OUTPUT TORQUE IS',F11.2,' NT-M'//)
40 FORMAT(T46,'INPUT SPEED IS',F11.2,' RPM.//T46,'OUTPUT SPEED IS'
&F11.2,' RPM.//)
50 FORMAT(//T18,'DATA FOR GEAR 1 (DRIVING GEAR)',T65,'*',T87,'DATA
&FOR GEAR 2 (DRIVEN GEAR)'//T18,T15(' '),T87,T15(' ')//)
60 FORMAT(T11,'NUMBER OF TEETH',T35,'=',T38,F4.0,T65,'*',T80,'NUMBER
&OF TEETH',T104,'=',T107,F4.0//)
&T11,'PITCH DIAMETER',T35,'=',T38,F8.4,3X,A3,T65,'*',T80,'PITCH DIA
&METER',T104,'=',T107,F8.4,3X,A3//)
&T11,'ADDENDUM CIRCLE RADIUS',T35,'=',T38,F8.4,3X,A3,T65,'*',T80,'ADDEND
&UM CIRCLE RADIUS',T104,'=',T107,F8.4,3X,A3//)
&T11,'BASE CIRCLE RADIUS',T35,'=',T107,F8.4,3X,A3,T65,'*',T80,'BASE
&CIRCLE RADIUS',T104,'=',T107,F8.4,3X,A3//)
&T11,'ROOT CIRCLE RADIUS',T35,'=',T38,F8.4,3X,A3,T65,'*',T80,'ROOT
&CIRCLE RADIUS',T104,'=',T107,F8.4,3X,A3//)
65 FORMAT(T11,'FILLET RADIUS',T35,'=',T38,F8.4,3X,A3,T65,'*',T80,'FI
&LLET RADIUS',T104,'=',T107,F8.4,3X,A3//)
&T11,'INSIDE RADIUS OF HUB',T35,'=',T38,F8.4,3X,A3,T65,'*',T80,'INS
&IDE RADIUS OF HUB',T104,'=',T107,F8.4,3X,A3//)
&T11,'RIM THICKNESS',T35,'=',T38,F8.4,3X,A3,T65,'*',
&T80,'RIM THICKNESS',T104,'=',T107,F8.4,3X,A3//)
&T11,'FACE WIDTH',T35,'=',T38,F8.4,3X,A3,T65,'*',T80,'FACE WIDTH',
&T104,'=',T107,F8.4,3X,A3//)
&T11,'YOUNG'S MODULUS',T35,'=',T39,2PE8.1,2X,A3,T65,'*',T80,'YOUNG'
&'S MODULUS',T104,'=',T108,F8.1,2X,A3//)
&T11,'SPECIFIC WEIGHT',T35,'=',T38,OPF8.3,3X,A3,T65,'*',T80,'SPECIF
&IC WEIGHT',T104,'=',T107,F8.3,3X,A3//)
&T11,'POISSON'S RATIO',T35,'=',T38,F8.4,T65,'*',T80,'POISSON'S RA
&TIO',T104,'=',T107,F8.4)
END

SUBROUTINE MAIN1(INF,LINF)
COMMON/DIMEN/OC,MODCOD
COMMON/HD/TITLE1(20),TITLE2(20),TITLE3(20),TAPE
COMMON/C1/PHI,PHID,DP,M,TG1,TG2,TP,DELTP
COMMON/C2/P1,F1,F2,R11,R12,E1,E2,G1,G2,PR1,PR2,GAMA1,GAMA2,RT1,RT2
COMMON/C4/TIN,TOUT,RPMIN,RPMOUT,OMEGA1,OMEGA2,RADEL2,CORT1,COR2,
COR3,COR4,DPSL11,DPSL12,DPEL1,DPEL2
COMMON/C6/L1,L2,PD1,PD2,RPC1,RPC2,RAC1,RAC2,RBC1,RBC2,RR1,RR2,
&RF1,RF2,C,CP,BP,UCUT1,UCUT2

```

C
C
C

```

COMMON/C7/YT11, YT12, YP1, YP2, YB11, YB12, RT11, RT12, RB11, RB12,
1RRO1, RRO2, XMIN1, XMIN2, SP, EP
COMMON/C8/X1(200), X2(200), Y1(200), Y2(200), THETA1(200), THETA2(200),
1RCURV1(200), RCURV2(200)
COMMON/C9/XC1(5,50), XC2(5,50), YC1(5,50), YC2(5,50), THETC1(200),
1THETC2(200), DCP1(200), DCP2(200), RC1(5,50), RC2(5,50), RCG1(5,50),
2RCC2(5,50), Q(5,50), TPS(5,50), NCP(50)
COMMON/C10/PS1(50), PS12(50), CMS(50), TDEF1(50), TDEF2(50),
1HDEF(50), CDEF(50), SVS(50), HZPS(50), PVS(50), U1(200), V1(200),
2W1(200), Z1(200), U2(200), V2(200), W2(200), Z2(200),
3PSIRD1(5), PSIRD2(5), PS11TP(5), PS12TP(5), UCP(5), VCP(5),
4ZCP1(5), ZCP2(5), WCP1(5), WCP2(5), XCP1(5), XCP2(5), YCP1(5), YCP2(5),
5RCP1(5), RCP2(5), RCCP1(5), RCCP2(5), TDCP1(5), TDCP2(5), H1(5), H2(5),
6THCP1(5), THCP2(5), TD(5), HD(5), CDEF1(5), STIFF(5), QTP(5), DM3(1855)
COMMON/C12/KG(50), CG(50), PSI(50), VELR(50), PSIS1, PSIS2, ITP, IEP, MNC

```

C

```

DIMENSION XP(50), Y1P(50), Y2P(50,2)
REAL M, JD, JG1, JG2, JL, KDS, KGP, AVG, KLS, KG, LDS, LLS, LCR
DIMENSION FORCE(2), SPEED(2), PRESS(2)
REAL LENGTH(2), MODLUS(2), LEN(2)
INTEGER OC
DOUBLE PRECISION XI, DX1
DATA NGEAR1, NGEAR2/1, 2/
DATA LENGTH/ 'IN.', 'MM.', /, FORCE/ 'LBF.', 'NTS.', /, LEN/ 'IN.', 'MT.', /,
&PRESS/ 'PSI.', 'MPA.', /, MODLUS/ 'PSI.', 'MPA.', /

```

C

```

P = TIN/RBC1
IF (OC.EQ.2) PMTRIC = P*4.448222
IF (OC.EQ.2) WRITE(6,2) PMTRIC, FORCE(OC)
IF (OC.EQ.1) WRITE(6,2) P, FORCE(OC)

```

C

```

CALL MOD(INF, CR)
IF (INF.EQ.1) GO TO 301
IF (INF.EQ.2) WRITE(6,5)
IF (INF.EQ.3) WRITE(6,6)
RETURN

```

C

```

2 FORMAT(///T30, 'THE NOMINAL TRANSMITTED FORCE ALONG THE LINE OF AC
&TION =', F10.2, 1X, AH/)
5 FORMAT(///T31, 'INVOLUTE INTERFERENCE OCCURS FOR THIS PAIR OF GEARS U
&NDER NO-LOAD CONDITIONS')
6 FORMAT(///T31, 'TIP INTERFERENCE OCCURS FOR THIS PAIR OF GEARS UNDER
&NO-LOAD CONDITIONS')
14 FORMAT(///T31, 'INTERFERENCE OCCURS FOR THIS PAIR OF GEARS UNDER LOAD

```

```

&ED CONDITIONS')
18 FORMAT(/126,'CONTACT RATIO FOR THIS PAIR OF GEARS UNDER LOAD IS E
&EQUAL TO OR LESS THAN UNITY')
20 FORMAT(146,'THE CONTACT RATIO UNDER LOAD =',F8.3/)

C
C TABLE 1 OUTPUT
301 WRITE(6,401)
IF(MODCOD.EQ.1) GO TO 400
WRITE(6,402)
400 WRITE(6,420) L1
WRITE(6,425) Y11,LENGTH(OC),YB11,LENGTH(OC),NGEAR1
WRITE(6,425) Y12,LENGTH(OC),YB12,LENGTH(OC),NGEAR2
WRITE(6,430) NGEAR1,Y11,LENGTH(OC)
WRITE(6,430) NGEAR2,Y12,LENGTH(OC)
WRITE(6,432) RR01,LENGTH(OC),RR02,LENGTH(OC)
WRITE(6,440) LENGTH(OC)
WRITE(6,450)

C
CONST=180./PI
DO 452 K=1,L1
THETA1=THETA1(K)*CONST
THETA2=THETA2(K)*CONST
WRITE(6,455) K,X1(K),Y1(K),THETA1,K,X2(K),Y2(K),THETA2
452 CONTINUE

C
401 FORMAT(137,'X-Y COORDINATES OF POINTS ALONG THE PROFILE OF THE GEA
&R TEETH'//)
402 FORMAT(137,'THE GEAR TEETH HAVE A STANDARD PROFILE WITH NO MODIFIC
&ATIONS'//)
420 FORMAT(14,'THE Y-AXIS CORRESPONDS TO THE LINE OF SYMMETRY OF THE T
&ROOT. THE ORIGIN OF THE X-Y COORDINATE SYSTEMS IS LOCATED AT THE
&/T4,'ROOT OF THE TOOTH A DISTANCE OF RR01 (OR RR02 FOR GEAR 2) FRO
&M THE GEAR CENTER. VALUES TABULATED BELOW REPRESENT POINTS ON THE
&/T4,'R.H. PROFILE OF THE TOOTH. POINT IS LOCATED AT THE ADDENDU
&M CIRCLE. POINT',14,' IS LOCATED AT THE ROOT CIRCLE./T4,'THETA V
&VALUES REPRESENT THE ANGLE BETWEEN THE NORMAL TO THE PROFILE AND TH
&E X-AXIS; COUNTERCLOCKWISE THETA IS DEFINED AS POSITIVE.'//)
425 FORMAT(115,'THE INVOLUTE STARTS AT Y =',F9.4,1X,A3,' AND ENDS AT
& Y =',F9.4,1X,A3,' ON THE TOOTH PROFILE OF GEAR',12,'.')
430 FORMAT(128,'THE PITCH CIRCLE INTERSECTS THE TOOTH PROFILE OF GEAR'
&,12,' AT Y =',F9.4,1X,A3)
432 FORMAT(156,'RR01 =',F9.4,1X,A3/T56,'RR02 =',F9.4,1X,A3)
440 FORMAT(140,'X AND Y VALUES ARE IN ',A3,' , THETA VALUES ARE IN

```

```

& DEGREES. '///T20, 'DATA FOR GEAR 1', T91, 'DATA FOR GEAR 2', T20, 15('*
&'), T91, 15( '*, ))
450 FORMAT(//T5, 'POINT', T21, 'X', T35, 'Y', T47, 'THETA', T76, 'POINT', T92,
&'X', T106, 'Y', T118, 'THETA'//)
455 FORMAT(T5, I3, 3X, 3F14.5, T76, I3, 3X, 3F14.5)

C
CALL SLOWM( INF, CR)

C
C
C TABLE 2 OUTPUT
WRITE(6, 500)
WRITE(6, 502)
WRITE(6, 510)
WRITE(6, 512)
WRITE(6, 514)
WRITE(6, 518)
WRITE(6, 530)
WRITE(6, 535) ((I, PSI1(I), PSI2(I), NCP(I), TPS(3, I), CMS(I), CG(I)), I=1
&, 50)
FORCE(OC), LEN(OC), FORCE(OC), LEN(OC), FORCE(OC), LEN(OC), FORCE(OC), LEN(OC)

C
500 FORMAT(1H1, T55, 'STATIC ANALYSIS', T55, 15('*')//)
502 FORMAT(T16, 'TABLES 2, 3 AND 4 LIST INFORMATION RESULTING FROM A ST
&TIC ANALYSIS OF THE GEAR PAIR (NEGLECTING INERTIA', T16, 'FORCFS).
& THE DATA PRESENTED IN THESE TABLES WERE OBTAINED BY ROTATING THE
& DRIVING GEAR THRU ONE CYCLE', T16, 'OF TOOTH ENGAGEMENT. IN EACH OF
& THESE TABLES POSITION 1 CORRESPONDS TO THE STARTING POINT OF CONT
&ACT WHILE', T16, 'POSITION 50 CORRESPONDS TO THE END POINT OF CONTACT
&T. '///)

C
510 FORMAT(T59, 'TABLE 2'//)
512 FORMAT(T30, 'PSI1 IS THE ANGLE OF ROTATION OF THE DRIVING GEAR IN D
&EGREES. ', T30, 'PSI2 IS THE ANGLE OF ROTATION OF THE DRIVEN GEAR IN
&DEGREES. ', T30, 'NCP IS THE NUMBER OF SEPARATE TOOTH PAIRS IN CONTACT
&T AT A PARTICULAR POSITION. ')
514 FORMAT(T30, 'PS IS THE TOOTH PAIR STIFFNESS IN ', A3, ' ', A2, ' AT A P
&ARTICULAR POSITION.', T30, 'KG IS THE COMBINED GEAR TOOTH SPRING CON
&STANT (STIFFNESS) IN ', A3, ' ', A2, ' AT A PARTICULAR POSITION. ', T30,
&'CG IS THE GEAR DAMPENING COEFFICIENT IN (', A2, '-SEC)/', A3)
518 FORMAT(//T24, 'NOTE: BOTH PSI1 AND PSI2 ARE MEASURED BETWEEN THE GEN
&TER LINE. '///)
530 FORMAT(T4, 'POSITION', T22, 'PSI1', T39, 'PSI2', T57, 'NCP', T77, 'PS', T100
&, 'KG', T126, 'CG'//)
535 FORMAT(5X, I3, 11X, F7.3, 10X, F7.3, 13X, I2, 11X, F13.1, 10X, F13.1, 10X, F13.
&1)

C
C
C TABLE 3 OUTPUT

```

```

WRITE(6,540) FORCE(OC),P, FORCE(OC)
WRITE(6,542) LENGTH(OC), LENGTH(OC)
WRITE(6,544) LENGTH(OC), LENGTH(OC)
IF(OC.EQ.1) WRITE(6,545)
IF(OC.EQ.2) WRITE(6,546)
WRITE(6,548) PRESS(OC)
WRITE(6,550) FORCE(OC), LEN(OC)
WRITE(6,560)
WRITE(6,570) ((I,Q(3,I),YC1(3,I),YC2(3,I),SVS(1),HZPS(1),PVS(1)),
&I=1,50)
C
540 FORMAT(1H1,I59,'TABLE 3'//)
542 FORMAT(1T7,'LOAD IS THE FORCE IN ',A4,' ACTING BETWEEN THE CONTACT
&ING TOOTH PAIR IN A DIRECTION NORMAL TO THE PROFILE.'/T17,'(THE TO
&TAL NOMINAL TRANSMITTED FORCE CARRIED BY ALL CONTACTING TOOTH PAIR
&S IS',F10.2,1X,A4,1')
544 FORMAT(1T7,'YC1 IS THE LOCATION OF THE CONTACT POINT ALONG THE TOO
&TH PROFILE OF GEAR 1; ',A3/T17,'YC2 IS THE LOCATION OF THE CONTACT
& POINT ALONG THE TOOTH PROFILE OF GEAR 2; ',A3/T17,'(YC1 AND YC2 A
&RE MEASURED RELATIVE TO THE X-Y COORDINATE SYSTEMS DEFINED IN TABL
&E 1)')
545 FORMAT(1T7,'SV IS THE SLIDING VELOCITY AT THE CONTACT POINT; F1/MI
&N.')
546 FORMAT(1T7,'SV IS THE SLIDING VELOCITY AT THE CONTACT POINT; N/SE
&C.')
548 FORMAT(1T7,'HZP IS THE MAXIMUM HERTZ CONTACT PRESSURE AT THE CONTA
&CT POINT; ',A4)
550 FORMAT(1T7,'PV IS THE HERTZ PRESSURE-SLIDING VELOCITY PRODUCT; ',
&A3,'/( ',A2,'-SEC.'/)
560 FORMAT(3X,'POSITION',T18,'LOAD',T39,'YC1',T59,'YC2',T79,'SV',T102,
&'HZP',T124,'PV'//)
570 FORMAT(5X,13,6X,F8.2,13X,F7.3,13X,F7.3,11X,E12.5,11X,E12.5,11X,E12
&.5)
C
C
C TABLE 4 OUTPUT
WRITE(6,580) LENGTH(OC), LENGTH(OC), LENGTH(OC), LENGTH(OC)
WRITE(6,590) LENGTH(OC), LENGTH(OC), LENGTH(OC), LENGTH(OC)
WRITE(6,600)
WRITE(6,605) ((I,TDEF1(1),TDEF2(1),HDEF(1),CDEF(1),VELR(1)),I=1
1,50)
C
580 FORMAT(1H1,I59,'TABLE 4'//)
590 FORMAT(136,'TD1 IS THE TOOTH DEFLECTION ON GEAR 1; ',A3/T36,'TD2 I
&S THE TOOTH DEFLECTION ON GEAR 2; ',A3/T36,'HD IS THE HERTZIAN DEF

```

```

&LECTION OF THE CONTACT POINT; 'A3/T36, 'CD IS THE COMBINED DEFLECT
&ION OF THE CONTACT POINT; 'A3/T36, (ALL DEFLECTIONS ARE MEASURED
&ALONG THE LINE OF ACTION.)/)
600 FORMAT(T20, 'POSITION', T42, 'TD1', T63, 'TD2', T83, 'HD', T103, 'CD', T123,
& 'VELR' /)
605 FORMAT(T22, I3, I3X, F10.7, I1X, F10.7, 10X, F10.7, 10X, F10.7, 10X, F10.7)
C
WRITE(6, 740) TAPE
740 FORMAT( ' ', TAPE COMMAND IS ' ', A4)
C
C
C
C
620 FORMAT(1H1////T44, 45( ' * ') / T44, ' * ', T88, ' * ' / T44, ' * ' X-Y PLOTS OF TH
&E STATIC ANALYSIS DATA ' * / T44, ' * ', T88, ' * ' / T44, 45( ' * '))
630 FORMAT(////T37, 'MUCH OF THE DATA PROVIDED IN TABLES 2, 3 AND 4 IS
& PRESENTED' / T43, 'GRAPHICALLY IN THE FOLLOWING TWELVE X-Y PLOTS. ' / /
& / T18, 'USING THE NOTATION DEFINED IN THE PREVIOUS TABLES, THE VARI
& ABLES GRAPHED IN THE TWELVE PLOTS ARE: ' / / /)
640 FORMAT(T45, 'PLOT 1 - TD1, TD2, HD AND CD VERSUS PS11' / T45, 'PLOT
& 2 - KG AND PS VERSUS PS11' / T45, 'PLOT 3 - LOAD VERSUS YC1' /
& T45, 'PLOT 4 - HZP VERSUS YC1' / T45, 'PLOT 5 - SV VERSUS YC1' /
& T45, 'PLOT 6 - PV VERSUS YC1' / T45, 'PLOT 7 - TD1, TD2, HD AND CD
& VERSUS PS12' / T45, 'PLOT 8 - KG AND PS VERSUS PS12' / T45, 'PLOT
& 9 - LOAD VERSUS YC2' / T45, 'PLOT 10 - HZP VERSUS YC2' / T45, 'PLOT
& 11 - SV VERSUS YC2' / T45, 'PLOT 12 - PV VERSUS YC2' /)
650 FORMAT(1H1/T64, 'PLOT ' , I1 / /)
652 FORMAT(1H1/T64, 'PLOT ' , I2 / /)
654 FORMAT(/T118, 'PSI ' , I1 / /)
656 FORMAT(/T118, 'YC ' , I1 / /)
660 FORMAT(I53, 'TD1, TD2, HD AND CD VERSUS PS1 ' , I1 / /)
661 FORMAT(I56, 'KG AND PS VERSUS PS1 ' , I1 / /)
662 FORMAT(I60, 'LOAD VERSUS YC ' , I1 / /)
663 FORMAT(I60, 'HZP VERSUS YC ' , I1 / /)
664 FORMAT(I61, 'SV VERSUS YC ' , I1 / /)
665 FORMAT(I61, 'PV VERSUS YC ' , I1 / /)
670 FORMAT(I12, 'TD1, TD2, HD OR CD' / /)
674 FORMAT(I16, 'LOAD' / /)
675 FORMAT(I17, 'HZP' / /)
676 FORMAT(I18, 'SV' / /)
678 FORMAT(I18, 'PV' / /)
680 FORMAT(I36, I1, ' - TD ' , I1, ' , THE TOOTH DEFLECTION ON GEAR ' , I1, ' ; '
& , A3)
682 FORMAT(I36, ' 3 - HD, THE HERTZIAN DEFLECTION OF THE CONTACT POINT;

```

```

& , A3)
684 FORMAT(T36, '4 - CD, THE COMBINED DEFLECTION OF THE CONTACT POINT:
& , A3)
686 FORMAT(T38, '(ALL DEFLECTIONS ARE MEASURED ALONG THE LINE OF ACTION
& ) )
688 FORMAT(T21, 'PSI1 IS THE ANGLE OF ROTATION OF THE DRIVING GEAR ( IN
& DEGREES) MEASURED FROM THE LINE OF CENTERS. )
689 FORMAT(T21, 'PSI2 IS THE ANGLE OF ROTATION OF THE DRIVEN GEAR ( IN D
& DEGREES) MEASURED FROM THE LINE OF CENTERS. )
690 FORMAT(T50, 'F - KG, THE GEAR STIFFNESS; , A3, ' / ' , A3/T50, 'X - THE T
& OOTH PAIR STIFFNESS; , A3, ' / ' , A3)
700 FORMAT(T32, 'LOAD IS THE FORCE IN ' , A4, ' ACTING BETWEEN THE CONTACT
& ING TOOTH PAIR. ' )
702 FORMAT(T26, 'YC, ' I1, ' IS THE LOCATION OF THE CONTACT POINT ALONG TH
& E TOOTH PROFILE OF GEAR , ' I1, ; , A3)
710 FORMAT(T32, 'HZP IS THE MAXIMUM HERTZ CONTACT PRESSURE AT THE CONTA
& CT POINT: , A4)
720 FORMAT(T30, 'SV IS THE SLIDING VELOCITY AT THE CONTACT POINT; FT/MI
& N. ' )
721 FORMAT(T30, 'SV IS THE SLIDING VELOCITY AT THE CONTACT POINT; M/SEC
& ' )
725 FORMAT(/T18, '(NOTE: THE ABSOLUTE VALUE OF SV IS SHOWN - THERE IS
& A SIGN REVERSAL IN SV AT THE PITCH POINT)')
730 FORMAT(T34, 'PV IS THE HERTZ PRESSURE-SLIDING VELOCITY PRODUCT; ' ,
& A3, ' / ( , A2, ' -SEC). ' )

C RETURN
C END
C
C
C
SUBROUTINE MOD(INF,CR)
COMMON/DIMEN/OC,MODCOD
COMMON/C1/PHI,PHID,DP,M,TG1,TG2,TP,DELTP
COMMON/C2/P1,F1,F2,R11,R12,E1,E2,G1,G2,PR1,PR2,GAMA1,CAMA2,RT1,RT2
COMMON/C3/PATM1,PATM2,STTM1,STTM2,RATM1,RATM2,PABM1,PABM2,STBM1,
&STBM2,RABM1,RABM2,PER1,PER2,PAP1,PAP2,CYC1,CYC2,IPIT11,IPIT12,
&IPIT21,IPIT22,DEEP1,DEEP2
COMMON/C6/L1,L2,PD1,PD2,RPC1,RPC2,RAC1,RAC2,RBC1,RBC2,RR1,RR2,
&RF1,RF2,C,CP,BP,UCUT1,UCUT2
COMMON/C7/YT11,YT12,YP1,YP2,YB11,YB12,RT11,RT12,RB11,RB12,
1RR01,RR02,XMIN1,XMIN2,SP,EP
COMMON/C8/X1(200),X2(200),Y1(200),Y2(200),THETA1(200),THETA2(200),
1RCURV1(200),RCURV2(200)

```

C

C

C

C

C

```

C          DIMENSION LENGTH(2)
C          REAL KL, LE1, KE1
C          DATA LENGTH/ 'IN', 'MM' /
C          TODEGR=360./(2.*PI)

C          TG-----NUMBER OF TEETH
C          DP-----DIAMETRAL PITCH
C          PHI-----PRESSURE ANGLE
C          AD-----ADDENDUM
C          WD-----WHOLE DEPTH (APPROXIMATE)
C          GRRF-----GENERATING RACK EDGE RADIUS
C          1-----IDENTIFIES GEAR 1
C          2-----IDENTIFIES GEAR 2
C          RF-----FILLET RADIUS

C*****WRITE PROFILE MODIFICATIONS
C          IF (MODCOD.EQ.0) GO TO 199
C          WRITE(6,50)

C          WRITE(6,54)
C          WRITE(6,60)
C          WRITE(6,103) PATM1, LENGTH(OC), PATM2, LENGTH(OC)
C          WRITE(6,105) PABM1, LENGTH(OC), PABM2, LENGTH(OC)
C          WRITE(6,110) STTM1, LENGTH(OC), STTM2, LENGTH(OC)
C          WRITE(6,113) STBM1, LENGTH(OC), STBM2, LENGTH(OC)
C          WRITE(6,115) RATM1, RATM2
C          WRITE(6,120) RABM1, RABM2
C          WRITE(6,122) PER1, LENGTH(OC), PER2, LENGTH(OC)
C          WRITE(6,125) CYC1, CYC2
C          WRITE(6,130) PAPI, PAP2
C          WRITE(6,131) IPIT11, IPIT12, IPIT21, IPIT22
C          WRITE(6,132) DEEP1, LENGTH(OC), DEEP2, LENGTH(OC)
C          WRITE(6,135)

50          FORMAT(1H1, T60, 'TABLE 1 '//T51, 'TOOTH PROFILE DEFINITION'/T51, 2H( '*
& ')//)
54          FORMAT(/T58, 'TABLE 1-A'//T51, 'PROFILE MODIFICATIONS'//T31, 'THE TE
&ETH OF ONE OR BOTH GEARS HAVE THE FOLLOWING MODIFICATIONS...'//)
60          FORMAT(T28, 'GEAR 1', T93, 'GEAR 2'//)
103         FORMAT(2(6X, 'PARABOLIC TIP MODIFICATION', 10X, '= ', F10.5, 2X, A3, 7X)//)
105         FORMAT(2(6X, 'PARABOLIC BOTTOM MODIFICATION', 7X, '= ', F10.5, 2X, A3,
& 7X)//)
110         FORMAT(2(6X, 'STRAIGHT LINE TIP MODIFICATION', 6X, '= ', F10.5, 2X, A3,
& 7X)//)
113         FORMAT(2(6X, 'STRAIGHT LINE BOTTOM MODIFICATION', 3X, '= ', F10.5, 2X, A3

```



```

&,7X)/)
115 FORMAT(2(6X,'ROLL ARC OF TIP MODIFICATION',8X,'=',F7.2,5X,'DEGREES
&',3X)/)
120 FORMAT(2(6X,'ROLL ARC OF BOTTOM MODIFICATION',5X,'=',F7.2,5X,'DEGR
&EES',3X)/)
122 FORMAT(2(6X,'SINUSODIAL PROFILE ERROR',12X,'=',F10.5,2X,A3,7X)/)
125 FORMAT(2(6X,'NUMBER OF CYCLES OF PROFILE ERROR',3X,'=',F7.2,5X,
&'CYCLES',3X)/)
130 FORMAT(2(6X,'PHASE ANGLE OF PROFILE ERROR',8X,'=',F7.2,5X,'DEGREES
&',3X)/)
131 FORMAT(2(6X,'PIT LOCATION',25X,'POSITIONS',13,' TO',13,3X)/)
132 FORMAT(2(6X,'DEPTH OF PIT',24X,'=',F10.5,2X,A3,7X)/)
135 FORMAT(1H1,T58,'TABLE 1-B'/)
C
C*****CHECK FOR INTERFERENCE
C
199 RCHK2 = SQRT(RPC2**2 + (C*SIN(PHI))**2)
IF (RCHK2.LE.RBC2)INF=2
C
C*****TIP INTERFERENCE CHECK, TAKEN FROM BUCKINGHAM, PAGE 129
C
ETA1=ACOS((RAC2**2 - RAC1**2 - C**2)/(2*C*RAC1))
ETA2=TG1*ETA1/TG2
C
THETT1=ASIN(SIN(ETA1)*RAC1/RAC2) - ETA2
C
PHI01=ACOS(RBC1/RAC1)
PHI02=ACOS(RBC2/RAC2)
FUNC1=TAN(PHI01) - PHI01
FUNC2=TAN(PHI02) - PHI02
FUNC3=TAN(PHI) - PHI
C
DEL=(TG1/TG2)*(FUNC1 - FUNC3) + FUNC3
C
Z2=DEL - THETT1
C
IF (FUNC2.GT.Z2) INF=3
IF (INF.EQ.3) GO TO 4563
C
IF (INF.EQ.2) GO TO 4563
ALPHA1=ARSIN(RF1/(RRC1+RF1))
RF2/(2.0*RTF22))
C
RTF11=(RRC1+RF1)*COS(ALPHA1)
RTF22=RRC2-RF2
ALPHA2=2.0*ARSIN(RF2/(2.0*RTF22))
CALCULATION OF LIMIT RADII (RLM1 AND RLM2)
C
C

```

```

AUX1=ARCOS(RBC1/RAC1)
AUX2=ARCOS(RBC2/RAC2)
C11=-RAC2*SIN(AUX2)+RPC2*SIN(PHI)
C12=RAC1*SIN(AUX1)-RPC1*SIN(PHI)
RALR1=ATAN((RPC1*SIN(PHI)-C11)/RBC1)
RALR2=ATAN((RPC2*SIN(PHI)+C12)/RBC2)
RLM1=RBC1/COS(RALR1)
RLM2=RTF22

C
RR1=RAC1-RLM1
RR2=RLM2-RAC2
IF (RLM1.LE.RRC1) RR1=RAC1-RTF11
IF (RLM2.GE.RRC2) RR2=RTF22-RAC2
IF (RLM1.LE.RRC1) WRITE(6,220) RLM1
IF (RLM2.GE.RRC2) WRITE(6,221) RLM2
220 FORMAT('0',2X,'NOTE: RADIUS OF THEORETICAL LAST POINT OF CONTACT
&' TO AVOID INTERFERENCE PROBLEMS, THIS TOOTH SHOULD BE UNDERCUT'//)
221 FORMAT('0',2X,'NOTE: RADIUS OF THEORETICAL LAST POINT OF CONTACT
&' TO AVOID INTERFERENCE PROBLEMS, THIS TOOTH SHOULD BE UNDERCUT'//)

C
L11=FIX((RR1/(RAC1-RRC1))*L1)
L12=FIX((RR2/(RRC2-RAC2))*L2)
RINC1=RR1/FLOAT(L11-1)
RINC12=RR2/FLOAT(L12-1)

C
RA-----ROLL ANGLE, GEAR
RATM----LENGTH OF TIP MODIFICATION IN DEGREES OF ROLL
RAT-----ROLL ANGLE AT TIP OF GEAR
RATI----ROLL ANGLE AT TOP OF INVOLUTE
RABI----ROLL ANGLE AT THE BOTTOM OF INVOLUTE
RABM----LENGTH OF ROOT MODIFICATION IN DEGREES OF ROLL
PATM----MAGNITUDE OF PARABOLIC MODIFICATION AT THE TIP
PABM----MAGNITUDE OF PARABOLIC MODIFICATION AT THE BOTTOM
STTM----MAGNITUDE OF STRAIGHT LINE MODIFICATION AT THE TIP
STBM----MAGNITUDE OF STRAIGHT LINE MODIFICATION AT THE BOTTOM
PER----MAX MANUFACTURED PROFILE ERROR
PAP----ANGLE FROM START OF SIN. ERROR TO START OF INVOLUTE
RTI----RADIUS TO TOP OF INVOLUTE
RBI----RADIUS TO BOTTOM OF INVOLUTE

C
C*****CALCULATION OF ROLL ANGLES TO INVOLUTE TOP, PITCH, AND BOTTOM; AND
C*****RADIAL DISTANCES TO (UN)MODIFIED INVOLUTE TOP, PITCH, AND BOTTOM
C

```

```

RAT1=TODEGR*SQRT((RAC1/RBC1)**2 - 1.)
RAT2=TODEGR*SQRT((RAC2/RBC2)**2 - 1.)
RAM1=RAT1-RATH1
RAM2=RAT2+RATH2
RT11=RBC1*SQRT((RAM1/TODEGR)**2 + 1.)
RT12=RBC2*SQRT((RAM2/TODEGR)**2 + 1.)

RAP=TODEGR*TAN(PHI)
RAT1P1=RAM1-RAP
RAT1P2=RAP-RAM2
RAB11=TODEGR*SQRT((RLM1/RBC1)**2 - 1.)
RAB12=TODEGR*SQRT((RLM2/RBC2)**2 - 1.)
RAN1=RAB11-RABM1
RAN2=RAB12+RABM2
RBI1=RBC1*SQRT((RAN1/TODEGR)**2 + 1.)
RBI2=RBC2*SQRT((RAN2/TODEGR)**2 + 1.)

C*****CALCULATION OF RRO
C
C 230 TP=PI*.5/DP
      PHIB1=ARCOS(RBC1/RLM1)
      BETAB1=PI/(2.*TG1)+(TAN(PHI)-PHI)-(TAN(PHIB1)-PHIB1)
      IF (RLM1.GE.RTF11) GO TO 285
      ARG1=((RRC1+RF1)**2 + RLM1**2 - RF1**2)/(2.*RLM1*(RRC1+RF1))
      ALPHA1=ARCOS(ARG1)
      RRO1=RRC1*COS(BETAB1+ALPHA1)

C
C 285 XMIN1=RTF11*SIN(BETAB1)
      PAP1=PAP1/TODEGR

C
C      PHIB2=ARCOS(RBC2/RLM2)
      BETAB2=PI/(2.*TG2)-(TAN(PHI)-PHI)+(TAN(PHIB2)-PHIB2)
      IF (RLM2.LE.RTF22) GO TO 290
      ARG2=((RRC2-RF2)**2 + RLM2**2 - RF2**2)/(2.*RLM2*(RRC2-RF2))
      ALPHA2=ARCOS(ARG2)
      RRO2=RRC2*COS(BETAB2+ALPHA2)

C
C 290 XMIN2=-RTF22*SIN(BETAB2)
      PAP2=PAP2/TODEGR

C
C*****CALCULATION OF INVOLUTE PROFILE COORDINATES, GEAR 1
C
C DO 330 J=1,L11
      ET1=0.
      PE1=0.
C

```

```

R1=RAC1-RINC11*(FLOAT(J-1))
PHI1=ARCOS(RBC1/R1)
BETA1=PI/(2.*TG1) + (TAN(PHI)-PHI) - (TAN(PHI1)-PHI1)
THETA1(J)=PHI1-BETA1
RA1=TODEGR*TAN(PHI1)
IF (J.EQ.1) RA1=RAT1

C*****CHECK FOR TIP MODIFICATIONS
C
IF (RATM1.EQ.0..OR.RA1.LT.RAM1) GO TO 300
IF (STTM1.EQ.0.) ET1=PATM1*(1.-SQRT((RAT1-RA1)/RATM1))
IF (PATM1.EQ.0.) ET1=STTM1*(RA1-RAM1)/RATM1

C*****CHECK FOR SINUSOIDAL ERRORS
C
300 IF (PER1.EQ.0.) GO TO 310
IF (RA1.GT.RAM1) PE1=PER1*SIN(PAP1)
IF (RA1.LT.RAM1)
& PE1=PER1*SIN((PI*(RAM1-RA1)*CYC1/RATIP1)+PAP1)

C*****CHECK FOR BOTTOM MODIFICATIONS
C
310 IF (RBM1.EQ.0..OR.RA1.GT.RAN1) GO TO 320
IF (STBM1.EQ.0.) ET1=PABM1*(1.-SQRT((RA1-RAB1)/RABM1))
IF (PABM1.EQ.0.) ET1=STBM1*(RA1-RAN1)/RABM1

C
320 X1(J)=R1*SIN(BETA1) + (ET1+PE1)/COS(THETA1(J))
Y1(J)=R1*COS(BETA1) - RRO1
IF (J.NE.1) THETA1(J-1)=ATAN((X1(J)-X1(J-1))/(Y1(J-1)-Y1(J)))
330 CONTINUE
C
C*****FILLET COORDINATE POINTS, GEAR 1
C
RINCBI=(R1-RRC1)/FLOAT(L1-LI1)
LI1=L1+1
DO 340 J=L11,L1
RFIL1=R1-RINCBI*FLOAT(J-LI1)
IF (RFIL1.GE.RTF1) ARCT=ALPHA1
IF (RFIL1.LT.RTF1)
&ARC1=ARCOS(((RRC1+RF1)**2+RFIL1**2-RF1**2)/(2.*RFIL1*(RRC1+RF1)))
BETA1=BETA1+ALPHA1-ARC1
X1(J)=RFIL1*SIN(BETA1)
Y1(J)=RFIL1*COS(BETA1) - RRO1
THETA1(J-1)=ATAN((X1(J)-X1(J-1))/(Y1(J-1)-Y1(J)))
340 THETA1(L1)=.5*PI - BETA1
C

```

```

C*****CALCULATION OF INVOLUTE PROFILE COORDINATES, GEAR 2
C
DO 380 J=1,L12
  ET2=0.
  PE2=0.

C
R2=RINC12*(FLOAT(J-1))+RAC2
PHI2=ARCOS(RBC2/R2)
BETA2=PI/(2.*TG2) - (TAN(PHI)-PHI) + (TAN(PHI2)-PHI2)
THETA2(J)=BETA2+PHI2
RA2=TODEGR*TAN(PHI2)
IF (J.EQ.1) RA2=RAT2

C
IF (RA1M2.EQ.0. .OR. RA2.GT.RAM2) GO TO 350
IF (STTM2.EQ.0.) ET2=PATM2*(1.-SQRT((RA2-RAT2)/RATM2))
IF (PATM2.EQ.0.) ET2=STTM2*(RAM2-RA2)/RATM2

C
IF (PER2.EQ.0.) GO TO 360
IF (RA2.LT.RAM2) PE2=PER2*SIN(PAP2)
IF (RA2.GT.RAM2)
  & PE2=PER2*SIN((PI*(RA2-RAM2)*CYC2/RAT1P2)+PAP2)

C
350 IF (RABM2.EQ.0. .OR. RA2.LT.RAN1) GO TO 370
IF (STBM2.EQ.0.) ET2=PABM2*(1.-SQRT((RAB12-RA2)/RABM2))
IF (PABM2.EQ.0.) ET2=STBM2*(RAN2-RA2)/RABM2

C
370 X2(J)=-R2*SIN(BETA2) + (ET2+PE2)/COS(THETA2(J))
Y2(J)=RR02 -R2*COS(BETA2)
IF (J.NE.1) THETA2(J-1)=ATAN((X2(J)-X2(J-1))/(Y2(J)-Y2(J-1)))
CONTINUE

C
380 C*****FILLET COORDINATE POINTS, GEAR 2
C
RINC2=(RRC2-R2)/FLOAT(L1-L12)

C
L12=L12+1
DO 390 J=L12,L2
  RFIL2=R2+RINC2*FLOAT(J-L12)
  GAP=RRC2-RFIL2
  IF (GAP.LT.RF2) GO TO 388
  BETA2=BETA2
  GO TO 389
388 ARC2=ARCOS(((RRC2-RF2)**2+RFIL2**2-RF2**2)/(2.*RFIL2*(RRC2-RF2)))
  BETA2=BETA2+ALPHA2-ARC2
389 X2(J)=-RFIL2*SIN(BETA2)

```

```

390 Y2(J)=-RFIL2*COS(BETAF2) + RR02
      THETA2(J-1)=ATAN((X2(J)-X2(J-1))/(Y2(J)-Y2(J-1)))
      THETA2(L2)=.5*PI - BETAF2
C
C CONTACT RATIO CALCULATIONS
C
      AB=SQRT(RAC1**2-RBC1**2)-SQRT(RAC2**2-RBC2**2)+C*SIN(PHI)
      E1B=SQRT(RAC1**2-RBC1**2)
      E1A=E1B-AB
      E1P=RPC1*SIN(PHI)
      AP=E1P-E1A
      PB=AB-AP
      SP=AP
      EP=PB
      CR=AB/BP
      CR1=SP/BP
      CR2=EP/BP
      WRITE(6,15) CR1,CR2,CR
C
      AUX1=ARCOS(RBC1/RT11)
      AUX2=ARCOS(RBC2/RT12)
      AL1=ARCOS(RBC1/(RB11))
      AL2=ARCOS(RBC2/(RB12))
      CRU1=RPC1*(SIN(PHI)-COS(PHI)*TAN(AL1))/BP
      CRU2=RPC2*(-SIN(PHI)+COS(PHI)*TAN(AL2))/BP
      CR1=-((RT12)*SIN(AUX2)-RPC2*SIN(PHI))/BP
      CR2=((RT11)*SIN(AUX1)-RPC1*SIN(PHI))/BP
      CRU12=CRU1+CRU2
      CR12=CR1+CR2
      WRITE(6,15) CRU1,CRU2,CRU12
      WRITE(6,15) CR1,CR2,CR12
15  FORMAT(' ',3X,3F11.7)
      IF((RBC1.GE.RB11).AND.(RBC2.LE.RB12)) GO TO 18
C
C IF(CRU1.LE.CR1) CR1=CRU1
C IF(CRU2.LE.CR2) CR2=CRU2
C IF(CRU1.GT.CR1) CR1=CR1
C IF(CRU2.GT.CR2) CR2=CR2
18  CR=CR1+CR2
      WRITE(6,12) CR
      SP=CR1*BP
      EP=CR2*BP
      SE=CR*BP
      INF = 1
12  FORMAT('T46, THE THEORETICAL CONTACT RATIO = ',F8.3/)
13  FORMAT(' ',3X,4F11.7)

```

```

14 FORMAT( ' ', 3X, 5F11.7, 14)
C
C****PIT INSERTION
C
IF (DEEP1.EQ.0.0) GO TO 4561
DO 4560 I=1PIT11, 1PIT12
4560 X1(I)=X1(I)-DEEP1
4561 IF (DEEP2.EQ.0.0) GO TO 4563
DO 4562 I=1PIT21, 1PIT22
4562 X2(I)=X2(I)+DEEP2
4563 CONTINUE
C****TO BE REMOVED
PHI11=ARCOS(RBC1/RT11)
BETAT1=PI/(2.*TG1)+(TAN(PHI)-PHI)-(TAN(PHI11)-PHI11)
YT11=RT11*COS(BETAT1)-RR01
PHIB1=ARCOS(RBC1/RB11)
BETAB1=PI/(2.*TG1)+(TAN(PHI)-PHI)-(TAN(PHIB1)-PHIB1)
YB11=RB11*COS(BETAB1)-RR01
YP1=RPC1*COS(PI/(2.*TG1))-RR01

PHI12=ARCOS(RBC2/RT12)
BETAT2=PI/(2.*TG2)-(TAN(PHI)-PHI)+(TAN(PHI12)-PHI12)
YT12=-RT12*COS(BETAT2)+RR02
PHIB2=ARCOS(RBC2/RB12)
BETAB2=PI/(2.*TG2)-(TAN(PHI)-PHI)+(TAN(PHIB2)-PHIB2)
YB12=-RB12*COS(BETAB2)+RR02
YP2=-RPC2*COS(PI/(2.*TG2))+RR02

C
RETURN
END
C
C
C
SUBROUTINE SLOWM(LCR, LINF)
COMMON/C1/PHI, PHID, DP, H, TG1, TG2, TP, DELTP
COMMON/HD/TITLE1(20), TITLE2(20), TITLE3(20), TAPE
COMMON/C2/PI, F1, F2, R11, R12, E1, E2, G1, G2, PR1, PR2, GAMA1, GAMA2, RT1, RT2
COMMON/C4/TIN, TOUT, RPMIN, RPMOUT, OMEGA1, OMEGA2, RADEL2, COR1, COR2,
1 COR3, COR4, DPSL11, DPSL12, DPEL1, DPEL2
COMMON/C5/JG1, JG2, JD, JL, KDS, KLS, KGPVAVG, ZETAS, ZETAG, CDS, CLS, CGPAVG,
1LDS, LLS, 1PLOT, CBD, CB1, CB2, CBL
COMMON/C6/L1, L2, PD1, PD2, RPC1, RPC2, RAC1, RAC2, RBC1, RBC2, RRC1, RRC2,
2RF1, RF2, C, CP, BP, UCUT1, UCUT2
COMMON/C7/YT11, YT12, YP1, YP2, YB11, YB12, RT11, RT12, RB11, RB12,
1RR01, RR02, XMIN1, XMIN2, SP, EP

```



```

V1(1)=0.0
W1(1) = X1(1)
Z1(1) = RRO1 + Y1(1)
R1(1)=SQRT(W1(1)**2+Z1(1)**2)
IF(R1(1).GT.RAC1) R1(1)=RAC1
2 CONTINUE
DO 3 I = 1,L1
  IPP=I
  IF(RPC1_GE.R1(I)) GO TO 4
3 CONTINUE
4 THPP1=ATAN(W1(IPP)/Z1(IPP))
  DO 5 I = 1,L2
    W2(1) = X2(I)
    Z2(1) = RRO2 - Y2(1)
    R2(1)=SQRT(W2(1)**2+Z2(1)**2)
    IF(R2(1).LT.RAC2) R2(1)=RAC2
    R11=SQRT(W1(1)**2+(C-Z1(1))**2)
    U2(1)=0.0
    V2(1)=0.0
5 CONTINUE
  DIFFF=(Y1(1)-Y1(L1))/(FLOAT(L1))
  DO 6 I = 1,50
    CMS(I) = 0.0
    SVS(I) = 0.0
    HZPS(I) = 0.0
    PVS(I) = 0.0
    PHIOP(I)=0.0
    VELR(I)=0.0
6 CONTINUE
  CDEF(1) = 0.0
  CDEF(50) = 0.0
  AB=SQRT(RAC1**2-RBC1**2)-SQRT(RAC2**2-RBC2**2)+C*SIN(PHI)
  E1B=SQRT(RAC1**2-RBC1**2)
  E1A=E1B-AB
  E1P=RPC1*SIN(PHI)
  AP=E1P-E1A
  PB=AB-AP
  SP=AP
  EP=PB
  US = -(SP + CDEF(1))*COS(PHI) + RPC1
  VS = -(SP + CDEF(1))*SIN(PHI)
  UE = (EP + CDEF(50))*COS(PHI)
  VE = (EP + CDEF(50))*SIN(PHI) + RPC1
  RTS = SQRT(US**2 + VS**2)

```



```

DO 8100 K=1,5
DO 8100 I=1,50
TDEF1(K,I)=0.0
TDEF2(K,I)=0.0
8100 CONTINUE
PSS1SL=PSI1SL
PSS1EL=PSI1EL
PSS2EL=PSI2EL
PSS2SL=PSI2SL
INT = 50
DO 47 J=1,2
IF(J.EQ.1) GO TO 8120
DO 8110 I=1,L2
Z2(I)=RR02-Y2(I) + RADEL2
8110 CONTINUE
WRITE(6,8111) RADEL2,COR1,COR2,COR3,COR4
8111 FORMAT('0',RADEL2='F9.5,5X',COR1='F9.5,5X',COR2='F9.5,
15X',COR3='F9.5,5X',COR4='F9.5)
WRITE(6,8112) DPSL1,DPSL2,DPEL1,DPEL2
8112 FORMAT('0',DPSL1='F9.5,5X',DPSL2='F9.5,5X',DPEL1='F9.5,5X,
1',DPEL2='F9.5)
8120 CONTINUE
C
WRITE(6,9001) PSI1SL,PSI1EL,PSI2SL,PSI2EL,DELTA1,DELTA2
9001 FORMAT('0',THEORETICAL INITIAL ANGLES OF CONTACT',1X,
& 4F11.7',THEORETICAL ANGULAR INCREMENTS -',2F11.7)
C
V1SP=0.0
U1SP=0.0
V2SP=0.0
U2SP=0.0
V1EP=0.0
U1EP=0.0
V2EP=0.0
U2EP=0.0
U11=0.0
U22=0.0
U12EP=0.0
U12SP=0.0
MTC=0
NMC=0
KKKK=(2*L1)+10
DELT=0.2
MLIM=75
UTEST=1000.
C
C
C
MLIM=MLIM

```

```

NLIM1=2*NLIM
MLIM1=2*MLIM
L11=L1-1
L22=L2-1
IRDEL=30
IR1S1=IR1S-IRDEL
IR1S2=IR1S+IRDEL
DELTA1 = (PSI1SL - PSI1EL)/49.
DELTA2 = (TG1/TG2)*DELTA1
P1SL=PSSI1SL+DELTA1*(FLOAT(NLIM-1))*DELT
P2SL=PSS2SL+DELTA2*(FLOAT(NLIM-1))*DELT
DIF1=(Y1(1)-Y1(L1))/(FLOAT(L1))
DIF2=(Y2(1)-Y2(L2))/(FLOAT(L2))
IF(DIF1.GE.DIF2) DIF=DIF1
IF(DIF2.GT.DIF1) DIF=DIF2
IF(IR1S1.LE.1) IR1S1=1
IF(IR1S2.GT.L1) IR1S2=L1-1
DIFF=9.99
WRITE(6,9015) TDEF1(3,1), TDEF2(3,1),
& FORMAT('0',I) TDEF1(3,INT), TDEF2(3,INT)
& ' DEFLECTIONS ADDED AT ENTRANCE -1,2F11.7/
& DEFLECTIONS ADDED AT EGRESS -1,2F11.7)
DPSI1S=0.0
ADD1=0.0
ADD2=0.0
IF(I1.EQ.2) ADD1=DPSLI1
IF(I1.EQ.2) ADD2=DPSLI2
49 CONTINUE
IF (MNC.EQ.8.OR.MMC.EQ.5) DIFF=DIFF+(DIFF/3.)
DO 50 N1=1,NLIM1
COR=COR1
PSI1SL=P1SL-DELTA1*(FLOAT(N1-1))*DELT - TG2/TG1*COR1*DPSI1S+ADD1
PSI2SL=P2SL-DELTA2*(FLOAT(N1-1))*DELT + COR2*DPSI1S +ADD2
DO 51 L=1,LLLL
LC=L
U2(L)=-Z2(L)*SIN(PSI2SL-.5*PI)-(W2(L)-TDEF2(3,1))*COS(PSI2SL-.5*
&PI)
V2(L)=Z2(L)*COS(PSI2SL-.5*PI)+(W2(L)-TDEF2(3,1))*SIN(PSI2SL-
&.5*PI)
U2SP=U2(LC)
V2SP=V2(LC)
DO 52 J=IR1S1,IR1S2
JC=J
U1(J)=(W1(J)+TDEF1(3,1))*SIN(PSI1SL)+Z1(J)*COS(PSI1SL)
U1(J+1)=(W1(J+1)+TDEF1(3,1))*SIN(PSI1SL)+Z1(J+1)*COS(PSI1SL)

```



```

IF(L.GT.1.AND.MMC.EQ.7) GO TO 49
IF (MMC.EQ.5) GO TO 49
DPSI2L=0.0
ADD3=0.0
ADD4=0.0
IF(I1.EQ.2) ADD3=DPEL1
IF(I1.EQ.2) ADD4=DPEL2
Y1S=Z1(JC)-RR01
Y2S=-Z2(LC)+RR02
V1SP=V2SP
U1SP=U2SP
MLIM=4
UTEST=1000.
MLIM1=8
DELT = 0.2
PIEL=PSS1EL-DELTA1*(FLOAT(MLIM-1))*DELT
P2EL=PSS2EL-DELTA2*(FLOAT(MLIM-1))*DELT
IR2E1=IR2E-IRDEL
IR2E2=IR2E+IRDEL
IF(IR2E1.LE.1) IR2E1=1
IF(IR2E2.GT.L2) IR2E2=L2-1

C
DO 60 M1=1,MLIM1
COR=COR2
PSI1EL=P1EL+DELTA1*(FLOAT(M1-1))*DELT -TG2/TG1*COR3*DPSI2L+ADD3
PSI2EL=P2EL+DELTA2*(FLOAT(M1-1))*DELT + COR4*DPSI2L +ADD4
DO 61 J=1,JJJJ
JE=J
U1(J)=(W1(J)+TDEF1(3,INT))*SIN(PSI1EL)+Z1(J)*COS(PSI1EL)
V1(J)=-(W1(J)+TDEF1(3,INT))*COS(PSI1EL)+Z1(J)*SIN(PSI1EL)+C
U1EP=U1(JE)
V1EP=V1(JE)
DO 62 LL=1,IR2E1
L=IR2E2+1-LL
LE=L
U2(L)=-((Z2(L)*SIN(PSI2EL-.5*PI)-(W2(L)-TDEF2(3,INT))*COS(PSI2EL
&-.5*PI))
U2(L-1)=-((Z2(L-1)*SIN(PSI2EL-.5*PI)-(W2(L-1)-TDEF2(3,INT))*
&COS(PSI2EL-.5*PI))
V2(L)=Z2(L)*COS(PSI2EL-.5*PI)+(W2(L)-TDEF2(3,INT))*SIN(PSI2EL
&-.5*PI)
V2(L-1)=Z2(L-1)*COS(PSI2EL-.5*PI)+(W2(L-1)-TDEF2(3,INT))*SIN(
&PSI2EL-.5*PI)
IF (V2(L-1).GT.V1EP) GO TO 62
IF (V2(L).LE.V1EP.AND.V2(L-1).LT.V1EP) GO TO 61

```

```

ARG22=V2(L)-V2(L-1)
ARGV22=(V1EP-V2(L-1))*(U2(L)-U2(L-1))
U22=(ARGV22/ARG22)+U2(L-1)
U12EP=U1EP-U22
V12EP=V2(L)-V1EP
NMC=5
IF(11.EQ.3) WRITE(6,9020) M1,J,L,U1(J),V1(J),U2(L),V2(L),
&U12EP,V12EP,NMC
IF (ABS(U12EP).GT.ABS(U1TEST)) GO TO 59
MTEST=M1
JTEST=J
LTEST=L
U1TEST=U1(J)
V1TEST=V1(J)
U2TEST=U22
V2TEST=V2(L)
U1TEST=U12EP
V1TEST=V12EP
C 59 IF (U1EP.GE.U22.AND.ABS(V12SP).LE.DIFF.AND.U12EP.LE.0.000080)
& GO TO 63
NMC=6
IF (ABS(U12EP).LE.0.000010.AND.ABS(V12EP).LE.DIFF) GO TO 63
62 CONTINUE
61 CONTINUE
60 CONTINUE
NMC=8
63 CONTINUE
C
IF(NMC.EQ.8) DPSI2L=ATAN(U2TEST/V1TEST)-ATAN(U1TEST/
&V1TEST)+DPSI2L
IF (NMC.EQ.8) WRITE(6,64) MTEST,JTEST,LTEST,U1TEST,V1TEST,U2TEST,
& V2TEST,U1TEST,V1TEST,DPSI2L
& 64 FORMAT('0','CLOSEST APPROACH CONDITIONS',1X,3I5,3(2F11.7,4X),2X,
& F11.7)
C
IF(NMC.EQ.8) GO TO 9011
IF(J.GT.1.AND.NMC.EQ.6) DPSI2L=ATAN(U22/V1(J))-ATAN(U1(J)/
&V1(J))+DPSI2L
WRITE(6,9020) M1,J,L,U1(J),V1(J),U22,V2(L),U12EP,V12EP,DPSI2L,
&NMC
9020 FORMAT(' ','ACTUAL END OF CONTACT',1X,
& 3I5,3(2F11.7,4X),F11.7,4X,'CONTACT CODE -',13)
& IF (J.GT.1.AND.NMC.EQ.6)GO TO 9011
C

```

```

9017 WRITE(6,9017)
      FORMAT('0', 'COORDINATES AT END OF CONTACT')
      DO 9019 I=1,3
        NO1=J+I-3
        NO2=L+I-2
        RAD1=SQRT(U1(NO1)**2 + V1(NO1)**2)
        RAD2=SQRT(U2(NO2)**2 + V2(NO2)**2)
9018 WRITE(6,9018) NO1,U1(NO1),V1(NO1),RAD1,NO2,U2(NO2),V2(NO2),RAD2
9019 FORMAT(' ',2(15,3F11.7,5X))
      CONTINUE

      Y1E=Z1(JE)-RRO1
      Y2E=-Z2(LE)+RR02
      V2EP=V1EP
      U2EP=U1EP
      R1S=SQRT(U1SP**2+V1SP**2)
      R1E=SQRT(U1EP**2+V1EP**2)
88 CONTINUE
      IF (MNC.EQ.8.OR.MMC.EQ.5) GO TO 49
      DELTA1 = (PSI1SL - PSI1EL)/(INT-1)
      DELTA2 = (PSI2SL-PSI2EL)/(INT-1)
      PRANG=ATAN(ABS(R1E*SIN(PSI1EL)-R1S*SIN(PSI1SL))/ABS(R1E*
      &COS(PSI1EL)-R1S*COS(PSI1SL)))*180./PI
C
C WRITE(6,9021) PSI1SL,PSI1EL,PSI2SL,PSI2EL,DELTA1,DELTA2
9021 FORMAT('0', 'ACTUAL INITIAL AND FINAL ANGLES OF CONTACT',/1X,
      &4F11.7/' ACTUAL ANGULAR INCREMENTS - ',2F11.7)
C
C WRITE(6,9030) MNC,MMC,PRANG
9030 FORMAT('0', 'CONTACT CODES: ',2I6/' PRESSURE ANGLE: ',F6.2)
C
      DO 7 I = 1,L1
        DCP1(I) = 0.0
        THETC1(I) = 0.0
        DCP2(I) = 0.0
        THETC2(I) = 0.0
7 CONTINUE
      Y1EE=Y1(L1)
      Y1SS=Y1(L1)
      I1EE=1
      I1SS=L1
      Y2SS=Y2(1)
      Y2EE=Y2(L2)
      I2SS=1
      I2EE=L2

```



```

10 CONTINUE
DO 23 K = 1,5
PSI11=PSI1TP(K)
PSI22=PSI2TP(K)
UCP(K) = 0.0
VCP(K) = 0.0
ZCP1(K) = 0.0
ZCP2(K) = 0.0
WCP1(K) = 0.0
WCP2(K) = 0.0
XCP1(K) = 0.0
XCP2(K) = 0.0
YCP1(K) = 0.0
YCP2(K) = 0.0
RCP1(K) = 0.0
RCP2(K) = 0.0
RCCP1(K)=0.0
RCCP2(K)=0.0
JCPT1=0
JCPT2=0
JCPB1=0
JCPB2=0
VEL1=0.0
VEL2=0.0
VEH01=0.0
VEH02=0.0
IR1S22=IR1S2+1
IF((PSI1TP(K).GT.PSI1LS).OR.(PSI1TP(K).LT.PSI1LE)) GO TO 23
IPRIME=0
IF (K.EQ.3) GO TO 8990
ARG=(PSI1TP(K)-PSI1TP(3))/DELTA1
IPRIME=FIX(ARG)+1
IF (ARG.LT.0) IPRIME=FIX(ARG)-1
8990 N=1-IPRIME
IF ((1-IPRIME).LE.0.OR.(1-IPRIME).GT.50) GO TO 23
REMEM1=TDEF1(3,N)
REMEM2=TDEF2(3,N)
IF (K.LE.3) GO TO 8993
TDEF1(3,N)=0.0
TDEF2(3,N)=0.0
IF (11.EQ.1) GO TO 8993
TDEF1(3,N)=RESIDL(1,N)
TDEF2(3,N)=RESIDL(2,N)
8993 CONTINUE
DO 901 J=1,IR1S22

```

```

U1(J)=(W1(J)+TDEFL1(3,N))*SIN(PSI1TP(K))+Z1(J)*COS(PSI1TP(K))
V1(J)=- (W1(J)+TDEFL1(3,N))*COS(PSI1TP(K))+Z1(J)*SIN(PSI1TP(K)) + C
901 CONTINUE
  IR2E22=IR2E2+1
  DO 902 L=1,IR2E2
    U2(L)=(Z2(L)*SIN(PSI2TP(K)-.5*PI)-(W2(L)-TDEFL2(3,N))
    *COS(PSI2TP(K)-.5*PI))
    V2(L)=Z2(L)*COS(PSI2TP(K)-.5*PI)+(W2(L)-TDEFL2(3,N))*SIN(PSI2
    *TP(K)-.5*PI)
902 CONTINUE
  TDEFL1(3,N)=REMEM1
  TDEFL2(3,N)=REMEM2
11 CONTINUE
C THIS SEGMENT LOCATES THE CONTACT POINT BETWEEN A GIVEN TOOTH PAIR
  IF((PSI1TP(K).GT.PSI1LS).OR.(PSI1TP(K).LT.PSI1LE)) GO TO 23
  DISTL = (RAC1 - RRC1)/(FLOAT(L1)*5.)
  GO TO 14
13 DISTL = 2.*DISTL
14 DO 15 J=1,IR1S2
  DIST = (ABS(TAN(PHI)*U1(J)-V1(J)+C+RPC1))/(SQRT((TAN(PHI))**2+1.))
  IF(DIST .LT.DISTL) GO TO 16
15 CONTINUE
  GO TO 13
16 IF(DIST.EQ.0.0) GO TO 21
  IF(J.EQ.1) GO TO 18
  IF(U1(J).EQ.0.0) GO TO 17
  ARGS = ABS(RPC1-V1(J)+C)/ABS(U1(J))
  SLOPE = ATAN(ARGS)
  IF((SLOPE.GT.PHI).AND.(U1(J).LT.0.0)) GO TO 19
  IF((SLOPE.LT.PHI).AND.(U1(J).GT.0.0)) GO TO 19
  GO TO 18
17 IF(V1(J)-C.LE.RPC1) GO TO 19
C POINT IS ABOVE THE LINE OF ACTION
18 UA = U1(J)
  VA = V1(J)-C
  UB = U1(J+1)
  VB = V1(J+1)-C
  GO TO 20
C POINT IS BELOW THE LINE OF ACTION
19 UA = U1(J-1)
  VA = V1(J-1)-C
  UB = U1(J)
  VB = V1(J)-C
20 SLOPE = (VA-VB)/(UA-UB)
  AT1 = TAN(PHI)

```

```

A12 = RPC1
A21 = SLOPE
A22 = VB - SLOPE*UB
UCP(K) = (A22-A12)/(A11-A21)
VCP(K) = A11*UCP(K) + A12
GO TO 22
21 UCP(K) = U1(J)
VCP(K) = V1(J)-C
22 CONTINUE
RCP2N = SQRT((UCP(K)**2) + ((C+VCP(K))**2))
JCP=J
JDEL=40
JCPB1=JCP+JDEL
JCPT1=JCP-JDEL
IF (JCPB1.GE.IR1S2) JCPB1=IR1S2
IF(JCPT1.LE.1) JCPT1=1
R2N=SQRT((C+VCP(K))**2+UCP(K)**2)
DO 165 L=1,IR2E2
LCP=L
IF(R2N.LE.R2(L)) GO TO 166
165 CONTINUE
166 JCPB2=LCP+JDEL
JCPT2=LCP-JDEL
IF (JCPB2.GE.IR2E2) JCPB2=IR2E2
IF(JCPT2.LE.1) JCPT2=1
U1U2P=U1(JCP)-U2(LCP)
V1V2P=V1(JCP)-V2(LCP)
IF((K.EQ.3).AND.(I.EQ.1).AND.(V2SP.NE.0.0)) VCP(K)=V2SP -C
IF((K.EQ.3).AND.(I.EQ.1).AND.(V2SP.NE.0.0)) UCP(K)=U2SP
IF((K.EQ.3).AND.(I.EQ.1).AND.(V2SP.NE.0.0)) GO TO 350
IF((K.EQ.3).AND.(I.EQ.INT).AND.(V1EP.NE.0.0)) VCP(K)=V1EP -C
IF((K.EQ.3).AND.(I.EQ.INT).AND.(V1EP.NE.0.0)) UCP(K)=U1EP
IF((K.EQ.3).AND.(I.EQ.INT).AND.(V1EP.NE.0.0)) GO TO 350
DV11=0.0
U11=0.0
U22=0.0
V11=0.0
C
TESTK=SQRT((U1(JCP)-U2(LCP))**2 + (V1(JCP)-V2(LCP))**2)
PHID1=ATAN((V1(JCP)-RPC2)/U1(JCP))*57.2957795
PHID2=ATAN((V2(LCP)-RPC2)/U2(LCP))*57.2957795
9063 ALIMIT=0.00001
C
DO 204 J=JCPT1,JCPB1
IF (J.EQ.JCPT1) COMPAR=100.0

```

```

IF (J.NE.JCPT1.AND.ABS(U12).LE.ABS(COMPARI)) COMPARI=U12
U11=U1(J)
V11=V1(J)
VCPT2=V2(JCPT2)-DIFF
IF (V11.LT.VCPT2) MMM=3
IF (V11.LT.VCPT2) GO TO 199
DO 202 L=JCPT2,JCPB2
IF (V2(L+1).GE.V11) GO TO 222
202 CONTINUE
MMM=7
GO TO 204
222 ARGV2=V2(L+1)-V2(L)
IF (ARGV2.NE.0.0) U22=((V11-V2(L))*(U2(L+1)-U2(L))/ARGV2)+U2(L)
IF (ARGV2.EQ.0.0) U22=U2(L)
U12=U11-U22
PHI1=ATAN(ABS(V11-C-RPC1)/ABS(U11))*180./PI
PHI2=ATAN(ABS(V11-C-RPC1)/ABS(U22))*180./PI
SLOPE1=ATAN(ABS(U1(J)-U1(J+1))/ABS(V1(J)-V1(J+1)))*180./PI
SLOPE2=ATAN(ABS(U2(L)-U2(L+1))/ABS(V2(L)-V2(L+1)))*180./PI
IF (U11.GE.U22) MMM=0
IF (U11.GE.U22) GO TO 349
IF (ABS(U12).LE.ALIMIT) MMM=18
IF (ABS(U12).LE.ALIMIT) GO TO 349
IF (V1(J+1).GT.V2(L)) GO TO 204
ARGV3=V1(J+1)-V1(J)
IF (ARGV3.NE.0.0) U11=((V2(L)-V1(J))*(U1(J+1)-U1(J))/ARGV3)+U1(J)
IF (ARGV3.EQ.0.0) U11=U1(J+1)
U12=U11-U2(L)
IF (U11.GE.U2(L)) MMM=72
IF (U11.GE.U2(L)) GO TO 349
IF (ABS(U12).LE.ALIMIT) MMM=73
IF (ABS(U12).LE.ALIMIT) GO TO 349
IF (L.EQ.1) GO TO 204
IF (V1(J+1).GT.V2(L-1)) GO TO 204
IF (ARGV3.NE.0.0) U11=((V2(L-1)-V1(J))*(U1(J+1)-U1(J))/V1(J+1)-
&V1(J))+U1(J)
IF (ARGV3.EQ.0.0) U11=U1(J+1)
U12=U11-U2(L-1)
IF (U11.GE.U2(L-1)) MMM=78
IF (U11.GE.U2(L-1)) GO TO 349
IF (ABS(U12).LE.ALIMIT) MMM=79
IF (ABS(U12).LE.ALIMIT) GO TO 349
204 CONTINUE
199 CONTINUE
IF (ABS(U12).LE.ABS(COMPARI)) COMPARI=U12
204 CONTINUE
199 CONTINUE

```

```

IF((MMM.EQ.3).AND.(PAS1.NE.0)) GO TO 504
IF((K.EQ.3).AND.(ABS(U1122).LE.ALIMIT)).AND.(MMM.EQ.3)) MMM=4
IF((K.EQ.3).AND.(ABS(U1122).LE.ALIMIT)).AND.(MMM.EQ.3)) GO TO 349
504 CONTINUE

```

C

```

UC1(K)=U1(JCP)
VC1(K)=V1(JCP) -C
UC2(K)=U2(LCP)
VC2(K)=V2(LCP)
XCP1(K)=0.0
XCP2(K)=0.0
YCP2(K)=0.0
YCP1(K)=0.0
RCP1(K)=0.0
RCP2(K)=0.0
RCCP1(K)=0.0
RCCP2(K)=0.0
ZCP1(K)=0.0
ZCP2(K)=0.0
WCP1(K)=0.0
WCP2(K)=0.0
UCP(K)=0.0
VCP(K)=0.0
UVDCP=0.0
MMM=15
VELR(1)=TG2/TG1
GO TO 360
349 CONTINUE

```

C

```

UCP(K)=U11
VCP(K)=V11 -C
350 CONTINUE
UVDCP=0.0
NCTP = NCTP +1
RCP1(K) = SQRT((UCP(K)**2) + (VCP(K)**2))
RCP2(K)=SQRT(UCP(K)**2+(C+VCP(K))**2)
ZCP2(K) = UCP(K)*COS(PSI2TP(K)) + (C+
1VCP(K))*SIN(PSI2TP(K))
ZCP1(K) = UCP(K)*COS(PSI1TP(K)) + VCP(K)*SIN(PSI1TP(K))
WCP1(K) = UCP(K)*SIN(PSI1TP(K)) - VCP(K)*COS(PSI1TP(K))
WCP2(K) = UCP(K) *SIN(PSI2TP(K)) -(C+
1VCP(K))*COS(PSI2TP(K))
RCCP1(K)=SQRT(ABS(RCP1(K)**2-RBC1**2))
RCCP2(K)=SQRT(ABS(RCP2(K)**2-RBC2**2))
IF(K.NE.3) GO TO 359

```

```

IF(K.EQ.3) THBUY(K)=ATAN(WCP1(K)/ZCP1(K))
ANG=ATAN(UCP(K)/VCP(K))
IF(UCP(K).LE.0.0) ANG1=ATAN(ABS(UCP(K))/VCP(K))
ANG2=ATAN(UCP(K)/(C+VCP(K)))
IF(UCP(K).LE.0.0) ANG2=ATAN(ABS(UCP(K))/(C+VCP(K)))
AN12=ANG1-ANG2
ANB1=ATAN(RCCP1(K)/RBC1)
AN1B=ANB1+ANG1
IF(UCP(K).GT.0.0) AN1B=ANB1-ANG1
AN11=PHI-ANG1
AN22=ANG2-PHI
IF(UCP(K).GE.0.0) AN11=PHI+ANG1
IF(UCP(K).GE.0.0) AN22=PHI+ANG2
RCCN1=SQRT(ABS(RBC1**2+RCP1(K)**2-2.*RBC1*RCP1(K)*COS(AN11)))
RCCN2=SQRT(ABS(RBC2**2+RCP2(K)**2-2.*RBC2*RCP2(K)*COS(AN22)))
PPND=RBC1/COS(AN1B)
RPMOTN=PPND*RPMIN/(C+PPND)
VELR(1)=RPMIN/RPMOTN
VEL1=RCP1(K)*RPMIN**2.*PI/12.
VEL2=RCP2(K)*RPMOTN**2.*PI/12.
PPP=PPND-RPC1
VEL11=VEL1
VEL22=RCP2(K)*RPMOUT**2.*PI/12.
SV12=SQRT(ABS(VEL1**2+VEL2**2-2.*VEL1*VEL2*COS(AN12)))
SVS(1)=SV12
SV11=SQRT(ABS(VEL11**2+VEL22**2-2.*VEL11*VEL22*COS(AN12)))
OMEGA1=2.*PI*RPMIN/60.
OMEGA2=2.*PI*RPMOUT/60.
SLIDV1=SQRT(ABS(RCP1(K)**2-RBC1**2))
SLIDV2=SQRT(ABS(RCP2(K)**2-RBC2**2))
SV13=(ABS(OMEGA2*SLIDV2-OMEGA1*SLIDV1))*5.
SVR=SVS(1)/SV13
RVELR=RPMOTN/RPMOUT
C INTERFERENCE CHECK
LINF=1
NNNN=1
IF((PAS.EQ.7).AND.((RCP1(K).LT.RBC1))) LINF=2
IF((PAS.EQ.7).AND.((RCP2(K).LT.RBC2))) LINF=2
IF((PAS.EQ.7).AND.((RCP1(K).LT.RB1))) LINF=2
IF((PAS.EQ.7).AND.((RCP2(K).GT.RB12))) LINF=2
C*****CHECK FOR INTERFERENCE, TAKEN FROM BUCKINGHAM, PAGE 129
C
C ETA1=ACOS((RAC2**2 - RAC1**2 - C**2)/(2*C*RAC1)
C ETA2=TG1*ETA1/TG2
C

```



```

TDCP1(K) = 0.0
TDCP2(K) = 0.0
THCP1(K) = 0.0
THCP2(K) = 0.0
TD(K) = 0.0
PSIRD1(K) = 0.0
PSIRD2(K) = 0.0
H1(K) = 0.0
H2(K) = 0.0
HD(K) = 0.0
CDEF(L(K)) = 0.0
STIFF(K) = 0.0
KT=0.0
TPS(K, I)=0.0
MM=7
IF((PAS.EQ.7).AND.((RCP1(K).EQ.0.0).OR.(RCP2(K).EQ.0.0))) MM=35
IF((PSI1TP(K).GT.PSI1LS).OR.(PSI1TP(K).LT.PSI1LE)) MM=36
IF((PAS.EQ.7).AND.((RCP1(K).EQ.0.0).OR.(RCP2(K).EQ.0.0))) GO TO 35
IF((PSI1TP(K).GT.PSI1LS).OR.(PSI1TP(K).LT.PSI1LE)) GO TO 35
DO 24 K1 = 1, L1
IF(Y1(K1).EQ.YCP1(K)) GO TO 30
IF(Y1(K1).LT.YCP1(K)) GO TO 31
24 CONTINUE
25 DO 26 K2 = 1, L2
IF(Y2(K2).EQ.YCP2(K)) GO TO 32
IF(Y2(K2).LT.YCP2(K)) GO TO 33
26 CONTINUE
30 TDCP1(K) = DCP1(K1)
THCP1(K) = THETC1(K1)
GO TO 25
31 CONTINUE
YINCRM=(Y1(K1-1)-YCP1(K))/(Y1(K1-1)-Y1(K1))
TDCP1(K)=DCP1(K1-1)+YINCRM*(DCP1(K1)-DCP1(K1-1))
THCP1(K)=THETC1(K1-1)+YINCRM*(THETC1(K1)-THETC1(K1-1))
GO TO 25
32 TDCP2(K) = DCP2(K2)
THCP2(K) = THETC2(K2)
GO TO 35
33 CONTINUE
YINCRM=(Y2(K2-1)-YCP2(K))/(Y2(K2-1)-Y2(K2))
TDCP2(K)=DCP2(K2-1)+YINCRM*(DCP2(K2)-DCP2(K2-1))
THCP2(K)=THETC2(K2-1)+YINCRM*(THETC2(K2)-THETC2(K2-1))
35 CONTINUE
C WRITE(6,9070) KT
9070 FORMAT('0',7) AT THE START OF DO 36, KT=',E13.6)

```

```

DO 36 K = 1,5
IF((PAS.EQ.7).AND.((RCP1(K).EQ.0.0).OR.(RCP2(K).EQ.0.0))) GO TO 36
IF((PS11TP(K).GT.PS11LS).OR.(PS11TP(K).LT.PS11LE)) GO TO 36
TD(K) = TDCP1(K) + TDCP2(K)
C1 = (4.*RCCP1(K)*RCCP2(K))/((PI*F)*(RCCP2(K)-RCCP1(K)))
BH = SQRT(C1*C2*Q1)
H1(K) = XCP1(K)/COS(THCP1(K))
H2(K) = -XCP2(K)/COS(THCP2(K))
ARG3 = (2.*H1(K))/BH
ARG4 = (2.*H2(K))/BH
HD(K)=(C3*(ALOG(ARG3)-C4)+C5*(ALOG(ARG4)-C6))*Q1
CDEF1(K) = TD(K) + HD(K)
STIFF(K) = 1.0/CDEF1(K)
KT = KT + STIFF(K)
TPS(K,1)=STIFF(K)
WRITE(6,9071) TDCP1(K),TDCP2(K),HD(K),CDEF1(K),TPS(K,1),KT
FORMAT(1,4(3X,E13.6),5X,2(E13.6,3X))
36 CONTINUE
CMS(1)=KT
DO 37 K = 1,5
QTP(K) = 0.0
IF (KT.NE.0.0) QTP(K)=(STIFF(K)/KT)*P
IF (PS11TP(K).GT.PS11LS.OR.PS11TP(K).LT.PS11LE) GO TO 37
V11 = QTP(K)*COS(THCP1(K))
T1 = V11*( YCP1(K)+ RR01)
PSIRD1(K) = (T1/(4.*PI*F1*G1))*(1./(R11**2))-1./(RR01**2))
PSIRD1(K) = PSIRD1(K) + PSIRD1(K)
V22 = QTP(K)*COS(THCP2(K))
T2 = V22*(-YCP2(K)+ RR02)
PSIRD2(K) = (T2/(4.*PI*F2*G2))*(1./(RR02**2))-1./(R12**2))
PSIRD2(K) = PSIRD2(K) + PSIRD2(K)
37 CONTINUE
KT=0.0
WRITE(6,9072) KT
FORMAT(10,1,1,AT THE START OF DO 40, KT=' ,E13.6)
DO 40 K = 1,5
IF((PAS.EQ.7).AND.((RCP1(K).EQ.0.0).OR.(RCP2(K).EQ.0.0))) GO TO 40
IF((PS11TP(K).GT.PS11LS).OR.(PS11TP(K).LT.PS11LE)) GO TO 40
THETAQ = ATAN(XCP1(K)/(RR01 + YCP1(K)))
ARG = ABS(THCP1(K) + THETAQ)
STIFF(K) = 1.0/CDEF1(K)
KT = KT + STIFF(K)
TPS(K,1)=STIFF(K)
TDCP1(K) = TDCP1(K)*QTP(K) + RCP1(K)*(PSIRD1(K)-PSIRD1(K))*COS(ARG)
THETAQ = ATAN(-XCP2(K)/(RR02-YCP2(K)))

```

```

ARG = ABS(THCP2(K) + THETAQ)
TDCP2(K) = TDCP2(K)*QTP(K) + RCP2(K)*(PSIR2T-PSIRD2(K))*COS(ARG)
TD(K) = TDCP1(K) + TDCP2(K)
BH = SQRT(C1*C2*QTP(K))
ARG3 = (2.*H1(K))/BH
ARG4 = (2.*H2(K))/BH
HD(K) = (C3*(ALOG(ARG3)-C4) + C5*(ALOG(ARG4)-C6))*QTP(K)
CHS(1)=KT
CDEF1(K) = TD(K) + HD(K)
WRITE(6,9071) TDCP1(K),TDCP2(K),HD(K),CDEF1(K),TPS(K,1),KT
C 40 CONTINUE
NCP(1) = NCTP
DO 4000 K=2,5
IF (PS11TP(K).GT.PS11LS.OR.PS11TP(K).LT.PS11LE) GO TO 4000
IF (QTP(K).NE.0.0) GO TO 4000
RCP11=SQRT(UC1(K)**2 + VC1(K)**2)
RCP22=SQRT(UC2(K)**2 + ( VC2(K))**2)
TDCP1(K)=RCP11*(PSIR1T-PSIRD1(K))
TDCP2(K)=RCP22*(PSIR2T-PSIRD2(K))
4000 CONTINUE
WRITE(6,9073) KT
C 9073 FORMAT('0', 'AT THE START OF DO 43, KT=',E13.6)
DO 43 K = 1,5
TPS(K,1)=STIFF(K)
Q(K,1) = QTP(K)
YC1(K,1) = YCP1(K)
XC1(K,1) = XCP1(K)
YC2(K,1) = YCP2(K)
XC2(K,1) = XCP2(K)
RC1(K,1) = RCP1(K)
RC2(K,1) = RCP2(K)
RCC1(K,1) = RCCP1(K)
RCC2(K,1)=RCCP2(K)
TDEF1(K,1)=TDCP1(K) + HD(K)*DELTA1/(DELTA1+DELTA2)
TDEF2(K,1)=TDCP2(K) + HD(K)*DELTA2/(DELTA1+DELTA2)
IF(K.NE.3) GO TO 41
RESIDL(1,1)=TDEF1(3,1)
RESIDL(2,1)=TDEF2(3,1)
IF((VCP(3).NE.0.0).AND.(UCP(3).LE.0.0)) THUVP(1)=ATAN(UCP(3)/VCP(3
1))-THBUV(1)+THPP1
IF((VCP(3).NE.0.0).AND.(UCP(3).GT.0.0)) THUVP(1)=ATAN(UCP(3)/VCP(3
1))-THBUV(1)+THPP1
IF(VCP(3).EQ.0.0) THUVP(1)=0.0
THUVP(1)=THUVP(1)*57.29576
41 CONTINUE
WRITE(6,9074) TDCP1(K),TDEF1(K,1),TDCP2(K),TDEF2(K,1),TPS(K,1)
C 9074 FORMAT('1',3X,2(E13.6),5X,2(E13.6),5X,E13.6)

```

```

43 CONTINUE
  TDEF1(1) = TDCP1(3)
  TDEF2(1) = TDCP2(3)
  HDEF(1) = HD(3)
  CDEF(1) = CDEF1(3)
  TPS(3,1)=STIFF(3)
  GO TO 45
44 TPS(3,1) = 0.0
45 PSI1TP(1) = PSI1TP(1)-DELTA1
  PSI2TP(1) = PSI2L - FLOAT(1)*DELTA2
  HZP=0.0
  IF (RC1(3,1).EQ.0.0.OR.RC2(3,1).EQ.0.0) GO TO 4500
  SRCN=1./RCN1-1./RCN2
  HZN=0.564*SQRT((Q(3,1)*SRCN)/(F*C2))
  SHZN=HZN*SVS(1)*0.2
  SRCC=1./RC1(3,1)-1./RC2(3,1)
  HZP=0.564*SQRT((Q(3,1)*SRCC)/(F*C2))
  SHZ1=HZP*SV13*0.2
  IF (.NOT.EQ.2) SHZ1=HZP*SV12*0.2
  RBCN=RBC1*VELR(1)
  RCC2(3,1)=SQRT(RC2(3,1)**2-RBCN**2)
4500 CONTINUE
46 CONTINUE
47 CONTINUE
  THMAX=THUVP(1)
  IIMAX=1
  IIMA=50-1
  DO 603 IKMA=1,IIMA
    THMA=THUVP(IKMA+1)-THMAX
    IF(THMA) 603,603,602
  602 THMAX=THUVP(IKMA+1)
  IIMAX=IKMA+1
  603 CONTINUE
  THMIN=THUVP(1)
  IIMIN=1
  IIMI=50-1
  DO 703 IKMI=1,IIMI
    THMI=THUVP(IKMI+1)-THMIN
    IF(THMI) 702,702,703
  702 THMIN=THUVP(IKMI+1)
  IIMIN=IKMI+1
  703 CONTINUE
  C LOADED CONTACT RATIO CALCULATION
  LCR=((ABS(THMAX)+ABS(THMIN))/57.29578)*RBC1)/BP
  EPL=SQRT(UE**2+(VE-RPC1)**2)

```

```

SPL=SQR(US**2+(RPC1-VS)**2)
CCR=(SPL+EPL+CDEF(1)+CDEF(50))/BP
IF(LCR.LE.1.0) GO TO 130
WRITE(6,56) LCR
96 FORMAT('0',T46,'THE LOADED CONTACT RATIO      =',F6.3)
C THIS SEGMENT CALCULATES THE HERTZIAN PRESSURE AND
C THE HERTZIAN PRESSURE - SLIDING VELOCITY PRODUCT
97 OMEGA1 = (2.*PI*RPMIN)/60.
98 OMEGA2 = (2.*PI*RPMAUT)/60.
DO 110 I = 1,50
IF((RC1(3,1).EQ.0.0).OR.(RC2(3,1).EQ.0.0)) GO TO 105
SRRC = 1./RCC1(3,1) - 1./RCC2(3,1)
HZPS(1) = 0.564*SQR(Q(3,1)*SRRC)/(F*C2)
IF((RCC1(3,1).EQ.0.0).OR.(RCC2(3,1).EQ.0.0))
&WRITE(6,104) RC1(3,1),RC2(3,1),RCC1(3,1),RCC2(3,1)
104 FORMAT(' ',4F10.4)
105 PVS(1) = HZPS(1)*SVS(1)*.2
110 CONTINUE
C NSTP IS THE NUMBER OF STIFFNESS TRANSITION POINTS
NSTP = 0
1160 CONTINUE
MNCP=2
IF (LCR.GE.2.051) MNCP=3
DO 1161 I=1,50
IF (TDEF1(4,I).NE.0.0) GO TO 1162
1161 CONTINUE
1162 IEP=1
      J=2
IF (MNCP.EQ.3) J=1
DO 1163 K=1,50
IF (TDEF1(J,K+1).EQ.0.0) GO TO 1164
1163 CONTINUE
1164 ITP=K
C*****TRANSMISSION RATIO INTERPOLATION*****
DO 11641 K=1,50
VELRAT(2*K-1)=VELR(K)
STATLD(2*K-1)=Q(3,K)
IF (K.EQ.50) GO TO 11642
VELRAT(2*K) = (VELR(K)+VELR(K+1))/2
STATLD(2*K) = (Q(3,K)+Q(3,K+1))/2
11641 VELRAT(100)=(VELR(50)**2)/VELR(49)
11642 STATLD(100)=(Q(3,50)**2)/Q(3,49)
C*****TRANSMISSION RATIO RE-CYCLING*****
IEP5=0
IF (MNCP.EQ.2) GO TO 1167

```

```

DO 1165 K=1,50
IF (IDEFL1(5,K).NE.0.0) GO TO 1166
1165 CONTINUE
1166 IEP5=K
1167 CONTINUE
DO 1168 K=1,50
IF (K.GE.IEP) VELR(K)=VELR(K+1-IEP)
IF (IEP5.NE.0.AND.K.GE.IEP5) VELR(K)=VELR(K+1-IEP5)
1168 CONTINUE
117 DO 118 J = 1,50
KG(J) = 0.0
PSI(J) = 0.0
118 CONTINUE
DO 120 J = 1,50
PSI(J) = (PSI(J) + ABS(PSI(1)))*(PI/180.)
KG(J) = CMS(J)
120 CONTINUE
PSI(1) = 0.0
PSI1 = PSI(1)*(PI/180.)
PSI2 = PSI(1)*(PI/180.)
C
IF (TAPE.EQ.NO) GO TO 1185
WRITE(8,1179) (Q(3,K),YC1(3,K),YC2(3,K),K=1,50)
FORMAT(3E14.7)
1179 WRITE(8,1180) ((XC1(I,J),XC2(I,J),YC1(I,J),YC2(I,J),RC1(I,J),
& RC2(I,J),RCC1(I,J),RCC2(I,J),TPS(I,J),I=1,5),J=1,50)
1180 FORMAT(9E14.7)
WRITE(8,1181) (Y1(I),Y2(I),THETC1(I),THETC2(I),DCP1(I),DCP2(I),
& I=1,L1)
1181 FORMAT(6E14.7)
WRITE(8,1182) (NCP(I),KG(I),CG(I),PSI(I),VELR(I),I=1,50)
1182 FORMAT(14,4E14.7)
WRITE(8,1183) PSI1,PSI2,RR01,RR02,RT1,RT2,ITP,IEP,MNCP
1183 FORMAT(6E14.7,3I5)
WRITE(8,1180) (STATLD(I),I=1,100)
1184 WRITE(8,1184) TITLE1,TITLE2,TITLE3
FORMAT(' ',20A4)
C
1185 CONTINUE
C 130 RETURN
END
SUBROUTINE DEFL(IG,YI,YL,KH,KL)
COMMON/C2/PI,F1,F2,R11,R12,E1,E2,G1,G2,PR1,PR2,GAMA1,GAMA2,RT1,RT2
COMMON/C6/L1,L2,PD1,PD2,RPC1,RPC2,RAC1,RAC2,RBC1,RBC2,RRC1,RRC2,

```

```

BRF1,RF2,C,CP,BP,UCUT1,UCUT2
COMMON/C7/YT11,YT12,YP1,YP2,YB11,YB12,RT11,RT12,RB11,RB12,
1RRO1,RR02,XMIN1,XMIN2,SP,EP
COMMON/C8/X1(200),X2(200),Y1(200),Y2(200),THETA1(200),THETA2(200),
1RCURV1(200),RCURV2(200)
COMMON/C9/XC1(5,50),XC2(5,50),YC1(5,50),YC2(5,50),THETC1(200),
1THETC2(200),DCP1(200),DCP2(200),RC1(5,50),RC2(5,50),RCC1(5,50),
2RCC2(5,50),Q(5,50),TPS(5,50),NCP(50)
COMMON/C11/X(200),Y(200),A(200),MI(200),THETA(200),DCP(200),
1THETAC(200),BML(200),PL(200),VL(200),DNH(3000)
REAL MI1,MI2,MI
IF(IG.EQ.2) GO TO 15
E = E1
G = G1
PR = PR1
YP = YP1
RRO = RRO1
RI = RI1
XMIN = XMIN1
F = F1
LL = L1
DO 10 I = 1,LL
X(I) = X1(I)
Y(I) = Y1(I)
THETA(I) = THETA1(I)
A(I) = 2.*X(I)*F
10 MI(I)=(F*(2.*X(I)**3)/12.
GO TO 25
15 E = E2
G = G2
PR = PR2
YP = YP2
RRO = RRO2
RI = 1.2*RRC2
XMIN = -XMIN2
F = F2
LL = L2
DO 20 I = 1,LL
X(I) = -X2(I)
Y(I) = Y2(I)
THETA(I) = THETA2(I)
A(I) = 2.*X(I)*F
20 MI(I)=(F*(2.*X(I)**3)/12.
BW=2.*XMIN
25 DO 30 L = 1,LL

```

```

KH = LL +1 - L
IF(Y(KH).GE.YH) GO TO 40
30 CONTINUE
40 DO 50 KL = 1,LL
IF(Y(KL).LE.YL) GO TO 60
50 CONTINUE
60 DO 70 L = 1,LL
DCP(L) = 0.0
70 THETAC(L)=0.0
QQ = 1.0
DO 110 K = KH, KL
THETAC(K) = THETA(K)
P = QQ*SIN(THETAC(K))
V = QQ*COS(THETAC(K))
YCT = Y(K) - X(K)*TAN(THETAC(K))
BR1 = (QQ*(COS(THETAC(K)))**2)/E
BR2 = (5.2*(YCT**2))/(BW**2) + YCT/BW
BR3 = 1.4*(1.+(TAN(THETAC(K)))**2)/3.1)
DCPBR = BR1*(BR2 + BR3)
IF (IG.EQ.2) GO TO 75
T = V*(Y(K) + RRO)
PSIRD = (T/(4.*PI*RT2*G))*(1./(R1**2)-1./(RRO**2))
RCP = SQRT((RRO + Y(K))**2 + X(K)**2)
THETAQ = ATAN(X(K)/(RRO + Y(K)))
ARG = ABS(THETAC(K) + THETAQ)
GO TO 76
75 T=V*(RRO-Y(K))
PSIRD=(T/(4.*PI*RT2*G))*(1./((RRO**2)-1./(R1**2))
RCP=SQRT((RRO-Y(K))**2 + X(K)**2)
THETAQ=ATAN(X(K)/(RRO-Y(K)))
ARG=ABS(THETAC(K) + THETAQ)
DCPRD = RCP*PSIRD*COS(ARG)
DO 80 L = 1,LL
BML(L) = 0.0
PL(L) = 0.0
80 VL(L)=0.0
DO 90 J = K,LL
BH = (Y(K)-Y(J))*V - X(K)*P
BML(J)=BM*BM/(M(J)*QQ)
PL(J)=P*P/(A(J)*QQ)
VL(J)=V*V/(A(J)*QQ)
90 DCPBM = 0.0
DCPP = 0.0
DCPV = 0.0
N = LL - 1

```



```

DO 100 J = K, N
DELTA = Y(J) - Y(J+1)
DCPBM = DCPBM + ((BML(J)+BML(J+1))*0.5)*DELTA
DCPP = DCPP + ((PL(J)+PL(J+1))*0.5)*DELTA
DCPV = DCPV + ((VL(J)+VL(J+1))*0.5)*DELTA
100 CONTINUE
DCP(K) = DCPRD + DCPBR + DCPBM/E + DCPP/E + (1.2*DCPV)/G
C
DCPBM=DCPBM/E
DCPP=DCPP/E
DCPV=(1.2*DCPV)/G
C WRITE(6,905) K,P,V,THETAC(K),DCP(K),DCPRD,DCPBR,DCPBM,DCPP,DCPV
905 FORMAT(1,12,3F10.6,2X,E14.6,2X,5E14.6)
C
110 CONTINUE
IF(1G.EQ.2) GO TO 120
DO 115 I = 1,LL
DCP1(I) = DCP(I)
115 THETC1(I)=THETAC(I)
RETURN
120 DO 125 I = 1,LL
DCP2(I) = DCP(I)
125 THETC2(I)=THETAC(I)
RETURN
END
//GO.SYSIN DD *
&HEDING TITLE1='HELLO
TITLE3=' HELLLLLL
&CONTROL INPUT='ENGL', OUTPUT='ENGL', TAPE='YES'&END
&PHYPAR E=2*30.E6, PR=2*0.285, GAMA=2*0.288, JG=0.0188, 1.5189 &END
&GENPAR DP=8, DELTP=0.01, TIN=1936.3, RPMIN=1000., ZETAS=0.005, ZETAG=0.05,
PHID=14.5, CBD=0., CB1=0., CB2=0., CBL=0., JD=0.9376, JL=0.93760,
KLS=885000., KDS=885000. &END
&GEOPAR TC=32.96, AD=2*0.125, WD=2*0.269625, GRRF=2*0.021625,
R1=.497, 8.0000, FW=2*1.0, RT1=1., RT2=0.8, RADEL2=.0000, COR1=0.51,
COR2=0.49, COR3=.10, COR4=.80 &END
&PARAM NLTH=75, MLIM=75, DELF=.2, JJJJ=9, LLLL=9, DPSSL1= 0.00000,
DPSSL2=-.00000, DPSEL1=-.000000, DPSEL2=0.000000 &END

```

```

DO 36 K = 1,5
IF((PAS.EQ.7).AND.((RCP1(K).EQ.0.0).OR.(RCP2(K).EQ.0.0))) GO TO 36
IF((PS11TP(K).GT.PS11LS).OR.(PS11TP(K).LT.PS11LE)) GO TO 36
TD(K) = TDCP1(K) + TDCP2(K)
C1 = (4.*RCCP1(K)*RCCP2(K))/((PI*F)*(RCCP2(K)-RCCP1(K)))
BH = SQRT(C1*C2*Q1)
H1(K) = XCP1(K)/COS(THCP1(K))
H2(K) = -XCP2(K)/COS(THCP2(K))
ARG3 = (2.*H1(K))/BH
ARG4 = (2.*H2(K))/BH
HD(K)=(C3*(ALOG(ARG3)-C4)+C5*(ALOG(ARG4)-C6))*Q1
CDEF1(K) = TD(K) + HD(K)
STIFF(K) = 1.0/CDEF1(K)
KT = KT + STIFF(K)
TPS(K,1)=STIFF(K)
WRITE(6,9071) TDCP1(K),TDCP2(K),HD(K),CDEF1(K),TPS(K,1),KT
9071 FORMAT(1,4(3X,E13.6),5X,2(E13.6,3X))
36 CONTINUE
CMS(1)=KT
DO 37 K = 1,5
QTP(K) = 0.0
IF (KT.NE.0.0) QTP(K)=(STIFF(K)/KT)*P
IF (PS11TP(K).GT.PS11LS.OR.PS11TP(K).LT.PS11LE) GO TO 37
V11 = QTP(K)*COS(THCP1(K))
T1 = V11*( YCP1(K)+ RR01)
PSIRD1(K) = (T1/(4.*PI*F1*G1))*(1./(R11**2)-1./(RR01**2))
PSIR1T = PSIR1T + PSIRD1(K)
V22 = QTP(K)*COS(THCP2(K))
T2 = V22*(-YCP2(K)+ RR02)
PSIRD2(K) = (T2/(4.*PI*F2*G2))*(1./(RR02**2)-1./(R12**2))
PSIR2T = PSIR2T + PSIRD2(K)
37 CONTINUE
KT=0.0
WRITE(6,9072) KT
9072 FORMAT(10,' ',AT THE START OF DO 40, KT=' ,E13.6)
DO 40 K = 1,5
IF((PAS.EQ.7).AND.((RCP1(K).EQ.0.0).OR.(RCP2(K).EQ.0.0))) GO TO 40
IF((PS11TP(K).GT.PS11LS).OR.(PS11TP(K).LT.PS11LE)) GO TO 40
THETAQ = ATAN(XCP1(K)/(RR01 + YCP1(K)))
ARG = ABS(THCP1(K) + THETAQ)
STIFF(K) = 1.0/CDEF1(K)
KT = KT + STIFF(K)
TPS(K,1)=STIFF(K)
TDCP1(K) = TDCP1(K)*QTP(K) + RCP1(K)*(PSIR1T-PSIRD1(K))*COS(ARG)
THETAQ = ATAN(-XCP2(K)/(RR02-YCP2(K)))

```

```

ARG = ABS(THCP2(K) + ITHETAQ)
TDCP2(K) = TDCP2(K)*QTP(K) + RCP2(K)*(PSIR2T-PSIRD2(K))*COS(ARG)
TD(K) = TDCP1(K) + TDCP2(K)
BH = SQRT(C1*C2*QTP(K))
ARG3 = (2.*H1(K))/BH
ARG4 = (2.*H2(K))/BH
HD(K) = (C3*(ALOG(ARG3)-C4) + C5*(ALOG(ARG4)-C6))*QTP(K)
CMS(1)=KT
CDEF1(K) = TD(K) + HD(K)
WRITE(6,9071) TDCP1(K), TDCP2(K), HD(K), CDEF1(K), TPS(K,1), KT
C 40 CONTINUE
NCP(1) = NCTP
DO 4000 K=2,5
IF (PSI1TP(K).GT.PSI11S.OR.PSI11TP(K).LT.PSI11LE) GO TO 4000
IF (QTP(K).NE.0.0) GO TO 4000
RCP11=SQRT(UC1(K)**2 + VC1(K)**2)
RCP22=SQRT(UC2(K)**2 + ( VC2(K)**2)
TDCP1(K)=RCP11*(PSIR1T-PSIRD1(K))
TDCP2(K)=RCP22*(PSIR2T-PSIRD2(K))
4000 CONTINUE
C WRITE(6,9073) KT
9073 FORMAT('0',1AT THE START OF DO 43, KT=',E13.6)
DO 43 K = 1,5
TPS(K,1)=STIFF(K)
Q(K,1) = QTP(K)
YC1(K,1) = YCP1(K)
XC1(K,1) = XCP1(K)
YC2(K,1) = YCP2(K)
XC2(K,1) = XCP2(K)
RC1(K,1) = RCP1(K)
RC2(K,1) = RCP2(K)
RCC1(K,1) = RCCP1(K)
RCC2(K,1)=RCCP2(K)
TDEF1(K,1)=TDCP1(K) + HD(K)*DELTA1/(DELTA1+DELTA2)
TDEF2(K,1)=TDCP2(K) + HD(K)*DELTA2/(DELTA1+DELTA2)
IF(K.NE.3) GO TO 41
RESIDL(1,1)=TDEF1(3,1)
RESIDL(2,1)=TDEF2(3,1)
IF((VCP(3).NE.0.0).AND.(UCP(3).LE.0.0)) THUVP(1)=ATAN(UCP(3)/VCP(3
1))-THBUY(1)+THPP1
IF((VCP(3).NE.0.0).AND.(UCP(3).GT.0.0)) THUVP(1)=ATAN(UCP(3)/VCP(3
1))-THBUY(1)+THPP1
IF(VCP(3).EQ.0.0) THUVP(1)=0.0
THUVP(1)=THUVP(1)*57.29578
41 CONTINUE
C WRITE(6,9074) TDCP1(K), TDEF1(K,1), TDCP2(K), TDEF2(K,1), TPS(K,1)
9074 FORMAT('1',3X,2(E13.6),5X,2(E13.6),5X,E13.6)

```

```

43 CONTINUE
TDEF1(1) = TDCP1(3)
TDEF2(1) = TDCP2(3)
HDEF(1) = HD(3)
GDEF(1) = CDEFL(3)
TPS(3,1) = STIFF(3)
GO TO 45

44 TPS(3,1) = 0.0
45 PSI1TP(1) = PSI1TP(1)-DELTA1
PSI2TP(1) = PSI2L - FLOAT(1)*DELTA2
H2P=0.0
IF (RC1(3,1).EQ.0.OR.RC2(3,1).EQ.0.0) GO TO 4500
SRCN=1./RCN1-1./RCN2
HZN=0.564*SQRT((Q(3,1)*SRCN)/(F*C2))
SHZN=HZN*SVS(1)*0.2
SRCC=1./RCC1(3,1)-1./RCC2(3,1)
H2P=0.564*SQRT((Q(3,1)*SRCC)/(F*C2))
SHZ1=H2P*SV13*0.2
IF (I1.EQ.2) SHZ1=H2P*SV12*0.2
RBCN=RBC1*VELR(1)
RCC2(3,1)=SQRT(RC2(3,1)**2-RBCN**2)
4500 CONTINUE
46 CONTINUE
47 THMAX=THUVP(1)
I1MAX=1
I1MA=50-1
DO 603 IKMA=1,I1MA
THMA=THUVP(IKMA+1)-THMAX
IF(THMA) 603,603,602
602 THMAX=THUVP(IKMA+1)
I1MAX=IKMA+1
603 CONTINUE
THMIN=THUVP(1)
I1MIN=1
I1MI=50-1
DO 703 IKMI=1,I1MI
THMI=THUVP(IKMI+1)-THMIN
IF(THMI) 702,702,703
702 THMIN=THUVP(IKMI+1)
I1MIN=IKMI+1
703 CONTINUE
C LOADED CONTACT RATIO CALCULATION
LCR=((ABS(THMAX)+ABS(THMIN))/57.29578)*RBC1)/BP
EPL=SQRT(UE**2+(VE-RPC1)**2)

```

```

SPL=SQRT(US**2+(RPC1-VS)**2)
CGR=(SPL+EPL+CDEF(1)+CDEF(50))/BP
IF(LCR.LE.1.0) GO TO 130
WRITE(6,96) LCR
96 FORMAT(0, I46, 'THE LOADED CONTACT RATIO      =', F6.3)
C THIS SEGMENT CALCULATES THE HERTZIAN PRESSURE AND
C THE HERTZIAN PRESSURE - SLIDING VELOCITY PRODUCT
97 OMEGA1 = (2.*PI*RPMIN)/60.
98 OMEGA2 = (2.*PI*RPMAUT)/60.
DO 110 I = 1,50
IF((RC1(3,1).EQ.0.0).OR.(RC2(3,1).EQ.0.0)) GO TO 105
SRRC = 1./RCC1(3,1) - 1./RCC2(3,1)
HZPS(1) = 0.564*SQRT((Q(3,1)*SRRC)/(F*C2))
IF((RCC1(3,1).EQ.0.0).OR.(RCC2(3,1).EQ.0.0))
&WRITE(6,104) RC1(3,1),RC2(3,1),RCC1(3,1),RCC2(3,1)
104 FORMAT (' ', 4F10.4)
105 PVS(1) = HZPS(1)*SVS(1)*.2
110 CONTINUE
C NSTP IS THE NUMBER OF STIFFNESS TRANSITION POINTS
NSTP = 0
1160 CONTINUE
MNCP=2
IF (LCR.GE.2.051) MNCP=3
DO 1161 I=1,50
IF (TDEF1(4,I).NE.0.0) GO TO 1162
1161 CONTINUE
1162 IEP=1
J=2
IF (MNCP.EQ.3) J=1
DO 1163 K=1,50
IF (TDEF1(J,K+1).EQ.0.0) GO TO 1164
1163 CONTINUE
1164 ITP=K
C*****TRANSMISSION RATIO INTERPOLATION*****
DO 11641 K=1,50
VELRAT(2*K-1)=VELR(K)
STATLD(2*K-1)=Q(3,K)
GO TO 11642
VELRAT(2*K) =(VELR(K)+VELR(K+1))/2
STATLD(2*K) =(Q(3,K)+Q(3,K+1))/2
11641 VELRAT(100)=(VELR(50)**2)/VELR(49)
11642 STATLD(100)=(Q(3,50)**2)/Q(3,49)
C*****TRANSMISSION RATIO RE-CYCLING*****
IEP5=0
IF (MNCP.EQ.2) GO TO 1167

```

```

DO 1165 K=1,50
IF (TDEF1(5,K).NE.0.0) GO TO 1166
1165 CONTINUE
1166 IEP5=K
1167 CONTINUE
DO 1168 K=1,50
IF (K.GE.IEP) VELR(K)=VELR(K+1-IEP)
IF (IEP5.NE.0.AND.K.GE.IEP5) VELR(K)=VELR(K+1-IEP5)
1168 CONTINUE
117 DO 118 J = 1,50
KG(J) = 0.0
PSI(J) = 0.0
118 CONTINUE
DO 120 J = 1,50
PSI(J) = (PSI1(J) + ABS(PSI1(1)))*(PI/180.)
KG(J) = CMS(J)
120 CONTINUE
PSI(1) = 0.0
PSIS1 = PSI1(1)*(PI/180.)
PSIS2 = PSI2(1)*(PI/180.)
C
IF (TAPE.EQ.NO) GO TO 1185
WRITE(8,1179) (Q(3,K),YC1(3,K),YC2(3,K),K=1,50)
FORMAT(3E14.7)
1179 WRITE(8,1180) ((XC1(I,J),XC2(I,J),YC1(I,J),YC2(I,J),RC1(I,J),
& RC2(I,J),RCC1(I,J),RCC2(I,J),TPS(I,J),I=1,5),J=1,50)
&
1180 FORMAT(9E14.7)
WRITE(8,1181) (Y1(I),Y2(I),THETC1(I),THETC2(I),DCPI(I),DCP2(I),
& I=1,L1)
&
1181 FORMAT(6E14.7)
WRITE(8,1182) (NCP(I),KG(I),CG(I),PSI(I),VELR(I),I=1,50)
1182 FORMAT(114.4E14.7)
WRITE(8,1183) PSIS1,PSIS2,RR01,RR02,RT1,RT2,ITP,IEP,MNGP
1183 FORMAT(6E14.7,3I5)
WRITE(8,1180) (STAILD(I),I=1,100)
1184 WRITE(8,1184) TITLE1,TITLE2,TITLE3
FORMAT(1,20A4)
C
1185 CONTINUE
C
130 RETURN
END
SUBROUTINE DEFL(IG,YH,YL,KH,KL)
COMMON/C2/PI,F1,F2,R11,R12,E1,E2,G1,G2,PR1,PR2,GAMA1,GAMA2,RT1,RT2
COMMON/C6/L1,L2,PD1,PD2,RPC1,RPC2,RAC1,RAC2,RBC1,RBC2,RR1,RR2,

```

```

&RF1,RF2,C,CP,BP,UCUT1,UCUT2
COMMON/C7/YT11,YT12,YP1,YP2,YB11,YB12,RT11,RT12,RB11,RB12,
1RR01,RR02,XMIN1,XMIN2,SP,EP
COMMON/C8/X1(200),X2(200),Y1(200),Y2(200),THETA1(200),THETA2(200),
1RCURV1(200),RCURV2(200)
COMMON/C9/XC1(5,50),XC2(5,50),YC1(5,50),YC2(5,50),THEIC1(200),
1THETC2(200),DCP1(200),DCP2(200),RCT(5,50),RC2(5,50),RCC1(5,50),
2RCC2(5,50),Q(5,50),TPS(5,50),NCP(50)
COMMON/C11/X(200),Y(200),A(200),MI(200),THETA(200),DCP(200),
1THETAC(200),BML(200),PL(200),VL(200),DM4(3000)
REAL MI1,MI2,MI
IF(IG.EQ.2) GO TO 15
E = E1
G = G1
PR = PR1
YP = YP1
RRO = RRO1
RI = RI1
XMIN = XMIN1
F = F1
LL = L1
DO 10 I = 1,LL
X(I) = X1(I)
Y(I) = Y1(I)
THETA(I) = THETA1(I)
A(I) = 2.*X(I)*F
10 MI(I)=(F*(2.*X(I)**3)/12.
15 E = E2
G = G2
PR = PR2
YP = YP2
RRO = RRO2
RI = 1.2*RRC2
XMIN = -XMIN2
F = F2
LL = L2
DO 20 I = 1,LL
X(I) = -X2(I)
Y(I) = Y2(I)
THETA(I) = THETA2(I)
A(I) = 2.*X(I)*F
20 MI(I)=(F*(2.*X(I)**3)/12.
25 BW=2.*XMIN
DO 30 I = 1,LL

```

```

KH = LL +1 - L
IF(Y(KH).GE.YH) GO TO 40
30 CONTINUE
40 DO 50 KL = 1,LL
  IF(Y(KL).LE.YL) GO TO 60
50 CONTINUE
60 DO 70 L = 1,LL
  DCP(L) = 0.0
70 THETAC(L)=0.0
  QQ = 1.0
  DO 110 K = KH,KL
    THETAC(K) = THETA(K)
    P = QQ*SIN(THETAC(K))
    V = QQ*COS(THETAC(K))
    YCT = Y(K) - X(K)*TAN(THETAC(K))
    BR1 = (QQ*(COS(THETAC(K)))**2)/E
    BR2 = (5.2*(YCT**2))/(BW**2) + YCT/BW
    BR3 = 1.4*(1.+(TAN(THETAC(K)))**2)/3.1)
    DCPBR = BR1*(BR2 + BR3)
    IF (IG.EQ.2) GO TO 75
    T = V*(Y(K) + RRO)
    PSIRD = (T/(4.*PI*RT1*G))*(1./(RI**2)-1./(RRO**2))
    RCP = SQRT((RRO + Y(K))**2 + X(K)**2)
    THETAQ = ATAN(X(K)/(RRO + Y(K)))
    ARG = ABS(THETAC(K) + THETAQ)
    GO TO 76
75  T=V*(RRO-Y(K))
    PSIRD=(T/(4.*PI*RT2*G))*(1./(RRO**2)-1./(RI**2))
    RCP=SQRT((RRO-Y(K))**2 + X(K)**2)
    THETAQ=ATAN(X(K)/(RRO-Y(K)))
    ARG=ABS(THETAC(K) + THETAQ)
    DCPRD = RCP*PSIRD*COS(ARG)
    DO 80 L = 1,LL
      BML(L) = 0.0
      PL(L) = 0.0
      VL(L)=0.0
80  DO 90 J = K,LL
      BM = (Y(K)-Y(J))*V - X(K)*P
      BML(J)=BM*BM/(MI(J)*QQ)
      PL(J)=P*P/(AJ)*QQ
      VL(J)=V*V/(AJ)*qq
90  DCPBM = 0.0
      DCPV = 0.0
      DCPJ = 0.0
      N = LL - 1

```



```

DO 100 J = K,N
DELTA = Y(J) - Y(J+1)
DCPBM = DCPBM + ((BML(J)+BML(J+1))*5)*DELTA
DCPP = DCPM + ((PL(J)+PL(J+1))*5)*DELTA
DCPV = DCPV + ((VL(J)+VL(J+1))*5)*DELTA
100 CONTINUE
DCP(K) = DCPRD + DCPBR + DCPBM/E + DCP/E + (1.2*DCPV)/G
C
DCPBM=DCPBM/E
DCPP=DCPP/E
DCPV=(1.2*DCPV)/G
WRITE(6,905) K,P,V,THETAC(K),DCP(K),DCPRD,DCPBR,DCPBM,DCPP,DCPV
905 FORMAT(1,12,3F10.6,2X,E14.6,2X,5E14.6)
C
110 CONTINUE
IF(IG.EQ.2) GO TO 120
DO 115 I = 1,LL
DCP1(I) = DCP(I)
115 THETC1(I)=THETAC(I)
RETURN
120 DO 125 I = 1,LL
DCP2(I) = DCP(I)
125 THETC2(I)=THETAC(I)
RETURN
END
//GO,SYSIN DD *
&HEDING, TITLE1='HELLO
TITLE3=' HELLLLLL
&CONTROL INPUT='ENGL', OUTPUT='ENGL', I PLOT=2, MODF='NO', NTYFF 1 &END
&PIVPAR E=2*30.E6, PR=2*0.285, GAMA=2*0.268, JG=C.0188, 1.518, &END
&GENPAR DP=8, DELTP=0.01, TIN=1936.3, RPHIN=1000., ZETAS=0.005, ZETAG=0.005,
PHID=14.5, CBD=0., CB1=0., CB2=0., JD=0.9376, JL=0.93760
&KLS=885000., KOS=885000. &END
&GEOPAR TG=32,96,AD=2*0.125, WD=2*0.269625, GRRF=2*0.021625,
RI=-497,8.0000, FW=2*1.0, RT1=1., RT2=0.8, RADEL2=.0000, COR1=0.51,
COR2=0.49, COR3=.10, COR4= 80 &END
&PARAM NLIN=75, MLIM=75, IELT=.2, JJJJ=9, ILLI=9, DPSLI1= 0.00000,
DPSLI2=-.00000, DPEL1=-.000000, DPEL2=0.0000000 &END

```

STATIC AND DYNAMIC ANALYSIS OF A GEAR PAIR SYSTEM

JOB RUN: 5/10/82 SUBMITTED BY A.PINTZ
 TEST FOR RADIAL DEFLECTIONS OF RING FILE
 DEFINITELY NOT WRITTEN TO TAPE

14.5 DEGREE PRESSURE ANGLE

DIAMETRAL PITCH IS 8.000
 INPUT TORQUE IS 1936.40 IN-LBF
 OUTPUT TORQUE IS 5809.20 IN-LBF
 INPUT SPEED IS 7000.00 RPM.
 OUTPUT SPEED IS 2333.33 RPM.

DATA FOR GEAR 1 (DRIVING GEAR)	*	DATA FOR GEAR 2 (DRIVEN GEAR)
*****		*****
NUMBER OF TEETH = 32.	*	NUMBER OF TEETH = 96.
PITCH DIAMETER = 4.0000 IN.	*	PITCH DIAMETER = 12.0000 IN.
ADDENDUM CIRCLE RADIUS = 2.1250 IN.	*	ADDENDUM CIRCLE RADIUS = 5.8750 IN.
BASE CIRCLE RADIUS = 1.9363 IN.	*	BASE CIRCLE RADIUS = 5.8089 IN.
ROOT CIRCLE RADIUS = 1.8554 IN.	*	ROOT CIRCLE RADIUS = 6.1446 IN.
FILLET RADIUS = 0.0201 IN.	*	FILLET RADIUS = 0.0169 IN.
INSIDE RADIUS OF HUB = 0.4977 IN.	*	INSIDE RADIUS OF HUB = 8.0000 IN.
RIM THICKNESS = 1.0000 IN.	*	RIM THICKNESS = 0.8000 IN.
FACE WIDTH = 1.0000 IN.	*	FACE WIDTH = 1.0000 IN.
YOUNG'S MODULUS = 30.0E+06 PSI	*	YOUNG'S MODULUS = 30.0E+06 PSI
SPECIFIC WEIGHT = 0.288 LBI	*	SPECIFIC WEIGHT = 0.288 LBI
POISSON'S RATIO = 0.2850	*	POISSON'S RATIO = 0.2850

THE NOMINAL TRANSMITTED FORCE ALONG THE LINE OF ACTION = 1000.05 LBF.

1.6396313 0.9854966 2.6251278
 1.6397820 0.9854782 2.6252594

THE THEORETICAL CONTACT RATIO = 2.625

X-Y COORDINATES OF POINTS ALONG THE PROFILE OF THE GEAR TEETH

THE GEAR TEETH HAVE A STANDARD PROFILE WITH NO MODIFICATIONS

THE Y-AXIS CORRESPONDS TO THE LINE OF SYMMETRY OF THE TOOTH. THE ORIGIN OF THE X-Y COORDINATE SYSTEMS IS LOCATED AT THE ROOT OF THE TOOTH A DISTANCE OF RR01 (OR RR02 FOR GEAR 2) FROM THE GEAR CENTER. VALUES TABULATED BELOW REPRESENT POINTS ON THE R.H. PROFILE OF THE TOOTH. POINT 100 IS LOCATED AT THE ADDENDUM CIRCLE. POINT 100 IS LOCATED AT THE ROOT CIRCLE. THETA VALUES REPRESENT THE ANGLE BETWEEN THE NORMAL TO THE PROFILE AND THE X-AXIS; COUNTERCLOCKWISE THETA IS DEFINED AS POSITIVE.

THE INVOLUTE STARTS AT Y = 0.2728 IN. AND ENDS AT Y = 0.0859 IN. ON THE TOOTH PROFILE OF GEAR 1.
 THE INVOLUTE STARTS AT Y = 0.2681 IN. AND ENDS AT Y = 0.0165 IN. ON THE TOOTH PROFILE OF GEAR 2.
 THE PITCH CIRCLE INTERSECTS THE TOOTH PROFILE OF GEAR 1 AT Y = 0.1462 IN.
 THE PITCH CIRCLE INTERSECTS THE TOOTH PROFILE OF GEAR 2 AT Y = 0.1434 IN.

RR01 = 1.8514 IN.
 RR02 = 6.1426 IN.

X AND Y VALUES ARE IN IN., THETA VALUES ARE IN DEGREES.

DATA FOR GEAR 1

POINT	X	Y	THETA	POINT	X	Y	THETA
1	0.05764	0.27280	22.67278	1	-0.07024	0.26806	9.37908
2	0.05881	0.27000	22.47890	2	-0.07070	0.26532	9.54995
3	0.05996	0.26721	22.26770	3	-0.07116	0.26258	9.73760
4	0.06110	0.26442	22.08023	4	-0.07163	0.25984	9.90594
5	0.06224	0.26163	21.85880	5	-0.07211	0.25709	10.06033
6	0.06336	0.25883	21.67349	6	-0.07259	0.25435	10.24472
7	0.06447	0.25604	21.45921	7	-0.07309	0.25161	10.39689
8	0.06557	0.25325	21.24742	8	-0.07359	0.24887	10.54142
9	0.06665	0.25045	21.04289	9	-0.07410	0.24613	10.72313
10	0.06773	0.24766	20.82654	10	-0.07462	0.24339	10.87461
11	0.06879	0.24486	20.62030	11	-0.07515	0.24065	11.01528
12	0.06984	0.24207	20.40486	12	-0.07568	0.23791	11.16992
13	0.07088	0.23927	20.18680	13	-0.07622	0.23517	11.32813
14	0.07191	0.23648	19.97523	14	-0.07677	0.23242	11.48463
15	0.07293	0.23368	19.75093	15	-0.07733	0.22968	11.62047
16	0.07393	0.23089	19.53282	16	-0.07789	0.22694	11.74957

DATA FOR GEAR 2

17	0.07492	19.30830	-0.07846	0.22420	11.89406
18	0.07590	19.07570	-0.07904	0.22146	12.03243
19	0.07667	18.86270	-0.07962	0.21872	12.17238
20	0.07782	18.62518	-0.08021	0.21599	12.31351
21	0.07877	18.39719	-0.08081	0.21325	12.44312
22	0.07970	18.16153	-0.08141	0.21051	12.58228
23	0.08061	17.92966	-0.08203	0.20777	12.71739
24	0.08152	17.68498	-0.08264	0.20503	12.84618
25	0.08241	17.45222	-0.08327	0.20229	12.96228
26	0.08329	17.20261	-0.08390	0.19955	13.10075
27	0.08416	16.96362	-0.08454	0.19681	13.21986
28	0.08501	16.71649	-0.08518	0.19407	13.35100
29	0.08585	16.46408	-0.08583	0.19133	13.48200
30	0.08667	16.20950	-0.08649	0.18860	13.59164
31	0.08749	15.94716	-0.08715	0.18586	13.72237
32	0.08829	15.69221	-0.08782	0.18312	13.84473
33	0.08907	15.43144	-0.08849	0.18038	13.95988
34	0.08984	15.16431	-0.08917	0.17765	14.08437
35	0.09060	14.88994	-0.08986	0.17491	14.19578
36	0.09134	14.61545	-0.09055	0.17217	14.30953
37	0.09207	14.34295	-0.09125	0.16943	14.43481
38	0.09279	14.05925	-0.09195	0.16670	14.55545
39	0.09349	13.77358	-0.09266	0.16396	14.65130
40	0.09417	13.47700	-0.09338	0.16122	14.77015
41	0.09484	13.18916	-0.09410	0.15849	14.89986
42	0.09549	12.88300	-0.09483	0.15575	14.98343
43	0.09613	12.58229	-0.09556	0.15301	15.11799
44	0.09676	12.26842	-0.09630	0.15028	15.21918
45	0.09736	11.94912	-0.09704	0.14754	15.33260
46	0.09795	11.62623	-0.09780	0.14481	15.44100
47	0.09853	11.29086	-0.09855	0.14207	15.53724
48	0.09909	10.95634	-0.09931	0.13934	15.65308
49	0.09963	10.61610	-0.10008	0.13660	15.76938
50	0.10015	10.25589	-0.10085	0.13387	15.85316
51	0.10065	9.89223	-0.10163	0.13113	15.96980
52	0.10114	9.51954	-0.10241	0.12840	16.07201
53	0.10161	9.13598	-0.10320	0.12566	16.17459
54	0.10205	8.73989	-0.10399	0.12293	16.28513
55	0.10248	8.33318	-0.10479	0.12020	16.38716
56	0.10289	7.90422	-0.10559	0.11746	16.48370
57	0.10328	7.46574	-0.10640	0.11473	16.58847
58	0.10364	7.01132	-0.10722	0.11199	16.68341
59	0.10398	6.52652	-0.10803	0.10926	16.78653
60	0.10430	6.02506	-0.10886	0.10653	16.90068
61	0.10459	5.49354	-0.10969	0.10380	16.97304
62	0.10486	4.92660	-0.11052	0.10106	17.08832
63	0.10510	4.31265	-0.11136	0.09833	17.19217
64	0.10531	3.64992	-0.11221	0.09560	17.26059
65	0.10549	2.92366	-0.11306	0.09287	17.38362
66	0.10563	2.07761	-0.11391	0.09014	17.48149
67	0.10573	1.08442	-0.11477	0.08740	17.56442
68	0.10578	-3.12494	-0.11564	0.08467	17.66570
69	0.10564	-3.12494	-0.11651	0.08194	17.74376

70	0.10549	0.08057	-3.12606	70	-0.11738	0.07921	17.85855
71	0.10535	0.07793	-3.12494	71	-0.11826	0.07648	17.94823
72	0.10520	0.07528	-3.12494	72	-0.11915	0.07375	18.03264
73	0.10506	0.07263	-3.12477	73	-0.12003	0.07102	18.11137
74	0.10491	0.06999	-3.12735	74	-0.12093	0.06829	18.22522
75	0.10477	0.06734	-3.12494	75	-0.12183	0.06556	18.31403
76	0.10462	0.06470	-3.12477	76	-0.12273	0.06283	18.41052
77	0.10448	0.06205	-3.12494	77	-0.12364	0.06010	18.50697
78	0.10433	0.05940	-3.12622	78	-0.12455	0.05737	18.58345
79	0.10419	0.05676	-3.12477	79	-0.12547	0.05464	18.68007
80	0.10405	0.05411	-3.12494	80	-0.12639	0.05191	18.76361
81	0.10390	0.05147	-3.12606	81	-0.12732	0.04918	18.87350
82	0.10376	0.04882	-3.12606	82	-0.12825	0.04645	18.94800
83	0.10361	0.04617	-3.12494	83	-0.12919	0.04373	19.03250
84	0.10347	0.04353	-3.12494	84	-0.13013	0.04100	19.12924
85	0.10332	0.04088	-3.12477	85	-0.13108	0.03827	19.21750
86	0.10318	0.03824	-3.12622	86	-0.13203	0.03554	19.30229
87	0.10303	0.03559	-3.12494	87	-0.13298	0.03282	19.39664
88	0.10289	0.03294	-3.12477	88	-0.13394	0.03009	19.47461
89	0.10275	0.03030	-3.12606	89	-0.13491	0.02736	19.55841
90	0.10260	0.02765	-3.12622	90	-0.13588	0.02464	19.64699
91	0.10246	0.02501	-3.12477	91	-0.13685	0.02191	19.73775
92	0.10231	0.02236	-2.44967	92	-0.13783	0.01918	19.81984
93	0.10220	0.01971	4.77381	93	-0.13881	0.01646	-3.22090
94	0.10242	0.01705	13.00435	94	-0.13867	0.01404	10.69113
95	0.10304	0.01436	20.43774	95	-0.13913	0.01165	14.08449
96	0.10405	0.01165	29.04039	96	-0.13973	0.00925	32.46616
97	0.10557	0.00891	38.72827	97	-0.14124	0.00687	35.21808
98	0.10780	0.00613	50.26900	98	-0.14291	0.00450	55.64484
99	0.11124	0.00327	69.78708	99	-0.14632	0.00217	67.65125
100	0.11992	0.00007	86.29399	100	-0.15186	-0.00011	88.58374

THEORETICAL INITIAL AND FINAL POINTS OF CONTACT
 68 0.0858650 1 0.2727957 85 0.0394440
 THEORETICAL AND ACTUAL RADII TO CONTACT POINTS
 1.9401731 1.9401722 5.8750000 5.8750000 2.1250000 2.1250000 6.1045961 6.1057749

THEORETICAL INITIAL AND FINAL ANGLES OF CONTACT
 1.9416542 1.4263802 1.6617460 1.4899321
 THEORETICAL ANGULAR INCREMENTS - 0.0105158 0.0035053

DEFLECTIONS ADDED AT ENTRANCE - 0.0 0.0
 DEFLECTIONS ADDED AT EGRESS - 0.0 0.0

ACTUAL START OF CONTACT
 75 67 1 -0.6035117 5.8464775 -0.6035038 5.8439198 -0.0000079 0.0025578
 ACTUAL END OF CONTACT

CONTACT CODE - 7

CONTACT CODE - 6

0.0

0.0022306

-0.0000097

6.0944958

0.3715599

6.0922651

0.3715502

6.0922651

0.3715502

COORDINATES AT END OF CONTACT

0.0

0.0

0.0

0.0

0.0

0.0

0.0

0.0

0.0

84 0.3717053 6.0916996 6.1030283

85 0.3709866 6.0944958 6.1057749

86 0.3702632 6.0972919 6.1085224

ACTUAL INITIAL AND FINAL ANGLES OF CONTACT

1.9416533 1.4221735 1.6617451 1.4885292

ACTUAL ANGULAR INCREMENTS - 0.0106016 0.0035350

CONTACT CODES: 6 7

PRESSURE ANGLE: 10.47

RADEL2 = 0.0 COR1= 0.10000 COR2= 0.80000 COR3= 0.10000 COR4= 0.80000

DPSL1= 0.0 DPSL2= 0.0 DPSL3= 0.0 DPSL4= 0.0

DPEL1= 0.0 DPEL2= 0.0 DPEL3= 0.0 DPEL4= 0.0

THEORETICAL INITIAL AND FINAL ANGLES OF CONTACT

1.9416533 1.4221735 1.6617451 1.4885292

THEORETICAL ANGULAR INCREMENTS - 0.0106016 0.0035350

DEFLECTIONS ADDED AT ENTRANCE - 0.0001727 0.0001572

DEFLECTIONS ADDED AT EGRESS - 0.0003092 0.0000302

ACTUAL START OF CONTACT

73 67 1 -0.6118452 5.8439608 -0.6119193 5.8430462 0.0000741 0.0009146

ACTUAL END OF CONTACT

58 1 82 0.4382711 6.0793200 0.4382645 6.0818081 0.0000066 0.0024881

COORDINATES AT END OF CONTACT

-1 0.0 0.0 0.0

0 0.0 0.0 0.0

1 0.4382711 6.0793200 6.0950975

81 0.4383404 6.0790052 6.0947876

82 0.4376647 6.0818081 6.0975351

83 0.4369853 6.0846100 6.1002808

ACTUAL INITIAL AND FINAL ANGLES OF CONTACT

1.9458933 1.3903341 1.6631584 1.4779167

ACTUAL ANGULAR INCREMENTS - 0.0113379 0.0037804

CONTACT CODES: 5 8

PRESSURE ANGLE: 9.27

THE LOADED CONTACT RATIO = 2.853

STATIC ANALYSIS

TABLES 2, 3 AND 4 LIST INFORMATION RESULTING FROM A STATIC ANALYSIS OF THE GEAR PAIR (NEGLECTING INERTIA FORCES). THE DATA PRESENTED IN THESE TABLES WERE OBTAINED BY ROTATING THE DRIVING GEAR THRU ONE CYCLE OF TOOTH ENGAGEMENT. IN EACH OF THESE TABLES POSITION 1 CORRESPONDS TO THE STARTING POINT OF CONTACT WHILE POSITION 50 CORRESPONDS TO THE END POINT OF CONTACT.

TABLE 2

PSI1 IS THE ANGLE OF ROTATION OF THE DRIVING GEAR IN DEGREES.
 PSI2 IS THE ANGLE OF ROTATION OF THE DRIVEN GEAR IN DEGREES.
 MCP IS THE NUMBER OF SEPARATE TOOTH PAIRS IN CONTACT AT A PARTICULAR POSITION.
 PS IS THE TOOTH PAIR STIFFNESS IN LBF/IN AT A PARTICULAR POSITION.
 KG IS THE COMBINED GEAR TOOTH SPRING CONSTANT (STIFFNESS) IN LBF/IN AT A PARTICULAR POSITION.
 CG IS THE GEAR DAMPENING COEFFICIENT IN (LB-SEC)/IN.

NOTE: BOTH PSI1 AND PSI2 ARE MEASURED BETWEEN THE CENTER LINE.

POSITION	PSI1	PSI2	MCP	PS	KG	CG
1	-21.491	-5.292	3	958039.7	3466220.0	0.0
2	-20.842	-5.075	3	964265.6	3450632.0	0.0
3	-20.192	-4.859	3	1006103.0	3468112.0	0.0
4	-19.543	-4.642	3	1025468.6	3485247.0	0.0
5	-18.893	-4.426	3	1057297.0	3476145.0	0.0
6	-18.243	-4.209	3	1061713.0	3461624.0	0.0
7	-17.594	-3.992	3	1092222.0	3445575.0	0.0
8	-16.944	-3.776	3	1120431.0	3450265.0	0.0
9	-16.295	-3.559	3	1135953.0	3463209.0	0.0
10	-15.645	-3.343	3	1161252.0	3483420.0	0.0
11	-14.995	-3.126	3	1174924.0	3489701.0	0.0
12	-14.346	-2.909	3	1197647.0	3497795.0	0.0
13	-13.696	-2.693	3	1218694.0	3506523.0	0.0
14	-13.046	-2.476	3	1237951.0	3504523.0	0.0
15	-12.397	-2.259	3	1255647.0	3505703.0	0.0
16	-11.747	-2.043	2	1271785.0	2522466.0	0.0
17	-11.098	-1.826	2	1286384.0	2521286.0	0.0
18	-10.448	-1.610	2	1304527.0	3480566.0	0.0
19	-9.798	-1.393	3	1315518.0	3457127.0	0.0
20	-9.149	-1.176	3	1325316.0	3494248.0	0.0
21	-8.499	-0.960	3	1333385.0	3475417.0	0.0
22	-7.850	-0.743	3	1340342.0	3477121.0	0.0
23	-7.200	-0.527	3	1347465.0	3477121.0	0.0
24	-6.550	-0.310	3	1351774.0	3450399.0	0.0
25	-5.901	-0.093	3	1354131.0	3458682.0	0.0
26	-5.251	0.123	3	1352619.0	3460157.0	0.0
27	-4.601	0.340	3	1349276.0	3470884.0	0.0
28	-3.952	0.556	3	1343711.0	3478630.0	0.0
29	-3.302	0.773	3	1336107.0	3494068.0	0.0
30	-2.653	0.990	3	1326361.0	3505421.0	0.0
31	-2.003	1.206	3	1314876.0	3513286.0	0.0
32	-1.353	1.423	3	1294555.0	3502281.0	0.0
33	-0.704	1.639	2	1271412.0	2533689.0	0.0
34	-0.054	1.856	2	1254025.0	2537960.0	0.0
35	0.595	2.073	2	1235582.0	2532838.0	0.0
36	1.245	2.289	3	1216163.0	3471868.0	0.0
37	1.895	2.506	3	1175208.0	3487532.0	0.0
38	2.544	2.722	3	1153571.0	3473196.0	0.0

39	3.194	2.939	1119666.0	3489985.0	0.0
40	3.844	3.156	1096707.0	3491731.0	0.0
41	4.493	3.372	1049302.0	3467946.0	0.0
42	5.143	3.589	1025214.3	3463281.0	0.0
43	5.792	3.805	988849.4	3457673.0	0.0
44	6.442	4.022	976052.6	3458911.0	0.0
45	7.092	4.239	975302.0	3480705.0	0.0
46	7.741	4.455	974454.1	3498281.0	0.0
47	8.391	4.672	973492.1	3511883.0	0.0
48	9.040	4.888	972410.7	3512479.0	0.0
49	9.690	5.105	971204.7	3519469.0	0.0
50	10.340	5.322	969876.9	3515886.0	0.0

TABLE 3

LOAD IS THE FORCE IN LBF. ACTING BETWEEN THE CONTACTING TOOTH PAIR IN A DIRECTION NORMAL TO THE PROFILE.
 (THE TOTAL NOMINAL TRANSMITTED FORCE CARRIED BY ALL CONTACTING TOOTH PAIRS IS 1000.05 LBF.)
 YC1 IS THE LOCATION OF THE CONTACT POINT ALONG THE TOOTH PROFILE OF GEAR 1; IN.
 YC2 IS THE LOCATION OF THE CONTACT POINT ALONG THE TOOTH PROFILE OF GEAR 2; IN.
 (YC1 AND YC2 ARE MEASURED RELATIVE TO THE X-Y COORDINATE SYSTEMS DEFINED IN TABLE 1)
 SV IS THE SLIDING VELOCITY AT THE CONTACT POINT; FT/MIN
 HZP IS THE MAXIMUM HERTZ CONTACT PRESSURE AT THE CONTACT POINT; PSI.
 PV IS THE HERTZ PRESSURE-SLIDING VELOCITY PRODUCT; LBF/(IN-SEC).

POSITION	LOAD	YC1	YC2	SV	HZP	PV
1	276.41	0.088	0.268	0.15949E+04	0.93940E+05	0.29964E+08
2	279.46	0.086	0.265	0.15283E+04	0.10443E+06	0.31919E+08
3	290.12	0.089	0.258	0.14797E+04	0.92030E+05	0.27235E+08
4	294.25	0.089	0.254	0.14208E+04	0.92555E+05	0.26300E+08
5	304.17	0.091	0.247	0.13677E+04	0.86000E+05	0.23525E+08
6	306.73	0.089	0.246	0.13038E+04	0.94203E+05	0.24563E+08
7	317.01	0.091	0.239	0.12527E+04	0.86984E+05	0.21793E+08
8	324.76	0.094	0.233	0.11981E+04	0.82258E+05	0.19711E+08
9	328.02	0.094	0.229	0.11422E+04	0.82126E+05	0.18761E+08
10	333.38	0.097	0.223	0.10886E+04	0.78170E+05	0.17018E+08
11	336.70	0.097	0.220	0.10311E+04	0.78272E+05	0.16142E+08
12	342.42	0.100	0.215	0.97779E+03	0.75118E+05	0.14690E+08
13	347.57	0.102	0.209	0.92398E+03	0.72493E+05	0.13396E+08
14	353.26	0.105	0.204	0.86995E+03	0.70348E+05	0.12240E+08
15	358.19	0.108	0.198	0.81569E+03	0.68440E+05	0.11165E+08
16	501.74	0.111	0.193	0.76118E+03	0.78494E+05	0.11950E+08
17	510.00	0.114	0.189	0.70651E+03	0.76872E+05	0.10862E+08
18	517.43	0.119	0.181	0.65330E+03	0.73802E+05	0.96430E+07
19	377.98	0.122	0.177	0.59903E+03	0.61573E+05	0.73768E+07
20	383.38	0.125	0.172	0.54247E+03	0.60636E+05	0.65786E+07
21	381.61	0.128	0.168	0.48941E+03	0.59175E+05	0.57921E+07
22	385.68	0.130	0.164	0.43400E+03	0.58265E+05	0.50574E+07
23	387.54	0.136	0.157	0.38124E+03	0.56431E+05	0.43028E+07
24	391.79	0.141	0.151	0.32815E+03	0.54981E+05	0.36083E+07
25	391.54	0.144	0.147	0.27241E+03	0.54012E+05	0.29427E+07
26	390.93	0.153	0.138	0.22062E+03	0.51912E+05	0.25906E+07
27	388.76	0.158	0.132	0.16647E+03	0.50462E+05	0.16801E+07
28	386.30	0.164	0.126	0.11236E+03	0.49100E+05	0.11033E+07

29	382.41	0.169	0.57965E+02	0.4774E+05	0.55350E+06
30	378.39	0.175	0.40000E+01	0.46463E+05	0.37170E+05
31	374.28	0.181	0.50279E+02	0.45249E+05	0.45502E+06
32	369.65	0.189	0.10096E+03	0.43789E+05	0.88414E+06
33	501.83	0.197	0.15487E+03	0.49474E+05	0.15407E+07
34	494.13	0.203	0.20919E+03	0.48476E+05	0.20281E+07
35	487.85	0.209	0.26294E+03	0.47331E+05	0.24890E+07
36	350.31	0.214	0.31784E+03	0.39422E+05	0.25060E+07
37	336.99	0.225	0.37053E+03	0.37659E+05	0.27908E+07
38	332.15	0.231	0.42417E+03	0.36804E+05	0.31222E+07
39	320.84	0.239	0.47942E+03	0.35451E+05	0.33992E+07
40	314.10	0.245	0.53275E+03	0.34557E+05	0.36820E+07
41	302.59	0.256	0.58667E+03	0.33161E+05	0.38909E+07
42	296.04	0.262	0.64007E+03	0.32339E+05	0.41399E+07
43	286.00	0.270	0.69394E+03	0.31234E+05	0.43349E+07
44	282.20	0.273	0.75124E+03	0.30678E+05	0.46094E+07
45	280.22	0.273	0.81003E+03	0.30304E+05	0.49094E+07
46	278.57	0.273	0.86849E+03	0.29934E+05	0.51994E+07
47	277.21	0.273	0.92674E+03	0.29563E+05	0.54795E+07
48	276.86	0.273	0.98471E+03	0.29228E+05	0.57563E+07
49	275.97	0.273	0.10424E+04	0.28846E+05	0.60137E+07
50	275.87	0.273	0.10998E+04	0.28444E+05	0.62650E+07

TABLE 4

TD1 IS THE TOOTH DEFLECTION ON GEAR 1; IN.
 TD2 IS THE TOOTH DEFLECTION ON GEAR 2; IN.
 HD IS THE HORIZIAN DEFLECTION OF THE CONTACT POINT; IN.
 CD IS THE COMBINED DEFLECTION OF THE CONTACT POINT; IN.
 (ALL DEFLECTIONS ARE MEASURED ALONG THE LINE OF ACTION.)

POSITION	TD1	TD2	HD	CD	VELR
1	0.0001371	0.0001469	0.00000462	0.0003302	2.9050817
2	0.0001384	0.0001445	0.0000479	0.0003308	2.9241858
3	0.0001386	0.0001403	0.0000479	0.0003268	2.9179687
4	0.0001392	0.0001367	0.0000486	0.0003245	2.9265528
5	0.0001413	0.0001326	0.0000490	0.0003229	2.9242868
6	0.0001410	0.0001320	0.0000506	0.0003236	2.9429636
7	0.0001433	0.0001283	0.0000509	0.0003225	2.9398413
8	0.0001452	0.0001239	0.0000512	0.0003203	2.9391937
9	0.0001458	0.0001210	0.0000517	0.0003185	2.9462233
10	0.0001476	0.0001162	0.0000518	0.0003156	2.9459581
11	0.0001481	0.0001139	0.0000523	0.0003143	2.9534197
12	0.0001501	0.0001097	0.0000525	0.0003124	2.9536076
13	0.0001521	0.0001057	0.0000527	0.0003105	2.9543543
14	0.0001542	0.0001020	0.0000530	0.0003093	2.9555330
15	0.0001563	0.000984	0.0000533	0.0003081	2.9570627
16	0.0001820	0.0001304	0.0000709	0.0003833	2.9588861
17	0.0001854	0.0001265	0.0000714	0.0003833	2.9609518
18	0.0001908	0.0001194	0.0000715	0.0003817	2.9586706
19	0.0001668	0.0000841	0.0000621	0.0003130	2.9050817
20	0.0001693	0.0000818	0.0000652	0.0003163	2.9241858
21	0.0001709	0.0000781	0.0000629	0.0003118	2.9179687

2.9265528
 2.9242868
 2.9429636
 2.9398413
 2.9391937
 2.9462233
 2.9459581
 2.9534197
 2.9536076
 2.9543543
 2.9555330
 2.9570627
 2.9588861
 2.9609518
 2.9050817
 2.9241858
 2.9179687
 2.9265528
 2.9242868
 2.9429636
 2.9398413
 2.9391937
 2.9462233
 2.9459581

0.0003127
 0.0003127
 0.0003145
 0.0003126
 0.0003122
 0.0003122
 0.0003124
 0.0003114
 0.0003109
 0.0003108
 0.0003131
 0.0003927
 0.0003929
 0.0003949
 0.0003269
 0.0003267
 0.0003309
 0.0003301
 0.0003314
 0.0003358
 0.0003377
 0.0003391
 0.0003398
 0.0003377
 0.0003359
 0.0003346
 0.0003347
 0.0003338
 0.0003338

0.0000634
 0.0000638
 0.0000645
 0.0000630
 0.0000619
 0.0000617
 0.0000614
 0.0000600
 0.0000587
 0.0000575
 0.0000569
 0.0000729
 0.0000707
 0.000693
 0.0000606
 0.0000566
 0.0000541
 0.0000529
 0.0000510
 0.0000499
 0.0000471
 0.0000465
 0.0000454
 0.0000444
 0.0000436
 0.0000429
 0.0000425

0.0000759
 0.0000715
 0.0000679
 0.0000655
 0.0000600
 0.0000564
 0.0000529
 0.0000496
 0.0000466
 0.0000438
 0.0000401
 0.0000497
 0.0000468
 0.0000442
 0.0000311
 0.0000274
 0.000238
 0.000226
 0.000203
 0.000193
 0.000179
 0.000176
 0.000178
 0.000180
 0.000183
 0.000186
 0.000190
 0.0000194

0.0001734
 0.0001774
 0.0001821
 0.0001841
 0.0001902
 0.0001941
 0.0001980
 0.0002018
 0.0002056
 0.0002095
 0.0002161
 0.0002701
 0.0002755
 0.0002814
 0.0002352
 0.0002427
 0.0002471
 0.0002522
 0.0002559
 0.0002645
 0.0002684
 0.0002741
 0.0002758
 0.0002745
 0.0002735
 0.0002727
 0.0002725
 0.0002719
 0.0002719

22
 23
 24
 25
 26
 27
 28
 29
 30
 31
 32
 33
 34
 35
 36
 37
 38
 39
 40
 41
 42
 43
 44
 45
 46
 47
 48
 49
 50

TAPE COMMAND IS YES

C-2 LISTING AND SAMPLE RUN OF THE DYNAMIC ANALYSIS PROGRAM
"INTERNAL DYNAMIC"

```

C ***** MODULE 2 *****
C ***** THIS PROGRAM IS STORED IN CHS, FILE - INTERNAL DYNAMIC *****
C ***** PROGRAM REQUIRES TAPE R8120.STATIC.OUTPUT *****
C ***** JOB CARD IS LABELED AUGUST5 *****
C *****
C *****
C *****
COMMON/DIMEN/OCODE,MODCOD,IBYPSS
COMMON/C1/PH1,PHID,DP,M,TG,TP,DELTP,TAPE
COMMON/C2/PI,FW,R1,E,G,PR,GAMA
COMMON/C4/TIN,TOUT,RPMIN,RPMOUT,OMEGA1,OMEGA2
COMMON/C5/JG,JD,JL,KDS,KLS,KGPAVG,ZETAS,ZETAG,CDS,CLS,CGPAVG,
1LDS,LLS,IPLLOT,CBD,CB1,CB2,CBL
COMMON/C6/L1,L2,PD1,PD2,RPC1,RPC2,RAC1,RAC2,RBC1,RBC2,RRC1,RRC2,
&RF1,&RF2,C,CP,BP,UCUT
COMMON/C10/VM1(4000)
COMMON/C11/VM2(5000)

C
REAL INPUT,MODF,LENGTH(2),LEN(2),MODLUS(2)
REAL M,JG(2),JD,JL,KDS,KGPAVG,KLS,KG,LDS,LLS
INTEGER OCODE,OC,IPT1(2),IPT2(2)
DIMENSION FORCE(2),SPEED(2),PRESS(2),SPWGHT(2)
DIMENSION G(2)
DIMENSION E(2),PR(2),GAMA(2),FW(2),TG(2),AD(2),WD(2),GRRF(2),RI(2)
DIMENSION PATM(2),STIM(2),RATM(2),PABM(2),STBM(2),RABM(2),
&PER(2),PAP(2),CYC(2),DEEP(2),UCUT(2)
DIMENSION X1(100),Y1(100),X2(100),Y2(100),PS1(50),PS12(50),
&NCP(50),TPS(5,50),CMS(50),CG(50),Q(5,50),YC1(5,50),YC2(5,50),
&SVS(50),HZPS(50),PVS(50)
DOUBLE PRECISION X1,DX1
EQUIVALENCE(OC,OCODE)

C
DATA TAUMAX/10000./
DATA SI,ENGL/'SI','ENGL'/,YES/'YES'/
DATA LENGTH/'IN','MM'/,FORCE/'LBF','N'/,LEN/'IN','M'/,
&PRESS/'MPA','MPA'/,MODLUS/'PSI','MPA'/,
&SPWGHT/'LB13','KGN3'/

C
NAMELIST/CONTRL/INPUT,OUTPUT,IPLLOT,MODF,NTYPE,FELGR
NAMELIST/PHYPAR/E,PR,GAMA,JG,TAPE
NAMELIST/GENPAR/DP,M,DELTP,TIN,RPMIN,ZETAS,ZETAG,PHID,CBD,CB1,CB2,

```

```

CBL,JD,JL,KDS,KLS,LDS,LLS
NAMELIST/GEOPAR/TG,AD,WD,GRRF,RI,FW,UCUT
PI=3.141592654
IBYPSS=0
1 READ(5,CONTRL,END=999)
  READ(5,PHYPAR)
  READ(5,GENPAR)
  READ(5,GEOPAR)
C
C IF (IBYPSS.EQ.1) GO TO 998
3 OCODE=1
C
C PHI=PHID*PI/180.
TOUT=TIN*TG(2)/TG(1)
RPMOUT=RPMIN*TG(1)/TG(2)
G(1)=0.5*E(1)/(1.+PR(1))
G(2)=0.5*E(2)/(1.+PR(2))
PD1=TG(1)/DP
PD2=TG(2)/DP
RPC1=0.5*PD1
RPC2=0.5*PD2
7 IF (RI(1).EQ.0.0) RI(1)=(16.*TIN/(PI*TAUMAX))**(1./3.)*.5
  IF (JG(1).EQ.0.) JG(1)=.5*GAMA(1)*PI*FW(1)*RPC1**4/386.
  IF (JG(2).EQ.0.) JG(2)=.5*GAMA(2)*PI*FW(2)*RPC2**4/386.
  C = RPC2 - RPC1
CP = PI/DP
BP = CP*COS(PHI)
RF1=.7*(GRRF(1)+(WD(1)-AD(1)-GRRF(1))**2/(.5*PD1+WD(1)-AD(1)-
&GRRF(1)))
RF2=.7*(GRRF(2)+(WD(2)-AD(2)-GRRF(2))**2/(.5*PD2+WD(2)-AD(2)-
&GRRF(2)))
RAC1=RPC1*AD(1)
RAC2=RPC2*AD(2)
  IF (RI(2).EQ.0.0) RI(2)= (RAC2+WD(2))
  RRC1=RAC1-WD(1)
  RRC2=RAC2-WD(2)
  RBC1 = RPC1*COS(PHI)
  RBC2 = RPC2*COS(PHI)
  DELR1 = RAC1 - RRC1
  DELR2 = RAC2 - RRC2
  DELTAR = DELR1
  IF(DELR2.GT.DELTAR) DELTAR = DELR2
  L1=DELTAR*100.

```

```

C
IF(DELTA.R.LE.1.0) L1 = 100
IF(DELTA.R.GE.2.0) L1 = 200
L2 = L1

WRITE(6,21)
WRITE(6,35) PHID
WRITE(6,37) DP,TIN,TOU
10 WRITE(6,40) RPMIN,RPMOUT
WRITE(6,50)
WRITE(6,60) TG,PD1,LENGTH(OC),PD2,LENGTH(OC),RAC1,LENGTH(OC),RAC2,
&LENGTH(OC),RBC1,LENGTH(OC),RBC2,LENGTH(OC),RRC1,LENGTH(OC),RRC2,
&LENGTH(OC)
WRITE(6,65) RF1,LENGTH(OC),RF2,LENGTH(OC),RI(1),LENGTH(OC),
&RI(2),LENGTH(OC),FW(1),LENGTH(OC),FW(2),LENGTH(OC),E(1),MODLUS(OC)
&,E(2),MODLUS(OC),GAMA(1),SPWGHT(OC),GAMA(2),SPWGHT(OC),PR

C
P = TIN/RBC1
998 CALL FAST
IBYPSS=1
GO TO 1
8 CONTINUE

C
21 FORMAT(1H1,T38,'STATIC AND DYNAMIC ANALYSIS OF A GEAR PAIR SYSTEM'
&/T38,49(' '))
35 FORMAT(T49,F5.1,' DEGREE PRESSURE ANGLE'//)
37 FORMAT(T49,'DIAMETRAL PITCH IS',F10.3//T46,'INPUT TORQUE IS',
&F11.2,'IN-LBF'//T46,'OUTPUT TORQUE IS',F11.2,'IN-LBF'//)
38 FORMAT(T53,'MODULE IS',F11.3//T46,'INPUT TORQUE IS',F11.2,'NT-M
&'//T46,'OUTPUT TORQUE IS',F11.2,'NT-M'//)
40 FORMAT(T46,'INPUT SPEED IS',F11.2,'RPM'//T46,'OUTPUT SPEED IS'
&,F11.2,'RPM. ')
50 FORMAT( //T18,'DATA FOR GEAR 1 (DRIVING GEAR)',T65,'*',T87,'DATA
&FOR GEAR 2 (DRIVEN GEAR)',T18,15(' '),'T87,15(' '))//
60 FORMAT( T11, NUMBER OF TEETH',T35, '=',T38,F4.0,T65,'*',T80,'NUMBER
&OF TEETH',T104, '=',T107,F4.0//
&T11,'PITCH DIAMETER',T35, '=',T38,F8.4,3X,A3,T65,'*',T80,'PITCH DIA
&METER',T104, '=',T107,F8.4,3X,A3//
&T11,'ADDENDUM CIRCLE RADIUS =',T38,F8.4,3X,A3,T65,'*',T80,'ADDEND
&UM CIRCLE RADIUS =',T104, '=',T107,F8.4,3X,A3//
&T11,'BASE CIRCLE RADIUS',T35, '=',T38,F8.4,3X,A3,T65,'*',T80,'BASE
&CIRCLE RADIUS',T104, '=',T107,F8.4,3X,A3//
&T11,'ROOT CIRCLE RADIUS',T35, '=',T38,F8.4,3X,A3,T65,'*',T80,'ROOT
&CIRCLE RADIUS',T104, '=',T107,F8.4,3X,A3)
65 FORMAT(/T11,'FILLET RADIUS',T35, '=',T38,F8.4,3X,A3,T65,'*',T80,'FI
&LLET RADIUS',T104, '=',T107,F8.4,3X,A3//

```



```

&VALUES REPRESENT THE ANGLE BETWEEN THE NORMAL TO THE PROFILE AND TH
&E X-AXIS; COUNTERCLOCKWISE THETA IS DEFINED AS POSITIVE. (//)
425 FORMAT(T5,'THE INVOLUTE STARTS AT Y =',F9.4,1X,A3,' AND ENDS AT
& Y =',F9.4,1X,A3,' ON THE TOOTH PROFILE OF GEAR',I2,'.')
430 FORMAT(T28,'THE PITCH CIRCLE INTERSECTS THE TOOTH PROFILE OF GEAR'
&,I2,' AT Y =',F9.4,1X,A3)
432 FORMAT(T56,'RRO1 =',F9.4,1X,A3/T56,'RRO2 =',F9.4,1X,A3)
440 FORMAT(T40,'X AND Y VALUES ARE IN',A3,' THETA VALUES ARE IN
& DEGREES. (//T20,'DATA FOR GEAR 1',T91,' DATA FOR GEAR 2',T20,15(
&'),T91,15(,'*'))
450 FORMAT(T15,'POINT',T21,'X',T35,'Y',T47,'THETA',T76,'POINT',T92,
&'X',T106,'Y',T118,'THETA')
455 FORMAT(T5,13,3X,3F14.5,T76,13,3X,3F14.5)
C
C TABLE 2 OUTPUT
WRITE(6,500)
WRITE(6,502)
WRITE(6,510)
WRITE(6,512)
WRITE(6,514)
WRITE(6,518)
WRITE(6,530)
WRITE(6,535) ((1,PS11(1),PS12(1),NCP(1),TPS(3,1),CMS(1),CG(1)),I=1
&,50)
C
500 FORMAT(1H1,T55,'STATIC ANALYSIS',T55,15(,'*')//)
502 FORMAT(T16,'TABLES 2, 3 AND 4 LIST INFORMATION RESULTING FROM A ST
&ATIC ANALYSIS OF THE GEAR PAIR (NEGLECTING INERTIA',T16,'FORCES).
& THE DATA PRESENTED IN THESE TABLES WERE OBTAINED BY ROTATING THE
&DRIVING GEAR THRU ONE CYCLE',T16,' OF TOOTH ENGAGEMENT. IN EACH OF
& THESE TABLES POSITION 1 CORRESPONDS TO THE STARTING POINT OF CONT
&ACT WHILE',T16,' POSITION 50 CORRESPONDS TO THE END POINT OF CONTACT
&T. (//)
510 FORMAT(T59,'TABLE 2')
512 FORMAT(T30,'PS11 IS THE ANGLE OF ROTATION OF THE DRIVING GEAR IN D
&EGREES.',T30,'PS12 IS THE ANGLE OF ROTATION OF THE DRIVEN GEAR IN
&DEGREES.',T30,'NCP IS THE NUMBER OF SEPARATE TOOTH PAIRS IN CONTACT
&T AT A PARTICULAR POSITION.')
514 FORMAT(T30,'PS IS THE TOOTH PAIR STIFFNESS IN',A3,'',A2,' AT A P
&ARTICULAR POSITION.',T30,'KG IS THE COMBINED GEAR TOOTH SPRING COH
&STANT (STIFFNESS) IN',A3,'',A2,' AT A PARTICULAR POSITION.',T30,
&'CG IS THE GEAR DAMPENING COEFFICIENT IN (',A2,'-SEC)',A3)
518 FORMAT(T24,'NOTE: BOTH PS11 AND PS12 ARE MEASURED BETWEEN THE GEN
&TER LINE. (//)

```



```

530 FORMAT(T4, 'POSITION', T22, 'PS11', T39, 'PS12', T57, 'NCP', T77, 'PS', T100
& 'KG', T126, 'CG', /)
535 FORMAT(5X, I3, 11X, F7.3, 10X, F7.3, 13X, I2, 11X, F13.1, 10X, F13.1, 10X, F13.
&1)

```

C
C

```

C TABLE 3 OUTPUT
WRITE(6, 540)
WRITE(6, 542) FORCE(OC), P, FORCE(OC)
WRITE(6, 544) LENGTH(OC), LENGTH(OC)
IF(OC.EQ.1) WRITE(6, 545)
IF(OC.EQ.2) WRITE(6, 546)
WRITE(6, 548) PRESS(OC)
WRITE(6, 550) FORCE(OC), LEN(OC)
WRITE(6, 570) ((I, Q(3, I), YC1(3, I), YC2(3, I), SVS(I), HZPS(I), PVS(I)),
&I=1, 50)

```

C

```

540 FORMAT(1H1, T59, 'TABLE 3', /)
542 FORMAT(T17, 'LOAD IS THE FORCE IN ', A4, ' ACTING BETWEEN THE CONTACT
&ING TOOTH PAIR IN A DIRECTION NORMAL TO THE PROFILE. '/T17, '(THE TO
&TAL NOMINAL TRANSMITTED FORCE CARRIED BY ALL CONTACTING TOOTH PAIR
&S IS', F10.2, 1X, A4, ', ' )
544 FORMAT(T17, 'YC1 IS THE LOCATION OF THE CONTACT POINT ALONG THE TOO
&TH PROFILE OF GEAR 1; ', A3/T17, 'YC2 IS THE LOCATION OF THE CONTACT
& POINT ALONG THE TOOTH PROFILE OF GEAR 2; ', A3/T17, '(YC1 AND YC2 A
&RE MEASURED RELATIVE TO THE X-Y COORDINATE SYSTEMS' DEFINED IN TABL
&E 1)')
545 FORMAT(T17, 'SV IS THE SLIDING VELOCITY AT THE CONTACT POINT; FT/MI
&N. ')
546 FORMAT(T17, 'SV IS THE SLIDING VELOCITY AT THE CONTACT POINT; M/SE
&C. ')
548 FORMAT(T17, 'HZP IS THE MAXIMUM HERTZ CONTACT PRESSURE AT THE CONTA
&CT POINT; ', A4)
550 FORMAT(T17, 'PV IS THE HERTZ PRESSURE-SLIDING VELOCITY PRODUCT; ',
&A3, /, (A2, '-SEC. ', /)
560 FORMAT(3X, 'POSITION', T18, 'LOAD', T39, 'YC1', T59, 'YC2', T79, 'SV', T102,
&'HZP', T124, 'PV', /)
570 FORMAT(5X, I3, 6X, F8.2, 13X, F7.3, 13X, F7.3, 11X, E12.5, 11X, E12.5, 11X, E12
&.5)

```

C
C
C
C
C

```

C TABLE 4 OUTPUT
WRITE(6, 580)
WRITE(6, 590) LENGTH(OC), LENGTH(OC), LENGTH(OC), LENGTH(OC)
WRITE(6, 600)

```

```

C   WRITE(6,605) ((I,TDEF1(I),TDEF2(I),HDEF(I),CDEF(I)),I=1,50)
C
580 FORMAT(1H1,T59,'TABLE 4'//)
590 FORMAT(T36,'TD1 IS THE TOOTH DEFLECTION ON GEAR 1; ',A3/T36,'TD2 I
&S THE TOOTH DEFLECTION ON GEAR 2; ',A3/T36,'HD IS THE HERTZIAN DEF
&LECTION OF THE CONTACT POINT; ',A3/T36,'CD IS THE COMBINED DEFLECT
&ION OF THE CONTACT POINT; ',A3/T36,'(ALL DEFLECTIONS ARE MEASURED
&ALONG THE LINE OF ACTION.)'//)
600 FORMAT(T20,'POSITION',T42,'TD1',T63,'TD2',T83,'HD',T103,'CD'//)
605 FORMAT(T22,I3,I3X,F10.7,11X,F10.7,10X,F10.7,10X,F10.7)

C   999 CONTINUE
      RETURN
      END

C
SUBROUTINE FAST
COMMON/DIMEN/OC,MODCOD,IBYPSS
COMMON/C1/PHI,PHID,DP,M,TG1,TG2,TP,DELTP,TAPE
COMMON/C2/P1,F1,F2,R11,R12,E1,E2,G1,G2,PR1,PR2,GAMA1,GAMA2
COMMON/C4/TIN,TOU,RPMIN,RPMOUT,OMEGA1,OMEGA2
COMMON/C5/JG1,JG2,JD,JL,KDS,KLS,KGPAVG,ZETAS,ZETAG,CDS,CLS,CGPAVG,
1LDS,LLS,1PLOT,CBD,CB1,CB2,CBL
COMMON/C6/L1,L2,PD1,PD2,RPC1,RPC2,RAC1,RAC2,RBC1,RBC2,RRC1,RRC2,
&RF1,RF2,C,CP,BP,UCUT1,UCUT2
COMMON/C7/YT11,YT12,YP1,YP2,YB11,YB12,RT11,RT12,RB11,RB12,
1RR01,RR02,XMIN1,XMIN2,SP,EP
COMMON/C8/X1(200),X2(200),Y1(200),Y2(200),THETA1(200),THETA2(200),
1RCURV1(200),RCURV2(200)
COMMON/C9/XC1(5,50),XC2(5,50),YC1(5,50),YC2(5,50),THETC1(200),
1THETC2(200),DCP1(200),DCP2(200),RC1(5,50),RC2(5,50),RCC1(5,50),
2RCC2(5,50),Q(5,50),TPS(5,50),NCP(50)
COMMON/C10/ADJG1(100),ADJG2(100),AVJG1(100),AVJG2(100),DLOAD(100),
1NCPD(100),TD1D(100),TD2D(100),TDD(100),HDD(100),CDEFD(100),
2SVD(100),HZPD(100),PVD(100),TIME(2500),DM5(100)
COMMON/C11/PS1(2500),PS2(2500)
COMMON/C12/KG(50),CG(50),PS1(50),VELR(50),PSIS1,PSIS2,ITP,IEP,MNCP
COMMON/C13/X1(8),DX1(8),NE,NP,NRK,IP,LPP,ISTORE,JEP,NCI
COMMON/C14/PS1D(2500),PS2D(2500),QDT(2500),STIFFK(2500)
COMMON/C15/XC1D(5,100),XC2D(5,100),YC1D(5,100),YC2D(5,100),
1THC1D(5,100),THC2D(5,100),RCTD(5,100),RC2D(5,100),RCC1D(5,100),
2RCC2D(5,100),QD(5,100),QDD(50),QZ(50),YZ1(50),YZ2(50)
COMMON/C16/PHIOP(50),VELRA1(100),STATLD(100)

C   DIMENSION SM(4,4),MM(4,4),X(4,4),EIGV(4),DPS1(50),DKG(50)

```

```

DIMENSION NFREQ(4), EGV(4,4), TFS(5), TWIST1(5), TWIST2(5), XP(100),
&Y1P(100)
REAL M,JD,JG1,JG2,JL,KDS,KGPAVG,KLS,KG,LDS,LLS,NFREQ,JDM,JG1M,JG2M
1,JLM,KDSM,KLSM,KGAVGM,KT
DIMENSION FORCE(2), SPEED(2), PRESS(2), DF1(100), DF2(100)
DIMENSION MM(100),XX(100),YY(100),ZZ(100)
REAL LENGTH(2),MODLUS(2),LEN(2)
INTEGER OC
DOUBLE PRECISION DPI,DDP,DTG1,DTG2,DGAMA1,DGAMA2,DPH1,DPD1,
1DPD2,DRPC1,DRPC2,DRBC1,DRBC2,DJD,DJG1,DJG2,DJL,DKDS,DKAVG,DKLS,
2DPH1D,SM,MM,X,EIGV,DPS1,DKG,DZETAS,DZETAG,DRPMIN,DOMGAD,DOMGAT,
3DOMGA2,DOMGAL,SNF,HNP,1TR,TSS,TTOTAL,HNF,SNP,DT,DDT,DTIN,TD,
4DTOUT,TL,DPS1D,DPS1I,DPS12,DPS1L,DPS1DD,DPS12D,DPS1LD,PSDP,
5PS1P,PS2P,PSLP,PSDPD,PS1PD,PS2PD,PSLPD,PSDPDD,PS1PDD,PS2PDD,PSLPDD,
6,PS1A,KGP,CGP,DFD,DFS,DFORCE,XI,DX1,DNCTR,DNC1,DPS1TP,DPS1EP,
7DKM1,DKM2,PRDK,DFDM,DFSM,DFRCEN,KGPM,CGPM,DR11,DR12,DLDS,DLLS,
8DGDS,DGLS,TRN,CSPF,CRM,DIBEP,DFW1,DFW2
DOUBLE PRECISION DRBCN,DCBD,DCB1,DCB2,DCB1
C
DATA DPI/3.14159265358979323846/
DATA N1,N2/1,2/
DATA LENGTH/IN,'MM','/',FORCE/'LBF','N','/',LEN/'IN','M'/' ,
& PRESS/'PSI','MPA','/',MODLUS/'PSI','MPA','/
DDELT=DELT
C
IF (IBYPSS.EQ.1) GO TO 1
C
READ(8,1179) (QZ(50),YZ1(50),YZ2(50),K=1,50)
FORMAT(3E14.7)
1179 READ(8,1180) ((XC1(I,J),XC2(I,J),YC1(I,J),YC2(I,J),RC1(I,J),
& RC2(I,J),RCC1(I,J),RCC2(I,J),I=1,5),J=1,50)
1180 FORMAT(9E14.7)
READ(8,1181) (Y1(I),Y2(I),THETC1(I),THETC2(I),DCP1(I),DCP2(I),
& I=1,L1)
1181 FORMAT(6E14.7)
READ(8,1182) (NCR(I),KG(I),CG(I),PSI(I),VELR(I),I=1,50)
1182 FORMAT(14,4E14.7)
READ(8,1183) PSIS1,PSIS2,RR01,RR02,RT1,RT2,ITP,IEP,MNCP
1183 FORMAT(6E14.7,3I5)
C
READ(8,1180) (STATLD(I),I=1,100)
C
DO 1 I = 1,50
DPSI(I) = PSI(I)
DKG(I) = KG(I)

```

1 CONTINUE

C
 DPSITP = (DPSI(ITP) + DPSI(ITP-1))/2.
 DPSIEP = (DPSI(IEP) + DPSI(IEP-1))/2.
 DDP = DP
 DTG1 = TG1
 DTG2 = TG2
 DGAMA1 = GAMA1
 DGAMA2 = GAMA2
 DFW1 = F1
 DFW2 = F2
 DPHID = PHID
 DPHI = (DPHID*DPI)/180.
 DPD1 = DTG1/DDP
 DPD2 = DTG2/DDP
 DRPC1 = DPD1/2.
 DRPC2 = DPD2/2.
 DRBC1 = (DPD1/2.)*DCOS(DPHI)
 DRBC2 = (DPD2/2.)*DCOS(DPHI)
 DJD = JD
 DJL = JL
 IF (JG1.EQ.0.) JG1 = (.5*DGAMA1*DPI*DFW1*(DRPC1**4))/386.
 IF (JG2.EQ.0.) JG2 = (.5*DGAMA2*DPI*DFW2*(R12**4-DRPC2**4))/386.)
 DJG1 = JG1
 DJG2 = JG2
 IF(JD.EQ.0.0) DJD = 50.*DJG1
 IF(JL.EQ.0.0) DJL = 50.*DJG1
 JD = DJD
 JL = DJL
 IBTP = ITP - 1
 IBEP = IEP - 1
 DKM1 = DKG(1)
 DKM2 = DKG(ITP)
 DKAVG=0.0
 DO 2020 I=1,IBEP
 2020 DKAVG=DKAVG+DKG(I)
 DIBEP=FLOAT(IEP)
 DKAVG=DKAVG/DIBEP
 KGPAVG = DKAVG
 DKDS = KDS
 DKLS = KLS
 IF(LDS.EQ.0.0) LDS = 6.
 IF(LLS.EQ.0.0) LLS = 6.
 IF((KDS.NE.0.0).AND.(KLS.NE.0.0)) GO TO 4
 DR11 = R11

```

DR12 = DR11*TG2/TG1
DLDS = LDS
DLLS = LLS
DGDS = 30000000./(2.*(1. + .285))
DGLS = 30000000./(2.*(1. + .285))
DKDS = (DPI*(2.*DR1)**4)*DGDS)/(32.*DLDS)
DKLS = (DPI*(2.*DR12)**4)*DGLS)/(32.*DLLS)
DKDS = DKDS
DKLS = DKLS
KDS = DKDS
KLS = DKLS
4 CONTINUE
DZETAS = ZETAS
DZETAG = ZETAG
DCDS = (2.*DZETAS*DSQRT(DKDS))/DSQRT((DJJ+DJG1)/(DJJ*DJG1))
DCLS = (2.*DZETAS*DSQRT(DKLS))/DSQRT((DJL+DJG2)/(DJL*DJG2))
DCBD = CBD
DCB1 = CB1
DCB2 = CB2
DCBL = CBL
CGPAVG = (2.*ZETAG*SQRT(KGPAVG))/SQRT((RBC1**2)/JG1+(RBC2**2)/JG2)
CDS = DCDS
CLS = DCLS
DO 5 I = 1,4
DO 5 J = 1,4
MM(1,J)=0.0
MM(1,1) = DJJ
MM(2,2) = DJG1
MM(3,3) = DJG2
MM(4,4) = DJL
SM(1,1) = DKDS
SM(1,2) = -DKDS
SM(1,3) = 0.0
SM(1,4) = 0.0
SM(2,1) = -DKDS
SM(2,2) = DKDS + DKAVG*(DRBC1**2)
SM(2,3) = -DKAVG*DRBC1*DRBC2
SM(2,4) = 0.0
SM(3,1) = 0.0
SM(3,2) = -DKAVG*DRBC1*DRBC2
SM(3,3) = DKLS + DKAVG*(DRBC2**2)
SM(3,4) = -DKLS
SM(4,1) = 0.0
SM(4,2) = 0.0
SM(4,3) = -DKLS
SM(4,4) = DKLS
5

```

```

CALL VIBS(SM,MM,X,EIGV)
DO 11 I = 1,4
NFREQ(I) = DSQRT(EIGV(I))/(2.*DPI)
DO 11 J = 1,4
11 EGVC(J,I)=X(J,I)
DRPMIN = RPMIN
DOMGA1 = 2.*DPI*(DRPMIN/60.)
DOMGAD = DOMGA1
DOMGA2 = (DRBC1/DRBC2)*DOMGA1
DOMGAL = DOMGA2
RPMOUT=DOMGA2*60./(2.*DPI)
SNF = DSQRT(EIGV(2))
HNP = (2.*DPI)/SNF
TTR = 5.*HNP
ARG = TTR*DTG1*(DRPMIN/60.)
NCTR = IFIX(ARG)
IF(NCTR.EQ.0) NCTR = 1
IF(MNCP.EQ.2) NCT = NCTR + 2
IF(MNCP.EQ.3) NCT = NCTR + 3
DNCTR = FLOAT(NCTR)
TTR = DNCTR/(DTG1*(DRPMIN/60.))
IF(MNCP.EQ.2) TSS = 2./(DTG1*(DRPMIN/60.))
IF(MNCP.EQ.3) TSS = 3./(DTG1*(DRPMIN/60.))
TTOTAL = TTR + TSS
HNF = DSQRT(EIGV(4))
SNP = (2.*DPI)/HNF
DDT = SNP/10.
LPK = 0
PRDK = DPSIEP/DOMGA1
IF(PRDK.LE.SNP) LPK = 1
IF((LPK.EQ.1).AND.(MNCP.EQ.2)) DDT = PRDK/100.
IF((LPK.EQ.1).AND.(MNCP.EQ.3)) DDT = PRDK/50.
DT = 0.0
KGP = DKG(1)
DTIN = TIN
TD = DTIN
DTOUT = (DRBC2/DRBC1)*DTIN
TL = DTOUT
DPSID = DTIN/DKDS
DPSI1 = 0.0
DPSI2 = -(DKDS*DPSID)/(KGP*DRBC1*DRBC2)
DPSI0 = DPSI2 - DTOUT/DKLS
DPSI0D = DOMGAD
DPSI1D = DOMGA1
DPSI2D = DOMGA2

```


&,'/T25,'KG AND CG ARE PERIODIC FUNCTIONS WITH A PERIOD EQUAL TO TH
 &E RECIPROCAL OF THE TOOTH'/T25,'MESHING FREQUENCY.'//)
 40 FORMAT(T42,'THE DAMPING FACTOR (ZETAS) OF THE SHAFT = ',F6.3//
 &T42,'THE DAMPING FACTOR (ZETAG) OF THE GEAR PAIR = ',F6.3//)

C
C
C

C NOMENCLATURE/SYSTEM PARAMETERS OUTPUT PAGE

```

WRITE(6,50)
WRITE(6,60)
WRITE(6,62)
WRITE(6,64)
WRITE(6,64)
WRITE(6,66)
WRITE(6,68)
WRITE(6,70)
WRITE(6,72)
WRITE(6,74)
WRITE(6,80)
  
```

C

50 FORMAT(IH1,T34,'THE SYMBOLS USED IN THE ABOVE FIGURE HAVE THE FOLL
 OWING DEFINITIONS: '//T36,'JD IS THE MASS MOMENT OF INERTIA OF TH
 &E PRIME MOVER (DRIVER) '//T36,'JG1 IS THE MASS MOMENT OF INERTIA OF
 & THE DRIVING GEAR (GEAR 1) '//T36,'JG2 IS THE MASS MOMENT OF INERTI
 &A OF THE DRIVEN GEAR (GEAR 2) '//T36,'JL IS THE MASS MOMENT OF INE
 &RTIA OF THE LOAD. '//T36,'KDS IS THE TORSIONAL SPRING STIFFNESS OF T
 &HE DRIVING SHAFT. '//T36,'KLS IS THE TORSIONAL SPRING STIFFNESS OF THE
 &GEAR PAIR. '//T36,'KLS IS THE TORSIONAL SPRING STIFFNESS OF THE LOAD
 & SHAFT. '//T36,'CDS IS THE TORSIONAL DAMPENING COEFFICIENT OF THE DR
 &IVING SHAFT. '//T36,'CG IS THE LINEAR DAMPENING COEFFICIENT OF THE
 &LOAD SHAFT. '//)

60 FORMAT('//T41,'THE SYSTEM PARAMETERS HAVE THE FOLLOWING SPECIFICATI
 &ONS: '//)
 62 FORMAT(T48,'JD = ',F9.4,' (',A2,'-',A3,'-(SEC**2))/RADIANT'//)
 64 FORMAT(T48,'JG1 = ',F9.4,' (',A2,'-',A3,'-(SEC**2))/RADIANT'//)
 66 FORMAT(T48,'JL = ',F9.4,' (',A2,'-',A3,'-(SEC**2))/RADIANT'//)
 68 FORMAT(T48,'KDS = ',F11.1,' (',A2,'-',A3,')/RADIANT'//)
 70 FORMAT(T48,'KLS = ',F11.1,' (',A2,'-',A3,')/RADIANT'//)
 72 FORMAT(T48,'CDS = ',F8.3,' (',A2,'-',A3,'-SEC)/RADIANT'//)
 74 FORMAT(T48,'CLS = ',F8.3,' (',A2,'-',A3,'-SEC)/RADIANT'//)
 80 FORMAT(T35,'KG AND CG ARE TABULATED IN TABLE 2 OF THE STATIC ANALY
 &SIS SECTION. '//T36,'CDS AND CLS WERE CALCULATED USING THE VALUE ZET
 &SIS QUOTED ABOVE. '//T36,'CG WAS CALCULATED USING THE VALUE ZETAG QUO
 &TED ABOVE. ')

C
C
C

C TABLE 5 OUTPUT


```

WRITE(6,90)
WRITE(6,95) KGPVAVG, FORCE(OC), LEN(OC)
WRITE(6,98)
WRITE(6,100) MFREQ(1), (EGVC(K,1), K=1,4)
WRITE(6,102) MFREQ(2), (EGVC(K,2), K=1,4)
WRITE(6,104) MFREQ(3), (EGVC(K,3), K=1,4)
WRITE(6,106) MFREQ(4), (EGVC(K,4), K=1,4)

C 90 FORMAT(1H1,T64,'TABLE 5'////T57,'SYSTEM VIBRATION DATA'/T57,21('*'
&///)
95 FORMAT(T11,'THE INFORMATION LISTED BELOW REPRESENTS THE SYSTEM NAT
&RURAL FREQUENCIES AND THE CORRESPONDING EIGANVECTORS. THIS'/T11,'I
&NFORMATION IS OBTAINED FROM THE "VIBS" SUBROUTINE WHICH SOLVES THE
& GENERAL EIGANPROBLEM USING A JACOBI ITERATION'/T11,'TECHNIQUE. N
&NOTE THAT THE FIRST MODE IS A RIGID BODY MODE AND NOTE THE EFFECT O
&F THE GEAR RATIO ON THE EIGANVECTORS.'/T11,'IN COMPUTING THIS VIBR
&ATION DATA AN AVERAGE VALUE FOR THE GEAR STIFFNESS EQUAL TO',F13.1
&,1X,A3,'/',A2,' WAS USED.'////)
98 FORMAT(T35,'NATURAL FREQUENCIES',T82,'EIGANVECTORS'//T38,'(CYCLES/
&SEC)',T66,'JD',T80,'JG1',T94,'JG2',T108,'JL'//)
100 FORMAT(T24,'1ST MODE',F14.1,T57,4F14.4/)
102 FORMAT(T24,'2ND MODE',F14.1,T57,4F14.4/)
104 FORMAT(T24,'3RD MODE',F14.1,T57,4F14.4/)
106 FORMAT(T24,'4TH MODE',F14.1,T57,4F14.4/)

C C
C C TABLE 6 OUTPUT
WRITE(6,110)
WRITE(6,115)
WRITE(6,120)
WRITE(6,122) RPMIN
WRITE(6,124) N1,RPMIN
WRITE(6,124) N2,RPMOUT
WRITE(6,126) RPMOUT
WRITE(6,130)
IF(OC.EQ.1) WRITE(6,131) TIN,TOUT
IF(OC.EQ.2) WRITE(6,132) TIN,TOUT
WRITE(6,134)
WRITE(6,136) DPSID
WRITE(6,138) N1,DPSI1
WRITE(6,138) N2,DPSI2
WRITE(6,140) DPSIL
WRITE(6,150) NCT,DDT,RT1,RT2

C C NUMERICAL INTEGRATION RESULTS (DYNAMIC)

```

```

IF(I PLOT,NE.0) GO TO 189
WRITE(6,160)
WRITE(6,162)
WRITE(6,164)
WRITE(6,164)
WRITE(6,166)
WRITE(6,168)
WRITE(6,168)
WRITE(6,170)
WRITE(6,172)
WRITE(6,174)
WRITE(6,176)
WRITE(6,178)
WRITE(6,180)
GO TO 275
N1,N1
N2,N2
N1,N1
N2,N2
FORCE(OC),LEN(OC)
FORCE(OC),LEN(OC)
FORCE(OC)
FORCE(OC)
FORCE(OC)
FORCE(OC)
C 189 WRITE(6,190)
WRITE(6,195)
WRITE(6,200)
FORCE(OC),LEN(OC),FORCE(OC)
IF(I PLOT, EQ.2) GO TO 225
WRITE(6,215)
GO TO 275
225 WRITE(6,210)
DELTPP=DELTP*25.4
IF (OC, EQ.2) RPMIN,DELTPP,LENGTH(OC)
WRITE(6,209) RPMIN,DELTPP,LENGTH(OC)
209 FORMAT(' ',T28,'INPUT SPEED IS ',F11.2,' RPM',28X,'BACKLASH I
&S ',F10.6,1X,A4//)
C 110 FORMAT(1H1,T63,'TABLE 6'//T36,'NUMERICAL INTEGRATION OF THE DIFFER
&ENTIAL EQUATIONS OF MOTION'/T36,61('*')//)
115 FORMAT(T20,'THE DIFFERENTIAL EQUATIONS OF MOTION OF THE SYSTEM VER
&E INTEGRATED NUMERICALLY USING A 4TH ORDER'/T20,'RUNGE-KUTTA INTEG
&RATION SCHEME. THE INITIAL CONDITIONS IMPLEMENTED FOR THE INTEGRA
&TION ARE:'//)
120 FORMAT(T53,'A. INITIAL ANGULAR VELOCITIES'//)
122 FORMAT(T43,'THE INITIAL VELOCITY OF JD IS ',F10.2,' RPM')
124 FORMAT(T43,'THE INITIAL VELOCITY OF JG',I1,' IS ',F10.2,' RPM')
126 FORMAT(T43,'THE INITIAL VELOCITY OF JL IS ',F10.2,' RPM')
130 FORMAT(T51,'B. INITIAL ANGULAR DISPLACEMENTS'//)
131 FORMAT(T24,'THE INITIAL DISPLACEMENTS ARE DUE TO A TORQUE PRELOAD
&OF ',F12.2,' IN-LBS ON THE'/T24,'INPUT SHAFT AND',F12.2,' IN-LBS
&ON THE OUTPUT SHAFT. THIS TORQUE PRELOAD IS')
132 FORMAT(T24,'THE INITIAL DISPLACEMENTS ARE DUE TO A TORQUE PRELOAD
&OF ',F12.2,' IN-MTS ON THE'/T24,'INPUT SHAFT AND',F12.2,' NT-MTS

```

```

&ON THE OUTPUT SHAFT. THIS TORQUE PRELOAD IS')
134 FORMAT(T24,'EQUAL TO THE NOMINAL STATIC TORQUE CARRIED BY THE SYST
&EM. THIS RESULTS IN THE FOLLOWING'/T24,'INITIAL ANGLES OF TWIST O
&R WIND-UP: '/')
136 FORMAT(T41,'THE INITIAL DISPLACEMENT OF JD IS',F10.5,' RADIANS')
138 FORMAT(T41,'THE INITIAL DISPLACEMENT OF JG',I1,' IS',F10.5,' RADI
&ANS')
140 FORMAT(T41,'THE INITIAL DISPLACEMENT OF JL IS',F10.5,' RADIANS'
&////////)
150 FORMAT(T23,'THE NUMERICAL INTEGRATION WAS CARRIED OUT FOR A LENGTH
& OF TIME EQUIVALENT TO',I5,' CYCLES'/T23,'OF STIFFNESS VARIATION.
& THIS TOTAL INTEGRATION TIME WAS ARRIVED AT ESSENTIALLY BY ADDING'
&
&T23,'THE TIME REQUIRED FOR THE START-UP TRANSIENT TO DECAY (THIS T
&IME IS ASSUMED TO BE EQUAL'/T23,'TO 5 TIMES THE LONGEST SYSTEM NAT
&URAL PERIOD) TO THE TIME REQUIRED FOR ONE ADDITIONAL'/T23,'TOOTH P
&ASSAGE CYCLE. THE DATA TABULATED IN TABLES 7 AND 8 BELOW COMES FR
&OM THIS LAST'/T23,'TOOTH PASSAGE CYCLE, THE ASSUMPTION BEING THAT
&THIS REPRESENTS A STEADY-STATE SITUATION.'/T23,'THE INTEGRATION TI
&ME STEP USED IS',F10.7,' SECONDS. THIS REPRESENTS EITHER ONE TEN
&TH'/T23,'OF THE SHORTEST SYSTEM NATURAL PERIOD OR A CERTAIN PERCENT
&STAGE OF THE PERIOD OF THE'/T23,'STIFFNESS FUNCTION, WHICHEVER IS S
&MALLEST./////////T23,'RT1,RT2 =',2F8.4)
160 FORMAT(IH1,T52,'C. NUMERICAL INTEGRATION RESULTS'////////T11,'THE RESU
&LTS OF THE NUMERICAL INTEGRATION ARE TABULATED BELOW. THE INFORMA
&TION LISTED IS IN DOUBLE PRECISION.'/T11,'NOTE THAT D+ON REPRESENT
&S 10 RAISED TO THE POSITIVE NTH POWER. THE FOLLOWING SYMBOLS ARE
&UTILIZED IN THIS TABLE: //)
162 FORMAT(T34,'TIME IS THE INTEGRATION TIME; SECONDS'/T34,'PSIDD IS
&THE ANGULAR VELOCITY OF JD; RADIANS/SEC')
164 FORMAT(T34,'PSI',I1,'D IS THE ANGULAR VELOCITY OF JG',I1,'; RADIAN
&S/SEC')
166 FORMAT(T34,'PSILD IS THE ANGULAR VELOCITY OF JL; RADIANS/SEC')
168 FORMAT(T34,'PSI',I1,' IS THE ANGULAR DISPLACEMENT OF JG',I1,'; RAD
&IANS')
170 FORMAT(T34,'KG IS THE GEAR STIFFNESS; ',A3,'/',',A2)
172 FORMAT(T34,'CG IS THE GEAR DAMPENING COEFFICIENT; ('',A2,'-SEC)'/',
&A2)
174 FORMAT(T34,'DFK IS THAT PORTION OF THE DYNAMIC FORCE CARRIED BY TH
&E GEAR PAIR SPRING; ',A3)
176 FORMAT(T34,'DFD IS THAT PORTION OF THE DYNAMIC FORCE CARRIED BY TH
&E GEAR PAIR DASHPOT; ',A3)
178 FORMAT(T34,'DF IS THE TOTAL DYNAMIC FORCE (SUM OF DFK AND DFD); '
&A3/T34,'INC IS THE CYCLE NUMBER OF THE STIFFNESS FUNCTION'////////)
180 FORMAT(T4,'TIME',4X,'PSIDD',4X,'PSILD',5X,'PSILD',5X,'P

```

```

&S11', 5X, 'PSI2', 8X, 'KG', 8X, 'CG', 7X, 'DFK', 7X, 'DFD', 9X, 'DF', 5X, 'NC'//
190 FORMAT(1H1, T50, 33(' '), T82, ' ', * /T50, ' ', * XT PLOT OF THE RES
&ULTS OF * /T50, ' ', * THE NUMERICAL INTEGRATION', T82, ' ', * /T50, ' ', * ,
&T82, ' ', * /T50, 33(' '), * /T50, ' ', * )//
195 FORMAT(T26, 'THE DATA DEPICTED IN THE FOLLOWING X VERSUS T PLOTS AR
&E OBTAINED BY NUMERICALLY /T26, ' INTEGRATING THE DIFFERENTIAL EQUAT
&IONS OF MOTION. IN THESE PLOTS: '///)
200 FORMAT(T47, 'TIME IS THE INTEGRATION TIME; SECONDS' /T49, 'KG IS THE
&GEAR STIFFNESS; 'A3, ' /, 'A2/T49, 'DF IS THE DYNAMIC FORCE; 'A3//
&T35, 'THE DYNAMIC FORCE PLOT DISPLAYS A NORMALIZED DYNAMIC FORCE, /
&T35, 'I.E. THE DYNAMIC FORCE DIVIDED BY THE NOMINAL TRANSMITTED FOR
&CE. '///)
210 FORMAT(T26, 'THIS PLOT REPRESENTS ONLY THAT TIME PERIOD IN THE NUME
&RICAL INTEGRATION SEQUENCE /T26, ' COVERING THE LAST PASSAGE OF A TO
&BOTH PAIR THRU THE CONTACT ZONE. IT IS ASSUMED' /T26, ' THAT THE SYST
&EM IS OPERATING IN A STEADY STATE CONDITION DURING THIS PERIOD. ' /
&/)
215 FORMAT(///)
C
275 ARG = DPSI1/DPSIEP
NC = IFIX(ARG) + 1
DNC1 = FLOAT(NC-1)
PSIA = DPSI1 - DNC1*DPSIEP
IF((PSIA.LE.DPSI(1)).OR.(PSIA.GT.DPSI(IEP))) GO TO 305
DO 280 I = 2, IEP
IF(PSIA.LE.DPSI(I)) GO TO 285
CONTINUE
IF(I.EQ. ITP) GO TO 295
IF(I.EQ. IEP) GO TO 300
KGP = DKG(I-1)*(DKG(I)-DKG(I-1))*((PSIA-DPSI(I-1))/
1(DPSI(I)-DPSI(I-1)))
VRATIO = VELR(I-1) + (VELR(I)-VELR(I-1))*((PSIA-DPSI(I-1))/
1(DPSI(I)-DPSI(I-1)))
GO TO 310
295 IF(PSIA.LT.DPSITP) KGP = DKG(ITP-1)
IF(PSIA.GE.DPSITP) KGP = DKG(ITP)
IF(PSIA.LT.DPSITP) VRATIO = VELR(ITP-1)
IF(PSIA.GE.DPSITP) VRATIO = VELR(ITP)
GO TO 310
300 IF(PSIA.LT.DPSIEP) KGP = DKG(IEP-1)
IF(PSIA.GE.DPSIEP) KGP = DKG(IEP)
IF(PSIA.LT.DPSIEP) VRATIO = VELR(IEP-1)
IF(PSIA.GE.DPSIEP) VRATIO = VELR(IEP)
GO TO 310
305 IF(PSIA.LE.DPSI(1)) KGP = DKG(1)

```

```

IF(PSIA.GT.DPSI(IEP)) KGP = DKG(IEP)
IF (PSIA.LE.DPSI(1)) VRATIO=VELR(1)
IF (PSIA.GT.DPSI(IEP)) VRATIO=VELR(IEP)
310 CGP=(2.*DZETAG*DSQRT(KGP))/DSQRT((DRBC1**2)/DJG1+(DRBC2**2)/DJG2)
TRN = VRATIO
TL = (TD - DCBD*(PSDPD+DOMGAD) - DCB1*(PS1PD+DOMGA1))*TRN
&
C*****EQUATIONS OF MOTION
DRBCN=DRBC1*TRN
CRM= (DRBC1*PS1P-DRBCN*PS2P)
PSDPDD = (-DCDS*((PSDPD+DOMGAD)-(PS1PD+DOMGA1))
& -DCBD*(PSDPD+DOMGAD)-DCB1*(PS1PD+DOMGA1)
& -DKDS*((PSDP+DT*DOMGAD)-(PS1P+DT*DOMGA1))+TD)/DJG
PSLPDD = (-DCLS*((PSLPD+DOMGAL)-(PS2PD+DOMGA2))
& -DCBL*((PSLPD+DOMGAL)-DCB2*(PS2PD+DOMGA2))
& -DKLS*((PSLP+DT*DOMGAL)-(PS2P+DT*DOMGA2))-TL)/DJL
IF (CRM.LE.0.0) GO TO 311
ICTR=1
PS1PDD = (-DCDS*((PS1PD+DOMGA1)-(PSDPD+DOMGAD))
& -DKDS*((PS1P+DT*DOMGA1)-(PSDP+DT*DOMGAD))
& -CGP*(DRBC1*(PS1PD+DOMGA1)-(DRBCN*PS2PD + DRBC2*DOMGA2))
& *DRBC1
& -KGP*(DRBC1*(PS1P+DT*DOMGA1)-(DRBCN*PS2P + DRBC2*DT
& *DOMGA2))*DRBC1)/DJG1
PS2PDD= (-DCLS*((PS2PD+DOMGA2)-(PSLPD+DOMGAL))
& -DKLS*((PS2P+DT*DOMGA2)-(PSLP+DT*DOMGAL))
& -CGP*((DRBCN*PS2PD+DRBC2*DOMGA2)-DRBC1*(PS1P+DOMGA1))
& *DRBCN
& -KGP*((DRBCN*PS2P+DRBC2*DT*DOMGA2)-DRBC1*(PS1P+DT*DOMGA1))
& *DRBCN)/DJG2
GO TO 314
311 IF (DABS(CRM).GE.DELT) GO TO 312
ICTR=2
PS1PDD = (-DCDS*((PS1PD+DOMGA1)-(PSDPD+DOMGAD))
& -DKDS*((PS1P+DT*DOMGA1)-(PSDP+DT*DOMGAD)))/DJG1
PS2PDD = (-DCLS*((PS2PD+DOMGA2)-(PSLPD+DOMGAL))
& -DKLS*((PS2P+DT*DOMGA2)-(PSLP+DT*DOMGAL)))/DJG2
GO TO 314
312 CONTINUE
ICTR=3
PS1PDD = (-DCDS*((PS1PD+DOMGA1)-(PSDPD+DOMGAD))
& -DKDS*((PS1P+DT*DOMGA1)-(PSDP+DT*DOMGAD))
& -CGP*(DRBC1*(PS1PD+DOMGA1)-(DRBCN*PS2PD + DRBC2*DOMGA2))
& *DRBC1
& -KGP*(DRBC1*(PS1P+DT*DOMGA1)-(DRBCN*PS2P + DRBC2*DT

```

```

& PS2PDD = (-DKLS*((PS2PD+DOMGA2)-(PSLP+DT*DOMGAL))
& -DKLS*((PS2P+DT*DOMGA2)-(PSLP+DT*DOMGAL))
& -CGP*((DRBCN*PS2PD+DRBC2*DOMGA2)-DRBC1*(PS1PD+DOMGA1))
& *DRBCN
& -KGP*((DRBCN*PS2P+DRBC2*DT*DOMGA2)-DRBC1*(PS1P+DT*DOMGA1)
& -DDELT) *DRBCN)/DJG1

314 CONTINUE
C*****
IF(NRK.EQ.1) GO TO 320
315 CALL RKUTIA(DT,DDT)
CALL MOREK(PSDP,PSDPD,DDT)
CALL MOREK(PS1P,PS1PD,DDT)
CALL MOREK(PS1PD,PS1PDD,DDT)
CALL MOREK(PS2P,PS2PD,DDT)
CALL MOREK(PSLP,PSLPD,DDT)
CALL MOREK(PSLPD,PSLPDD,DDT)
DPS11 = PS1P + DT*DOMGA1
GO TO 275
320 IF(NC.GT.NCT) GO TO 340
DPSID = PSDP + DT*DOMGAD
DPSI2 = PS2P + DT*DOMGA2
DPSIL = PSLP + DT*DOMGAL
DPSIDD = PSDPD + DOMGAD
DPSI1D = PS1PD + DOMGA1
DPSI2D = PS2PD + DOMGA2
DPSILD = PSLPD + DOMGAL
DFD=CGP*((DRBC1*PS1PD - DRBCN*PS2PD)
DFS=KGP*((DRBC1*PS1P - DRBCN*PS2P)
D'FORCE = DFD + DFS
IF (ICTR.EQ.2) DFORCE=0.0
T = DT
DYNF = DFORCE
SKGP = KGP
IF(IPLT.NE.0) GO TO 340
WRITE(6,325) DT,DPSIDD,DPSI1D,DPSILD,DPSI2,KGP,CGP,
& DFS,DFD,DFORCE,TL,ARG,ICTR
325 FORMAT(' ',F8.6,1X,F7.3,2F10.5,F8.3,1X,2F9.5,1X,D12.5,F7.4,1X,
& 3F9.2,F7.1,F6.2,12)
340 IF(IPLT.NE.1) GO TO 350
CALL STORE(T,DELTA,PRI,PT,TSP,TEP,SKGP,DYNF,NC)
350 IF(NC.GT.NCT) GO TO 360
IF((NC.LE.(NCT-MNCP)).OR.(LP.EQ.1)) GO TO 315

```

```

J = J + 1
IF(J.EQ.1) TIMES = T
IF(J.EQ.1) PS1S = DPSI1
IF(J.EQ.1) PS2S = DPSI2
IF(NC.EQ.NCT) LC = 1
IF((LC.EQ.1).AND.(PS1A.GT.DPSITP)) LP = 1
IF(LP.EQ.1) JEP = J - 1
IF(LP.EQ.1) GO TO 315
TIME(J) = T
PS1(J) = DPSI1
PS2(J) = DPSI2
PS1D(J) = DPSI1D
PS2D(J) = DPSI2D
QDT(J) = DFORCE
STIFFK(J) = SKGP
IF(J.LT.2500) GO TO 315
WRITE(6,355)
355 FORMAT(5X,'THE J INDEX IN THE FAST SUBROUTINE EXCEEDS 2500 - INCR
1EASE THE DIMENSIONS OF ALL THE ARRAYS IN COMMON BLOCK C14')
STOP
360 NC = 0
IF(I.PLOT.NE.2) GO TO 375
TSP = TIME(1)
TEP = TIME(JEP)
PT = TSP
DO 370 I = 1,JEP
XTM = TIME(I)
IF(OC.EQ.2) GO TO 365
Y1E = STIFFK(I)
Y2E = QDT(I)
CALL STORE(XTM,DELTAT,PRI,PT,TSP,TEP,Y1E,Y2E,NC)
GO TO 370
365 Y1M = STIFFK(I)*175.12685
Y2M = QDT(I)*4.448222
CALL STORE(XTM,DELTAT,PRI,PT,TSP,TEP,Y1M,Y2M,NC)
370 CONTINUE
375 CONTINUE
PS2(1) = 0.0
PS1(1) = 0.0
DO 400 I = 2,JEP
PS1(I) = PS1(I) - PS1S
PS2(I) = PS2(I) - PS2S
400 CONTINUE
PS1(JEP) = PS1(50)
ADJG1(1) = PS1(1)

```

```

ADJG2(1) = PS2(1)
AVJG1(1) = PS1D(1)
AVJG2(1) = PS2D(1)
DLOAD(1) = QDT(1)
ADJG1(100) = PS1(JEP)
ADJG2(100) = PS2(JEP)
AVJG1(100) = PS1D(JEP)
AVJG2(100) = PS2D(JEP)
DLOAD(100) = QDT(JEP)
DELANG = PS1(JEP)/99.
DO 407 I = 2,99
  PS1DA = FLOAT(I-1)*DELANG
DO 402 J = 2,JEP
  IF(PS1(J).EQ.PS1DA) GO TO 404
  IF(PS1(J).GT.PS1DA) GO TO 406
402 CONTINUE
404 ADJG1(1) = PS1(J)
   ADJG2(1) = PS2(J)
   AVJG1(1) = PS1D(J)
   AVJG2(1) = PS2D(J)
   DLOAD(1) = QDT(J)
   GO TO 407
406 ADJG1(1) = PS1DA
   VINCR = (PS1DA-PS1(J-1))/(PS1(J)-PS1(J-1))
   TINC = TIME(J-1) + VINCR*(TIME(J)-TIME(J-1))
   TINCR = (TM-TIME(J-1))/(TIME(J)-TIME(J-1))
   ADJG2(1) = PS2(J-1) + TINCR*(PS2(J)-PS2(J-1))
   AVJG1(1) = PS1D(J-1) + TINCR*(PS1D(J)-PS1D(J-1))
   AVJG2(1) = PS2D(J-1) + TINCR*(PS2D(J)-PS2D(J-1))
   DLOAD(1) = QDT(J-1) + TINCR*(QDT(J)-QDT(J-1))
407 CONTINUE
DO 422 I = 1,100
  KT = 0.0
DO 408 JJ = 1,50
  IF(PS1(JJ).GE.ADJG1(1)) GO TO 409
408 CONTINUE
409 NCPD(1) = NCP(JJ)
DO 418 K = 1,50
DO 412 JJ = 1,50
  IF(PS1(JJ).GE.ADJG1(1)) GO TO 413
412 CONTINUE
413 XC1D(K,1) = XC1(K, JJ)
   YC1D(K,1) = YC1(K, JJ)
   XC2D(K,1) = XC2(K, JJ)
   YC2D(K,1) = YC2(K, JJ)

```



```

RC1D(K, I) = RC1(K, JJ)
RC2D(K, I) = RC2(K, JJ)
RCC1D(K, I) = RCC1(K, JJ)
RCC2D(K, I) = RCC2(K, JJ)
TPSD(K) = TPS(K, JJ)
IF((PSI(JJ)).EQ.ADJG1(I)).OR.(YC1(K, JJ).LT..000001)) GO TO 416
VINGR = (ADJG1(I)-PSI(JJ-1))/(PSI(JJ)-PSI(JJ-1))
XC1D(K, I) = XC1(K, JJ-1) + VINGR*(XC1(K, JJ)-XC1(K, JJ-1))
YC1D(K, I) = YC1(K, JJ-1) + VINGR*(YC1(K, JJ)-YC1(K, JJ-1))
XC2D(K, I) = XC2(K, JJ-1) + VINGR*(XC2(K, JJ)-XC2(K, JJ-1))
YC2D(K, I) = YC2(K, JJ-1) + VINGR*(YC2(K, JJ)-YC2(K, JJ-1))
RC1D(K, I) = RC1(K, JJ-1) + VINGR*(RC1(K, JJ)-RC1(K, JJ-1))
RC2D(K, I) = RC2(K, JJ-1) + VINGR*(RC2(K, JJ)-RC2(K, JJ-1))
RCC1D(K, I) = RCC1(K, JJ-1) + VINGR*(RCC1(K, JJ)-RCC1(K, JJ-1))
RCC2D(K, I) = RCC2(K, JJ-1) + VINGR*(RCC2(K, JJ)-RCC2(K, JJ-1))
IF(ADJG1(I).LT.((PSI(JJ)+PSI(JJ-1))/2.)) TPSD(K) = TPS(K, JJ-1)
IF(ADJG1(I).GE.((PSI(JJ)+PSI(JJ-1))/2.)) TPSD(K) = TPS(K, JJ)
416 KT = KT + TPSD(K)
418 CONTINUE
DO 420 K = 1, 5
QD(K, I)=0.0
IF (KT.EQ.0.0) GO TO 420
QD(K, I) = (TPSD(K)/KT)*DLOAD(I)
420 CONTINUE
422 CONTINUE
F = F1
IF(F2.LT.F1) F = F2
C2 = (1.-PR1**2)/E1 + (1.-PR2**2)/E2
C3 = (2.*(1.-PR1**2))/(PI*F*E1)
C4 = PR1/(2.*(1.-PR1))
C5 = (2.*(1.-PR2**2))/(PI*F*E2)
C6 = PR2/(2.*(1.-PR2))
D0 465 I = 1, 100
TD1D(I) = 0.0
TU2D(I) = 0.0
HDD(I) = 0.0
SVD(I) = 0.0
HZPD(I) = 0.0
PVD(I) = 0.0
CDEFLO(I)=0.0
D0 450 K = 1, 5
THC1E(K, I) = 0.0
THC2D(K, I) = 0.0
TWIST1(K) = 0.0
450 TWIST2(K)=0.0

```

```

DO 459 K = 1,5
IF(QD(K,I).LT..0001) GO TO 459
DO 451 K1 = 1,L1
IF(Y1(K1).EQ.YC1D(K,I)) GO TO 454
IF(Y1(K1).LT.YC1D(K,I)) GO TO 455
451 CONTINUE
452 DO 453 K2 = 1,L2
IF(Y2(K2).EQ.YC2D(K,I)) GO TO 456
IF(Y2(K2).LT.YC2D(K,I)) GO TO 457
453 CONTINUE
454 TD1D(I) = QD(K,I)*DCP1(K1)
THC1D(K,I) = THETC1(K1)
GO TO 452
455 YINCRM = (Y1(K1-1)-YC1D(K,I))/(Y1(K1-1)-Y1(K1))
TD1D(I) = QD(K,I)*(DCP1(K1-1) + YINCRM*(DCP1(K1)-DCP1(K1-1)))
THC1D(K,I) = THETC1(K1-1) + YINCRM*(THETC1(K1)-THETC1(K1-1))
GO TO 452
456 TD2D(I) = QD(K,I)*DCP2(K2)
THC2D(K,I) = THETC2(K2)
GO TO 458
457 YINCRM = (Y2(K2-1)-YC2D(K,I))/(Y2(K2-1)-Y2(K2))
TD2D(I) = QD(K,I)*(DCP2(K2-1) + YINCRM*(DCP2(K2)-DCP2(K2-1)))
THC2D(K,I) = THETC2(K2-1) + YINCRM*(THETC2(K2)-THETC2(K2-1))
458 CONTINUE
459 CONTINUE
TWISTP = 0.0
TWISTG = 0.0
DO 460 K = 1,5
IF (QD(3,I).LT.0.0001) GO TO 465
V11 = QD(K,I)*COS(THC1D(K,I))
T1 = V11*(YC1D(K,I) + RR01)
TWIST1(K) = (T1/(4.*PI*F1*G1))*(1./(R11**2)-1./(RR01**2))
TWISTP = TWISTP + TWIST1(K)
V22 = QD(K,I)*COS(THC2D(K,I))
T2 = V22*(-YC2D(K,I) + RR02)
TWIST2(K) = (T2/(4.*PI*F2*G2))*(1./(RR02**2)-1./(R12**2))
TWISTG = TWISTG + TWIST2(K)
460 CONTINUE
THETAQ = ATAN(XC1D(3,I)/(RR01 + YC1D(3,I)))
ARG = ABS(THC1D(3,I) + THETAQ)
TD1D(I) = TD1D(I) + RC1D(3,I)*(TWISTP - TWIST1(3))*COS(ARG)
THETAQ = ATAN(-XC2D(3,I)/(RR02 - YC2D(3,I)))
ARG = ABS(THC2D(3,I) + THETAQ)

```

```

TD2D(1) = TD2D(1) + RC2D(3,1)*(TWISTG - TWIST2(3))*COS(ARG)
TDD(1) = TD1D(1) + TD2D(1)
IF((RCC1D(3,1).EQ.0.0).OR.(RCC2D(3,1).EQ.0.0)) GO TO 463
C1 = (4.*RCC1D(3,1)*RCC2D(3,1))/((PI*F)*(-RCC1D(3,1)+RCC2D(3,1)))
BH = Sqrt(C1*C2*QD(3,1))
H1D = XC1D(3,1)/COS(THC1D(3,1))
H2D = -XC2D(3,1)/COS(THC2D(3,1))
ARG1 = (2.*H1D)/BH
ARG2 = (2.*H2D)/BH
HDD(1) = (C3*(ALOG(ARG1)-C4) + C5*(ALOG(ARG2)-C6))*QD(3,1)
463 CONTINUE
CDEFD(1) = TDD(1) + HDD(1)
DO 11641 K=1,50
VELRAT(2*K-1)=VELR(K)
IF (K.EQ.50) GO TO 11642
VELRAT(2*K)=(VELR(K) + VELR(K+1))/2
11641 CONTINUE
11642 VELRAT(100)=(VELR(50)**2)/VELR(49)
RBCN=RBC1*VELRAT(1)
SLIDV2 = ((RC2D(3,1)**2)-(RBCN**2))
SLIDV1 = ((RC1D(3,1)**2)-(RBC1**2))
IF((SLIDV1.LT.0.0).OR.(SLIDV2.LT.0.0)) GO TO 461
IF((RC1D(3,1).EQ.0.0).OR.(RC2D(3,1).EQ.0.0)) GO TO 461
SLIDV1 = Sqrt((RC1D(3,1)**2)-(RBC1**2))
SLIDV2 = Sqrt((RC2D(3,1)**2)-(RBCN**2))
SVD(1) = (ABS(AVJG2(1)*SLIDV2 - AVJG1(1)*SLIDV1))*5.
461 IF((RCC1D(3,1).EQ.0.0).OR.(RCC2D(3,1).EQ.0.0)) GO TO 462
SRRC = 1./RCC1D(3,1) - 1./RCC2D(3,1)
HZPD(1) = 0.564*Sqrt((QD(3,1)*SRRC)/(F*C2))
462 PVD(1) = HZPD(1)*SVD(1)**.2
465 CONTINUE
DO 470 I = 1,100
C*****METRIC CONVERSION*****
C *****TABLE 7 CONVERSION***
IF (OC.NE.2) GO TO 469
DLOAD(1) = DLOAD(1)*4.448222
YC1D(3,1) = YC1D(3,1)*25.4
YC2D(3,1) = YC2D(3,1)*25.4
SVD(1) = SVD(1)*(0.3048/60.)
HZPD(1) = HZPD(1)*0.006894757
PVD(1) = PVD(1)*(4.448222/0.0254)
*****TABLE 8 CONVERSION***
C QD(3,1) = QD(3,1)*4.448222
TD1D(1) = TD1D(1)*25.4

```

```

T02D(1) = T02D(1)*25.4
HDD(1) = HDD(1)*25.4
CDEFD(1) = CDEFD(1)*25.4
469 CONTINUE
ADJG1(1) = ADJG1(1) + PSIS1
470 ADJG2(1) = ADJG2(1) + PSIS2

```

C

C

```

C TABLE 7 OUTPUT
WRITE(6,500)
WRITE(6,505)
WRITE(6,510)
WRITE(6,520) FORCE(OC)
WRITE(6,530) N1,N1,LENGTH(OC)
WRITE(6,530) N2,N2,LENGTH(OC)
IF(OC.EQ.1) WRITE(6,535)
IF(OC.EQ.2) WRITE(6,536)
WRITE(6,540) PRESS(OC)
WRITE(6,545) FORCE(OC),LEN(OC)
WRITE(6,550)

```

C

```

WRITE(6,560)
COST=180./PI
DO 500 I=1,100
ADJG1(1)=ADJG1(1)*CONST
ADJG2(1)=ADJG2(1)*CONST
562 WRITE(6,565) I,ADJG1(1),ADJG2(1),DLOAD(1),YCID(3,1),
&YC2D(3,1),SVD(1),HZPD(1),PVD(1)

```

C

```

500 FORMAT(1H1,T63,'TABLE 7',///)
505 FORMAT(T26,'THE INFORMATION IN THIS TABLE COMES FROM AN ANALYSIS O
&F THE NUMERICAL INTEGRATION',T26,'SEQUENCE COVERING THE LAST PASSA
&GE OF A TOOTH PAIR THROUGH THE CONTACT ZONE.',T26,'POSITION 1 CORR
&RESPONDS TO THE STARTING POINT OF CONTACT WHILE POSITION 100',T26,'
&'CORRESPONDS TO THE END POINT OF CONTACT. THE FOLLOWING SYMBOLS, A
&RE UTILIZED IN',T26,'THIS TABLE:',///)
510 FORMAT(T28,'PS11 IS THE ANGLE OF ROTATION OF THE DRIVING GEAR; DE
&Grees.',T28,'PS12 IS THE ANGLE OF ROTATION OF THE DRIVEN GEAR; DE
&Grees.',T28,'NCP IS THE NUMBER OF SEPARATE TOOTH PAIRS IN CONTACT
&AT A PARTICULAR POSITION')
520 FORMAT(T28,'DF IS THE TOTAL DYNAMIC FORCE BEING TRANSMITTED ALONG
& THE LINE OF ACTION;',A1)
530 FORMAT(T28,'YC',I1,' IS THE LOCATION OF THE CONTACT POINT ALONG TH
&E TOOTH PROFILE OF GEAR ',I1,',',A3)
535 FORMAT(T28,'SV IS THE SLIDING VELOCITY AT THE CONTACT POINT; FT/

```

```

&MIN.' )
536 FORMAT(T28,'SV IS THE SLIDING VELOCITY AT THE CONTACT POINT; M/
&SEC.' )
540 FORMAT(T28,'A4) IS THE MAXIMUM HERTZ CONTACT PRESSURE AT THE CONTA
&CT POINT;' )
545 FORMAT(T28,'PV IS THE HERTZ PRESSURE-SLIDING VELOCITY PRODUCT; '
&A3,'/(,'A2,'-SEC)')
550 FORMAT(T26,'BOTH PSI1 AND PSI2 ARE MEASURED BETWEEN THE CENTER LIN
&E OF THE CONTACTING TOOTH AND THE LINE OF//T26,'CENTERS. AN ANGLE
&AKEN AS POSITIVE.//T26,'YC1 AND YC2 ARE MEASURED RELATIVE TO THE X
&Y-COORDINATE SYSTEMS DEFINED IN TABLE 1'//)
560 FORMAT(T4,'POSITION',5X,'PSI1',7X,'PSI2',6X,'NCP',7X,'DF',11X,'YC1
&',9X,'YC2',11X,'SV',16X,'H2P',14X,'PV'//)
565 FORMAT(T5,14,2X,2(4X,F7.3),5X,12,5X,F8.2,2(5X,F7.3),3(5X,E12.5))
C
C
C TABLE 8 OUTPUT
WRITE(6,570)
WRITE(6,505)
WRITE(6,575) FORCE(OC)
WRITE(6,580) N1,N1,LENGTH(OC)
WRITE(6,580) N2,N2,LENGTH(OC)
WRITE(6,585) LENGTH(OC)
WRITE(6,590) LENGTH(OC)
WRITE(6,592)
C
WRITE(6,595)
DO 569 I=1,100
569 WRITE(6,598) I,QD(3,I),TD1D(I),TD2D(I),HDD(I),CDEFD(I)
C
570 FORMAT(1H1,T63,'TABLE 8'//)
575 FORMAT(T36,'LOAD IS THE FORCE IN ',A4,' ACTING BETWEEN THE CONTACT
&ING TOOTH PAIR.//T38,'(THE LOAD IS DIRECTED NORMAL TO THE TOOTH PR
&OF FILE.)')
580 FORMAT(T36,'TD',11,' IS THE TOOTH DEFLECTION ON GEAR ',11,'; ',
&A3)
585 FORMAT(T36,'HD IS THE HERTZIAN DEFLECTION OF THE CONTACT POINT;
&',A3)
590 FORMAT(T36,'CD IS THE COMBINED DEFLECTION OF THE CONTACT POINT;
&',A3)
592 FORMAT(T38,'(ALL DEFLECTIONS ARE MEASURED ALONG THE LINE OF ACTION
&)' )
595 FORMAT(//T11,'POSITION',14X,'LOAD',17X,'TD1',17X,'TD2',18X,'HD',
&18X,'CD'//)

```

598 FORMAT(T12, I4, 14X, F8.2, 2X, 4(10X, F10.7))

C
C
C

TABLE 9 OUTPUT

```
WRITE(6, 5900)
WRITE(6, 505)
WRITE(6, 5901) FORCE(OC)
WRITE(6, 520) FORCE(OC)
WRITE(6, 5902)
WRITE(6, 5903) FORCE(OC), FORCE(OC)
WRITE(6, 5904)
P = TIN/DRBC1
IF (OC.EQ.2) P=P*4.448222
DO 59000 I=1,100
DF1(I) = DLOAD(I)/P
IF (STATLD(I).NE.0.0)GOTO 801
DF2(I)=0.0
```

GEA00070
GEA00080
GEA00090

GOTO 802

801 IF (OC.EQ.2) STATLD(I)=STATLD(I)*4.448222

DF2(I)=QD(3,I)/STATLD(I)

DO 700 K=1,50

QDD(K) =QD(3,2*K-1)

700 CONTINUE

C WRITE (9, 710) (QDD(K), YC1(3, K), YC2(3, K), K=1, 50)

C10 FORMAT(3E14.7)

C

802 CONTINUE

WRITE(6, 5905) I, P, DLOAD(I), DF1(I), STATLD(I), QD(3, I), DF2(I)

5900 CONTINUE

5900 FORMAT(IH1, T63, 'TABLE 9'//)

5901 FORMAT(T28, 'SF IS THE NOMINAL TRANSMITTED FORCE ALONG THE LINE OF
&ACTION; ,A4)

5902 FORMAT(T28, 'DF1 IS THE DYNAMIC LOAD FACTOR FOR THE GEAR PAIR, ADJA
&CENT SHAFTS AND BEARINGS')

5903 FORMAT(T28, 'SL IS THE FORCE IN ,A4, ' ACTING BETWEEN THE CONTACT IN
&G TOOTH PAIR FROM THE STATIC ANALYSIS'/T28, 'DL IS THE FORCE IN ,

&A4, ' ACTING BETWEEN THE CONTACTING TOOTH PAIR FROM THE DYNAMIC ANA
&LYSIS'/T28, 'DF2 IS THE DYNAMIC FACTOR FOR AN INDIVIDUAL GEAR TOOTH

& PAIR TRAVERSING THE MESH ARC'//

5904 FORMAT(//T24, 'POSITION', 12X, 'SF', 10X, 'DF', 10X, 'DF1', 14X, 'SL', 10X,
&'DL', 10X, 'DF2'//)

5905 FORMAT(' ', 24X, 13, 12X, 2(F7.2, 4X, F8.2, 5X, F7.2, 10X))

C

5906 CONTINUE

C

GEA00110

```

RETURN
END

SUBROUTINE VIBS(A,B,X,EIGV)
IMPLICIT REAL*8(A-H,O-Z)
ABS(X) = DABS(X)
SQRT(X) = DSQRT(X)
DIMENSION A(4,4),B(4,4),X(4,4),EIGV(4),D(4)
N = 4
NSMAX = 15
RTOL = +10.D-12
AAVG = 0.0
BAVG = 0.0
DO 2 I = 1,N
  AAVG = AAVG + A(I,I)
  BAVG = BAVG + B(I,I)
  AAVG = AAVG/N
  BAVG = BAVG/N
ROH = -(AAVG/BAVG)
DO 5 I = 1,N
DO 5 J = 1,N
  5 A(I,J) = A(I,J) - ROH*B(I,J)
DO 10 I = 1,N
  D(I) = A(I,I)/B(I,I)
DO 30 I = 1,N
DO 20 J = 1,N
  20 X(I,J) = 0.
  30 X(I,I) = 1.
  NSWEEP = 0
  NR = N - 1
  40 NSWEEP = NSWEEP + 1
  EPS = (.01**NSWEEP)**2
  DO 210 J = 1, NR
  JJ = J + 1
  DO 210 K = JJ, N
    EPTOLA = (A(J,K)*A(J,K))/(A(J,J)*A(K,K))
    EPTOLB = (B(J,K)*B(J,K))/(B(J,J)*B(K,K))
    IF((EPTOLA.LT.EPS).AND.(EPTOLB.LT.EPS)) GO TO 210
    AKK = A(K,K)*B(J,K) - B(K,K)*A(J,K)
    AJJ = A(J,J)*B(J,K) - B(J,J)*A(J,K)
    AB = A(J,J)*B(K,K) - A(K,K)*B(J,J)
    CHECK = (AB*AB + 4.*AKK*AJJ)/4.
  60 SQCH = SQRT(CHECK)

```

C C

```

D1 = AB/2. + SQCH
D2 = AB/2. - SQCH
DEN = D1
IF(ABS(D2).GT.ABS(D1)) DEN = D2
IF(DEN) 80, 70, 80
70 CA = 0.
CG = -A(J,K)/A(K,K)
GO TO 90
80 CA = AKK/DEN
CG = -AJJ/DEN
90 IF(N-2) 100, 190, 100
100 JP1 = J + 1
JM1 = J - 1
KP1 = K + 1
KM1 = K - 1
IF(JM1 - 1) 130, 110, 110
110 DO 120 I = 1, JM1
AJ = A(I, J)
BJ = B(I, J)
AK = A(I, K)
BK = B(I, K)
A(I, J) = AJ + CG*AK
B(I, J) = BJ + CG*BK
A(I, K) = AK + CA*AJ
B(I, K) = BK + CA*BJ
120 IF(KP1-N) 140, 140, 160
130 DO 150 I = KP1, N
AJ = A(J, I)
BJ = B(J, I)
AK = A(K, I)
BK = B(K, I)
A(J, I) = AJ + CG*AK
B(J, I) = BJ + CG*BK
A(K, I) = AK + CA*AJ
B(K, I) = BK + CA*BJ
150 IF(JP1 - KM1) 170, 170, 190
160 DO 180 I = JP1, KM1
AJ = A(J, I)
BJ = B(J, I)
AK = A(I, K)
BK = B(I, K)
A(J, I) = AJ + CG*AK
B(J, I) = BJ + CG*BK
A(I, K) = AK + CA*AJ
B(I, K) = BK + CA*BJ
180

```



```

190 AK = A(K,K)
    BK = B(K,K)
    A(K,K) = AK + 2.*CA*A(J,K) + CA*CA*A(J,J)
    B(K,K) = BK + 2.*CA*B(J,K) + CA*CA*B(J,J)
    A(J,J) = A(J,J) + 2.*CG*A(J,K) + CG*CG*AK
    B(J,J) = B(J,J) + 2.*CG*B(J,K) + CG*CG*BK
    A(J,K) = 0.
    B(J,K) = 0.
DO 200 I = 1, N
  XJ = X(I,J)
  XK = X(I,K)
  X(I,J) = XJ + CG*XK
200 X(I,K) = XK + CA*XJ
210 CONTINUE
C
DO 220 I = 1, N
  EIGV(I) = A(I,I)/B(I,I)
220 DO 240 I = 1, N
  TOL = RTOL*D(I)
  DIF = ABS(EIGV(I) - D(I))
  IF(DIF.GT.TOL) GO TO 280
240 CONTINUE
  EPS = RTOL**2
  DO 250 J = 1, NR
  JJ = J + 1
  DO 250 K = JJ, N
    EPSA = (A(J,K)*A(J,K))/(A(J,J)*A(K,K))
    EPSB = (B(J,K)*B(J,K))/(B(J,J)*B(K,K))
    IF((EPSA.LT.EPS).AND.(EPSB.LT.EPS)) GO TO 250
  GO TO 280
250 CONTINUE
255 DO 260 I = 1, N
  DO 260 J = 1, N
    A(J,I) = A(I,J)
260 B(J,I) = B(I,J)
  DO 270 J = 1, N
  BB = SQRT(B(J,J))
  DO 270 K = 1, N
    X(K,J) = X(K,J)/BB
270 DO 272 I = 1, N
  EIGV(I) = EIGV(I) + ROH
272 DO 275 J = 1, N
  DO 274 I = 1, N
  IBW = N - I + 1
  X(IBW,J) = X(IBW,J)/X(1,J)

```

```

IF(ABS(X(IBM,J)).LT.0.0001) X(IBM,J) = 0.0
274 CONTINUE
275 CONTINUE
IH = N - 1
DO 279 I = 1, IH
  JL = I + 1
  DO 278 J = JL, N
    IF(EIGV(I).LE.EIGV(J)) GO TO 278
    TEMP = EIGV(I)
    EIGV(I) = EIGV(J)
    EIGV(J) = TEMP
  DO 277 K = 1, N
    XTEMP = X(K,I)
    X(K,I) = X(K,J)
    X(K,J) = XTEMP
  277 CONTINUE
278 CONTINUE
279 CONTINUE
DO 276 I = 1, N
  IF(ABS(EIGV(I)).LT.0.001) EIGV(I) = 0.0
276 CONTINUE
  RETURN

```

C

```

280 DO 290 I = 1, N
290 D(I) = EIGV(I)
  IF(NSWEEP.LT.NSMAX) GO TO 40
  GO TO 255
END

```

C

```

SUBROUTINE RKUTTA(T,DT)
COMMON/C13/XI(8),DXI(8),NE,NP,NRK,IP,LPP,ISTORE,JEP,NCI
DOUBLE PRECISION XI,DXI,T,DT
NE = 0
NP = NP + 1
NRK = 0
IF(NP.EQ.5) NP = 1
IF(NP.EQ.1) GO TO 1
IF(NP.EQ.2) RETURN
IF(NP.EQ.3) GO TO 2
IF(NP.EQ.4) NRK = 1
RETURN
1 DT = DT/2.
  T = T + DT
  RETURN
2 T = T + DT

```

```
DT = 2.*DT
RETURN
END
```

C C

```
SUBROUTINE MORERK(X,DX,DT)
COMMON/C13/XI(8),DXI(8),NE,NP,MRK,IP,LPP,ISTORE,JEP,NCT
DOUBLE PRECISION X,DX,XI,DXI,T,DT
NE = NE + 1
GO TO (1,2,3,4),NP
1 XI(NE) = X
DXI(NE) = DX
X = X + DX*DT
RETURN
2 DXI(NE) = DXI(NE) + 2.*DX
X = XI(NE) + DX*DT
RETURN
3 DXI(NE) = DXI(NE) + 2.*DX
X = XI(NE) + DX*DT
RETURN
4 DXI(NE) = (DXI(NE) + DX)/6.
X = XI(NE) + DXI(NE)*DT
RETURN
END
```

C C

```
SUBROUTINE STORE(T,DT,PRI,PT,TSP,TEP,X2,X3,NC)
COMMON/C1/PHI,PHID,DP,M,TG1,TG2,TP,DELTP
COMMON/C4/TIN,TOUT,RPMIN,RPMOUT,OMEGA1,OMEGA2
COMMON/C5/JG1,JG2,JD,JL,KDS,KLS,KGPAVG,ZETAS,ZETAG,CDS,CLS,CGPAVG,
1LDS,LLS,IPLOT,CBD,CB1,CB2,CBL
COMMON/C6/L1,L2,PD1,PD2,RPC1,RPC2,RAC1,RAC2,RBC1,RBC2,RR1,RR2,
&RF1,RF2,C,CP,BP,UCUT1,UCUT2
COMMON/C13/XI(8),DXI(8),NE,NP,MRK,IP,LPP,ISTORE,JEP,NCT
DIMENSION XT(3,400)
REAL M,JD,JG1,JG2,JL,KDS,KGPAVG,KLS,LDS,LLS
DOUBLE PRECISION XI,DXI
IF(T.LT.TSP) RETURN
IF(IPLOT.EQ.2) GO TO 1
IF(NC.GT.NCT) LPP = 1
IF(LPP.EQ.1) GO TO 4
1 IF((T.GT.(TEP+DT/2.)).AND.(LPP.EQ.1)) RETURN
IF(T.GT.(PT-DT/2.)) GO TO 2
RETURN
2 IP = IP + 1
```

```

XT(1,IP) = PT
XT(2,IP) = X2
XT(3,IP) = X3
PT = PT + PRI
IF (IP.EQ.400) CALL XTPLOT(XT, ILP, NXTP)
IF (T.GT.(TEP-PR)/2.) LPP = 1
4 IF (LPP.EQ.1) ILP = IP
  IF (LPP.EQ.1) CALL XTPLOT(XT, ILP, NXTP)
RETURN
END

SUBROUTINE XTPLOT(XT, ILP, N)
COMMON/CI/PHI, PHID, DP, M, IC1, IC2, TP, DELTP
COMMON/C4/TIN, TOUT, RPMIN, RPMOUT, OMEGA1, OMEGA2
COMMON/C5/JG1, JG2, JD, JL, KDS, KLS, KGPAVG, ZETAS, ZETAG, CDS, CLS, CGPAVG,
1LDS, LLS, IPLOT, CBD, CB1, CB2, CBL
COMMON/C6/L1, L2, PD1, PD2, RPC1, RPC2, RAC1, RAC2, RBC1, RBC2, RRC1, RRC2,
&RF1, RF2, C, CP, BP, UCUT1, UCUT2
COMMON/C13/XI(8), DXI(8), NE, NP, NRK, IP, LPP, ISTORE, JEP, NCT
DIMENSION LINEK(41), LINEF(41), XLK(5), XLF(5), XT(3,400)
DATA JLL/1H*/ , JN, JP, JI, JBLANK, JZ/1H-, 1H+, 1H1, 1H , 1HS/
REAL M, JD, JG1, JG2, JL, KDS, KGPAVG, KLS, LDS, LLS
DOUBLE PRECISION XI, DXI
IF (LPP.EQ.1) AND. (ILP.EQ.0) GO TO 134
IF (LPP.EQ.0) ILP = 400
IF (ISTORE.NE.0) GO TO 36
WRITE(6,1)
1 FORMAT(///)
DO 15 I = 1, 41
LINEK(I) = JBLANK
15 LINEF(I) = JBLANK
N = 0
SFORCE = TIN/RBC1
IF (UNITS.EQ.2) SFORCE = SFORCE*4.448222
XTKMAX = XT(2,1)
XTKMIN = XT(2,1)
XTFMAX = XT(3,1)/SFORCE
XTFMIN = 0.0
DO 16 J = 2, ILP
IF (XTKMAX.LT.XT(2,J)) XTKMAX = XT(2,J)
IF (XTKMIN.GT.XT(2,J)) XTKMIN = XT(2,J)
IF (XTFMAX.LT.(XT(3,J)/SFORCE)) XTFMAX = XT(3,J)/SFORCE
16 CONTINUE
XTKMIN = .95*XTKMIN

```

C C

```

XTKMAX = 1.05*XTKMAX
XTFMAX = 1.25*XTFMAX
RK = XTKMAX - XTKMIN
DELTAK = RK/4.
RF = XTFMAX - XTFMIN
DELTAF = RF/4.
XLK(1) = XTKMIN
XLF(1) = XTFMIN
DO 17 I = 2,5
  XLK(I) = XLK(I-1) + DELTAK
  XLF(I) = XLF(I-1) + DELTAF
17 WRITE(6,30)
30 FORMAT(4X,'TIME',16X,'GEAR STIFFNESS',21X,'KG',20X,'NORMALIZED DYN
1AMIC FORCE',16X,'DF')
WRITE(6,32) (XLK(I), I = 1,5), (XLF(I), I = 1,5)
32 FORMAT(6X,5(E10.3),15X,5(F5.2,5X))
GO TO 45
36 N = ISTORE*400
GO TO 45
40 IF(N/10-(N-1)/10) 55,55,45
45 ND = 0
DO 50 I = 1,4
  ND = ND + 1
LINEK(ND) = JP
LINEF(ND) = JP
DO 50 J = 1,9
  ND = ND + 1
LINEK(ND) = JN
LINEF(ND) = JN
LINEK(41) = JP
LINEF(41) = JP
GO TO 65
55 DO 60 I = 1,41,10
  LINEK(I) = JI
60 LINEF(I) = JI
65 IF(ISTORE.EQ.0) N1 = N + 1
  IF(ISTORE.NE.0) N1 = N - (ISTORE*400) + 1
DO 90 I = 2,3
  IF(1.EQ.2) JA = IFIX(40.*(XT(2,N1)-XTKMIN)/RK)+1.5)
  IF(1.EQ.3) JA = IFIX(40.*(XT(3,N1)/(SFORCE*XTFMAX))+1.5)
  IF(JA-41) 70,85,75
70 IF(JA) 80,80,85
75 IF(1.EQ.2) LINEK(41) = JZ
  IF(1.EQ.3) LINEF(41) = JZ
GO TO 90

```

```

80 IF(I.EQ.2) LINEK(1) = JZ
   IF(I.EQ.3) LINEF(1) = JZ
   GO TO 90
85 IF(I.EQ.2) LINEK(JA) = JLL
   IF(I.EQ.3) LINEF(JA) = JLL
90 CONTINUE
   IF(N.EQ.0) GO TO 95
   IF(N/10-(N-1)/10) 105, 105, 95
95 WRITE(6,100) XT(1,N1),LINEK,XT(2,N1),LINEF,XT(3,N1)
100 FORMAT(3X,F8.5,41A1,1X,1PE12.5,8X,41A1,1X,1PE12.5)
   GO TO 115
105 WRITE(6,110) LINEK,XT(2,N1),LINEF,XT(3,N1)
110 FORMAT(11X,41A1,1X,1PE12.5,8X,41A1,1X,1PE12.5)
115 DO 120 I = 1,41
   LINEK(I) = JBLANK
120 LINEF(I) = JBLANK
125 N = N + 1
127 IF(N1-ILP) 40,130,130
130 IP = 0
   ILP = 0
   ISTORE = ISTORE + 1
   DO 132 I = 1,3
   DO 132 J = 1,400
132 XT(I,J)=0.0
   IF(LPP.EQ.0) RETURN
134 RN = FLOAT(N)
   NTENS = IFIX(RN/10.)
   TENS = FLOAT(NTENS)
   REM = RN - 9.99999*TENS
   IREM = IFIX(REM)
   IF(IREM.EQ.0) GO TO 145
   IF(IREM.EQ.1) GO TO 165
   IREM1 = 10 - IREM
   DO 135 I = 1,41,10
   LINEK(I) = JI
135 LINEF(I)=JI
   DO 140 I = 1,IREM1
140 WRITE(6,141) LINEK,LINEF
141 FORMAT(11X,41A1,21X,41A1)
145 DO 150 I = 1,41
   LINEK(I) = JN
150 LINEF(I)=JN
   DO 155 I = 1,41,10
   LINEK(I) = JP
155 LINEF(I)=JP

```

```
WRITE(6,141) LINEK,LINEF
DO 165 I = 1,41
LINEK(I) = JBLANK
165 LINEF(I)=JBLANK
RETURN
END
//GO. SYSIN DD *
&CONTRL INPUT='ENGL', OUTPUT='ENGL', IPLOT=2, NTYPE=2, MODF='NO' &END
&PHYPAR E=2*30.E6, PR=2*0.285, GAMA=2*0.288, JG=0.0188, 2.3000, TAPE='YES'
&END
&GEHPAR DP=8, DELTP=0.01, TIN=1936.3, RPMIN=8000., ZETAS=.005, ZETAG=.05,
PHID=14.5, CBD=0., CB1=0., CB2=0., CBL=0., JD=0.93, JL=0.93760 &END
&GEOPAR TG=32, 96, AD=2*0.125, WD=2*0.269625, GR=2*0.021625,
FW=2*1.0 &END
```

14.5 DEGREE PRESSURE ANGLE
 STATIC AND DYNAMIC ANALYSIS OF A GEAR PAIR SYSTEM

DIAMETRAL PITCH IS 8.000
 INPUT TORQUE IS 1936.30 IN-LBF
 OUTPUT TORQUE IS 5808.90 IN-LBF
 INPUT SPEED IS 8000.00 RPM.
 OUTPUT SPEED IS 2666.67 RPM.

DATA FOR GEAR 1 (DRIVING GEAR)		*	DATA FOR GEAR 2 (DRIVEN GEAR)	
*****			*****	
NUMBER OF TEETH	= 32.	*	NUMBER OF TEETH	= 96.
PITCH DIAMETER	= 4.0000 IN.	*	PITCH DIAMETER	= 12.0000 IN.
ADDENDUM CIRCLE RADIUS	= 2.1250 IN.	*	ADDENDUM CIRCLE RADIUS	= 5.8750 IN.
BASE CIRCLE RADIUS	= 1.9363 IN.	*	BASE CIRCLE RADIUS	= 5.8089 IN.
ROOT CIRCLE RADIUS	= 1.8554 IN.	*	ROOT CIRCLE RADIUS	= 6.1446 IN.
FILLET RADIUS	= 0.0201 IN.	*	FILLET RADIUS	= 0.0169 IN.
INSIDE RADIUS OF HUB	= 0.4977 IN.	*	INSIDE RADIUS OF HUB	= 8.0000 IN.
FACE WIDTH	= 1.0000 IN.	*	FACE WIDTH	= 1.0000 IN.
YOUNG'S MODULUS	= 30.0E+06 PSI	*	YOUNG'S MODULUS	= 30.0E+06 PSI
SPECIFIC WEIGHT	= 0.288 LBI	*	SPECIFIC WEIGHT	= 0.288 LBI
POISSON'S RATIO	= 0.2850	*	POISSON'S RATIO	= 0.2850
			DYNAMIC ANALYSIS	

THE SYSTEM USED IN THE DYNAMIC ANALYSIS IS PICTURED BELOW.

JG1 IS THE MASS MOMENT OF INERTIA OF THE DRIVING GEAR (GEAR 1)
 JG2 IS THE MASS MOMENT OF INERTIA OF THE DRIVEN GEAR (GEAR 2)
 JL IS THE MASS MOMENT OF INERTIA OF THE LOAD
 KDS IS THE TORSIONAL SPRING STIFFNESS OF THE DRIVING SHAFT
 KG IS THE LINEAR SPRING STIFFNESS OF THE GEAR PAIR
 KLS IS THE TORSIONAL SPRING STIFFNESS OF THE LOAD SHAFT
 CDS IS THE TORSIONAL DAMPENING COEFFICIENT OF THE DRIVING SHAFT
 CG IS THE LINEAR DAMPENING COEFFICIENT OF THE LOAD SHAFT.

THE SYSTEM PARAMETERS HAVE THE FOLLOWING SPECIFICATIONS:

JD = 0.9376 (IN-LBF-(SEC**2))/RADIAN
 JG1 = 0.0188 (IN-LBF-(SEC**2))/RADIAN
 JG2 = 2.3000 (IN-LBF-(SEC**2))/RADIAN
 JL = 0.9376 (IN-LBF-(SEC**2))/RADIAN
 KDS = 902413.0 (IN-LBF)/RADIAN
 KLS = 902413.0 (IN-LBF)/RADIAN
 CDS = 1.290 (IN-LBF-SEC)/RADIAN
 CLS = 7.753 (IN-LBF-SEC)/RADIAN

KG AND CG ARE TABULATED IN TABLE 2 OF THE STATIC ANALYSIS SECTION.
 CDS AND CLS WERE CALCULATED USING THE VALUE ZETAS QUOTED ABOVE.
 CG WAS CALCULATED USING THE VALUE ZETAG QUOTED ABOVE.
 TABLE 5

SYSTEM VIBRATION DATA

THE INFORMATION LISTED BELOW REPRESENTS THE SYSTEM NATURAL FREQUENCIES AND THE CORRESPONDING EIGENVECTORS. THIS INFORMATION IS OBTAINED FROM THE "VIBS" SUBROUTINE WHICH SOLVES THE GENERAL EIGENPROBLEM USING A JACOBI ITERATION TECHNIQUE. NOTE THAT THE FIRST MODE IS A RIGID BODY MODE AND NOTE THE EFFECT OF THE GEAR RATIO ON THE EIGENVECTORS. IN COMPUTING THIS VIBRATION DATA AN AVERAGE VALUE FOR THE GEAR STIFFNESS EQUAL TO 3318517.0 LBF/IN WAS USED.

NATURAL FREQUENCIES (CYCLES/SEC)	EIGENVECTORS			
	JD	JG1	JG2	JL
1ST MODE	1.0000	1.0000	0.3333	0.3333
2ND MODE	1.0000	0.0073	-0.0216	-2.9475
3RD MODE	1.0000	-3.5448	-1.2837	0.3621
4TH MODE	1.0000	-783.9355	18.0099	-0.0230

TABLE 6

NUMERICAL INTEGRATION OF THE DIFFERENTIAL EQUATIONS OF MOTION

THE DIFFERENTIAL EQUATIONS OF MOTION OF THE SYSTEM WERE INTEGRATED NUMERICALLY USING A 4TH ORDER RUNGE-KUTTA INTEGRATION SCHEME. THE INITIAL CONDITIONS IMPLEMENTED FOR THE INTEGRATION ARE:

A. INITIAL ANGULAR VELOCITIES

THE INITIAL VELOCITY OF JD IS 8000.00 RPM
 THE INITIAL VELOCITY OF JG1 IS 8000.00 RPM
 THE INITIAL VELOCITY OF JG2 IS 2666.67 RPM
 THE INITIAL VELOCITY OF JL IS 2666.67 RPM

B. INITIAL ANGULAR DISPLACEMENTS

THE INITIAL DISPLACEMENTS ARE DUE TO A TORQUE PRELOAD OF 1936.30 IN-LBS ON THE INPUT SHAFT AND 5808.90 IN-LBS ON THE OUTPUT SHAFT. THIS TORQUE PRELOAD IS EQUAL TO THE NOMINAL STATIC TORQUE CARRIED BY THE SYSTEM. THIS RESULTS IN THE FOLLOWING INITIAL ANGLES OF TWIST OR WIND-UP:

THE INITIAL DISPLACEMENT OF JD IS 0.00215 RADIANS
 THE INITIAL DISPLACEMENT OF JG1 IS 0.0 RADIANS
 THE INITIAL DISPLACEMENT OF JG2 IS -0.00005 RADIANS
 THE INITIAL DISPLACEMENT OF JL IS -0.00649 RADIANS

THE NUMERICAL INTEGRATION WAS CARRIED OUT FOR A LENGTH OF TIME EQUIVALENT TO 140 CYCLES THE TIME REQUIRED FOR THE START-UP TRANSIENT TO DECAY (THIS TIME IS ASSUMED TO BE EQUALING TO 5 TIMES THE LONGEST SYSTEM NATURAL PERIOD) TO THE TIME REQUIRED FOR ONE ADDITIONAL TOOTH PASSAGE CYCLE. THE DATA TABULATED IN TABLES 7 AND 8 BELOW COMES FROM THIS LAST

TOOTH PASSAGE CYCLE. THE ASSUMPTION BEING THAT THIS REPRESENTS A STEADY-STATE SITUATION. THE INTEGRATION TIME STEP USED IS 0.0000229 SECONDS. THIS REPRESENTS EITHER ONE TENTH OF THE SHORTEST SYSTEM NATURAL PERIOD OR A CERTAIN PERCENTAGE OF THE PERIOD OF THE STIFFNESS FUNCTION, WHICHEVER IS SMALLEST.

RT1, RT2 = 1.0000 0.8000

```
*****
*
* XT PLOT OF THE RESULTS OF
* THE NUMERICAL INTEGRATION
*
*****
```

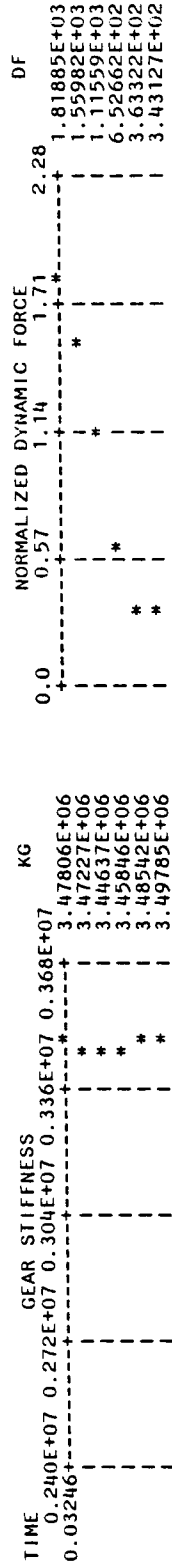
THE DATA DEPICTED IN THE FOLLOWING X VERSUS T PLOTS ARE OBTAINED BY NUMERICALLY INTEGRATING THE DIFFERENTIAL EQUATIONS OF MOTION. IN THESE PLOTS:

TIME IS THE INTEGRATION TIME; SECONDS
 KG IS THE GEAR STIFFNESS; LBF/IN
 DF IS THE DYNAMIC FORCE; LBF

THE DYNAMIC FORCE PLOT DISPLAYS A NORMALIZED DYNAMIC FORCE, I.E. THE DYNAMIC FORCE DIVIDED BY THE NOMINAL TRANSMITTED FORCE.

THIS PLOT REPRESENTS ONLY THAT TIME PERIOD IN THE NUMERICAL INTEGRATION SEQUENCE COVERING THE LAST PASSAGE OF A TOOTH PAIR THRU THE CONTACT ZONE. IT IS ASSUMED THAT THE SYSTEM IS OPERATING IN A STEADY STATE CONDITION DURING THIS PERIOD.

INPUT SPEED IS 8000.00 RPM BACKLASH IS 0.010000 IN.



2	-21.170	-5.185	3	1787.17	0.087	0.17150E+04	0.13167E+06	0.45162E+18
3	-20.848	-5.078	3	1800.28	0.086	0.16878E+04	0.13995E+06	0.47243E+18
4	-20.527	-4.971	3	1813.40	0.087	0.16553E+04	0.13047E+06	0.43192E+18
5	-20.205	-4.863	3	1774.40	0.089	0.16293E+04	0.12291E+06	0.40050E+18
6	-19.884	-4.756	3	1698.37	0.089	0.15919E+04	0.11985E+06	0.38303E+18
7	-19.562	-4.649	3	1622.34	0.089	0.15686E+04	0.11789E+06	0.36983E+18
8	-19.241	-4.541	3	1536.65	0.090	0.15387E+04	0.10984E+06	0.33804E+18
9	-18.919	-4.434	3	1406.05	0.091	0.15096E+04	0.10232E+06	0.30892E+18
10	-18.598	-4.326	3	1275.44	0.090	0.14729E+04	0.10086E+06	0.29712E+18
11	-18.276	-4.219	3	1144.84	0.089	0.14449E+04	0.10031E+06	0.28989E+18
12	-17.955	-4.111	3	1009.91	0.090	0.13952E+04	0.81744E+05	0.25777E+18
13	-17.633	-4.003	3	873.68	0.091	0.13615E+04	0.72461E+05	0.19731E+18
14	-17.312	-3.896	3	737.52	0.092	0.13310E+04	0.65096E+05	0.17328E+18
15	-16.990	-3.788	3	620.60	0.094	0.12965E+04	0.60032E+05	0.15566E+18
16	-16.669	-3.681	3	535.62	0.094	0.12669E+04	0.55160E+05	0.13977E+18
17	-16.347	-3.573	3	450.63	0.095	0.12408E+04	0.48460E+05	0.12026E+18
18	-16.026	-3.466	3	365.63	0.097	0.12103E+04	0.46977E+05	0.11371E+18
19	-15.704	-3.359	3	357.56	0.097	0.11733E+04	0.46286E+05	0.10861E+18
20	-15.382	-3.251	3	351.64	0.097	0.11427E+04	0.46038E+05	0.10522E+18
21	-15.061	-3.144	3	345.71	0.098	0.11184E+04	0.47370E+05	0.10596E+18
22	-14.739	-3.037	3	381.21	0.099	0.10879E+04	0.50591E+05	0.11008E+18
23	-14.418	-2.930	3	448.81	0.101	0.10559E+04	0.53081E+05	0.11210E+18
24	-14.096	-2.823	3	516.46	0.102	0.10252E+04	0.55808E+05	0.11443E+18
25	-13.775	-2.716	3	586.70	0.104	0.99376E+03	0.58587E+05	0.11644E+18
26	-13.453	-2.609	3	672.41	0.105	0.96331E+03	0.61552E+05	0.11859E+18
27	-13.132	-2.502	3	758.13	0.106	0.93192E+03	0.63805E+05	0.11892E+18
28	-12.810	-2.395	3	843.85	0.108	0.90158E+03	0.65370E+05	0.11787E+18
29	-12.489	-2.289	3	903.66	0.109	0.87048E+03	0.77711E+05	0.13529E+18
30	-12.167	-2.182	2	953.69	0.110	0.84011E+03	0.81176E+05	0.13138E+18
31	-11.846	-2.075	2	1003.68	0.112	0.80923E+03	0.81176E+05	0.13138E+18
32	-11.524	-1.968	2	1091.35	0.113	0.77934E+03	0.86901E+05	0.13545E+18
33	-11.203	-1.861	2	1266.25	0.115	0.75470E+03	0.90784E+05	0.13703E+18
34	-10.881	-1.754	2	1441.26	0.118	0.72391E+03	0.94577E+05	0.13693E+18
35	-10.560	-1.648	2	1616.26	0.118	0.69392E+03	0.95068E+05	0.17795E+18
36	-10.238	-1.541	3	1685.74	0.120	0.66392E+03	0.95068E+05	0.18471E+18
37	-9.917	-1.434	3	1740.52	0.121	0.63392E+03	0.81584E+05	0.17041E+18
38	-9.595	-1.327	3	1795.30	0.123	0.60392E+03	0.81584E+05	0.15500E+18
39	-9.273	-1.220	3	1806.01	0.124	0.57392E+03	0.81834E+05	0.15276E+18
40	-8.952	-1.112	3	1764.89	0.125	0.54392E+03	0.80011E+05	0.15006E+18
41	-8.630	-1.005	3	1723.76	0.127	0.51392E+03	0.78034E+05	0.13879E+18
42	-8.309	-0.898	3	1679.27	0.128	0.48392E+03	0.76212E+05	0.12605E+18
43	-7.987	-0.790	3	1570.08	0.130	0.45392E+03	0.69727E+05	0.11724E+18
44	-7.666	-0.683	3	1460.82	0.132	0.42392E+03	0.66099E+05	0.10763E+18
45	-7.344	-0.575	3	1351.63	0.135	0.39392E+03	0.61655E+05	0.86877E+07
46	-7.023	-0.467	3	1214.78	0.137	0.36392E+03	0.57092E+05	0.67826E+07
47	-6.701	-0.360	3	1062.93	0.140	0.33392E+03	0.52240E+05	0.60948E+07
48	-6.380	-0.252	3	911.16	0.142	0.30392E+03	0.47599E+05	0.55282E+07
49	-6.058	-0.145	3	770.13	0.144	0.27392E+03	0.43510E+05	0.47868E+07
50	-5.737	-0.037	3	662.13	0.146	0.24392E+03	0.39015E+05	0.39347E+07
51	-5.415	0.070	3	554.13	0.150	0.21392E+03	0.34456E+05	0.30089E+07
52	-5.094	0.178	3	446.13	0.154	0.18392E+03	0.32085E+05	0.24204E+07
53	-4.772	0.285	3	398.97	0.134	0.15392E+03	0.30228E+05	0.21030E+07
54	-4.451	0.393	3	362.96	0.131	0.12392E+03	0.30228E+05	0.21030E+07

55	-4.129	0.500	326.95	0.162	0.128	0.31893E+03	0.28258E+05	0.18025E+07
56	-3.808	0.607	324.21	0.165	0.125	0.25914E+03	0.27813E+05	0.14415E+07
57	-3.486	0.714	364.17	0.168	0.122	0.15964E+03	0.28997E+05	0.11578E+07
58	-3.164	0.821	404.12	0.171	0.120	0.17028E+03	0.30208E+05	0.10288E+07
59	-2.843	0.928	445.50	0.173	0.117	0.14119E+03	0.31209E+05	0.88126E+06
60	-2.521	1.035	548.96	0.176	0.114	0.11077E+03	0.34277E+05	0.75938E+06
61	-2.200	1.142	652.42	0.179	0.111	0.80647E+02	0.36780E+05	0.59323E+06
62	-1.878	1.249	755.88	0.182	0.108	0.44232E+02	0.39136E+05	0.34621E+06
63	-1.557	1.356	816.55	0.186	0.104	0.11414E+01	0.39894E+05	0.91067E+04
64	-1.235	1.463	849.00	0.190	0.100	0.42328E+02	0.47235E+05	0.39987E+06
65	-0.914	1.570	881.43	0.195	0.096	0.85166E+02	0.47080E+05	0.80192E+06
66	-0.592	1.676	924.53	0.198	0.093	0.12432E+03	0.47679E+05	0.11855E+07
67	-0.271	1.783	1016.41	0.201	0.090	0.15513E+03	0.49165E+05	0.15254E+07
68	0.051	1.890	1108.35	0.204	0.088	0.18660E+03	0.50888E+05	0.18991E+07
69	0.372	1.997	1200.24	0.207	0.086	0.21786E+03	0.52163E+05	0.22729E+07
70	0.694	2.104	1350.05	0.209	0.083	0.28441E+02	0.54849E+05	0.31199E+06
71	1.015	2.211	1518.44	0.212	0.081	0.14419E+03	0.48872E+05	0.14094E+07
72	1.337	2.318	1686.93	0.216	0.078	0.50671E+02	0.51007E+05	0.51692E+06
73	1.658	2.425	1796.91	0.221	0.073	0.58827E+02	0.50960E+05	0.59957E+06
74	1.980	2.532	1790.75	0.226	0.068	0.73461E+02	0.50290E+05	0.73886E+06
75	2.301	2.639	1784.60	0.229	0.066	0.72448E+02	0.49454E+05	0.71656E+06
76	2.623	2.746	1778.44	0.232	0.064	0.12453E+03	0.48959E+05	0.12194E+07
77	2.945	2.854	1694.47	0.236	0.060	0.18499E+03	0.46501E+05	0.17204E+07
78	3.266	2.961	1603.99	0.240	0.057	0.20520E+03	0.44822E+05	0.18395E+07
79	3.588	3.068	1513.46	0.243	0.055	0.21727E+03	0.42762E+05	0.18582E+07
80	3.909	3.176	1394.46	0.246	0.052	0.30603E+03	0.40712E+05	0.24918E+07
81	4.231	3.283	1248.95	0.252	0.048	0.41153E+03	0.37395E+05	0.30778E+07
82	4.552	3.391	1103.44	0.257	0.043	0.45866E+03	0.34788E+05	0.30326E+07
83	4.874	3.499	960.30	0.259	0.041	0.44509E+03	0.31876E+05	0.28375E+07
84	5.195	3.606	835.12	0.262	0.039	0.46580E+03	0.29510E+05	0.27492E+07
85	5.517	3.714	709.95	0.266	0.036	0.49414E+03	0.26512E+05	0.26202E+07
86	5.838	3.821	584.77	0.270	0.033	0.58523E+03	0.21824E+05	0.26081E+07
87	6.160	3.929	501.11	0.272	0.033	0.59778E+03	0.20200E+05	0.25543E+07
88	6.481	4.036	434.01	0.273	0.033	0.60327E+03	0.18428E+05	0.22234E+07
89	6.803	4.144	366.88	0.273	0.034	0.63629E+03	0.17239E+05	0.21938E+07
90	7.124	4.251	323.94	0.273	0.036	0.67017E+03	0.17389E+05	0.23307E+07
91	7.446	4.358	334.58	0.273	0.037	0.67806E+03	0.17580E+05	0.23841E+07
92	7.767	4.465	345.23	0.273	0.037	0.68630E+03	0.17719E+05	0.24321E+07
93	8.089	4.572	355.87	0.273	0.040	0.69527E+03	0.18543E+05	0.25784E+07
94	8.411	4.631	393.68	0.273	0.041	0.70444E+03	0.19367E+05	0.27286E+07
95	8.732	4.684	434.55	0.273	0.043	0.71525E+03	0.20149E+05	0.28823E+07
96	9.054	4.737	475.46	0.273	0.043	0.72641E+03	0.20846E+05	0.30286E+07
97	9.375	4.790	516.37	0.273	0.046	0.73891E+03	0.21530E+05	0.31817E+07
98	9.697	4.843	557.23	0.273	0.047	0.75177E+03	0.22167E+05	0.33330E+07
99	10.018	4.896	598.14	0.273	0.049	0.77039E+03	0.22769E+05	0.35083E+07
100	10.340	4.949	639.06	0.273				

TABLE 8

THE INFORMATION IN THIS TABLE COMES FROM AN ANALYSIS OF THE NUMERICAL INTEGRATION SEQUENCE COVERING THE LAST PASSAGE OF A TOOTH PAIR THROUGH THE CONTACT ZONE. POSITION 1 CORRESPONDS TO THE STARTING POINT OF CONTACT WHILE POSITION 100 CORRESPONDS TO THE END POINT OF CONTACT. THE FOLLOWING SYMBOLS ARE UTILIZED IN

THIS TABLE:

LOAD IS THE FORCE IN LBF ACTING BETWEEN THE CONTACTING TOOTH PAIR.

(THE LOAD IS DIRECTED NORMAL TO THE TOOTH PROFILE.)

TD1 IS THE TOOTH DEFLECTION ON GEAR 1; IN.

TD2 IS THE TOOTH DEFLECTION ON GEAR 2; IN.

HD IS THE HERTZIAN DEFLECTION OF THE CONTACT POINT; IN.

CD IS THE COMBINED DEFLECTION OF THE CONTACT POINT; IN.

(ALL DEFLECTIONS ARE MEASURED ALONG THE LINE OF ACTION)

POSITION	LOAD	TD1	TD2	HD	CD
1	490.34	0.0002432	0.0002606	0.0000773	0.0005811
2	493.96	0.0002458	0.0002590	0.0000788	0.0005836
3	503.08	0.0002491	0.0002602	0.0000811	0.0005904
4	506.75	0.0002498	0.0002537	0.0000803	0.0005838
5	514.75	0.0002459	0.0002493	0.0000801	0.0005754
6	492.70	0.0002354	0.0002338	0.0000771	0.0005463
7	477.34	0.0002258	0.0002220	0.0000750	0.0005228
8	452.13	0.0002144	0.0002040	0.0000708	0.0004892
9	427.66	0.0001986	0.0001869	0.0000668	0.0004524
10	387.94	0.0001798	0.0001681	0.0000619	0.0004098
11	351.13	0.0001615	0.0001512	0.0000573	0.0003700
12	309.75	0.0001427	0.0001297	0.0000509	0.0003234
13	276.95	0.0001251	0.0001125	0.0000457	0.0002833
14	233.79	0.0001059	0.0000922	0.0000390	0.0002372
15	201.53	0.0000901	0.0000772	0.0000340	0.0002013
16	173.94	0.0000778	0.0000654	0.0000298	0.0001730
17	147.82	0.0000657	0.0000547	0.0000258	0.0001462
18	119.93	0.0000535	0.0000432	0.0000213	0.0001180
19	119.20	0.0000527	0.0000418	0.0000211	0.0001156
20	117.22	0.0000519	0.0000404	0.0000208	0.0001130
21	116.40	0.0000512	0.0000395	0.0000206	0.0001113
22	128.35	0.0000566	0.0000425	0.0000224	0.0001216
23	153.67	0.0000673	0.0000495	0.0000262	0.0001430
24	176.84	0.0000778	0.0000555	0.0000295	0.0001628
25	203.91	0.0000891	0.0000624	0.0000333	0.0001849
26	267.80	0.0001168	0.0000697	0.0000374	0.0002097
27	233.70	0.0001026	0.0000779	0.0000420	0.0002367
28	298.08	0.0001305	0.0000846	0.0000460	0.0002611
29	323.67	0.0001411	0.0000896	0.0000493	0.0002799
30	472.33	0.0001714	0.0001267	0.0000682	0.0003663
31	503.57	0.0001824	0.0001319	0.0000718	0.0003861
32	547.55	0.0001994	0.0001400	0.0000769	0.0004163
33	645.75	0.0002343	0.0001613	0.0000884	0.0004840
34	735.00	0.0002691	0.0001780	0.0000982	0.0005453
35	836.26	0.0003072	0.0001954	0.0001090	0.0006116
36	872.21	0.0003228	0.0001985	0.0001126	0.0006338
37	657.85	0.0002124	0.0001594	0.0000883	0.0004600
38	678.55	0.0002302	0.0002564	0.0000904	0.0005769
39	692.35	0.0002323	0.0002570	0.0000917	0.0005810

40	676.58	0.0002268	0.0002455	0.0000897	0.0005620
41	657.78	0.0002244	0.0002392	0.0000874	0.0005510
42	640.80	0.0002182	0.0002273	0.0000852	0.0005307
43	605.52	0.0002060	0.0002135	0.0000810	0.0005006
44	563.39	0.0001916	0.0001950	0.0000759	0.0004625
45	523.79	0.0001787	0.0001800	0.0000710	0.0004297
46	470.75	0.0001606	0.0001588	0.0000646	0.0003840
47	416.43	0.0001419	0.0001397	0.0000579	0.0003396
48	356.97	0.0001219	0.0001170	0.0000506	0.0002894
49	301.52	0.0001048	0.0000984	0.0000436	0.0002468
50	259.23	0.0000904	0.0000822	0.0000382	0.0002107
51	216.62	0.0000770	0.0000684	0.0000325	0.0001779
52	174.40	0.0000621	0.0000539	0.0000268	0.0001428
53	155.10	0.0000559	0.0000479	0.0000241	0.0001279
54	141.10	0.0000509	0.0000429	0.0000222	0.0001159
55	126.29	0.0000462	0.0000385	0.0000201	0.0001047
56	125.24	0.0000459	0.0000374	0.0000199	0.0001031
57	139.25	0.0000523	0.0000415	0.0000217	0.0001156
58	154.53	0.0000583	0.0000449	0.0000238	0.0001269
59	168.57	0.0000652	0.0000489	0.0000256	0.0001397
60	207.71	0.0000807	0.0000587	0.0000306	0.0001700
61	244.17	0.0000974	0.0000691	0.0000351	0.0002015
62	282.90	0.0001131	0.0000784	0.0000397	0.0002312
63	301.82	0.0001234	0.0000847	0.0000418	0.0002499
64	434.16	0.0001465	0.0001185	0.0000569	0.0003218
65	442.30	0.0001565	0.0001209	0.0000576	0.0003350
66	463.93	0.0001659	0.0001222	0.0000597	0.0003478
67	502.22	0.0001871	0.0001316	0.0000637	0.0003824
68	547.64	0.0002059	0.0001390	0.0000683	0.0004132
69	585.51	0.0002270	0.0001489	0.0000721	0.0004479
70	658.59	0.0002563	0.0001644	0.0000793	0.0005000
71	531.90	0.0001755	0.0000904	0.0000660	0.0003320
72	590.91	0.0002185	0.0002431	0.0000719	0.0005334
73	605.51	0.0002387	0.0002601	0.0000730	0.0005718
74	603.44	0.0002375	0.0002524	0.0000725	0.0005624
75	592.73	0.0002388	0.0002501	0.0000711	0.0005600
76	590.68	0.0002384	0.0002458	0.0000706	0.0005549
77	543.62	0.0002323	0.0002349	0.0000656	0.0005329
78	475.36	0.0002097	0.0002161	0.0000624	0.0004977
79	437.98	0.0001932	0.0001841	0.0000582	0.0004715
80	377.90	0.0001765	0.0001657	0.0000540	0.0004313
81	333.87	0.0001560	0.0001438	0.0000425	0.0003898
82	284.27	0.0001375	0.0001251	0.0000369	0.0003423
83	247.22	0.0001197	0.0001067	0.0000327	0.0002996
84	203.04	0.0001043	0.0000907	0.0000275	0.0002591
85	167.24	0.0000861	0.0000727	0.0000232	0.0002224
86	141.40	0.0000745	0.0000621	0.0000200	0.0001819
87	122.47	0.0000645	0.0000529	0.0000176	0.0001566
88	102.80	0.0000553	0.0000442	0.0000151	0.0001350
89	90.77	0.0000490	0.0000380	0.0000135	0.0001146
90	93.20	0.0000512	0.0000388	0.0000138	0.0001005
91	96.16	0.0000530	0.0000389	0.0000142	0.0001038
92					0.0001062

93	98.65	0.0000554	0.0000397	0.0000145	0.0001095
94	109.13	0.0000614	0.0000428	0.0000158	0.0001200
95	120.30	0.0000682	0.0000471	0.0000171	0.0001324
96	131.63	0.0000746	0.0000508	0.0000185	0.0001439
97	142.49	0.0000821	0.0000546	0.0000197	0.0001564
98	153.77	0.0000889	0.0000575	0.0000210	0.0001674
99	165.00	0.0000966	0.0000611	0.0000223	0.0001800
100	176.29	0.0001036	0.0000638	0.0000235	0.0001909

TABLE 9

THE INFORMATION IN THIS TABLE COMES FROM AN ANALYSIS OF THE NUMERICAL INTEGRATION SEQUENCE COVERING THE LAST PASSAGE OF A TOOTH PAIR THROUGH THE CONTACT ZONE. POSITION 1 CORRESPONDS TO THE STARTING POINT OF CONTACT WHILE POSITION 100 CORRESPONDS TO THE END POINT OF CONTACT. THE FOLLOWING SYMBOLS ARE UTILIZED IN THIS TABLE:

SF IS THE NOMINAL TRANSMITTED FORCE ALONG THE LINE OF ACTION; LBF
 DF IS THE TOTAL DYNAMIC FORCE BEING TRANSMITTED ALONG THE LINE OF ACTION; LBF
 DF1 IS THE DYNAMIC FORCE FOR THE GEAR PAIR, ADJACENT SHAFTS, AND BEARINGS
 SL IS THE DYNAMIC LOAD FACTOR FOR THE CONTACTING TOOTH PAIR FROM THE STATIC ANALYSIS
 DL IS THE FORCE IN LBF ACTING BETWEEN THE CONTACTING TOOTH PAIR FROM THE DYNAMIC ANALYSIS
 DF2 IS THE FORCE IN LBF ACTING BETWEEN THE CONTACTING TOOTH PAIR FROM THE DYNAMIC ANALYSIS
 DL2 IS THE DYNAMIC FACTOR FOR AN INDIVIDUAL GEAR TOOTH PAIR TRAVERSING THE MESH ARC

POSITION	SF	DF	DF1	SL	DL	DF2
1	1000.00	1774.07	1.77	276.41	490.34	1.77
2	1000.00	1787.17	1.79	277.93	493.96	1.78
3	1000.00	1800.28	1.80	279.46	503.08	1.80
4	1000.00	1813.40	1.81	284.79	506.75	1.78
5	1000.00	1774.40	1.77	290.12	514.75	1.77
6	1000.00	1698.37	1.70	292.18	492.70	1.69
7	1000.00	1622.34	1.62	294.25	477.34	1.62
8	1000.00	1536.65	1.54	299.21	452.13	1.51
9	1000.00	1406.05	1.41	304.17	427.66	1.41
10	1000.00	1275.44	1.28	305.45	387.94	1.27
11	1000.00	1144.84	1.14	306.73	351.13	1.14
12	1000.00	1009.91	1.01	311.87	309.75	0.99
13	1000.00	873.68	0.87	317.01	276.95	0.87
14	1000.00	737.52	0.74	320.88	233.79	0.73
15	1000.00	620.60	0.62	324.76	201.53	0.62
16	1000.00	535.62	0.54	326.39	173.94	0.53
17	1000.00	450.65	0.45	328.02	147.82	0.45
18	1000.00	365.63	0.37	330.70	119.93	0.36
19	1000.00	357.56	0.36	333.38	119.20	0.36
20	1000.00	351.64	0.35	335.04	117.22	0.35
21	1000.00	345.71	0.35	336.70	116.40	0.35
22	1000.00	381.21	0.38	339.56	128.35	0.38
23	1000.00	448.81	0.45	342.42	153.67	0.45
24	1000.00	516.46	0.52	344.99	176.84	0.51

25	1000.00	586.70	0.59	347.57	203.91	0.59
26	1000.00	672.41	0.67	350.42	233.70	0.67
27	1000.00	758.13	0.76	353.26	267.80	0.76
28	1000.00	843.85	0.84	355.73	298.08	0.84
29	1000.00	903.66	0.90	358.19	323.67	0.90
30	1000.00	953.69	0.95	429.97	472.33	1.10
31	1000.00	1003.68	1.00	501.74	503.57	1.00
32	1000.00	1091.35	1.09	505.87	547.55	1.08
33	1000.00	1266.25	1.27	510.00	645.75	1.27
34	1000.00	1441.26	1.44	513.72	735.00	1.43
35	1000.00	1616.26	1.62	517.43	836.26	1.62
36	1000.00	1685.74	1.69	447.71	872.21	1.95
37	1000.00	1740.52	1.74	377.98	657.85	1.74
38	1000.00	1795.30	1.80	380.68	678.55	1.78
39	1000.00	1806.01	1.81	383.38	692.35	1.81
40	1000.00	1764.89	1.76	382.50	676.58	1.77
41	1000.00	1723.76	1.72	381.61	657.78	1.72
42	1000.00	1679.27	1.68	383.65	640.80	1.67
43	1000.00	1570.08	1.57	385.68	605.52	1.57
44	1000.00	1460.82	1.46	386.61	563.39	1.46
45	1000.00	1351.63	1.35	387.54	523.79	1.35
46	1000.00	1214.78	1.21	389.67	470.75	1.21
47	1000.00	1062.93	1.06	391.79	416.43	1.06
48	1000.00	911.16	0.91	391.67	356.97	0.91
49	1000.00	770.13	0.77	391.54	301.52	0.77
50	1000.00	662.13	0.66	391.24	259.23	0.66
51	1000.00	554.13	0.55	390.93	216.62	0.55
52	1000.00	446.13	0.45	389.85	174.40	0.45
53	1000.00	398.97	0.40	388.76	155.10	0.40
54	1000.00	362.96	0.36	387.53	141.10	0.36
55	1000.00	326.95	0.33	386.30	126.29	0.33
56	1000.00	324.21	0.32	384.35	125.24	0.33
57	1000.00	364.17	0.36	382.41	139.25	0.36
58	1000.00	404.12	0.40	380.40	154.53	0.41
59	1000.00	445.50	0.45	378.39	168.57	0.45
60	1000.00	548.96	0.55	376.34	207.71	0.55
61	1000.00	652.42	0.65	374.28	244.17	0.65
62	1000.00	755.88	0.76	371.97	282.90	0.76
63	1000.00	816.55	0.82	369.65	301.82	0.82
64	1000.00	849.00	0.85	435.74	434.16	1.00
65	1000.00	881.43	0.88	501.83	442.30	0.88
66	1000.00	924.53	0.92	497.98	463.93	0.93
67	1000.00	1016.41	1.02	494.13	502.22	1.02
68	1000.00	1108.35	1.11	490.99	547.64	1.12
69	1000.00	1200.24	1.20	487.85	585.51	1.20
70	1000.00	1350.05	1.35	419.08	658.59	1.57
71	1000.00	1518.44	1.52	350.31	531.90	1.52
72	1000.00	1686.93	1.69	343.65	590.91	1.72
73	1000.00	1796.91	1.80	336.99	605.51	1.80
74	1000.00	1790.75	1.79	334.57	603.44	1.80
75	1000.00	1784.60	1.78	332.15	592.73	1.78
76	1000.00	1778.44	1.78	326.50	590.68	1.81
77	1000.00	1694.47	1.69	320.84	543.62	1.69

78	1000.00	1603.99	1.60	317.47	514.59	1.62
79	1000.00	1513.46	1.51	314.10	475.36	1.51
80	1000.00	1394.46	1.39	308.35	437.98	1.42
81	1000.00	1248.95	1.25	302.59	377.90	1.25
82	1000.00	1103.44	1.10	299.31	333.87	1.12
83	1000.00	960.30	0.96	296.04	284.27	0.96
84	1000.00	835.12	0.84	291.02	247.22	0.85
85	1000.00	709.95	0.71	286.00	203.04	0.71
86	1000.00	584.77	0.58	284.10	167.24	0.59
87	1000.00	501.11	0.50	282.20	141.40	0.50
88	1000.00	434.01	0.43	281.21	122.47	0.44
89	1000.00	366.88	0.37	280.22	102.80	0.37
90	1000.00	323.94	0.32	279.39	90.77	0.32
91	1000.00	334.58	0.33	278.57	93.20	0.33
92	1000.00	345.23	0.35	277.89	96.16	0.35
93	1000.00	355.87	0.36	277.21	98.65	0.36
94	1000.00	393.68	0.39	277.04	109.13	0.39
95	1000.00	434.55	0.43	276.86	120.30	0.43
96	1000.00	475.46	0.48	276.41	131.63	0.48
97	1000.00	516.37	0.52	275.97	142.49	0.52
98	1000.00	557.23	0.56	275.92	153.77	0.56
99	1000.00	598.14	0.60	275.87	165.00	0.60
100	1000.00	639.06	0.64	275.77	176.29	0.64

C-3 LISTING AND SAMPLE RUN OF THE STRESS ANALYSIS PROGRAM
"INTERNAL STRESS"

```

C *****
C ***** MODULE 3 *****
C ***** INTERNAL STRESS *****
C* THIS MODULE CALCULATES THE MAXIMUM TOOTH BENDING STRESS USING *****
C* ***** CORNELL'S METHOD *****
C
COMMON/DIMEN/OCODE,MODCOD
COMMON/C1/PHI,PHID,DP,M,TG,TP,DELTP
COMMON/C2/P1,FW,R1,E,G,PR,GAMA
COMMON/C4/TIN,TOUT,RPMIN,RPMOUT,OMEGA1,OMEGA2
COMMON/C6/L1,L2,PD1,PD2,RPC1,RPC2,RAC1,RAC2,RBC1,RBC2,RRC1,RRC2,
1 RF1,RF2,C,CP,BP,UCUT
COMMON/C9/Q(50),YC1(50),YC2(50),IDIR
REAL INPUT,MODF,LENGTH(2),LEN(2),MODULUS(2)
REAL M,JG(2),JD,JL,KDS,KGPAVG,KLS,KG,LDS,LLS
INTEGER OCODE,OC,IPIT1(2),IPIT2(2)
DIMENSION FORCE(2),SPEED(2),PRESS(2),SPWGHT(2)
DIMENSION G(2)
DIMENSION E(2),PR(2),GAMA(2),FW(2),TG(2),AD(2),WD(2),GRRF(2),R1(2)
DOUBLE PRECISION XI,DXI
EQUIVALENCE(OC,OCODE)
C
DATA TAUMAX/10000./
DATA SI,ENGL,'SI',ENGL,'YES','YES'/'
DATA LENGTH,'IN.','MM.'/'
&PRESS,'PSI.','MPA.'/'
&SPWGHT,'LBI3.','KGM3'/'
C
NAMELIST/CONTRL/INPUT,OUTPUT,I PLOT,MODF,NTYPE,FELGR,IDIR
NAMELIST/PHYPAR/E,PR,GAMA,JG
NAMELIST/GENPAR/DP,M,DELTP,TIN,RPMIN,ZETAS,ZETAG,PHID,CBD,CB1,CB2,
&
NAMELIST/GEOPAR/TG,AD,WD,GRRF,R1,FW,UCUT
PI=3.141592654
IBYPSS=0
C
1 READ(5,CONTRL,END=999)
READ(5,PHYPAR)
READ(5,GENPAR)
READ(5,GEOPAR)
C
GO TO (11,12,14),IDIR
11 READ(8,1180)(Q(K),YC1(K),YC2(K),K=1,50)
1180 FORMAT(3E14.7)

```

```

GO TO 14
12 READ(9,1180) (Q(K),YC1(50),YC2(50),K=1,50)
14 CONTINUE
C
C 3 OCODE=1
C IF (OUTPUT.EQ.SI) OCODE = 2
C IF (INPUT.EQ.SI) DP=1/M
C ICHNG=0
C
6 PHI=PHID*PI/180.
TOUT=TIN*TG(2)/TG(1)
RPMOUT=RPMIN*TG(1)/TG(2)
G(1)=0.5*E(1)/(1.+PR(1))
G(2)=0.5*E(2)/(1.+PR(2))
PD1=TG(1)/DP
PD2=TG(2)/DP
RPC1=0.5*PD1
RPC2=0.5*PD2
IF (INPUT.EQ.ENGL) GO TO 7
IF (RI(1).EQ.0.0) RI(1)=(16.*TIN/(PI*TAUMAX))**(1./3.)*26.270218
IF (RI(2).EQ.0.0) RI(2)=(16.*TOUT/(PI*TAUMAX))**(1./3.)*26.270218
7 IF (RI(1).EQ.0.0) RI(1)=(16.*TIN/(PI*TAUMAX))**(1./3.)*.5
IF (RI(2).EQ.0.0) RI(2)=(16.*TOUT/(PI*TAUMAX))**(1./3.)*.5
IF (JG(1).EQ.0.) JG(1)=.5*GAMA(1)*PI*FW(1)*RPC1**4/386.
IF (JG(2).EQ.0.) JG(2)=.5*GAMA(2)*PI*FW(2)*RPC2**4/386.
C =-RPC1 + RPC2
CP = PI/DP
BP = CP*COS(PHI)
RF1=.7*(GRRF(1)+(WD(1)-AD(1)-GRRF(1))**2/(.5*PD1+WD(1)-AD(1)-
&GRRF(1)))
RF2=.7*(GRRF(2)+(WD(2)-AD(2)-GRRF(2))**2/(.5*PD2+WD(2)-AD(2)-
&GRRF(2)))
RF2=RF1
RAC1=RPC1+AD(1)
RAC2=RPC2-AD(2)
RRC1=RAC1-WD(1)
RRC2=RAC2+WD(2)
RBC1 = RPC1*COS(PHI)
RBC2 = RPC2*COS(PHI)
DELR1 = RAC1 - RRC1
DELR2 =-RAC2 + RRC2
DELTAR = DELR1

```

```

IF(DELTR2.GT.DELTAR) DELTAR = DELR2
L1=DELTAR*100.
IF(DELTAR.LE.1.0) L1 = 100
IF(DELTAR.GE.2.0) L1 = 200
L2 = L1

C      IF(OCODE.EQ.2) GO TO 8
      GO TO 10
      8 CONTINUE
      10 CONTINUE

C      CALL MAIN1(INF,LINF)
      IF ((INF.EQ.2).OR.(LINF.EQ.2)) GO TO 1

C      GO TO 1
      999 STOP

C      21 FORMAT(1H1, T38, 'STATIC AND DYNAMIC ANALYSIS OF A GEAR PAIR SYSTEM'
      &/T38,49(' '))
      35 FORMAT(T49,F5.1, ' DEGREE PRESSURE ANGLE'//)
      37 FORMAT(T49, ' DIAMETRAL PITCH IS',F10.3//T46, ' INPUT TORQUE IS',
      &F11.2, ' IN-LBF'//T46, ' OUTPUT TORQUE IS',F11.2, ' IN-LBF'//)

      38 FORMAT(T53, 'MODULE IS', F11.3//T46, ' INPUT TORQUE IS', F11.2, ' NT-M
      & //T46, ' OUTPUT TORQUE IS', F11.2, ' NT-M'//)
      40 FORMAT(T46, ' INPUT SPEED IS', F11.2, ' RPM. //T46, ' OUTPUT SPEED IS',
      &F11.2, ' RPM.//)
      50 FORMAT( //T18, 'DATA FOR GEAR 1 (DRIVING GEAR)', T65, '*' , T87, 'DATA
      &FOR GEAR 2 (DRIVEN GEAR)'/T18,15(' ' ), T87,15(' ' )//)
      60 FORMAT( T11, 'NUMBER OF TEETH', T35, '=', T38, F4.0, T65, '*', T80, 'NUMBER
      & OF TEETH', T104, '=', T107, F4.0//)
      &T11, 'PITCH DIAMETER', T35, '=', T38, F8.4, 3X, A3, T65, '*', T80, 'PITCH DIA
      &METER', T104, '=', T107, F8.4, 3X, A3//)
      &T11, 'ADDENDUM CIRCLE RADIUS =', T38, F8.4, 3X, A3, T65, '*', T80, 'ADDEND
      &UM CIRCLE RADIUS =', T104, '=', T107, F8.4, 3X, A3//)
      &T11, 'BASE CIRCLE RADIUS', T35, '=', T38, F8.4, 3X, A3, T65, '*', T80, 'BASE
      &CIRCLE RADIUS', T104, '=', T107, F8.4, 3X, A3//)
      &T11, 'ROOT CIRCLE RADIUS', T35, '=', T38, F8.4, 3X, A3, T65, '*', T80, 'ROOT
      &CIRCLE RADIUS', T104, '=', T107, F8.4, 3X, A3//)
      65 FORMAT(/T11, 'FILLET RADIUS', T35, '=', T38, F8.4, 3X, A3, T65, '*', T80, 'FI
      &LLET RADIUS', T104, '=', T107, F8.4, 3X, A3//)
      &T11, 'INSIDE RADIUS OF HUB', T35, '=', T38, F8.4, 3X, A3, T65, '*', T80, 'INS
      &IDE RADIUS OF HUB', T104, '=', T107, F8.4, 3X, A3//)
      &T11, 'FACE WIDTH', T35, '=', T38, F8.4, 3X, A3, T65, '*', T80, 'FACE WIDTH',
      &T104, '=', T107, F8.4, 3X, A3//)

```



```

&T11, 'YOUNG'S MODULUS', T35, '= ', T39, 2PE8.1, 2X, A3, T65, '* ', T80, 'YOUNG'
&'S MODULUS', T104, '= ', T108, E8.1, 2X, A3//
&T11, 'SPECIFIC WEIGHT', T35, '= ', T38, OPF8.3, 3X, A3, T65, '* ', T80, 'SPECIF
&IC WEIGHT', T104, '= ', T107, F8.3, 3X, A3//
&T11, 'POISSON'S RATIO', T35, '= ', T38, F8.4, T65, '* ', T80, 'POISSON'S RA
&TIO', T104, '= ', T107, F8.4)
END

```

C
C
C

```

SUBROUTINE MAIN1(INF, LINF)
COMMON/DIMEN/OC,MODCOD
COMMON/C1/PHI, PHID, DP, M, TG1, TG2, TP, DELTP
COMMON/C2/P1, F1, F2, R11, R12, E1, E2, G1, G2, PR1, PR2, GAMA1, GAMA2
COMMON/C4/TIN, TOUT, RPMIN, RPMOUT, OMEGA1, OMEGA2
COMMON/C6/L1, L2, PD1, PD2, RPC1, RPC2, RAC1, RAC2, RBC1, RBC2, RRC1, RRC2,
&RF1, RF2, C, CP, BP, UCUT1, UCUT2
COMMON/C7/YT11, YT12, YP1, YP2, YB11, YB12, RT11, RT12, RB11, RB12,
1RR01, RR02, XMIN1, XMIN2, SP, EP
COMMON/C8/X1(200), X2(200), Y1(200), Y2(200), THETA1(200), THETA2(200),
1RCURV1(200), RCURV2(200)

```

C

```

DIMENSION XP(50), Y1P(50), Y2P(50, 2)
REAL M, JD, JG1, JG2, JL, KDS, KGPAVG, KLS, KG, LDS, LLS, LCR
DIMENSION FORCE(2), SPEED(2), PRESS(2)
REAL LENGTH(2), MODLUS(2), LEN(2)
INTEGER OC
DOUBLE PRECISION X1, DX1
DATA NGEAR1, NGEAR2/1, 2/
DATA LENGTH/ 'IN.', 'MM.', '/', FORCE/'LBF.', 'NTS.', '/', LEN/'IN.', 'MT.'/,
&PRESS/'PSI.', 'MPA.', '/', MODLUS/'PSI.', 'MPA.'/

```

C

```

P = TIN/RBC1
IF (OC.EQ.2) PMTRIC = P*4.448222
CALL MOD(INF, CR)
IF (INF.EQ.1) GO TO 301
RETURN

```

C

```

2 FORMAT(////T30, 'THE NOMINAL TRANSMITTED FORCE ALONG THE LINE OF AC
&TION =', F10.2, 1X, A4/)
5 FORMAT(//T31, 'INTERFERENCE OCCURS FOR THIS PAIR OF GEARS UNDER NO-L
&LOAD CONDITIONS')
14 FORMAT(//T31, 'INTERFERENCE OCCURS FOR THIS PAIR OF GEARS UNDER LOAD
&ED CONDITIONS')

```

```

18 FORMAT(//T26,'CONTACT RATIO FOR THIS PAIR OF GEARS UNDER LOAD IS E
&QUAL TO OR LESS THAN UNITY')
20 FORMAT(T46,'THE CONTACT RATIO UNDER LOAD =',F8.3/)
C
C
C TABLE 1 OUTPUT
301 CONTINUE
IF(MODCOD.EQ.1) GO TO 400
400 CONTINUE
C
CONST=180./PI
DO 452 K=1,L1
THET1=THETA1(K)*CONST
THET2=THETA2(K)*CONST
452 CONTINUE
C
401 FORMAT(T37,'X-Y COORDINATES OF POINTS ALONG THE PROFILE OF THE GEA
&R TEETH')
402 FORMAT(T37,'THE GEAR TEETH HAVE A STANDARD PROFILE WITH NO MODIFIC
&ATIONS')
420 FORMAT(T4,'THE Y-AXIS CORRESPONDS TO THE LINE OF SYMMETRY OF THE I
&OOTH. THE ORIGIN OF THE X-Y COORDINATE SYSTEMS IS LOCATED AT THE'
&/T4,'ROOT OF THE TOOTH A DISTANCE OF RR01 (OR RR02 FOR GEAR 2) FRO
&M THE GEAR CENTER. VALUES TABULATED BELOW REPRESENT POINTS ON THE
&/T4,'R.H. PROFILE OF THE TOOTH. POINT IS LOCATED AT THE ADDENDU
&M CIRCLE. POINT',I4,' IS LOCATED AT THE ROOT CIRCLE. /T4,'THETA V
&ALUES REPRESENT THE ANGLE BETWEEN THE NORMAL TO THE PROFILE AND TH
&E X-AXIS; COUNTERCLOCKWISE THETA IS DEFINED AS POSITIVE. //')
425 FORMAT(T15,'THE INVOLUTE STARTS AT Y =',F9.4,1X,A3,' AND ENDS AT
& Y =',F9.4,1X,A3,' ON THE TOOTH PROFILE OF GEAR',I2,'')
430 FORMAT(T28,'THE PITCH CIRCLE INTERSECTS THE TOOTH PROFILE OF GEAR'
&,I2,' AT Y =',F9.4,1X,A3)
432 FORMAT(//T56,'RR01 =',F9.4,1X,A3/T56,'RR02 =',F9.4,1X,A3)
440 FORMAT(//T40,'X AND Y VALUES ARE IN',A3,' , THETA VALUES ARE IN
& DEGREES. //T20,'DATA FOR GEAR 1',T91,' DATA FOR GEAR 2',T20,T15('*
&'),T91,T15('*'))
450 FORMAT(//T5,'POINT',T21,'X',T35,'Y',T47,'THETA',T76,'POINT',T92,
&'X',T106,'Y',T118,'THETA')
455 FORMAT(T5,13,3X,3F14.5,T76,13,3X,3F14.5)
C
RETURN
END
C
C
C

```



```

105 FORMAT(2(6X, 'PARABOLIC BOTTOM MODIFICATION', 7X, '= ', F10.5, 2X, A3,
&7X)/)
110 FORMAT(2(6X, 'STRAIGHT LINE TIP MODIFICATION', 6X, '= ', F10.5, 2X, A3,
&7X)/)
113 FORMAT(2(6X, 'STRAIGHT LINE BOTTOM MODIFICATION', 3X, '= ', F10.5, 2X, A3
& 7X)/)
115 FORMAT(2(6X, 'ROLL ARC OF TIP MODIFICATION', 8X, '= ', F7.2, 5X, 'DEGREES
& ', 3X)/)
120 FORMAT(2(6X, 'ROLL ARC OF BOTTOM MODIFICATION', 5X, '= ', F7.2, 5X, 'DEGR
&EES', 3X)/)
122 FORMAT(2(6X, 'SINUSOIDAL PROFILE ERROR', 12X, '= ', F10.5, 2X, A3, 7X)/)
125 FORMAT(2(6X, 'NUMBER OF CYCLES OF PROFILE ERROR', 3X, '= ', F7.2, 5X,
&'CYCLES', 3X)/)
130 FORMAT(2(6X, 'PHASE ANGLE OF PROFILE ERROR', 8X, '= ', F7.2, 5X, 'DEGREES
& ', 3X)/)
131 FORMAT(2(6X, 'PIT LOCATION', 25X, 'POSITIONS ', 13, ' TO ', 13, 3X)/)
132 FORMAT(2(6X, 'DEPTH OF PIT', 24X, '= ', F10.5, 2X, A3, 7X)/)
135 FORMAT(1H1, T58, 'TABLE 1-8'/)
C
C*****CHECK FOR INTERFERENCE
C
C 199 RCHK1 = SQRT(RBC1**2 + (C*SIN(PHI))**2)
C 199 RCHK2 = SQRT(RPC2**2 + (C*SIN(PHI))**2)
C      IF (RCHK2.LE.RBC2) INF=2
C      IF (INF.EQ.2) GO TO 4563
C      ALPHA1=ARSIN(RF1/(RRC1+RF1))
C      ALPHA2=ARSIN(RF2/(RRC2+RF2))
C      RTF11=(RRC1+RF1)*COS(ALPHA1)
C      RTF22= (RRC2+RF2)*COS(ALPHA2)
C      ALPHA2=2.0*ARSIN(RF2/(2.0*RTF22))
C
C WRITE(6,9000) RRC2,RF2,RTF22,ALPHA2
C000 FORMAT(0, 'RRC2,RF2,RTF22,ALPHA2', 3X,4F14.7)
C
C CALCULATION OF LIMIT RADII (RLM1 AND RLM2)
C
C AUX1=ARCOS(RBC1/RAC1)
C AUX2=ARCOS(RBC2/RAC2)
C C11=-RAC2*SIN(AUX2)+RPC2*SIN(PHI)
C C12= RAC1*SIN(AUX1)-RPC1*SIN(PHI)
C RALR1=ATAN((RPC1*SIN(PHI)-C11)/RBC1)
C RALR2=ATAN((RPC2*SIN(PHI)+C12)/RBC2)
C RLM1=RBC1/COS(RALR1)
C RLM2=RBC2/COS(RALR2)
C

```

```

RR1=RAC1-RLM1
RR2=RLM2-RAC2
IF (RLM1.LE.RRC1) RR1=RAC1-RTF11
IF (RLM2.GE.RRC2) RR2=RTF22-RAC2
220 FORMAT('0',2X,'NOTE: RADIUS OF THEORETICAL LAST POINT OF CONTACT
&ON GEAR 1 IS LESS THAN THE ROOT CIRCLE RADIUS.'/)
&' TO AVOID INTERFERENCE PROBLEMS, THIS TOOTH SHOULD BE UNDERCUT'//)
221 FORMAT('0',2X,'NOTE: RADIUS OF THEORETICAL LAST POINT OF CONTACT
&ON GEAR 2 IS LESS THAN THE ROOT CIRCLE RADIUS.'/)
&' TO AVOID INTERFERENCE PROBLEMS, THIS TOOTH SHOULD BE UNDERCUT'//)

C
L11=IFIX((RR1/(RAC1-RRC1))*L1)
L12=IFIX((RR2/(RRC2-RAC2))*L2)
RINC1=RR1/FLOAT(L11-1)
RINC2=RR2/FLOAT(L12-1)

C
RA1-----ROLL ANGLE, GEAR 1
RATM1----LENGTH OF TIP MODIFICATION IN DEGREES OF ROLL, GEAR 1
RAT1-----ROLL ANGLE AT TIP OF GEAR 1
RAT11----ROLL ANGLE AT TOP OF INVOLUTE, GEAR 1
RAB11----ROLL ANGLE AT THE BOTTOM OF INVOLUTE, GEAR 1
RABM1----LENGTH OF ROOT MODIFICATION IN DEGREES OF ROLL, GEAR 1
PATM1----MAGNITUDE OF PARABOLIC MODIFICATION AT THE TIP, GEAR 1
PABM1----MAGNITUDE OF PARABOLIC MODIFICATION AT THE BOTTOM, GEAR 1
STTM1----MAGNITUDE OF STRAIGHT LINE MODIFICATION AT THE TIP, GEAR 1
STBM1----MAGNITUDE OF STRAIGHT LINE MODIFICATION AT THE BOTTOM, GEAR 1
PER1----MAX MANUFACTURED PROFILE ERROR, GEAR 1
PAP1----ANGLE FROM START OF SIN. ERROR TO START OF INVOLUTE, GEAR 1
RT11----RADIUS TO TOP OF INVOLUTE, GEAR 1
RB11----RADIUS TO BOTTOM OF INVOLUTE, GEAR 1

C
C*****CALCULATION OF ROLL ANGLES TO INVOLUTE TOP, PITCH, AND BOTTOM; AND
C*****RADIAL DISTANCES TO (UN)MODIFIED INVOLUTE TOP, PITCH, AND BOTTOM
C
RAT1=TODEGR*SQRT((RAC1/RBC1)**2 - 1.)
RAT2=TODEGR*SQRT((RAC2/RBC2)**2 - 1.)
RAM1=RAT1-RATM1
RAM2=RAT2+RATM2
RT11=RBC1*SQRT((RAM1/TODEGR)**2 + 1.)
RT12=RBC2*SQRT((RAM2/TODEGR)**2 + 1.)
RAP=TODEGR*TAN(PHI)
RATIPI=RAM1-RAP

```

```

RAT1P2=RAP-RAM2
RAB11=TODEGR*SQRT((RLM1/RBC1)**2 - 1.)
RAB12=TODEGR*SQRT((RLM2/RBC2)**2 - 1.)
RAN1=RAB11-RABM1
RAN2=RAB12+RABM2
RBI1=RBC1*SQRT((RAN1/TODEGR)**2 + 1.)
RBI2=RBC2*SQRT((RAN2/TODEGR)**2 + 1.)
C
C*****CALCULATION OF RRO
C
C 230 TP=PI*.5/DP
PHIB1=ARCOS(RBC1/RLM1)
BETAB1=PI/(2.*TG1)+(TAN(PHI)-PHI)-(TAN(PHIB1)-PHIB1)
IF (RLM1.GE.RTF11) GO TO 285
ARG1=((RRC1+RF1)**2 + RLM1**2 - RF1**2)/(2.*RLM1*(RRC1+RF1))
ALPHA1=ARCOS(ARG1)
RRO1=RRC1*COS(BETAB1+ALPHA1)
C
C XMIN1=RTF11*SIN(BETAB1)
PAP1=PAP1/TODEGR
C
PHIB2=ARCOS(RBC2/RLM2)
BETAB2=PI/(2.*TG2)-(TAN(PHI)-PHI)+(TAN(PHIB2)-PHIB2)
IF (RLM2.LE.RTF22) GO TO 290
ARG2=((RRC2-RF2)**2 + RLM2**2 - RF2**2)/(2.*RLM2*(RRC2-RF2))
ALPHA2=ARCOS(ARG2)
RRO2=RRC2*COS(BETAB2+ALPHA2)
C
C 290 RRO2=RRC2*COS(BETAB2+ALPHA2)
C
C WRITE(6,9010) RBC2,RLM2,BETAB2,ARG2,ALPHA2,RRO2
C 10 FORMAT('01','RBC2,RLM2,BETAB2,ARG2,ALPHA2,RRO2',3X,6F14.7)
C
C XMIN2=-RTF22*SIN(BETAB2)
PAP2=PAP2/TODEGR
C
C*****CALCULATION OF INVOLUTE PROFILE COORDINATES, GEAR 1
C
C DO 330 J=1,LI1
ET1=0.
PET=0.
C
R1=RAC1-RINC11*(FLOAT(J-1))
PHI1=ARCOS(RBC1/R1)
BETA1=PI/(2.*TG1) + (TAN(PHI)-PHI) - (TAN(PHI1)-PHI1)
THETA1(J)=PHI1-BETA1
RA1=TODEGR*TAN(PHI1)

```

```

C      IF (J.EQ.1) RA1=RAT1
C****CHECK FOR TIP MODIFICATIONS
C
C      IF (RATM1.EQ.0. .OR. RA1.LT.RAM1) GO TO 300
C      IF (STIM1.EQ.0.) ET1=PATM1*(1.-SQRT((RAT1-RA1)/RATM1))
C      IF (PATM1.EQ.0.) ET1=STIM1*(RA1-RAM1)/RATM1
C****CHECK FOR SINUSOIDAL ERRORS
C
C      IF (PER1.EQ.0.) GO TO 310
C      IF (RA1.GT.RAM1) PE1=PER1*SIN(PAP1)
C      IF (RA1.LT.RAM1)
C      * PE1=PER1*SIN((PI*(RAM1-RA1)*CYC1/RATIPI)+PAP1)
C****CHECK FOR BOTTOM MODIFICATIONS
C
C      IF (RABM1.EQ.0. .OR. RA1.GT.RAN1) GO TO 320
C      IF (STBM1.EQ.0.) ET1=PABM1*(1.-SQRT((RA1-RAB11)/RABM1))
C      IF (PABM1.EQ.0.) ET1=STBM1*(RA1-RAN1)/RABM1
C
C      X1(J)=R1*SIN(BETA1) + (ET1+PE1)/COS(THETA1(J))
C      Y1(J)=R1*COS(BETA1) - RRO1
C      IF (J.NE.1) THETA1(J-1)=ATAN((X1(J)-X1(J-1))/(Y1(J-1)-Y1(J)))
C      CONTINUE
C
C****FILLET COORDINATE POINTS, GEAR 1
C
C      BETA1=ATAN(X1(L11)/(Y1(L11)+RRO1))
C      RINCB1=(R1-RRC1)/FLOAT(L1-L11)
C      LI1=L11+1
C      DO 340 J=L11,LI
C      RFIL=R1-RINCB1*FLOAT(J-L11)
C      IF (RFIL1.GE.RTF11) ARC1=ALPHA1
C      IF (RFIL1.LT.RTF11)
C      &ARC1=ARCOS(((RRC1+RF1)**2+RFIL1**2-RF1**2)/(2.*RFIL1*(RRC1+RF1)))
C      BETAF1=BETA1+ALPHA1-ARC1
C      X1(J)=RFIL1*SIN(BETAF1)
C      Y1(J)=RFIL1*COS(BETAF1) - RRO1
C      THETA1(J-1)=ATAN((X1(J)-X1(J-1))/(Y1(J-1)-Y1(J)))
C      THETA1(L1)=.5*PI-BETAF1
C
C****CALCULATION OF INVOLUTE PROFILE COORDINATES, GEAR 2
C
C      DO 380 J=1,L12

```

```

C
ET2=0.
PE2=0.
R2=RAC2+RINC12*(FLOAT(J-1))
PHI2=ARCOS(RBC2/R2)
BETA2=PI/(2.*TG2) - (TAN(PHI)-PHI) + (TAN(PHI2)-PHI2)
THETA2(J)=PHI2+BETA2
C
WRITE(6,9020) R2,PHI2,BETA2,THETA2(J)
FORMAT('0',1R2,PHI2,BETA2,THETA(J),4F14.7)
C
RA2=TODEGR*TAN(PHI2)
IF (J.EQ.1) RA2=RAT2
C
IF (RATM2.EQ.0..OR.RA2.LT.RAM2) GO TO 350
IF (STM2.EQ.0.) ET2=PATM2*(1.-SQRT((RA2-RAT2)/RATM2))
IF (PATM2.EQ.0.) ET2=STTM2*(RAM2-RA2)/RATM2
C
IF (PER2.EQ.0.) GO TO 360
IF (RA2.GT.RAM2) PE2=PER2*SIN(PAP2)
IF (RA2.LT.RAM2)
& PE2=PER2*SIN(PI*(RA2-RAM2)*CYC2/RAT1P2)+PAP2)
C
350 IF (RABM2.EQ.0..OR.RA2.GT.RAN1) GO TO 370
IF (STBM2.EQ.0.) ET2=PABM2*(1.-SQRT((RA2-RAB12)/RABM2))
IF (PABM2.EQ.0.) ET2=STBM2*(RA2-RAN2)/RABM2
C
370 X2(J)=-R2*SIN(BETA2) + (ET2+PE2)/COS(THETA2(J))
Y2(J)=-R2*COS(BETA2) + RR02
IF (J.NE.1) THETA2(J-1)=ATAN((X2(J)-X2(J-1))/(Y2(J)-Y2(J-1)))
380 CONTINUE
C
C*****FILLET COORDINATE POINTS, GEAR 2
C
RINC2=(-R2+RRC2)/FLOAT(L2-L12)
BETA2=ATAN(X2(L12)/(+Y2(L12)-RR02))
C
L12=L12+1
DO 390 J=L12,L2
RFIL2=R2+RINC2*FLOAT(J-L12)
IF (RFIL2.LE.RTF22) ARC2=ALPHA2
IF (RFIL2.GT.RTF22)
&ARC2=ARCOS(((RRC2-RF2)**2+RFIL2**2-RF2**2)/(2.*RFIL2*(RRC2-RF2)))
BETA2=BETA2+ALPHA2-ARC2
C
WRITE(6,9040) RFIL2,BETA2,BETA2,ALPHA2,ARC2

```



```

C 40  FORMAT('0',1RF1L2,BETA2,BETA2,ALPHA2,ARC2',3X,5F14.7)
C
C 390  X2(J)=-RF1L2*SIN(BETA2)
      Y2(J)=-RF1L2*COS(BETA2) + RR02
      THETA2(J-1)=ATAN((X2(J)-X2(J-1))/(Y2(J)-Y2(J-1)))
      THETA2(L2)=.5*PI - BETA2
C
C      CONTACT RATIO CALCULATIONS
C
      AUX1=ARCOS(RBC1/RT11)
      AUX2=ARCOS(RBC2/RT12)
      AL1=ARCOS(RBC1/(RB11))
      AL2=ARCOS(RBC2/(RB12))
      CRU1=RPC1*SIN(PHI)-COS(PHI)*TAN(AL1)/BP
      CRU2=RPC2*SIN(PHI)-COS(PHI)*TAN(AL2)/BP
      CR1=((RT12)*SIN(AUX2)-RPC2*SIN(PHI))/BP
      CR2=((RT11)*SIN(AUX1)-RPC1*SIN(PHI))/BP
      IF((RBC1.GE.RB11).AND.(RBC2.GE.RB12)) GO TO 18
      IF(CRU1.LE.CR1) CR1=CRU1
      IF(CRU2.LE.CR2) CR2=CRU2
      IF(CRU1.GT.CR1) CR1=CR1
      IF(CRU2.GT.CR2) CR2=CR2
      18 CR=CR1+CR2
      SP=CR1*BP
      EP=CR2*BP
      SE=CR*BP
      INF = 1
      12 FORMAT('THEORETICAL CONTACT RATIO =',F8.3/)
      13 FORMAT(' ',3X,4F11.7)
C
C*****PIT INSERTION
C
      IPIT11=45
      IPIT12=50
      DEEP1=0.02
      IF (DEEP1.EQ.0.0) GO TO 4561
      DO 4560 I=IPIT11,IPIT12
      4560 X1(I)=X1(I)-DEEP1
      4561 IF (DEEP2.EQ.0.0) GO TO 4563
      DO 4562 I=IPIT21,IPIT22
      4562 X2(I)=X2(I)-DEEP2
      4563 CONTINUE
C
      KK=L1+NF
      DO 4610 I=1,KK
      C      WRITE(6,4601) X1(I),Y1(I),I,THETA1(I)

```



```

COMMON/C9/LOAD1(50),YC1(50),YC2(50),IDIR
COMMON/C22/X(400,2),Y(400,2),THETA(400,2),YC(100,2)
REAL P1,H1,LOAD1,H,J,J,L
DELTAX=1./{(100.0*DP)}
L122=L12
DO 403 L5=1,L1
WRITE(6,404)XA(L5),YA(L5),THET1(L5),XB(L5),YB(L5),THET2(L5)
C 404 FORMAT(2X,'X1= ',F8.6,5X,'Y1= ',F8.6,5X,'THETA1= ',F8.6,15X,'X2= ',
C 1,F8.6,5X,'Y2= ',F8.6,5X,'THETA2= ',F8.6)
C 403 CONTINUE
NF=90
C
C LOAD INTO "YC" ARRAY VALUES FROM DATA SET
C
DO 111 J=1,2
DO 110 I=1,50
IF(J.EQ.1) GO TO 109
YC(I,J)=YC2(I)
GO TO 110
109 CONTINUE
YC(I,J)=YC1(I)
110 CONTINUE
111 CONTINUE
C
C ***** GEAR NUMBER #1 *****
LOAD EXTERNAL PLOT VALUES INTO X,Y, AND THETA ARRAY UNTIL FILLET
AREA OF INVOLUTE PROFILE IS REACHED
DO 5 J=1,L1
RMIN=SQRT(XA(J)**2+(YA(J)+RRO1)**2)
IF(RMIN.LE.RTF11) GO TO 6
X(J,1)=XA(J)
Y(J,1)=YA(J)
THETA(J,1)=THET1(J)
5 CONTINUE
6
X(J,1)=RTF11*SIN(BETA1)
Y(J,1)=RTF11*COS(BETA1)-RRO1
THETA(J,1)=THETA(J-1,1)
KK=L1+NF-J
RPHI=((RRC1+RF1)**2+RF1**2)-RTF11**2)/(2.*RF1*(RRC1+RF1))
R11=RPHI/(FLOAT(KK))
J=J+1

```

```

KK=L1+NF
DO 345 JJJ=J, KK
RPHI=RPHI-R11
RX1=SQRT(RF1**2+(RRC1+RF1)**2 -2.*RF1*(RRC1+RF1)*COS(RPHI))
ARC1=ARSIN((RF1/RX1)*SIN(RPHI))
BETA1=BETA1+ALPHA1-ARC1
X(JJJ, 1)=RX1*SIN(BETA1)
Y(JJJ, 1)=RX1*COS(BETA1)-RR01
IF(JJJ.EQ.J) GO TO 345
THETA(JJJ-1, 1)=ATAN((X(JJJ, 1)-X(JJJ-2, 1))/(Y(JJJ, 1)-Y(JJJ-2, 1)))
345 CONTINUE
THETA(JJJ, 1)=.5*PI-BETA1
C
C ***** GEAR NUMBER #2 *****
C LOAD EXTERNAL PLOT INVOLUTE COORDINATES INTO ARRAY X, Y, THETA
C UNTIL FILLET PORTION OF INVOLUTE IS REACHED
C
DO 7 J=1, L1
RMIN=SQRT(XB(J)**2+(-YB(J)+RR02)**2)
IF(RMIN.GE.RTF22)GO TO 8
X(J, 2)=XB(J)
Y(J, 2)=YB(J)
7 THETA(J, 2)=THETA(J)
8 CONTINUE
X(J, 2)=-RTF22*SIN(BETA2)
Y(J, 2)=-RTF22*COS(BETA2)+RR02
THETA(J, 2)=THETA(J-1, 2)
KK=L1+NF-J
RPHI=((RRC2-RF2)**2+RF2**2)-RTF22**2)/(2.*RF2*(RRC2-RF2))
RPHI=ARGCOS(RPHI)
RRPHI=PI-RPHI
R12=RRPHI/(FLOAT(KK))
J=J+1
KK=L1+NF
DO 346 JJJ=J, KK
RPHI=RPHI+R12
RX2=SQRT(RF2**2+(RRC2-RF2)**2 -2.*RF2*(RRC2-RF2)*COS(RPHI))
ARC2=ARSIN((RF2/RX2)*SIN(RPHI))
BETA2=BETA2+ALPHA2-ARC2
X(JJJ, 2)=-RX2*SIN(BETA2)
Y(JJJ, 2)=-RX2*COS(BETA2)+RR02
IF(JJJ.EQ.J) GO TO 346
THETA(JJJ-1, 2)=ATAN((X(JJJ, 2)-X(JJJ-2, 2))/(Y(JJJ, 2)-Y(JJJ-2, 2)))
346 CONTINUE
THETA(JJJ, 2)=.5*PI-BETA2

```



```

DO 101 I1=1,2
IF(I1.EQ.2)GO TO 110
GO TO 109
110 CONTINUE
LI=LI22
RFIL=RF2
RR03= RR02
RRCA= RRC2
ALPHA=ALPHA2
BETA=BETA2
109 CONTINUE
RHO=PI/2.-(BETA+ALPHA)
YDIST=RR03-SIN(RHO)*(RRCA-RFIL)
HO=2.*(SIN(ALPHA+BETA)*(RRCA-RFIL)-RFIL)
WRITE(6,94)11
94 FORMAT(50X,'CORNELL METHOD FOR GEAR NUMBER ',I3//)
WRITE(6,95)
95 FORMAT(5X,' POSITION',5X,'Y-POS OF LOAD',5X,'LOAD ANGLE',5X,
1'STRESS CON. FAC.',5X,'GAM.CON. ANGLE',5X,'CORNELL J+',5X,
2'LOAD',5X,'CORNELL STRESS'//)
C ***** BEGIN INNER LOOP CALCULATIONS *****
C
C LN=LI
DO 100 I=1,50
LI=LN
DEL=DELTA X
36 CONTINUE
J=1
15 CONTINUE
IF(ABS(YC(I,I))-Y(J,I)).LE.DEL) GO TO 11
J=J+1
IF(J.GT.LI)GO TO 35
GO TO 15
CONTINUE
DEL=DEL+DELTA X
GO TO 36
11 CONTINUE
IF(I1.EQ.2) X(J,2)=-X(J,2)
LO=Y(J,11)-ABS(X(J,11))*TAN(THETA(J,11))
IF((LO-YDIST).LE.0.0)WRITE(6,99)1
99 FORMAT(5X,I3,20X,'CORNELL METHOD DID NOT CONVERGE FOR THIS POSITIO
N')
IF((LO-YDIST).LE.0.0)GO TO 100
C ***** START ITERATIVE PROCEDURE FOR GAMMA MAX *****
C
C
C

```

```

DEL=DELTA
IT=1
10 CONTINUE
   GAMMA=.2
12 CONTINUE
   AI=HO/RFIL*2.*(1.-COS(GAMMA))
   BI=ABS(LO-YDIST)/RFIL+SIN(GAMMA)
   RIGHT=((1.+16*(AI**.7))*AI)/(BI*(4.+416*(AI**.7))-(1./3.+016
1*(AI**.7)*ATAN(THETA(J,1))))
   RLEFT=ATAN(RIGHT)
   WRITE(6,90)AI,BI,RIGHT,RLEFT
C 900 FORMAT(2X,'AI = ',F10.5,5X,'BI = ',F10.5,5X,'RIGHT = ',F10.6,5X,
C 1'RLEFT = ',F10.6)
   IF(ABS(GAMMA-RLEFT).LE.DEL)GO TO 20
   IT=IT+1
   IF(IT.GT.10)WRITE(6,96)IT
C 96 FORMAT(2X,'SOLUTION FOR GAMMA MAX DID NOT CONVERGE,GAMMA = ',13)
   GAMMA=RLEFT
   GO TO 12
20 CONTINUE

***** GAMMA CONVERGENCE COMPLETE *****
***** SEARCH FILLET FOR CORRESPONDING ANGLE *****

DEL=DELTA
30 CONTINUE
   LI=LN
31 CONTINUE
   IF(ABS(GAMMA-THETA(LI,1)).LE.DEL)GO TO 80
   LI=LI+1
   IF(LI.GT.KK)GO TO 33
   GO TO 31
33 CONTINUE
   DEL=DEL+DELTA
   IF(DEL.GT.1)WRITE(6,92)GAMMA
C 92 FORMAT(2X,'DELTA TOO LARGE ',5X,'GAMMA= ',F10.7)
   IF(DEL.GT.2)STOP
   GO TO 30
80 CONTINUE
   QLOAD=LOAD1(1)
C THE FOLLOWING EQUATIONS ARE FOR THE VARIOUS FACTORS NEEDED
C TO EVALUATE THE BENDING STRESS FOR CORNELL'S METHOD
C
C SCF - STRESS CONCENTRATION FACTOR

```

```

C      BCBS - BEAM CANTILEVER BENDING STRESS FACTOR
C      BLPS - BENDING LOAD PROXIMITY STRESS FACTOR
C      ALPS - AXIAL LOAD PROXIMITY STRESS FACTOR
C      AXS - AXIAL STRESS FACTOR
      IF(11.EQ.2) X(LI,2) =-X(LI,2)
      SCF=((2.*ABS(X(LI,11)))/(2.*RFIL))**.7)*.26+1.
      BCBS=(6.*(LO-Y(LI,11)))/(2.*ABS(X(LI,11)))*2)
      BLPS=SQRT(.72/(2.*ABS(X(LI,11))*(Y(J,11)-Y(LI,11))))
      ALPS=(1.-(2.*ABS(X(J,11))*25*TAN(THETA(J,11)))/(2.*ABS(X(LI,11))))
1)    AXS=TAN(THETA(J,11))/(2.*ABS(X(LI,11)))
      SIG= QLOAD*COS(THETA(J,11))*SCF*(BCBS+BLPS*ALPS-AXS)/FW
      XPLUS=(QLOAD*DP)/(SIG*FW)
      GAMMA=GAMMA*180./PI
      THETA=THETA(J,11)*180./PI
      WRITE(6,40)1, YC(1,11), THETA, SCF, GAMMA, XPLUS, LOAD1(1), SIG
      40  FORMAT(5X,13,9X,F10.6,8X,F10.6,9X,F10.6,5X,F10.6,2X,
      1F10.2,6X,F10.2)
100  CONTINUE
      WRITE(6,1)
      1  FORMAT(1H1)
101  CONTINUE
      RETURN
      END
//GO. SYSIN DD *
&CONTRL  INPUT='ENGL', OUTPUT='ENGL', I PLOT=2, MODF='NO ', NTYPE=2,
IDIR=1 &END
&PHYPAR  E=2*30.E6, PR=2*0.285, GAMA=2*0.288, JG=0.0188, 1.5189 &END
&GENPAR  DP=8, DELT=0.01, TIN=1.9363, RPMIN=1000., ZETAS=0.005, ZETAG=0.05,
PHID=14.5, CBD=0., CB1=0., CB2=0., CBL=0., JD=0.9376, JL=0.93760,
KLS=885000., KDS=885000. &END
&GEOPAR  TC=32,96,AD=2*0.12500,WD=2*0.269600, GRRF=0.0216250, 0.021625,
R1=1.8554,6.1446,FW=2*1.0 &END
&PRDEF  PATM1=-0.0000, PATM2=-0.0000, RATM1=0.0, RATM2=0.0 &ERD
//GO. FT08F001 DD DSN=R8120. STATIC. OUTPUT,
// DISP=OLD
**
//

```


14.500000, 1.851447
 2.000000
 RPC
 1.940172
 RLM
 1.875414
 RTF
 1.855399
 RRC
 999

NUMBER OF TEETH ON GEAR #1 = 32.

NUMBER OF TEETH ON GEAR #2 = 96.

CORNELL METHOD FOR GEAR NUMBER 1

POSITION	Y-POS OF LOAD	LOAD ANGLE	STRESS CON. FAC.	GAM. CON. ANGLE	CORNELL J+	LOAD	CORNELL STRESS
1	0.087664	1.084418	1.835004	38.324188	0.259927	276.41	8507.36
2	0.085862	-3.128635	1.832846	36.595352	0.241963	279.46	9239.87
3	0.088628	1.084418	1.835004	38.324188	0.259927	290.12	8929.16
4	0.088627	1.084418	1.835004	38.324188	0.259927	294.25	9056.25
5	0.091159	2.077615	1.835004	38.020828	0.261483	304.17	9305.96
6	0.088627	1.084418	1.835004	38.324188	0.259927	306.72	9440.20
7	0.091395	2.077615	1.835004	38.020828	0.261484	317.00	9698.56
8	0.093923	2.923657	1.833914	37.626602	0.262010	324.74	9915.50
9	0.094165	2.923657	1.833914	37.626602	0.262010	328.01	10015.23
10	0.096859	3.649922	1.833914	37.161850	0.261961	333.37	10180.71
11	0.096938	3.649922	1.833914	37.161850	0.261961	336.69	10282.00
12	0.099712	4.312653	1.832846	36.665619	0.261340	342.40	10481.40
13	0.102488	4.926600	1.832846	36.149338	0.260537	347.55	10671.74
14	0.105265	5.493335	1.831800	35.614746	0.259275	353.24	10899.32
15	0.108044	6.025059	1.830776	35.070389	0.257781	358.17	11115.40
16	0.110822	6.526517	1.830776	34.521088	0.256203	501.72	15666.29
17	0.113603	7.011321	1.829776	33.974304	0.254392	509.97	16037.27
18	0.119050	7.904217	1.828799	32.877731	0.250402	517.40	16530.24
19	0.121894	8.333175	1.827846	32.339279	0.248254	377.95	12179.36
20	0.124599	8.739887	1.827846	31.802948	0.246071	383.34	12462.78
21	0.127519	9.135977	1.826917	31.274109	0.243752	381.58	12523.45
22	0.130307	9.519541	1.826917	30.752243	0.241454	385.65	12777.44
23	0.135880	10.255890	1.825130	28.933868	0.230006	387.50	13478.07
24	0.141459	10.956341	1.824274	27.942917	0.224969	391.75	13930.92
25	0.144248	11.290858	1.823442	27.461838	0.222404	390.89	14082.34
26	0.152592	12.268422	1.823442	26.899099	0.221888	390.89	14093.30
27	0.158165	12.883000	1.822637	26.013245	0.216953	388.72	14333.87
28	0.163748	13.477004	1.821856	25.173904	0.212074	386.26	14570.68
29	0.169335	14.059245	1.821101	24.372284	0.207300	382.38	14756.41
30	0.174932	14.615447	1.820373	23.602249	0.202575	378.36	14941.96
31	0.180530	15.164305	1.819669	22.867752	0.197983	374.24	15122.25
32	0.188942	15.947165	1.818992	21.821884	0.191255	369.62	15460.87

POSITION	Y-POS OF LOAD	LOAD ANGLE	* STRESS CON. FAC.	GAM. CON. ANGLE	CORNELL J+	LOAD	CORNELL STRESS
33	0.197323	16.716492	1.818341	20.846527	0.184835	501.80	21718.98
34	0.202922	17.202606	1.817719	20.228867	0.180653	494.11	21861.02
35	0.208515	17.684998	1.817719	19.639038	0.176626	487.83	22095.54
36	0.214108	18.161530	1.817122	19.075043	0.172716	350.29	16224.90
37	0.225312	19.075699	1.816552	18.015625	0.165219	336.97	16316.48
38	0.230884	19.532822	1.816010	17.520599	0.161674	332.14	16434.89
39	0.239315	20.186798	1.816010	16.883820	0.155222	320.83	16397.82
40	0.244861	20.620300	1.815495	16.427321	0.152322	314.09	16398.41
41	0.256103	21.459213	1.815007	15.569323	0.146942	302.58	16473.58
42	0.261625	21.858795	1.815007	15.165621	0.143923	296.04	16455.26
43	0.270002	22.478897	1.814548	14.592818	0.139637	286.00	16385.52
44	0.272794	22.672791	1.814548	14.408601	0.138231	282.20	16332.14
45	0.272794	22.672791	1.814548	14.408601	0.138231	280.22	16217.43
46	0.272794	22.672791	1.814548	14.408601	0.138231	278.57	16121.98
47	0.272794	22.672791	1.814548	14.408601	0.138231	277.22	16043.70
48	0.272794	22.672791	1.814548	14.408601	0.138231	276.86	16023.16
49	0.272794	22.672791	1.814548	14.408601	0.138231	276.45	15999.43
50	0.272794	22.672791	1.814548	14.408601	0.138231	275.87	15965.93

CORNELL METHOD FOR GEAR NUMBER 2

POSITION Y-POS OF LOAD LOAD ANGLE * STRESS CON. FAC. GAM. CON. ANGLE CORNELL J+ LOAD CORNELL STRESS

1	0.268063	9.370547	2.097627	18.419540	0.163392	276.41	13533.69
2	0.265137	9.560156	2.098140	18.639404	0.165309	279.46	13524.38
3	0.258019	10.058612	2.098140	19.241974	0.171164	290.12	13559.67
4	0.253717	10.230891	2.098679	19.477798	0.173223	294.25	13589.23
5	0.246580	10.717623	2.098679	20.217972	0.179653	304.17	13544.78
6	0.245606	10.717623	2.099241	21.012177	0.186491	317.00	13658.39
7	0.239133	11.169379	2.099629	21.576355	0.191337	324.74	13598.57
8	0.232878	11.465735	2.099829	21.867233	0.193797	328.01	13540.42
9	0.229338	11.596176	2.100440	22.477463	0.199010	333.37	13401.06
10	0.223165	11.886320	2.100440	23.120728	0.204456	336.69	13173.90
11	0.220191	12.169178	2.101075	23.796112	0.210134	342.40	13035.51
12	0.214523	12.423953	2.101735	24.514740	0.216194	347.55	12860.62
13	0.209012	12.699697	2.102419	25.271576	0.222510	353.24	12700.20
14	0.203664	12.950659	2.102419	26.077988	0.229215	358.17	12500.67
15	0.198476	13.217940	2.103126	26.493484	0.232636	501.72	17253.32
16	0.193450	13.323896	2.103855	27.373474	0.239913	509.97	17005.12
17	0.188582	13.576272	2.103855	28.797165	0.251575	517.40	16453.19
18	0.181203	13.941792	2.105385	29.820374	0.259883	377.95	11634.35
19	0.176640	14.169509	2.106183	30.362442	0.264336	383.34	11601.64
20	0.172259	14.299187	2.107005	31.486649	0.273365	381.58	11666.80
21	0.168008	14.512162	2.107849	32.088669	0.278303	385.65	11085.61
22	0.163932	14.650782	2.109601	33.988205	0.293474	387.50	10563.23
23	0.157307	14.972322	2.110509	35.374130	0.304497	391.75	10292.44
24	0.150832	15.200427	2.114353	36.099991	0.310249	391.50	10095.01
25	0.147225	15.304362	2.114353	39.283463	0.335307	390.89	9326.19
26	0.138331	15.735962	2.116396	41.051071	0.349135	388.72	8907.11
27	0.132305	15.943896	2.118517	42.956116	0.364003	386.26	8489.10
28	0.126425	16.158340					

29	0.120695	16.350021	2.121839	44.990204	0.379811	382.38	8054.03
30	0.115110	16.559341	2.124143	47.189651	0.396797	378.36	7628.26
31	0.109678	16.770874	2.126515	49.556931	0.415009	374.24	7214.19
32	0.101653	17.046829	2.131456	53.401413	0.442446	369.62	6656.14
33	0.093735	17.343719	2.137971	57.761093	0.476887	501.80	8417.98
34	0.088737	17.543900	2.142041	60.863144	0.500229	494.11	7902.14
35	0.083697	17.735809	2.147636	64.147202	0.524836	487.83	7435.92
36	0.079188	17.813187	2.150498	65.766403	0.537106	350.29	5217.39
37	0.069030	18.194321	2.160801	73.085129	0.589921	336.97	4577.52
38	0.064630	18.373795	2.168373	76.971466	0.614674	332.14	4322.78
39	0.057508	18.560501	2.174521	80.995102	0.638854	320.83	4017.55
40	0.053406	18.734406	2.168373	77.058731	0.658775	314.09	3814.29
41	0.043730	19.004150	2.159306	71.251266	0.681571	302.58	3551.60
42	0.039912	1.224213	2.153399	68.301498	0.347916	296.04	6807.07
43	0.033362	1.227212	2.156336	69.734253	0.345643	286.00	6619.60
44	0.032619	1.227212	2.156336	69.734253	0.345644	282.20	6531.62
45	0.034884	1.227212	2.156336	69.734253	0.345644	280.22	6485.74
46	0.037327	1.227212	2.156336	69.734253	0.345643	278.57	6447.57
47	0.039949	1.224213	2.153399	68.301498	0.347916	277.22	6374.35
48	0.042748	19.079468	2.159306	69.404099	0.685009	276.86	6233.39
49	0.045726	19.004150	2.159306	71.251266	0.681570	276.45	6244.89
50	0.048878	18.927048	2.162303	73.136276	0.675914	275.87	6265.19

C-4 ENTERING OF INPUT DATA

The three modules of the ISG drive computer package require input data which are obtainable from the namelist arrays or the two data files. Numerical data may be entered without format statements, and fields are generated as required. The variables required for the namelist arrays along with their respective headings are:

/HEDING/

TITLE 1 any suitable title or information
 TITLE 2 can be entered on three lines from
 TITLE 3 Title 1 through Title 3
 TAPE - Alphanumeric code to indicate whether certain information is to be filed on tape. Tape 8 is used for the dynamic analysis (Module 2) and Tape 9 is for the stress analysis (Module 3).
 'YES' - write on tape
 'NO' - do not write on tape

/CONTRL/

INPUT - alphanumeric code used to designate type of input data
 'ENGL' - English (lbf, in., sec.)
 'SI' - metric (newtons, mm, sec.)
 OUTPUT - alphanumeric code used to designate output; codes used are same as for input
 MODF - alphanumeric code used to designate whether or not profile modifications are input
 'NO' - no modifications
 'YES' - modifications listed under /PRFDEF/

/PHYPAR/ (two data points required per variable)

E - Young's modulus
 PR - Poisson's ratio
 GAMA - specific weight
 JG - polar moment of inertia; optional, program
 will generate if no value entered

/GENPAR/

DP - diametral pitch (English input only)
 M - gear module (metric module only)
 DELTP - backlash
 TIN - input torque
 RPMIN - input RPM
 ZETAS - damping coefficient of shaft
 ZETAG - damping coefficient between gear teeth
 PHID - pressure angle (degrees)
 * JD - mass moment of inertia of driver
 * JL - mass moment of inertia of load
 * KDS - torsional spring stiffness of driving shaft
 * KLS - torsional spring stiffness of load shaft
 * LDS - length of drive shaft
 * LLS - length of load shaft

/GEOPAR/ (two data points required per variable)

TG - number of gear teeth
 AD - addendum
 WD - working depth
 GRRF - fillet radius of basic rack
 * RI - hub radius

FW - face width
 UCUT - undercut
 RT - rim thickness
 RADEL - radial deflection
 COR12 - modifier for tooth center angle
 COR34 - modifier for tooth center angle
 /PARAME/
 NLIM - angular sweep parameter - Gear 1
 MLIM - angular sweep parameter - Gear 2
 DELT - increment
 JJJJ - adjustable do loop parameter - Gear 1
 LLLL - adjustable do loop parameter - Gear 2
 DPSLI1 - angular correction due to radial deflection -
 Gear 1
 DPSLI2 - angular correction due to radial deflection -
 Gear 2
 DPEL1 - modifier for tooth center angle - Gear 1
 DPEL2 - modifier for tooth center angle - Gear 2
 * optional, program will generate if no value entered

In addition to evaluating purely involute gear teeth, the gear tooth profile can be modified to simulate tip relief or undercutting. Also, sinusoidal errors can be introduced, as well as pits, to simulate involute errors due to manufacturing and surface damage, respectively. These modifications are introduced in the /PRFDEF/ namelist. If MODF = NO, /PRFDEF/ is not included in the data card set.

/PRFDEF/ (two data points required per variable)

PATM - parabolic tip modification
STTM - straight line tip modification
RATM - roll angle of tip modification
PABM - parabolic bottom modification
STBM - straight line bottom modification
RABM - roll angle of bottom modification
PER - amplitude of sinusoidal error
PAP - phase angle of sinusoidal error
CYC - number of cycles of sinusoidal errors
IPIT - profile coordinate points over which pit
occurs
DEEP - depth of pit

Use of the namelist arrays offers a simple, unformatted means of inputting data and is very convenient for looping more than one data set. After the initial data set, subsequent data sets need just two input revisions. If a later namelist array contains no revisions, only a card with the array heading and ending need be submitted. Unlisted variables default to the previous values. Examples of input data card sets illustrate the following namelist data card format.

1. Column one is blank.
2. '&' is used to signify new namelist array.
3. '&' is followed by the namelist name.
4. A blank separates the namelist name and the first variable name. Subsequent variables are separated by commas.

5. There are two methods for defining the two element variables. The elements are defined in the order they are to be entered in the variable and separated by commas, i.e., $TG=32, 96$ defines $TG(1) = 32$ and $TG(2)=96$. If both elements are equal, they may be entered by listing the number of identical values, the multiplication symbol, and then the value itself, i.e., $AD=2*0.125$, defines $AD(1)=0.125$ and $AD(2)=0.125$.
6. The last listed array value is followed by a blank and then the symbol from column 2 is repeated. The word END immediately follows the symbol and signifies the end of that array.

Because of the modular approach it is necessary to store certain information from one module for use in another module. Tape 8 stores the pertinent data from the static analysis which is needed for the dynamic analysis. Tape 9 stores the pertinent data from the dynamic analysis for use in the stress analysis. This tape contains some of the previously transferred static analysis data on Tape 8. The stress analysis then has logic to initiate a static or dynamic stress analysis.

The modules have the capability for accepting either SI or English gear input data and have options to print the results in either SI or English units. Input and output do not necessarily have to be of the same regime, i.e., SI output can be obtained from English input and vice-versa. Data submitted under the 'ENGL' code should be in pounds-force, inches and seconds. The data submitted under the 'SI' code should be in newtons, millimeters and seconds. The only exception to this is the density value under the 'SI' code should be in kg/m^3 .

GLOSSARY OF TERMS

<u>Text</u>	<u>Computer Program</u>	<u>Description</u>
a	AD	addendum
A		area
b		ring gear width maximum thickness of tooth
B	BGM	backlash
c	CR	loaded contact ratio
	C	center distance of gears
	C_B	damping coefficient
	CYC	number of sinusoidal error cycles
d	DED	dedendum
DF1, DF2	DF1, DF2	dynamic load factors
D		ball diameter
DEEP	DEEP	depth of pit
E	E	Young's modulus
F	FW	face width geometry factor
F_r		radial load of bearings
F_t		tangential load of gears
G		modulus of torsion
h		ring gear thickness
HSF	HSF	hub/ring torsional stiffness factor
h_t	HT	whole depth
I		moment of inertia
ISG		internal gear drive
J		polar mass moment of inertia
[J]	[MM]	inertia matrix
KG		gear mesh stiffness
KP		gear pair stiffness

<u>Text</u>	<u>Computer Program</u>	<u>Description</u>
[K]	[SM]	stiffness matrix
L		length of roller
L.A.		line of action
m_G	MG	gear ratio
m_P	CR	contact ratio
M		bending moment module
N	TG	normal load
	OMG	number of teeth constant angular velocity
p	CP	circular pitch
p_b	BP	base pitch
p		applied load at contacting point
	PABM	magnitude of parabolic modification at bottom
	PAP	angle from start of sinusoidal error to start of involute
	PATM	magnitude of parabolic modification at tip
	PE	profile error
	PER	maximum profile error
	PH	Hertzian pressure
	PM	profile modification
	PPD'	instantaneous pitch radius
	PSITP	static angular position
r	RPC	radius at pitch circle
r_A	RAC	radius at addendum circle
r_b	RBC	base radius circle
	RABI	RA at the bottom of involute
	RABM	length of root modification in degrees of roll
	RABOT	RA at bottom of involute
	RAM	roll angle at end of modification at tip
	RAN	RA at end of modification at bottom
	RAPP	RA at pitch point
	RAT	RA at tip
	RATIP	RA from end of modification to RA at the pitch point
	RATM	length of tip modification in degrees of roll

<u>Text</u>	<u>Computer Program</u>	<u>Description</u>
RCCP	RCC	instantaneous radius of curvature
r_F	RF	fillet radius
r_L	RLM	limit radius
r_T	RT	edge radius of generating tool
Q	Q(k) _i	static gear pair load
Q _t	QT	total mesh static load
QD	QD(k) _i	dynamic gear pair load
QD _t	QDT(I)	total mesh dynamic load
Q _{max}		maximum radial bearing load
	STBM	magnitude of straight line modification at bottom
	STTM	magnitude of straight line modification at tip
SV		sliding velocity
T		torque
T _{IN}	TD	input torque
T _{LA}		theoretical line of action
TR, TR'	TDIN	theoretical and instantaneous transmission ratio
T _{OUT}	TOUT	output torque
U ₁ , U ₂		interval of contact
U		abscissa in global coordinate system
V		shear velocity ordinate in global coordinate system
W		abscissa in rotating coordinate system of gears
X		abscissa in local tooth coordinate system

<u>Text</u>	<u>Computer Program</u>	<u>Description</u>
Y		ordinate in local tooth coordinate system
Z		ordinate in rotating coordinate system of gears number of balls or rollers-bearings

GREEK SYMBOLS

α		contact angle - bearings
β		angle between point of contact and center of tooth
γ		angle between pitch point and center of tooth
γ_s		maximum fillet stress angle
δ	TDEFL	deflection
ϵ	RA	roll angle
θ		involute polar angle
θ	PSP	dynamic displacement
$\dot{\theta}$	PSPD	dynamic velocity
$\ddot{\theta}$	PSPDD	dynamic acceleration
μ	PR	Poisson's ratio
ϵ_G	ZETAG	critical damping ratio - gear
ϵ_S	ZETAS	critical damping ratio - shafts
π	PI	3.141592654
σ		stress
τ		torsional stress
ϕ		pressure angle at any point
ϕ_n		normal pressure angle

<u>Text</u>	<u>Computer Program</u>	<u>Description</u>
-------------	-------------------------	--------------------

IDENTIFIERS

1		external gear
2		internal gear
D		driving element
G		gear
i		mesh arc position
k		tooth number
s		shafting
'		instantaneous

1. Report No. NASA CR-3692	2. Government Accession No.	3. Recipient's Catalog No.	
4. Title and Subtitle DYNAMIC EFFECTS OF INTERNAL SPUR GEAR DRIVES		5. Report Date June 1983	6. Performing Organization Code
		8. Performing Organization Report No. None	
7. Author(s) Adam Pintz, R. Kasuba, J. L. Frater, and R. August		10. Work Unit No.	
9. Performing Organization Name and Address Cleveland State University Mechanical Engineering Department Cleveland, Ohio 44115		11. Contract or Grant No. NAG3-186	
		13. Type of Report and Period Covered Contractor Report	
12. Sponsoring Agency Name and Address National Aeronautics and Space Administration Washington, D. C. 20546		14. Sponsoring Agency Code 505-40-42 (E-1620)	
		15. Supplementary Notes Final report. Project Manager, John J. Coy, U. S. Army Research and Technology Laboratories (AVRADCOM), Propulsion Laboratory, Lewis Research Center, Cleveland, Ohio 44135. Based on a dissertation submitted by Adam Pintz in partial fulfillment of the requirements for the degree Doctor of Philosophy to Cleveland State University, Cleveland, Ohio in June 1982.	
16. Abstract This research work has developed a comprehensive method for analyzing the static and dynamic loading and stresses of internal spur gear (ISG) drives. Prior to this study, there were no established methods for dynamic analysis of ISG drives. The currently published design techniques for ISG drives reflect the technology of the 1950' s. Consequently, this comprehensive methodology represents a definite advancement of the ISG drive design techniques. The analysis can be applied to involute and noninvolute spur gearing as well as to the high contact ratio gear systems. In addition, the developed method sets the groundwork for studies of planetary gear dynamics. The developed methods are combined in a digital computer program so that the static and dynamic behavior of an ISG drive can be investigated in an uninterrupted sequence. In addition to the geometry and nominal load relations, the computer program takes into account the following: <ol style="list-style-type: none"> 1. Variable gear mesh stiffness due to changes in single and multiple tooth contacts. 2. Deformations of the internal gear rings. 3. Actual tooth geometry including any errors and defects. 4. Elastic and inertial effects of the entire rotating system. 5. Effect of load on contact ratio, mesh stiffness and premature or delayed engagement. The variable mesh stiffness is combined with the drive train stiffness, inertia and damping to solve by numerical methods the nonlinear differential equations of motion for the dynamic loading of the gear teeth. Utilizing the computer program, parametric studies were made to determine the contributions of errors, damping and component stiffness on the dynamic behavior of ISG drives. The results of the analyses indicated an impressive list of advantages of the ISG drive over the external spur gear (ESG) drive. The principal reason for these advantages can be attributed to the high contact ratio of the ISG drive. The new methodology has finally provided an analysis procedure exclusively for the ISG drive. It reflects the latest state-of-the-art understanding of involute and noninvolute spur gear performance and is capable of analyzing the "very high contact ratio" (VHCR) gearing encountered with ISG drives.			
17. Key Words (Suggested by Author(s)) Gear dynamics Gear deflections and stresses Planetary gear systems Vibrations Internal gears		18. Distribution Statement Unclassified - unlimited STAR Category 37	
19. Security Classif. (of this report) Unclassified	20. Security Classif. (of this page) Unclassified	21. No. of Pages 284	22. Price* A13

* For sale by the National Technical Information Service, Springfield, Virginia 22161